TECHNOLOGICAL ADVANCES IN MICROBIOLOGICAL RISK ASSESSMENT

EDITED BY: Jun Wang, Bruce Michael Applegate, Fereidoun Forghani, Biao Suo and Gongliang Zhang

PUBLISHED IN: Frontiers in Microbiology

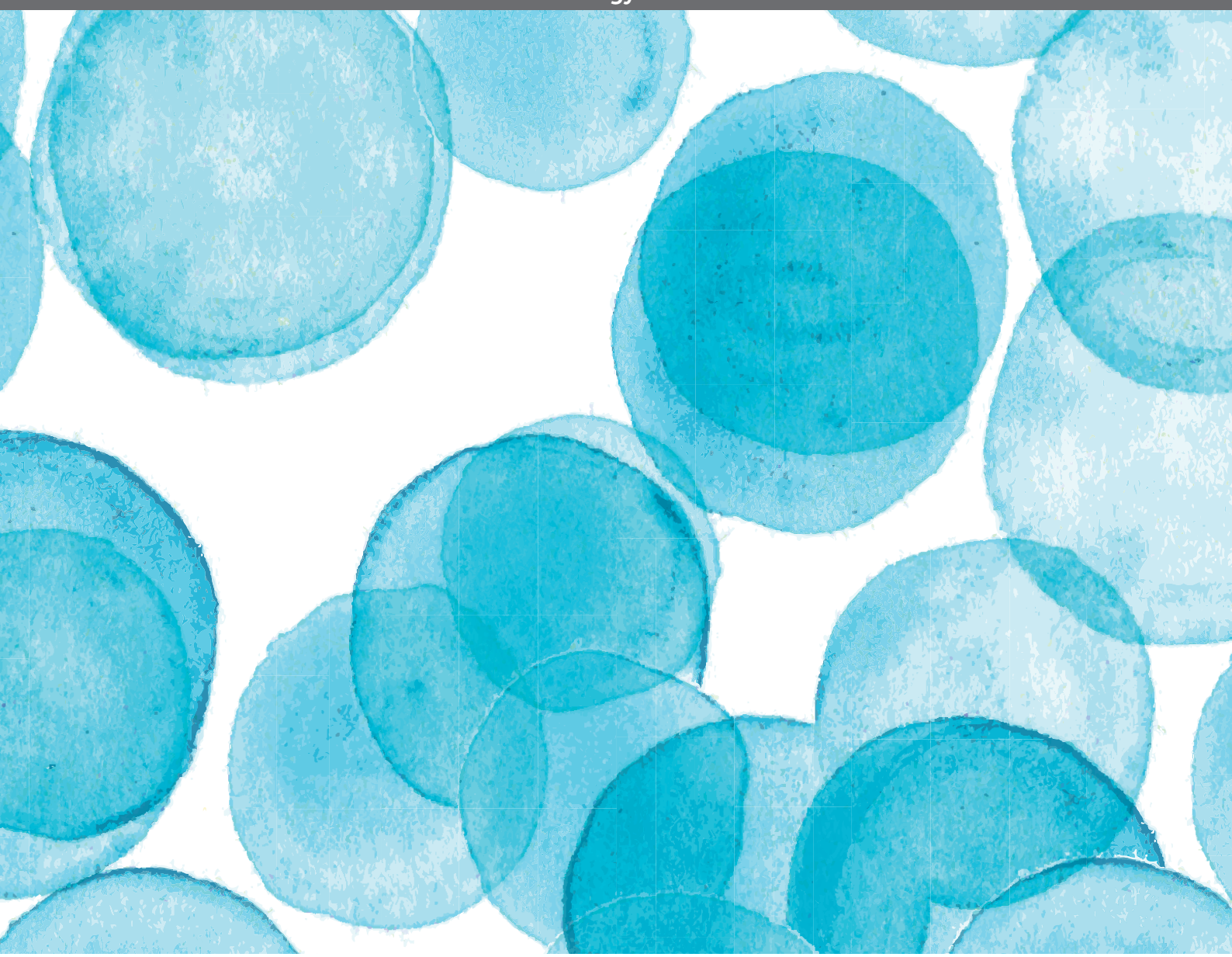

frontiers Research Topics

ISSN 1664-8714
ISBN 978-2-88974-879-2
DOI 10.3389/978-2-88974-879-2

About Frontiers

Frontiers is more than just an open-access publisher of scholarly articles: it is a pioneering approach to the world of academia, radically improving the way scholarly research is managed. The grand vision of Frontiers is a world where all people have an equal opportunity to seek, share and generate knowledge. Frontiers provides immediate and permanent online open access to all its publications, but this alone is not enough to realize our grand goals.

Frontiers Journal Series

The Frontiers Journal Series is a multi-tier and interdisciplinary set of open-access, online journals, promising a paradigm shift from the current review, selection and dissemination processes in academic publishing. All Frontiers journals are driven by researchers for researchers; therefore, they constitute a service to the scholarly community. At the same time, the Frontiers Journal Series operates on a revolutionary invention, the tiered publishing system, initially addressing specific communities of scholars, and gradually climbing up to broader public understanding, thus serving the interests of the lay society, too.

Dedication to Quality

Each Frontiers article is a landmark of the highest quality, thanks to genuinely collaborative interactions between authors and review editors, who include some of the world's best academicians. Research must be certified by peers before entering a stream of knowledge that may eventually reach the public - and shape society; therefore, Frontiers only applies the most rigorous and unbiased reviews.
Frontiers revolutionizes research publishing by freely delivering the most outstanding research, evaluated with no bias from both the academic and social point of view. By applying the most advanced information technologies, Frontiers is catapulting scholarly publishing into a new generation.

What are Frontiers Research Topics?

Frontiers Research Topics are very popular trademarks of the Frontiers Journals Series: they are collections of at least ten articles, all centered on a particular subject. With their unique mix of varied contributions from Original Research to Review Articles, Frontiers Research Topics unify the most influential researchers, the latest key findings and historical advances in a hot research area! Find out more on how to host your own Frontiers Research Topic or contribute to one as an author by contacting the Frontiers Editorial Office: frontiersin.org/about/contact

TECHNOLOGICAL ADVANCES IN MICROBIOLOGICAL RISK ASSESSMENT

Topic Editors:
Jun Wang, Qingdao Agricultural University, China
Bruce Michael Applegate, Purdue University, United States
Fereidoun Forghani, IEH Laboratories and Consulting Group, United States
Biao Suo, Henan Agricultural University, China
Gongliang Zhang, Dalian Polytechnic University, China

Citation: Wang, J., Applegate, B. M., Forghani, F., Suo, B., Zhang, G., eds. (2022). Technological Advances in Microbiological Risk Assessment. Lausanne: Frontiers Media SA. doi: 10.3389/978-2-88974-879-2

Table of Contents

frontiers in Microbiology

EDITORIAL
published: 17 March 2022
doi: 10.3389/fmicb.2022.872879

Editorial: Technological Advances in Microbiological Risk Assessment

Jun Wang[1]*, *Biao Suo*[2], *Fereidoun Forghani*[3], *Gongliang Zhang*[4] and *Bruce Applegate*[5,6]

[1] College of Food Science and Engineering, Qingdao Agricultural University, Qingdao, China, [2] College of Food Science and Technology, Henan Agricultural University, Zhengzhou, China, [3] Molecular Epidemiology, Inc., Lake Forest Park, WA, United States, [4] School of Food Science and Technology, Dalian Polytechnic University, Dalian, China, [5] Department of Food Science, Purdue University, West Lafayette, IN, United States, [6] Department of Biological Sciences, Purdue University, West Lafayette, IN, United States

Keywords: microbiological risk assessment, predictive microbiology, rapid detection, growth model, inactivation model

Editorial on the Research Topic

Technological Advances in Microbiological Risk Assessment

This Research Topic focused on current advances of research related to microbiological risk assessment (MRA). To minimize the adverse impact of foodborne pathogens on human health, MRA has been regarded as a structured and effective approach to improve food control systems and evaluate microbial risks. Generally, MRA is conducted in response to well defined risk management questions, requiring huge available data input to provide relevant results. In response to recent scientific and technical advances, and public demands, 10 articles were collected according to the objectives of this topic and could be divided into the following four aspects:

IMPROVING EXPOSURE ASSESSMENT STEP OF MRA

In MRA, predictive models play an important role for exposure assessment of foodborne pathogens to describe the microbial response over time and the growth dynamics affected by environmental conditions during the food chain from farm to table. Hiura et al. developed a Bayesian statistical modeling based on a generalized linear model (GLM) to fit observed bacterial inactivation data and growth data for *Bacillus simplex* and *Listeria monocytogenes*, respectively. Accordingly, the bacterial inactivation or growth, considering variability and uncertainty was simulated. The developed models enable a more explicit illustration of the variation in bacterial behavior *via* probability distributions. The novel method could clearly explain the variability and uncertainty in bacterial population behavior and could provide as useful information for risk assessment related to food borne pathogens. In another study by Zhou et al. the Weibull model was designed to evaluate the effectiveness of a newly developed 360-degree radiation thermosonication system (TS) in inactivating the *Staphylococcus aureus* in milk. In addition, the Bigelow and Log-linear model with tail were successfully used for describing the thermal inactivation kinetics of *Listeria monocytogenes* under mild heat, lactic acid, benzalkonium chloride, and nisin treatments, while the model- derived extended lag time of the survivors can be used to evaluate the cell growth kinetics following the treatments (Fang et al.).

OPEN ACCESS

Edited and reviewed by:
Giovanna Suzzi,
University of Teramo, Italy

***Correspondence:**
Jun Wang
faithmate@gmail.com

Specialty section:
This article was submitted to Food Microbiology, a section of the journal Frontiers in Microbiology

Received: *10 February 2022*
Accepted: *17 February 2022*
Published: *17 March 2022*

Citation:
Wang J, Suo B, Forghani F, Zhang G and Applegate B (2022) Editorial: Technological Advances in Microbiological Risk Assessment. Front. Microbiol. 13:872879. doi: 10.3389/fmicb.2022.872879

SUPPORTING MRA IN HAZARD IDENTIFICATION

In hazard identification, food contamination surveillance data, together with product/process evaluations needs to be collected, appraised, and interpreted to aid the identification of hazard–food combinations. In the study by Yan et al. the serotypes, MLST, and cgMLST of *Salmonella enterica* isolates from different sources in nine provinces in China from 2004 to 2019 were examined and used to investigate their phenotyping and genotyping diversities and genetic relationships. This article clarifies the temporal and spatial distribution characteristics of phenotyping and genotyping diversity of *S. enterica* isolates in China in the recent 16 years, which could provide valuable information for prevention and control of *Salmonella* in China with strain resources and genetic information. In another study by Qu et al. the prevalence of *B. cereus* in lettuce and farm environments distributed in China was investigated to determine the possible transmission of *B. cereus* on lettuce farms in China and its enterotoxicity. The results showed that soil and pesticides are the main sources of *B. cereus* on lettuce farms in China, and the possible transmission routes are as follows: soil-lettuce, manure-lettuce, pesticide-lettuce, manure-soil-lettuce, and water-manure-soil-lettuce. Furthermore, the *B. cereus* isolates, whether from lettuce or the environment, pose a potential risk to health. Liu et al. focused on the investigation of *Escherichia coli* strains isolated from raw milk of dairy cattle in Northern China and their antimicrobial susceptibility and essential virulence genes. The importance of this topic comes from the fact that *E. coli* is commonly associated with animals and is a major cause of toxic mastitis in dairy cows. Results obtained in the study showed that 34.4% of the samples were positive for *E. coli*, and that among the positive samples, several of them were harboring toxic genes and/or showed antimicrobial resistance. This aligned well with other literature emphasizing that antimicrobial resistance should be of concern to the public health authorities and in this particular case, that antibiotics should be cautiously used for the treatment of *E. coli* caused mastitis in dairy cows.

IMPROVING MRA AND PREVENTION APPROACHES

Bahk and Lee developed a user-friendly Microbial-MLE Tool, which can be easily used without requiring complex mathematical knowledge of MLE using an Excel spreadsheet. The tool, which is designated to adjust log-normal distributions to observed counts and implemented for food microbial censored data, would provide an accessible and easily comprehensible means for performing MLE and useful calculation to improve the outcome of MRA.

RAPID DETECTION OR APPROACHES REDUCING RISK

Effective and rapid detection of foodborne pathogens based on emerging technologies is critical for reliably assessing the pathogenic factors and reducing microbial risk. The review by Huang et al. explained how the aptasensors have been applied to risk assessment in foodborne pathogens using *Staphylococcus aureus* as a representation. The review concluded that the aptasensors have a good competitiveness for using as a tool for risk assessment of foodborne pathogens, in terms of time, sensitivity, specificity, and cost, especially with the developments of nanomaterials and portable detection instruments in future. Mustafa et al. assessed the heavy metal resistance in *Salmonella* Typhimurium and its association with disinfectant and antibiotic resistance. The research conclusion was that excessive use of metals and disinfectants as feed additive in animal care may have the potential to promote antibiotic resistance through co-selection and maintain and promote antibiotic resistance even in the absence of antibiotics. Xu and Zhu investigated the positive effects of complete replacement of nitrite with a *Lactobacillus fermentum* on the quality and safety of Chinese fermented sausages, and evaluated the risk of this strain. The results showed that replacing nitrite completely with the *L. fermentum* strain could be a potential strategy to produce healthier and safer acceptable sausages through decreasing the risk of nitrite and improving nutrition and quality of the sausages.

By compiling these 10 articles into this topic, the advances in MRA including development of growth/inactivation model, the rapid detection method, prevalence and molecular characterization of foodborne pathogens from different matrices, as well as emerging technologies on the inactivation of foodborne pathogens were covered, providing useful information for the target audience.

AUTHOR CONTRIBUTIONS

JW: conceptualization, writing the original draft, funding acquisition, writing—review, and editing. BS: writing the original draft, writing—review, and editing. FF: writing the original draft, writing—review, and editing. GZ: writing—review and editing. BA: conceptualization, writing—review, and editing. All authors approved the submitted version.

FUNDING

Research in the JW lab was supported by the Grant from China National Center for Food Safety Risk Assessment (20210349-6602421216), BS was supported by Natural Science Foundation of Henan Province (222300420455), and National Risk Assessment Major Special Project of Milk Product Quality and Safety (GJFP2019027).

ACKNOWLEDGMENTS

We would like to express our gratitude to all the authors who proposed their work, all the researchers who reviewed the submissions to this Research Topic.

Conflict of Interest: FF was employed by the company IEH Laboratories and Consulting Group, United States.

The remaining authors declare that the research was conducted in the absence of any commercial or financial relationships that could be construed as a potential conflict of interest.

Publisher's Note: All claims expressed in this article are solely those of the authors and do not necessarily represent those of their affiliated organizations, or those of the publisher, the editors and the reviewers. Any product that may be evaluated in this article, or claim that may be made by its manufacturer, is not guaranteed or endorsed by the publisher.

frontiers in Microbiology

ORIGINAL RESEARCH
published: 19 March 2021
doi: 10.3389/fmicb.2021.646735

Inactivation and Subsequent Growth Kinetics of *Listeria monocytogenes* After Various Mild Bactericidal Treatments

*Taisong Fang[1], Yufan Wu[2], Yani Xie[1], Linjun Sun[1], Xiaojie Qin[1], Yangtai Liu[1], Hongmei Li[1], Qingli Dong[1] and Xiang Wang[1]**

[1] School of Medical Instrument and Food Engineering, University of Shanghai for Science and Technology, Shanghai, China, [2] Research Centre of Analysis and Test, School of Chemistry and Molecular Engineering, East China University of Science and Technology, Shanghai, China

This study was carried out to investigate the effects of mild heat, lactic acid, benzalkonium chloride and nisin treatments on the inactivation, sublethal injury, and subsequent growth of *Listeria monocytogenes*. Results showed that the Bigelow model successfully described the thermal inactivation kinetics, while the Log-linear model with tail consistently offered the most accurate fit to LA, BC, and nisin inactivation curves of cells. Differential plating indicated that percentage of sublethal injury for nisin treated cells was significantly higher than that for the other three treatments. Compared to non-treated cells, significant extension of lag time was observed for all treated cells. The longer exposures to heat treatment contributed to the extended lag time of the survivors. While for LA, BC and nisin treated cells, the longest lag time was not observed at the most severe treatment conditions. The correlation analysis of sublethal injury percentage on the duration of lag time revealed that only heat treatment showed the significant correlation. Overall, the lag time analysis could evaluate a wide range of bacterial injury. Lag time of treated cells was significantly influenced by stress treatments and temperatures of recovery, however, there were not any significant changes in the maximum specific growth rate between treated and non-treated cells under isothermal recovery conditions. The information generated from this study is valuable for utilizing intervention strategies in the elimination or growth inhibition of *L. monocytogenes*.

Keywords: *Listeria monocytogenes*, inactivation, growth parameters, sublethal injury, pathogens control

OPEN ACCESS

Edited by:
Biao Suo,
Henan Agricultural University, China

Reviewed by:
Ting Fang,
Fujian Agriculture and Forestry University, China
Yong Zhao,
Shanghai Ocean University, China

***Correspondence:**
Xiang Wang
xiang.wang@usst.edu.cn

Specialty section:
This article was submitted to Food Microbiology, a section of the journal Frontiers in Microbiology

Received: *28 December 2020*
Accepted: *01 March 2021*
Published: *19 March 2021*

Citation:
Fang T, Wu Y, Xie Y, Sun L, Qin X, Liu Y, Li H, Dong Q and Wang X (2021) Inactivation and Subsequent Growth Kinetics of Listeria monocytogenes After Various Mild Bactericidal Treatments. Front. Microbiol. 12:646735. doi: 10.3389/fmicb.2021.646735

INTRODUCTION

Listeria monocytogenes is the causative agent of human listeriosis, a life threatening foodborne disease commonly associated with consumption of contaminated food products, especially ready-to-eat (RTE) foods (Swaminathan and Gerner-Smidt, 2007). Previous studies reported that fatality rate of listeriosis was up to 15.6% in European Union in 2018 (European Centre for Disease Prevention and Control [ECDC], 2019). In China, in spite of rare listeriosis outbreaks, high contamination rate was reported in retail foods, which could also cause a high potential risk to human health (Wu et al., 2016). Due to high fatality rate of listeriosis and high tolerance

of *L. monocytogenes* against food processing stresses such as low temperature, pH, a_w or high salinity, the bacterium has been identified as the one of the most dangerous pathogens associated with food products (Ferrentino et al., 2015). Therefore, it is vital to understand the response of *L. monocytogenes* to multiple food related stresses, and take into account growth kinetic parameters of survivors in different environments in order to design appropriate intervention strategies to control the level of *L. monocytogenes* in food chain.

Two important parameters inherent to *L. monocytogenes* growth kinetics are the lag time (λ) and the maximum specific growth rate (μ_{max}), and it is necessary to predict the two parameters accurately because outgrowth of *L. monocytogenes* is unacceptable in food products. The lag time reflects an adjustment period during which bacterial cells repair injuries caused by any stress, and modify themselves in order to initiate exponential growth in the new environment. Compared to reliable information on the maximum specific growth rate, the lag time is usually difficult to be predicted accurately due to poor understanding of initial physiological state of cells and/or repair of injured cell structures (D'Arrigo et al., 2006). The duration of lag time depends on numerous factors, including actual growth environments such as physical or chemical conditions. In addition, the history (physiological state in previous environments) of cells can also significantly influence the lag time in the actual growth environments, many studies have demonstrated that bacterial cells show shorter lag time when changes are smaller between previous and actual growth conditions (Francois et al., 2007; Yue et al., 2019). However, *L. monocytogenes* is routinely exposed to bactericidal treatments such as heat, organic acids, quaternary ammonium compounds and bacteriocins stresses (Shi et al., 2013; Humayoun et al., 2018) in food or food processing environments, and mild bactericidal treatments for food preservation are being utilized to obtain microbiologically safe food products and satisfy consumers' demands for minimally processed foods. The mild process may result in surviving *L. monocytogenes* cell populations, which most likely exhibited the state of sublethal injury. This suboptimal physiological state of cells could considerably extend the duration of lag time because of self-repairing process of injured cells in the appropriate growth environments (Yuste et al., 2004). After resuscitation, *L. monocytogenes* possesses full virulence, giving rise to a threat to public health. Therefore, injury induced by exposure to the mild bactericidal treatments influences the growth behavior of surviving cells. This emphasizes the importance of understanding the growth of *L. monocytogenes* after different mild bactericidal treatments.

In the present study, we investigated the effects of three types of treatments (physical, chemical, and biological bactericidal treatments) with heat, lactic acid (LA), benzalkonium chloride (BC) and nisin on the inactivation, sublethal injury, and subsequent growth of *L. monocytogenes*. Stress exposure conditions were selected to encompass various potential sublethal stresses encountered by *L. monocytogenes* in foods or food processing environments. In addition, the effects of various recovery temperatures (20, 25, 30, and 37°C) on growth parameters of treated *L. monocytogenes* were also determined.

MATERIALS AND METHODS

Bacterial Strain and Culture Conditions

Listeria monocytogenes (ATCC 19112) purchased from the China Center of Industrial Culture Collection (Beijing, China) was used in this study. Frozen stocks of bacteria were maintained in Tryptone Soy Yeast Extract Broth (TSB-YE; Beijing Land Bridge Technology Co., Ltd., Beijing, China) with 50% glycerol at −80°C. Working stocks were stored at 4°C on Tryptone Soy Agar with 0.6% Yeast Extract (TSA-YE; Beijing Land Bridge Technology Co., Ltd., Beijing, China) and were renewed monthly. Prior to each experiment, a single colony was inoculated into 10 mL of TSB-YE and incubated in a shaker with 110 rpm at 37°C for 16–18 h. Then 100 μL of overnight culture was transferred into 10 mL of fresh TSB-YE and incubated at same conditions to yield stationary phase cells which contained approximately 10^9 CFU/mL cells.

Mild Bactericidal Treatments

Four mild bactericidal treatments included one physical treatment with heat, two chemical treatments with LA and BC, and one biological treatment with nisin. Before each treatment experiment, 1 mL stationary phase cultures were centrifuged at 5,000 *g* for 10 min (Thermo Fisher Scientific Co., Ltd., Shanghai, China). Harvested cells were washed twice with 0.85% saline solution and re-suspended in 1 mL 0.85% saline solution to yield a cell density of ca. 10^9 CFU/mL. Stress exposure conditions were adjusted to suitable parameters leading to approximately 1.5–2.5 log CFU/mL reduction in cell counts. After each stress exposure, the surviving cells were placed at 25°C for recovery and subsequent growth. The lag time was monitored by using TTD (Time to Detection) method based on optical measurements (see below).

Heat Treatment

Mild heat treatment of *L. monocytogenes* was performed at 48°C for different treatment time (30, 60, 90, 120, and 150 min) according to preliminary experiments. It was carried out using thin walled PCR tubes (Shanghai Generay Biotech Co., Ltd., Shanghai, China) containing 30 μL culture and a thermal cycler instrument (Analytik Jena AG, Germany). The heating program was initially set at 37°C for 1 min in order to reduce and standardize the time to reach the target heat treatment temperature, and test tubes were removed at the set time intervals after the cultures had reached 48°C (Wang et al., 2017). After heat treatment, PCR tubes were immersed immediately in an ice-water bath for 1 min. Subsequently, decimal dilutions were made and plated, and then incubated at 37°C for 48 h before surviving cells' enumeration.

Lactic Acid, Benzalkonium Chloride, and Nisin Treatments

Stress treatments were performed by incubating *L. monocytogenes* cells with corresponding solutions at 25°C in a static incubator (Keer Equipment Co., Ltd., Nanjing, China). LA (40 mmol/L, Kuling Fine Chemical Co., Ltd., Shanghai, China), BC (70 mg/L, Macklin Biochemical Co., Ltd., Shanghai, China)

and nisin solution (900 IU/mL, Meryer Chemical Technology Co., Ltd., Shanghai, China) was separately prepared by dissolving the solute in 0.85% saline, and sterilized by filtration through 0.22 μm membrane filter units. For LA stress exposure, 1 mL harvested stationary cells were re-suspended in 1 mL LA solution for different treatment time (20, 40, 60, 80, and 100 min). For BC treatment, *L. monocytogenes* cells were incubated for 12, 24, 36, 48, 60, and 72 min, respectively. For nisin, cells were treated from 12 to 60 min and removed at a time interval of 12 min. Treated cells were harvested by centrifugation at 5,000 *g* for 10 min, and re-suspended in 1 mL TSB-YE for further analysis.

Viable and Sublethally Injured Cell Counts

The counts of *L. monocytogenes* were enumerated by a traditional plating method. Each sample was serially (1:10) diluted with 0.85% NaCl solution and appropriate dilutions were plated on TSA-YE (the non-selective medium) and TSA-YE with 5% NaCl (the selective medium) (Uyttendaele et al., 2008). Both vital and injured cells were able to grow on TSA-YE, while those which appeared on TSA-YE with 5% NaCl were regarded as only uninjured cells (Ray et al., 1978). Following formula (Busch and Donnelly, 1992) was used to calculate the percentage of sublethally injured cells:

$$\text{The injury rate (\%)} = \left(1 - \frac{\text{counts on selective medium}}{\text{counts on non} - \text{selective medium}}\right) \times 100\% \quad (1)$$

Time-averaged injured cells coefficient (TICC) was calculated to quantify the sublethally injured cells for the whole treatment time, and the equation is as follows (Miller et al., 2006):

$$TICC = \frac{\int_{t_{\text{initial}}}^{t_{\text{final}}} [\%\text{Sublethal Injury } (t)]dt}{t_{\text{final}} - t_{\text{initial}}} \quad (2)$$

Where t is the bactericidal treatment time, $t_{initial}$ and t_{final} are the first and last sampling time, respectively.

Optical Density Measurements

The effects of heat, LA, BC, and nisin treatments on the subsequent growth of *L. monocytogenes* were determined by growth curves using an automatic Bioscreen C system (Oy Growth Curves Ab Ltd., Helsinki, Finland). Treated and non-treated cultures were serially diluted (1:10) in TSB-YE, and 200 μL volume of different dilutions with concentrations ranged from 10^6 to 10^2 CFU/mL were added to 200 wells of two honeycomb plates. The honeycomb plates were placed in the Bioscreen C at an incubation temperature of 25°C, and the growth of *L. monocytogenes* was monitored by reading OD_{600} of the wells at 10 min intervals. For each well, the time to reach an OD_{600} of 0.15 from the start of incubation (OD_{600} = 0.10) was determined, and a cell concentration of approximately 10^7 CFU/mL corresponding to an OD_{600} value of 0.15 was determined by the count of plated viable cells. Honeycomb plates were shaken at medium intensity for 20 s before every measurement, and each stress experiment was repeated three times. After heat treatment for 150 min, LA treatment for 20 min, BC treatment for 48 min and nisin treatment for 24 min, treated cells were incubated at 20, 25, 30, and 37°C to compare the effects of recovery temperatures on growth parameters of treated *L. monocytogenes* by using TTD method described above.

Estimation of Growth Parameters of *Listeria monocytogenes*

The growth parameters of treated and non-treated *L. monocytogenes* were calculated based on TTD method. The μ_{max} value was calculated as the reciprocal of the absolute value of the regression slope of T_d (detection time) versus natural logarithm of initial cell concentration. The initial cell concentration for each dilution was determined by serial dilution and plating on TSA-YE, followed by incubation at 37°C for 48 h. Lag time of *L. monocytogenes* was estimated based on the following equation (Baranyi and Pin, 1999):

$$\lambda = T_d - \left[\frac{ln(N_d) - ln(N_0)}{\mu_{max}}\right] \quad (3)$$

Where, N_d is the bacterial number at the turbidity detection level (CFU/mL); N_0 is the initial concentration of cells (CFU/mL); T_d is the turbidity detection time (h); μ_{max} is the maximum specific growth rate (h^{-1}) under the experimental conditions described above.

Modeling Inactivation Kinetics of *Listeria monocytogenes*

After each treatment time, the counts of *L. monocytogenes* were converted to $\log_{10}$ values, and the survivors ($\log_{10}$ N_t) were represented vs. the treatment time (min for heat, LA, BC and nisin treatments) to construct survival curves. The Bigelow model and Log-linear model with tail were, respectively, used to fit the linear and non-linear inactivation kinetics obtained in our selected conditions, and inactivation parameters were obtained on the software GInaFiT (version 1.6) (Geeraerd et al., 2005). The goodness of fitting was evaluated by root mean squared error (RMSE). The equations and relevant parameters of the selected models are as follows (Bigelow, 1921; Geeraerd et al., 2000):

$$Log_{10}(N_t) = Log_{10}(N_0) - k_{max}t/Ln(10) \quad (4)$$

$$Log_{10}(N_t) = Log_{10}\left\{\left[10^{Log_{10}(N_0)} - 10^{Log_{10}(N_{res})}\right] \times e^{-k_{max}t} + 10^{Log_{10}(N_{res})}\right\} \quad (5)$$

Where, N_t represents the counts of survivors (CFU/mL); N_0 represents the initial counts (CFU/mL); k_{max} is the specific inactivation rate (min^{-1}); t is the exposure time of each treatment (min); N_{res} represents the residual population (CFU/mL).

Modeling the Effects of Different Temperatures on Growth Parameters

The λ and μ_{max} values of non-treated and treated *L. monocytogenes* cells were further analyzed as a function of recovery temperatures to develop the secondary model. The

equations and relevant parameters of the models are as follows (Ratkowsky et al., 1982):

$$\sqrt{\mu_{max}} = b \times (T - T_0) \quad (6)$$

$$\frac{1}{\sqrt{\lambda}} = b \times (T - T_0) \quad (7)$$

Where, λ is the lag time (h); μ_{max} is the maximum specific growth rate (h^{-1}); b is the regression constant; T_0 is the minimum temperature required for growth of *L. monocytogenes* (°C); T is the recovery temperature (°C).

Statistical Analysis

All experiments were repeated three times, means and standard deviations were determined from independent triplicate trials. Single-factor analysis of variance (ANOVA) and Tukey's test by SPSS 25 (SPSS Inc., Chicago, IL, United States) was used to test for any significant difference between means for sake of multiple comparisons. Correlation coefficients were calculated to conduct the correlation analysis of stresses for λ value. A significant level of 0.05 with p value was used in each case.

RESULTS AND DISCUSSION

Inactivation of *Listeria monocytogenes* by Mild Bactericidal Treatments

The survival of *L. monocytogenes* subjected to the four bactericidal treatments was evaluated, and the survival curves obtained from selective and non-selective media are shown in **Figure 1**. Overall, the inactivation curves exhibited two different patterns, log-linear and log-linear with tail. The Bigelow model successfully described the inactivation curves of heat treated cells. Similar thermal inactivation kinetics were also observed by Wang et al. (2017) and Haskaraca et al. (2019) while performing mild heat treatments of *L. monocytogenes*. The Bigelow model and relevant D value parameter have been extensively used to describe the microbial thermal inactivation in many studies. However, more and more reports have emphasized that non-linear models are more suitable than log-linear model for describing microbial heat inactivation curves, especially for mild heat treatments (Augustin et al., 2010; Aryani et al., 2015). A study of Marcén et al. (2019) indicated that mild heat (58°C) inactivation curve showed a shoulder. Similar results were also found in the thermal inactivation kinetics of *Salmonella enterica* (Wang et al., 2017). The Shoulder phenomena can be attributed to the presence of sublethally injured cells in the treated population, and their subsequent accumulation leading to sublethal injury during the manifestation of shoulders (Lou and Yousef, 1997). In fact, many studies have supported that heat inactivation kinetics present shoulders or tails, which are often fitted with the Weibull model (Aryani et al., 2015; Arioli et al., 2019). In this context, when estimating the effectiveness of heat treatments, non-linear kinetics could be taken into account upon existence of shoulders or tails.

The log-linear model with tail consistently offered the most accurate fit to LA, BC, and nisin inactivation curves of cells recovered from both media based on the small RMSE values (RMSE $\leq$ 0.133, data not shown). Many authors focused their attention on inactivation level of foodborne pathogens after exposure to a fixed LA or BC treatment time (Shi et al., 2017; Kang et al., 2019; Andrade et al., 2020), but there are limited studies on relevant inactivation kinetics of *L. monocytogenes*. In this study, tails appeared at an inactivation level of approximate 2 log cycles, especially for nisin treatment. When 900 IU/mL nisin was applied, the *L. monocytogenes* counts reduced significantly ($p < 0.05$) as the treatment time increased from 0 to 12 min, and counts of survival cells remained approximate 7 log CFU/mL in 12–60 min stress exposure. The inactivation kinetics of *L. monocytogenes* cells to nisin treatment obtained in the present study were in agreement with that of Shi's study (Shi et al., 2013). The occurrence of tails could be attributed to different factors, such as the presence of resistant cells subpopulation, adaptation phenomena along the treatment time.

Results in our study reflected differences among inactivation curves depending on the treatments applied, especially the inactivation kinetics of *L. monocytogenes* cells exposure to three treatments showing tail phenomena, which indicated possible adaptation phenomena along the treatment time. Therefore, from a practical point of view, when mild bactericidal treatments are designed, determination of inactivation kinetics should be taken into account to select process conditions applicable and avoid overestimation of bactericidal effectiveness, and further studies can be conducted by a deeper knowledge of their mode of action on foodborne pathogens to obtain a better profit of all these bactericidal technologies.

Stresses Induced Sublethal Injury Based on Differential Plating

The percentage of *L. monocytogenes* injury based on differential plating and TICC values after exposure to heat, LA, BC and nisin stresses are shown in **Figure 2**. The percentage of injury to heat, LA, BC, and nisin stresses ranged from 24.80–73.79, 20.05–50.93, 6.35–47.70, and 94.98–98.85%, respectively, which indicated the existing of different level of injured cells. Percentage of injury for non-treated cells was equal to zero (data not shown). In case of nisin treatment, the estimated ratio of injured bacterial cells was over 95% after 12 min exposure, and it was close to 100% as the treatment time went on (**Figure 2D**). As a whole, the percentage of injury in nisin treated cells was significantly higher than that in the other three treatments ($p < 0.05$), and this is also confirmed by the TICC value for the whole nisin treatment time (87.62%). Nisin has effective antimicrobial activities against Gram-positive bacteria including *L. monocytogenes*, and the cytoplasmic membrane is the target for nisin action (Martins et al., 2010). The TICC value in the present study revealed that nisin stress caused the high degree of cell membrane damage, which was also an indication of mechanism of relevant antimicrobial action. The possible reason for high sublethal damage rather than direct inactivation is that adaption phenomena along the treatment time induced the emergence of nisin-resistant cells subpopulation. This is demonstrated by Harris et al. (1991), which has described the

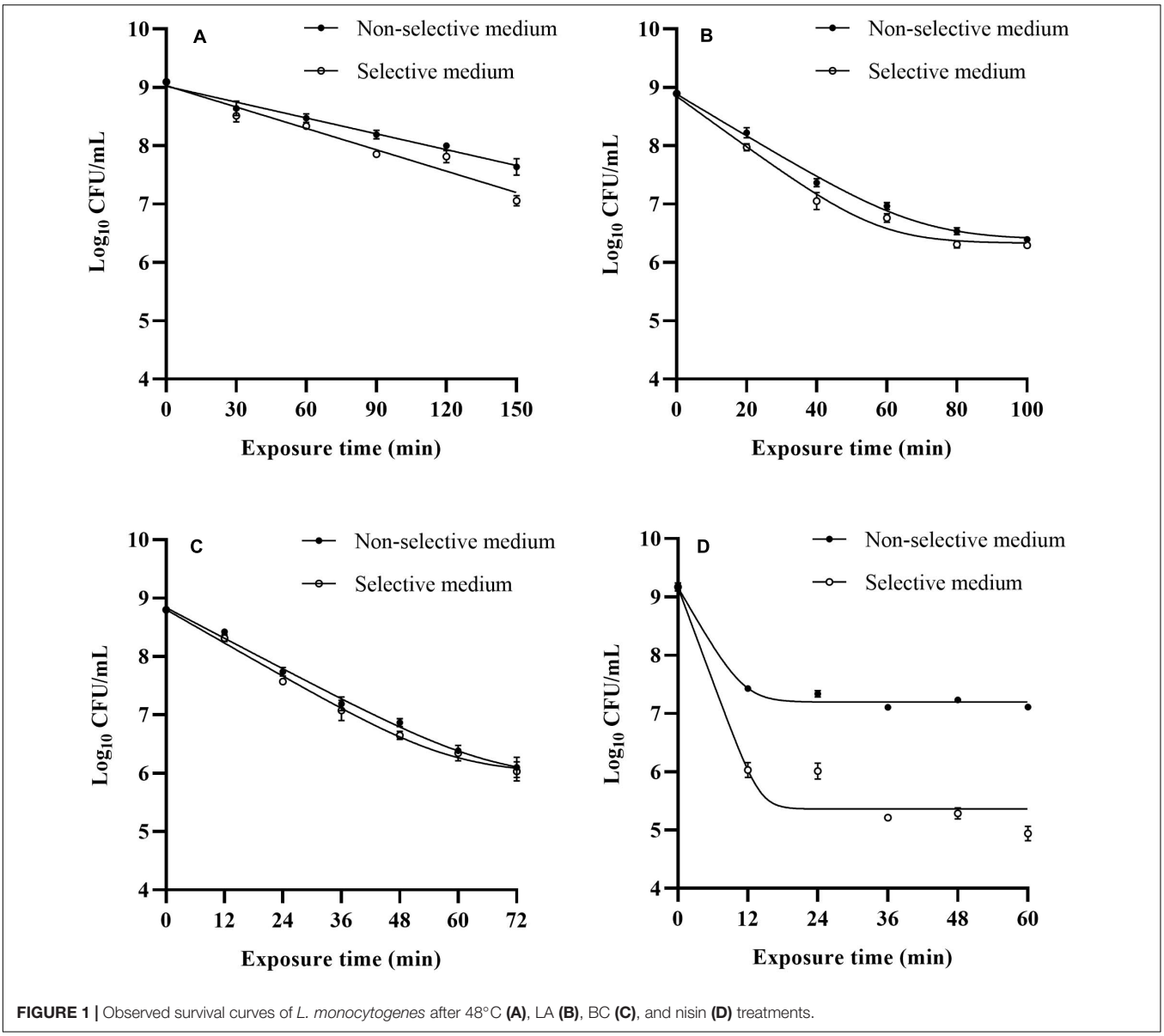

FIGURE 1 | Observed survival curves of *L. monocytogenes* after 48°C **(A)**, LA **(B)**, BC **(C)**, and nisin **(D)** treatments.

presence of nisin-resistant mutants after exposure of nisin-sensitive *L. monocytogenes* cells to relatively high concentrations of nisin. Resistance could be associated with a barrier including changes in fatty acid and phospholipid composition of the cytoplasmic membrane which prevent the nisin from crossing the barrier (Davies et al., 1996). Actually in food matrices, nisin has low solubility and can interact with phospholipids and proteins, which lead the efficacy of nisin to last for only a short time (Chen et al., 2014). From a practical point of view, combination of other bactericidal technologies and nisin could overcome the limitation of nisin. Moreover, the application of nisin at lower concentrations could also reduce the rate of emergence of nisin-resistant cells along the treatment time.

When subjected to the other three stresses (heat, LA, and BC), *L. monocytogenes* had low percentage of injury, especially for BC treatment. For heat treatment, the evaluated proportion of heat injured cells had an increasing trend with increasing treatment time (0–150 min). Kawasaki et al. (2018) have reported similar results for *Salmonella* Enteritidis in PBS and ground beef at 52.5°C for 0–60 min. As is shown in **Figure 2**, the TICC values of heat, LA and BC induced injured *L. monocytogenes* cells were only 35.20, 36.60, and 20.89%, respectively. It has been described before that the LA treatment (1,000 mmol/L, 4 min) resulted in almost 100% sublethal injury of *E. coli* O157:H7 (Smigic et al., 2009). This could be associated with the different bacteria, different concentrations and exposure time of LA used in their studies. The use of LA has been an authorized decontaminating treatment in beef production, which was proposed by the European Food Safety Authority in 2011 (EFSA Panel on Biological Hazards [BIOHAZ], 2011). In addition, BC, as a kind of Quaternary Ammonium Compounds (QACs), has been widely used for disinfecting the surfaces in food production

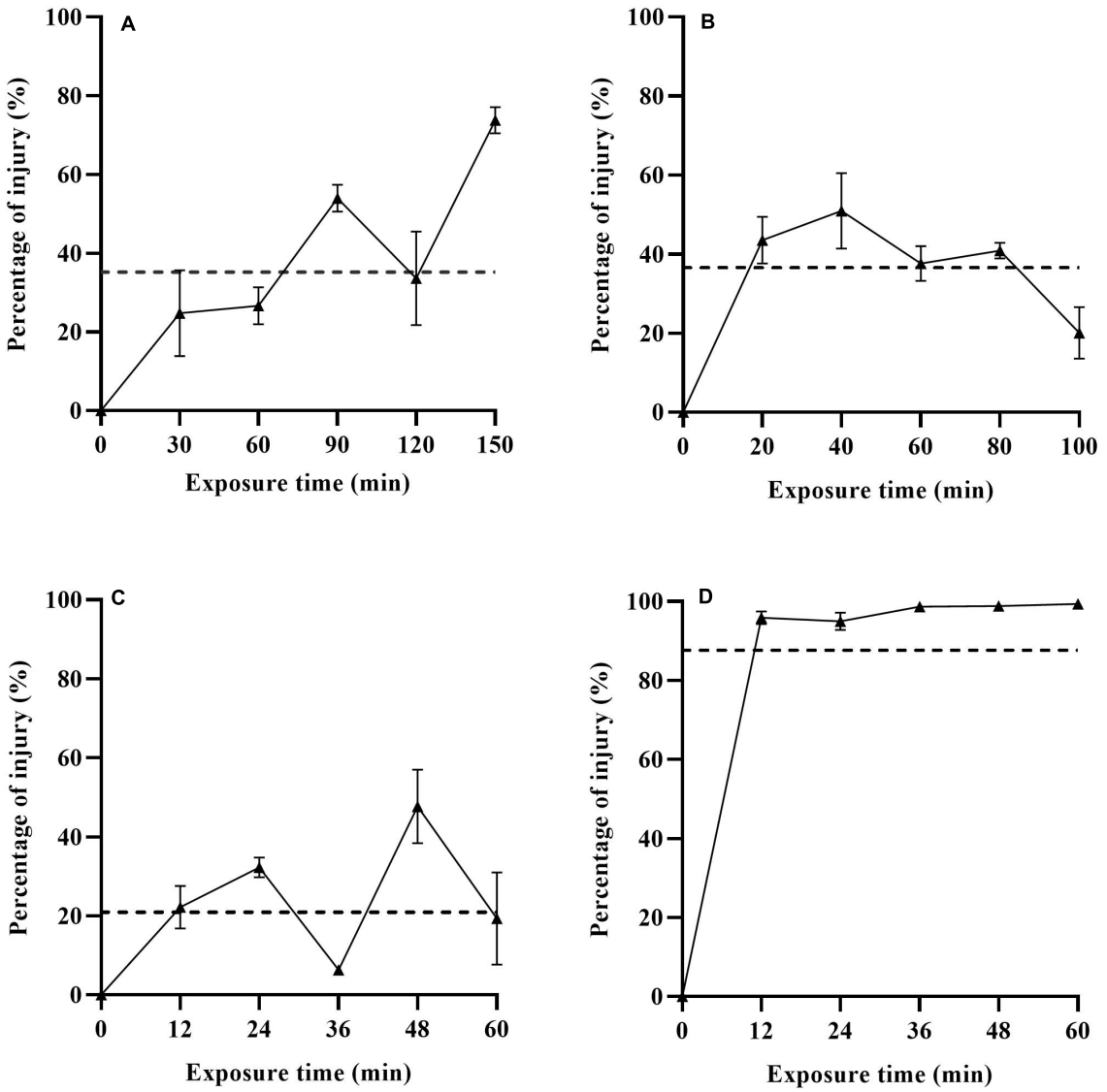

FIGURE 2 | Percentage of sublethal injured *L. monocytogenes* cells and TICC values (dashed line) after exposure to heat **(A)**, LA **(B)**, BC **(C)**, and nisin **(D)** stresses based on differential plating.

environments (To et al., 2002). In food industry, bacteria are inevitably exposed to sublethal concentrations of sanitizing compounds, and this could induce injured cells subpopulation or adaption of initially susceptible bacteria. Therefore, evaluation of the degree of sublethal injury is critical to the safety of final products that have undergone food processing.

Growth Lag Time of *Listeria monocytogenes* After Mild Bactericidal Treatments

The lag time prediction of foodborne pathogens is useful for microbial risk assessment. To accurately predict and then control the growth of *L. monocytogenes* in food products, it is important to understand the effects of various stresses experienced history on the lag time. In the present study, TTD method based on the Baranyi growth model was used to monitor *L. monocytogenes* growth after mild bactericidal treatments. This method is known for its high efficacy to estimate the λ and μ_{max} values without requirement of calibration between cell numbers and absorbance. The effects of heat, LA, BC, and nisin stresses on the lag time of *L. monocytogenes* are shown in **Figure 3**. Compared to non-treated cells, observed significant extension of lag time was a direct consequence of prior sublethal injury ($p < 0.05$). When the final reductions in the number of viable cells were 1.5–2.5 log units, lag time was significantly different among the four treatments with heat treated cells exhibiting the longest lag time, followed by that of nisin, LA and finally BC treated cells. Heat treated cells showed the lag time in the range of 5.86–9.68 h. The longer time the heat treatment was the longer was the lag time of

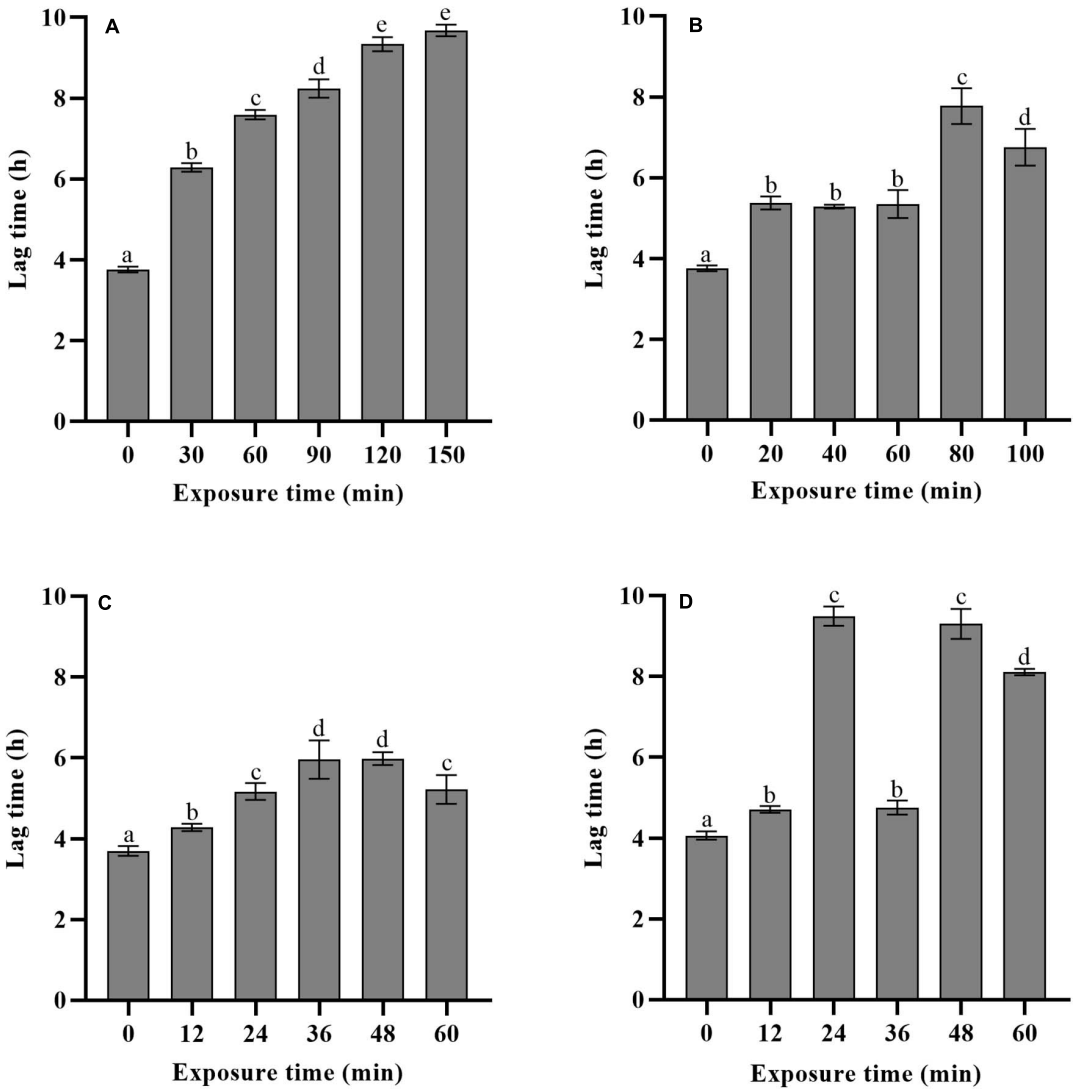

FIGURE 3 | Effects of different exposure time of heat **(A)**, LA **(B)**, BC **(C)**, and nisin **(D)** stresses on the lag time of *L. monocytogenes*.

survivors. In contrast, for LA, BC, and nisin treated cells, longer exposure time did not reveal the longer lag time. Moreover, it did not correspond to the maximum level of injury obtained by differential plating. To compare the effects of sublethal injury percentage on lag time, the correlation coefficients have been evaluated and illustrated in **Figure 4**. The correlation coefficient of heat treatment for lag time was highest (0.850), and value close to 1 indicated almost linear positive correlations ($p < 0.05$). Furthermore, the correlation coefficients of LA, BC and nisin treatments were 0.42, 0.51, and 0.52, respectively. However, the results of statistical analysis revealed no significant correlations between percentage of injury and lag time of LA, BC, and nisin treated cells ($p > 0.05$). As a whole, these results would indicate that only heat induced injury and lag time of *L. monocytogenes* exhibited a significant correlation.

Four mild bactericidal treatments used in the present study are some of the most studied decontamination treatments with heat, organic acids, quaternary ammonium compounds and peptide antimicrobial agents. As expected, compared to non-treated cells, significant extension of lag time revealed the existence of the injured cells in the surviving population for all conditions tested, which was consistent with the results of other studies. For instance, in the study of Xuan et al. (2017), the effect of injury caused by heat (55°C) on the growth parameters indicated that larger λ value was observed in heat injured *L. monocytogenes* as compared to control group. Similar results were also found in the λ value of injured *L. monocytogenes* cells after acid (pH 4.2), osmotic (10% NaCl) and heat (55°C) stresses (Sibanda and Buys, 2017). Up to now, many authors have focused their attention on the lag time of injured foodborne pathogens after exposure to a fixed bactericidal treatment time, however, not much literature is available on how the lag time changes after different treatment time.

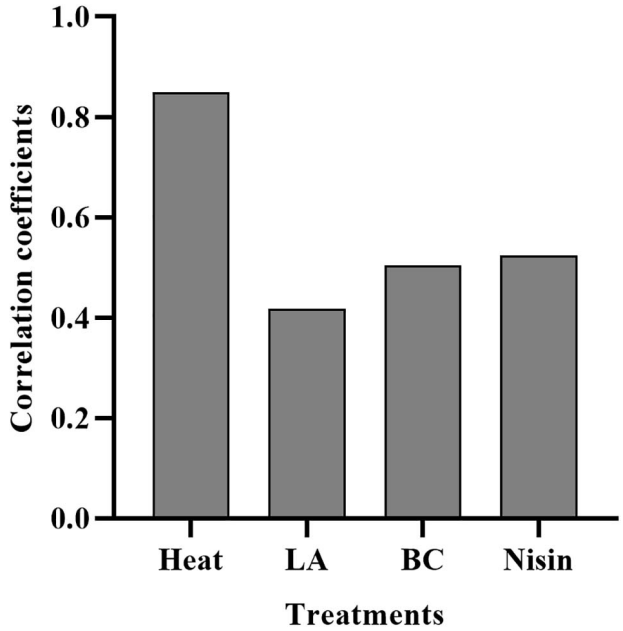

FIGURE 4 | Correlation coefficients of heat, LA, BC, and nisin treatments induced percentage of injury for lag time.

Sublethal injury of foodborne pathogens has huge implications on food safety, and ability to detect injured microorganisms is critical since injured cells can resuscitate and then possess full virulence in a favorable environment. To estimate the amount of sublethally injured cells after bactericidal treatments, conventional selective techniques and other detection methods such as flow cytometry and fluorescent metabolic probes have been used in most studies (Uyttendaele et al., 2008; Zhang et al., 2020). According to these methods, the proportion of injured cells in the population can be calculated, with the outcome largely dictated by incubation conditions (such as temperatures and atmospheres) and detection methods. Sibanda and Buys (2017) assessed the degree of stress induced injury by using differential plating and flow cytometry coupled with membrane integrity indicators. The results indicated that both methods showed significant difference among stress treatments, and membrane integrity was not a sufficient indicator of heat stress injury. For differential plating method, due to the differences in recovery ability of bacteria, the percentages of injury also depend on the types of selective media. For instance, selective media based on NaCl supplement can only detect the sublethal membrane damage of cells, while several other damaged cellular targets such as enzymes, RNA and DNA can't be detected, so this outcome implies a potential for under-estimation of injury (Miller et al., 2006). In addition, calculated percentage of injury based on differential plating method only indicates the portions of amounts of injured cells in the population (it may range from 0 to 100%), which reflect all cells in the population are at the same degree of injury. However, due to individual cell heterogeneity, responses to stress exposures differ among stress sensitive and resistant cell subpopulations, so injured populations are often a mixture of cells in different physiological states (various degree of injury) (Casadesús and Low, 2013), some cells in the population are more damaged than others. Therefore, although differential plating method can evaluate percentage of amounts of injured cells, this method only reflect the level of injury (based on the amounts of injured cells) rather than the degree of injury (based on different physiological states).

It is well known that compared to uninjured cells, injured cells can present the extension of lag time due to the resuscitation behavior, so the lag time length of injured cells might be useful for evaluating the degree of sublethal injury. Kawasaki et al. (2018) described the growth delay time (GDT, the difference of λ value between treated and non-treated cells) of *Salmonella* Enteritidis by real-time PCR monitoring assay, which was then compared with traditional culture method. Results showed that calculated percentage of injured cells was 100% during 24–48 min treatment since bacterial colonies were not detected on selective medium. The differential plating method was only able to evaluate the degree of injury until a stress exposure time of 12 min. However, the GDT significantly increased with the prolonged treatment time (24–48 min), which indicated that GDT could evaluate a wider range of bacterial injury than the traditional culture method. In the present study, as are shown in **Figures 2**, **3**, a similar finding was also observed in case of nisin treatment, the estimated ratio of injured bacterial cells was 98.71% after 36 min exposure, which was not significantly different among different treatment time (36–60 min), thus indicating constant level of sublethal injury along the treatment time by traditional culture method. However, the λ value obtained by TTD method revealed that injury to microbial cells was still in a dynamic change. The present findings revealed the significance of lag time analysis to evaluate a wide range of bacterial injury, which can quantify the degree of injury more accurately than differential plating method.

Growth Parameters Under Different Recovery Temperatures

The λ and μ_{max} values of *L. monocytogenes* after heat, LA, BC, and nisin treatments at recovery temperatures of 20, 25, 30, and 37°C were evaluated (**Table 1**). For all the treatments, significant shorter λ and higher μ_{max} values were observed at higher recovery temperatures. Stress treatments and recovery temperatures had significant effects on λ values ($p < 0.05$), while regardless of stress treatments, μ_{max} only varied significantly at recovery temperature from 20 to 37°C ($p < 0.05$). When compared to non-treated cells, λ values for treated cells were significantly higher ($p < 0.05$) at each recovery temperature, and there were no great change in the μ_{max} values between treated and non-treated cells under isothermal recovery conditions in spite of results of statistical analysis indicating significant difference in some cases.

In bacterial growth kinetics, the λ value of cell population is influenced by the physiological state prior to environmental change, especially sublethal injury induced by various stresses (Augustin et al., 2000). From the results of our study, compared to other recovery temperatures, the observed shorter λ values at

TABLE 1 | Growth parameters of *L. monocytogenes* at 20, 25, 30, and 37°C after heat, LA, BC, and nisin treatments.

Treatment conditions	Recovery temperature (°C)	λ (h)	μ_{max} (h^{-1})
Control	20	5.34 ± 0.20 Aa	0.430 ± 0.009Aa
	25	3.72 ± 0.09 Ba	0.626 ± 0.019Ba
	30	3.41 ± 0.10Ca	0.850 ± 0.011Ca
	37	2.45 ± 0.03Da	0.963 ± 0.003Da
Heat	20	11.04 ± 0.16Ab	0.387 ± 0.007Ab
	25	9.68 ± 0.15Bb	0.641 ± 0.007Ba
	30	7.82 ± 0.21Cb	0.837 ± 0.039Ca
	37	4.39 ± 0.11Db	0.956 ± 0.010Da
LA	20	8.49 ± 0.09Ab	0.433 ± 0.011Aa
	25	5.38 ± 0.16Bb	0.632 ± 0.006Ba
	30	4.63 ± 0.10Cb	0.890 ± 0.007Cb
	37	3.94 ± 0.10Db	0.943 ± 0.022Db
BC	20	7.06 ± 0.47Ab	0.428 ± 0.004Aa
	25	5.98 ± 0.16Bb	0.632 ± 0.025Ba
	30	4.37 ± 0.10Cb	0.869 ± 0.007Ca
	37	3.81 ± 0.26Db	0.927 ± 0.024Db
Nisin	20	12.88 ± 0.38Ab	0.435 ± 0.011Aa
	25	9.49 ± 0.24Bb	0.705 ± 0.005Bb
	30	8.06 ± 0.17Cb	0.873 ± 0.012Ca
	37	5.16 ± 0.19Db	0.971 ± 0.010Da

Values are expressed as means ± standard deviations of three replicate experiments. Means with different uppercase letters in the same column for each treatment condition indicate significant differences ($p < 0.05$). For each recovery temperature, means with different lowercase letters indicate significant differences ($p < 0.05$) between control and each stress treatment.

37°C for each treatment could be attributed to a quicker repair rate. This could be associated with the relevant protein synthesis, particularly enzymes that contribute to synthesis of membrane lipids necessary for repairing damaged cell membranes (García et al., 2006). In fact, for stress induced injured cells, other functional components such as DNA and RNA of bacterial cells can also be damaged (Chilton et al., 2001), which need to be repaired before cells can commence division again. The μ_{max} of treated *L. monocytogenes* cells showed no significant variation among treatments and was expectedly decreased from 37 to 20°C, which reflected temperature dependence of bacterial growth in the exponential phase. Similar results were also observed in Francois et al.'s (2007), which showed that recovery temperature affected both λ and μ_{max} values, whereas stresses influenced λ value only. To evaluate the effects of recovery temperatures on growth parameters of stresses treated *L. monocytogenes* cells, the square root model was tested. As shown in **Figure 5**, the reciprocal of square root of λ and the square root of μ_{max} showed linear relationships with recovery temperature in the control and all treatments, and the small RMSE values (RMSE $\leq$ 0.064, data not shown) indicated that the established secondary models showed good performances. Sant'Ana et al. (2012) used the square root model to investigate the changes in growth parameters (λ and μ_{max}) of *S. enterica* and *L. monocytogenes* in minimally processed lettuce as a function of temperature. The results also showed that models obtained were accurate and suitable for modeling the growth of *S. enterica* and *L. monocytogenes*. In addition, other secondary models such as hyperbolic and polynomial models have also been reported (Swinnen et al., 2004; Aguirre et al., 2013). From a practical point of view, temperature is a major environmental factor affecting bacterial growth parameters in foods. Furthermore, since the *L. monocytogenes* cells are damaged rather than being entirely killed after mild bactericidal treatments, therefore information on the growth kinetics of injured cells should be developed to help obtain reliable outputs when injured cells of foodborne pathogens are taken into account in the risk assessment.

CONCLUSION

This study sought to evaluate the effects of four mild bactericidal treatments (heat, LA, BC, and nisin) on the inactivation, sublethal injury, and subsequent growth of *L. monocytogenes* cells, and the growth parameters at different recovery

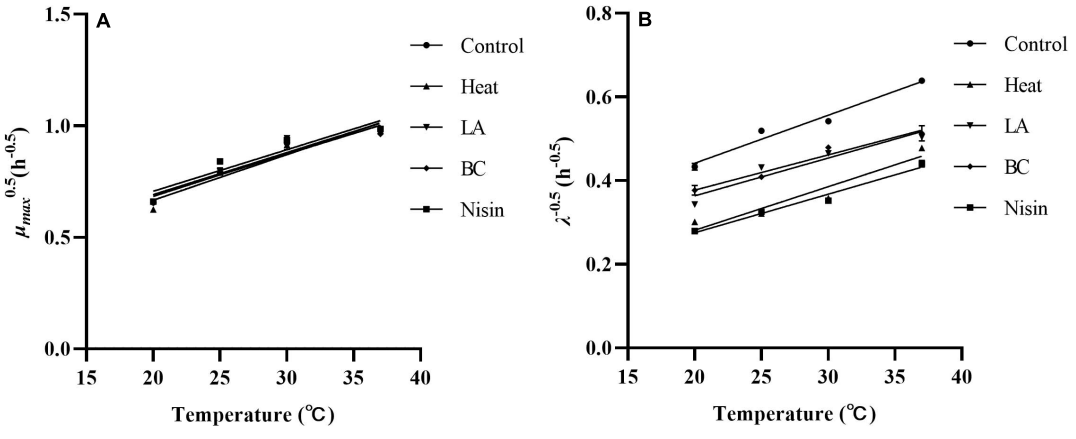

FIGURE 5 | The square root of the μ_{max} **(A)** and reciprocal of square root of the λ **(B)** of *L. monocytogenes* after various treatments as a function of recovery temperatures.

temperatures (20, 25, 30, and 37°C) were further determined. The obtained results demonstrated that the four bactericidal treatments induced sublethally injured cells. Percentage of sublethal injury was shown to be dependent on the type of selected bactericidal treatments. Compared to non-treated cells, mild bactericidal treatments induced significant extension of lag time of *L. monocytogenes*. Based on the correlation analysis of sublethal injury percentage on lag time, it indicated that only heat treatment showed the significant correlation. In addition, information regarding λ value of treated *L. monocytogenes* from this study was useful for determining a wide range of bacterial injury levels. Once repairing the cellular damage, the μ_{max} parameter of treated *L. monocytogenes* cells was not different from non-treated cells regardless of different forms of stresses. As a whole, the results obtained in our study are valuable for helping understand the behavior of *L. monocytogenes* under various mild bactericidal treatments, and the resuscitation behavior of sublethal injured bacterial cells should be taken into account in the predictive modeling and risk assessment studies to reduce the potential food safety risks of stress injured *L. monocytogenes* cells.

DATA AVAILABILITY STATEMENT

The raw data supporting the conclusions of this article will be made available by the authors, without undue reservation.

AUTHOR CONTRIBUTIONS

TF was responsible for the experimental work, article writing, and data analysis. XW and QD conceived of the study and participated in its design and coordination. YW, YX, LS, XQ, YL, and HL participated in the experimental work. All authors reviewed and approved the final manuscript.

FUNDING

This study was funded by the National Natural Science Foundation of China (grant no. 31801455).

REFERENCES

Aguirre, J. S., González, A., Özçelik, N., Rodriguez, M. R., and De Fernando, G. D. G. (2013). Modeling the *Listeria innocua* micropopulation lag phase and its variability. *Int. J. Food Microbiol.* 164, 60–69. doi: 10.1016/j.ijfoodmicro.2013.03.003

Andrade, J. C., António, L. J., Alonso, C. D. S., Barreto, A. S., and Henriques, A. R. (2020). Genetic subtyping, biofilm-forming ability and biocide susceptibility of *Listeria monocytogenes* strains isolated from a ready-to-eat food industry. *Antibiotics (Basel)* 9:416. doi: 10.3390/antibiotics9070416

Arioli, S., Montanari, C., Magnani, M., Tabanelli, G., Patrignani, F., Lanciotti, R., et al. (2019). Modelling of *Listeria monocytogenes* scott a after a mild heat treatment in the presence of thymol and carvacrol: effects on culturability and viability. *J. Food Eng.* 240, 73–82. doi: 10.1016/j.jfoodeng.2018.07.014

Aryani, D. C., Den Besten, H. M. W., Hazeleger, W. C., and Zwietering, M. H. (2015). Quantifying variability on thermal resistance of *Listeria monocytogenes*. *Int. J. Food Microbiol.* 193, 130–138. doi: 10.1016/j.ijfoodmicro.2014.10.021

Augustin, J. C., Carlier, V., and Rozier, J. (2010). Mathematical modelling of the heat resistance of *Listeria monocytogenes*. *J. Appl. Microbiol.* 84, 185–191. doi: 10.1046/j.1365-2672.1998.00317.x

Augustin, J. C., Rosso, L., and Carlier, V. (2000). A model describing the effect of temperature history on lag time for *Listeria monocytogenes*. *Int. J. Food Microbiol.* 57, 169–181. doi: 10.1016/S0168-1605(00)00260-9

Baranyi, J., and Pin, C. (1999). Estimating bacterial growth parameters by means of detection times. *Appl. Environ. Microb.* 65, 732–736.

Bigelow, W. D. (1921). The logarithmic nature of thermal death time curves. *J. Infect. Dis.* 29, 528–536. doi: 10.1093/infdis/29.5.528

Busch, S. V., and Donnelly, C. W. (1992). Development of a repair-enrichment broth for resuscitation of heat-injured *Listeria monocytogenes* and *Listeria innocua*. *Appl. Environ. Microb.* 58, 14–20. doi: 10.1128/AEM.58.1.14-20.1992

Casadesús, J., and Low, D. A. (2013). Programmed heterogeneity: epigenetic mechanisms in bacteria. *J. Biol. Chem.* 288, 13929–13935. doi: 10.1074/jbc.R113.472274

Chen, H. Q., Davidson, P. M., and Zhong, Q. X. (2014). Antimicrobial properties of nisin after glycation with lactose, maltodextrin and dextran and the thyme oil emulsions prepared thereof. *Int. J. Food Microbiol.* 191, 75–81. doi: 10.1016/j.ijfoodmicro.2014.09.005

Chilton, P., Isaacs, N. S., Manas, P., and Mackey, B. M. (2001). Biosynthetic requirements for the repair of membrane damage in pressure-treated *Escherichia coli*. *Int. J. Food Microbiol.* 71, 101–104. doi: 10.1016/S0168-1605(01)00566-9

D'Arrigo, M., De Fernando, G. D. G., De Diego, R. V., Ordonez, J. A., George, S. M., and Pin, C. (2006). Indirect measurement of the lag time distribution of single cells of *Listeria innocua* in food. *Appl. Environ. Microb.* 72, 2533–2538. doi: 10.1128/AEM.72.4.2533-2538.2006

Davies, E. A., Falahee, M. B., and Adams, M. R. (1996). Involvement of the cell envelope of *Listeria monocytogenes* in the acquisition of nisin resistance. *J. Appl. Microbiol.* 81, 139–146. doi: 10.1111/j.1365-2672.1996.tb04491.x

EFSA Panel on Biological Hazards [BIOHAZ] (2011). Scientific Opinion on the evaluation of the safety and efficacy of lactic acid for the removal of microbial surface contamination of beef carcasses, cuts and trimmings. *EFSA J.* 9:2317. doi: 10.2903/j.efsa.2011.2317

European Centre for Disease Prevention and Control [ECDC] (2019). The European Union one health 2018 zoonoses report. *EFSA J.* 17:5926. doi: 10.2903/j.efsa.2019.5926

Ferrentino, G., Tamburini, S., Bath, K., Foladori, P., Spilimbergo, S., and Jousson, O. (2015). Application of culture-independent methods for monitoring *Listeria monocytogenes* inactivation on food products. *Process Biochem.* 50, 188–193. doi: 10.1016/j.procbio.2014.12.014

Francois, K., Valero, A., Geeraerd, A. H., Van Impe, J. F., Debevere, J., Garcia-Gimeno, R. M., et al. (2007). Effect of preincubation temperature and pH on the individual cell lag phase of *Listeria monocytogenes*, cultured at refrigeration temperatures. *Food Microbiol.* 24, 32–43. doi: 10.1016/j.fm.2006.03.011

García, D., Mañas, P., Gómez, N., Raso, J., and Pagan, R. (2006). Biosynthetic requirements for the repair of sublethal membrane damage in *Escherichia coli* cells after pulsed electric fields. *J. Appl. Microbiol.* 100, 428–435. doi: 10.1111/j.1365-2672.2005.02795.x

Geeraerd, A. H., Herremans, C. H., and Van Impe, J. F. (2000). Structural model requirements to describe microbial inactivation during a mild heat treatment. *Int. J. Food Microbiol.* 59, 185–209. doi: 10.1016/S0168-1605(00)00362-7

Geeraerd, A. H., Valdramidis, V. P., and Van Impe, J. F. (2005). GInaFiT, a freeware tool to assess non-log-linear microbial survivor curves. *Int. J. Food Microbiol.* 102, 95–105. doi: 10.1016/j.ijfoodmicro.2006.04.002

Harris, L. J., Fleming, H. P., and Klaenhammer, T. R. (1991). Sensitivity and resistance of *Listeria monocytogenes* ATCC 19115, Scott A, and UAL500 to Nisin. *J. Food Protect.* 54, 836–840. doi: 10.4315/0362-028X-54.11.836

Haskaraca, G., Juneja, V. K., Mukhopadhyay, S., and Kolsarici, N. (2019). The effects of grapefruit seed extract on the thermal inactivation of *Listeria monocytogenes* in sous-vide processed Döner Kebabs. *Food Control* 95, 71–76. doi: 10.1016/j.foodcont.2018.07.006

Humayoun, S. B., Hiott, L. M., Gupta, S. K., Barrett, J. B., Woodley, T. A., Johnstone, J. J., et al. (2018). An assay for determining the susceptibility

of *Salmonella* isolates to commercial and household biocides. *PLoS One* 13:e0209072. doi: 10.1371/journal.pone.0209072

Kang, J. H., Park, J. B., and Song, K. B. (2019). Inhibitory activities of quaternary ammonium surfactants against *Escherichia coli* O157:H7, *Salmonella* Typhimurium, and *Listeria monocytogenes* inoculated on spinach leaves. *LWT Food Sci. Technol.* 102, 284–290. doi: 10.1016/j.lwt.2018.12.046

Kawasaki, S., Hosotani, Y., Noviyanti, F., Koseki, S., and Inatsu, Y. (2018). Growth delay analysis of heat-injured *Salmonella* Enteritidis in ground beef by real-time PCR. *LWT Food Sci. Technol.* 90, 499–504. doi: 10.1016/j.lwt.2017.12.066

Lou, Y. Q., and Yousef, A. E. (1997). Adaptation to sublethal environmental stress protects *Listeria monocytogenes* against lethal preservation factors. *Appl. Environ. Microb.* 63, 1252–1255. doi: 10.1128/AEM.63.4.1252-1255.1997

Marcén, M., Cebrian, G., Ruiz-Artiga, V., Condon, S., and Manas, P. (2019). Cellular events involved in *E. coli* cells inactivation by several agents for food preservation: a comparative study. *Food Microbiol.* 84, 1–9. doi: 10.1016/j.fm.2019.103246

Martins, J. T., Cerqueira, M. A., Souza, B. W. S., Avides, M. D., and Vicente, A. A. (2010). Shelf life extension of ricotta cheese using coatings of galactomannans from nonconventional sources incorporating nisin against *Listeria monocytogenes*. *J. Agric. Food Chem.* 58, 1884–1891. doi: 10.1021/jf902774z

Miller, F. A., Brandao, T. R. S., Teixeira, P., and Silva, C. L. M. (2006). Recovery of heat-injured *Listeria innocua*. *Int. J. Food Microbiol.* 112, 261–265. doi: 10.1016/j.ijfoodmicro.2006.04.013

Ratkowsky, D. A., Olley, J., McMeekin, T. A., and Ball, A. (1982). Relationship between temperature and growth rate of bacterial cultures. *J. Bacteriol.* 149, 1–5. doi: 10.1128/JB.149.1.1-5.1982

Ray, B., Hawkins, S. M., and Hackney, C. R. (1978). Method for the detection of injured *Vibrio parahaemolyticus* in seafoods. *Appl. Environ. Microb.* 35, 1121–1127.

Sant'Ana, A. S., Franco, B. D. G. M., and Schaffner, D. W. (2012). Modeling the growth rate and lag time of different strains of *Salmonella enterica* and *Listeria monocytogenes* in ready-to-eat lettuce. *Food Microbiol.* 30, 267–273. doi: 10.1016/j.fm.2012.11.015

Shi, H., Chen, Z. Z., Chen, D., and Kan, J. Q. (2017). Sublethal injury and recovery of *Escherichia coli* O157:H7 and K-12 after exposure to lactic acid. *Food Control* 82, 190–195. doi: 10.1016/j.foodcont.2017.06.017

Shi, H., Trinh, Q., Xu, W. T., Luo, Y. B., Tian, W. Y., and Huang, K. L. (2013). The transcriptional response of virulence genes in *Listeria monocytogenes* during inactivation by nisin. *Food Control* 31, 519–524. doi: 10.1016/j.foodcont.2012.11.008

Sibanda, T., and Buys, E. M. (2017). Resuscitation and growth kinetics of sublethally injured *Listeria monocytogenes* strains following fluorescence activated cell sorting (FACS). *Food Res. Int.* 100, 150–158. doi: 10.1016/j.foodres.2017.08.020

Smigic, N., Rajkovic, A., Antal, E., Medic, H., Lipnicka, B., Uyttendaele, M., et al. (2009). Treatment of *Escherichia coli* O157:H7 with lactic acid, neutralized electrolyzed oxidizing water and chlorine dioxide followed by growth under sub-optimal conditions of temperature, pH and modified atmosphere. *Food Microbiol.* 26, 629–637. doi: 10.1016/j.fm.2009.04.010

Swaminathan, B., and Gerner-Smidt, P. (2007). The epidemiology of human listeriosis. *Microbes Infect.* 9, 1236–1243. doi: 10.1016/j.micinf.2007.05.011

Swinnen, I. A. M., Bernaerts, K., Dens, E. J. J., Geeraerd, A. H., and Van Impe, J. F. (2004). Predictive modelling of the microbial lag phase: a review. *Int. J. Food Microbiol.* 94, 137–159. doi: 10.1016/j.ijfoodmicro.2004.01.006

To, M. S., Favrin, S., Romanova, N., and Griffiths, M. W. (2002). Postadaptational resistance to benzalkonium chloride and subsequent physicochemical modifications of *Listeria monocytogenes*. *Appl. Environ. Microb.* 68, 5258–5264. doi: 10.1128/AEM.68.11.5258-5264.2002

Uyttendaele, M., Rajkovic, A., Houteghem, N. V., Boon, N., Thas, O., Debevere, J., et al. (2008). Multi-method approach indicates no presence of sub-lethally injured *Listeria monocytogenes* cells after mild heat treatment. *Int. J. Food Microbiol.* 123, 262–268. doi: 10.1016/j.ijfoodmicro.2008.02.015

Wang, X., Devlieghere, F., Geeraerd, A., and Uyttendaele, M. (2017). Thermal inactivation and sublethal injury kinetics of *Salmonella enterica* and *Listeria monocytogenes* in broth versus agar surface. *Int. J. Food Microbiol.* 243, 70–77. doi: 10.1016/j.ijfoodmicro.2016.12.008

Wu, S., Wu, Q. P., Zhang, J. M., Chen, M. T., and Guo, W. P. (2016). Analysis of multilocus sequence typing and virulence characterization of *Listeria monocytogenes* isolates from Chinese retail ready-to-eat food. *Front. Microbiol.* 7:168. doi: 10.3389/fmicb.2016.00168

Xuan, X. T., Ding, T., Li, J., Ahn, J. H., Zhao, Y., Chen, S. G., et al. (2017). Estimation of growth parameters of *Listeria monocytogenes* after sublethal heat and slightly acidic electrolyzed water (SAEW) treatment. *Food Control* 71, 17–25. doi: 10.1016/j.foodcont.2016.06.018

Yue, S. Y., Liu, Y. T., Wang, X., Xu, D. P., Qiu, J. X., Liu, Q., et al. (2019). Modeling the effects of the preculture temperature on the lag phase of *Listeria monocytogenes* at 25°C. *J. Food Protect.* 82, 2100–2107. doi: 10.4315/0362-028X.JFP-19-117

Yuste, J., Capellas, M., Fung, D. Y. C., and Mor-Mur, M. (2004). Inactivation and sublethal injury of foodborne pathogens by high pressure processing: evaluation with conventional media and thin agar layer method. *Food Res. Int.* 37, 861–866. doi: 10.1016/j.foodres.2004.05.002

Zhang, H. J., Zhao, Y. Y., Gong, C. T., and Jiao, S. S. (2020). Effect of radio frequency heating stress on sublethal injury of *Salmonella* Typhimurium in red pepper powder. *LWT Food Sci. Technol.* 117:108700. doi: 10.1016/j.lwt.2019.108700

Conflict of Interest: The authors declare that the research was conducted in the absence of any commercial or financial relationships that could be construed as a potential conflict of interest.

frontiers in Microbiology

ORIGINAL RESEARCH
published: 24 June 2021
doi: 10.3389/fmicb.2021.674364

Bayesian Generalized Linear Model for Simulating Bacterial Inactivation/Growth Considering Variability and Uncertainty

Satoko Hiura, Hiroki Abe, Kento Koyama and Shige Koseki*

Graduate School of Agricultural Science, Hokkaido University, Sapporo, Japan

Conventional regression analysis using the least-squares method has been applied to describe bacterial behavior logarithmically. However, only the normal distribution is used as the error distribution in the least-squares method, and the variability and uncertainty related to bacterial behavior are not considered. In this paper, we propose Bayesian statistical modeling based on a generalized linear model (GLM) that considers variability and uncertainty while fitting the model to colony count data. We investigated the inactivation kinetic data of *Bacillus simplex* with an initial cell count of 10^5 and the growth kinetic data of *Listeria monocytogenes* with an initial cell count of 10^4. The residual of the GLM was described using a Poisson distribution for the initial cell number and inactivation process and using a negative binomial distribution for the cell number variation during growth. The model parameters could be obtained considering the uncertainty by Bayesian inference. The Bayesian GLM successfully described the results of over 50 replications of bacterial inactivation with average of initial cell numbers of 10^1, 10^2, and 10^3 and growth with average of initial cell numbers of 10^{-1}, 10^0, and 10^1. The accuracy of the developed model revealed that more than 90% of the observed cell numbers except for growth with initial cell numbers of 10^1 were within the 95% prediction interval. In addition, parameter uncertainty could be expressed as an arbitrary probability distribution. The analysis procedures can be consistently applied to the simulation process through fitting. The Bayesian inference method based on the GLM clearly explains the variability and uncertainty in bacterial population behavior, which can serve as useful information for risk assessment related to food borne pathogens.

Keywords: parameter estimation, Bayesian inference, generalized linear model, poisson distribution, negative binomial distribution, model residual

OPEN ACCESS

Edited by:
Bruce Michael Applegate, Purdue University, United States

Reviewed by:
Alexandra Lianou, University of Patras, Greece
Antonio Valero, University of Córdoba, Spain

****Correspondence:***
Kento Koyama
kento.koyama@frontier.hokudai.ac.jp

Specialty section:
This article was submitted to Food Microbiology, a section of the journal Frontiers in Microbiology

Received: *01 March 2021*
Accepted: *17 May 2021*
Published: *24 June 2021*

Citation:
Hiura S, Abe H, Koyama K and Koseki S (2021) Bayesian Generalized Linear Model for Simulating Bacterial Inactivation/Growth Considering Variability and Uncertainty. Front. Microbiol. 12:674364. doi: 10.3389/fmicb.2021.674364

INTRODUCTION

Predictive microbiology models explain bacterial number variations over time and how growth/inactivation rates are affected by environmental conditions (Lammerding and Fazil, 2000). In the development process of mathematical or statistical models, experimental data are collected, a model is selected, and curve fitting is applied to the data for parameter estimation. Least-squares estimation has been the most widely used curve fitting procedure (Gil et al., 2017). The least-squares

methods in frequentist statistics assume that the experimental error follows a normal distribution, and studies conducted thus far have described the experimental error using a normal distribution (van Boekel, 2020). In the case of bacterial growth or inactivation kinetics, the model residual with respect the logarithmic number of cells has been assumed to follow a normal distribution (Ratkowsky et al., 1996), though the reason for this assumption is unclear given the variability and uncertainty in bacterial population behavior. The current model residual based on the normal distribution cannot clarify the origin of the error, which means that we need to identify what type of error is included, how the error can be separated, and how large the error is.

A predictive model has been employed for exposure assessment in risk assessment to quantify the changes in the number of bacteria along the farm-to-fork chain. Exposure assessment is necessary to qualitatively and/or quantitatively assess the likelihood of ingestion of pathogens (FAO/WHO, 2008). A quantitative exposure assessment requires the development of a model that mathematically describes all the relationships between the factors influencing the exposure (FAO/WHO, 2008). Since point estimation is performed using the mean values in the kinetic model (FAO/WHO, 2008), it is difficult to appropriately estimate the changes in bacterial behavior characterized by individual cell variation. To describe the variation in bacterial behavior considering the variability and uncertainty, the need to distinguish between variability and uncertainty has been pointed out (Nauta, 2000).

The generalized linear model (GLM) is an approach incorporating various probability distributions into a fitting procedure to describe variability. The GLM, introduced by Nelder and Wedderburn (1972), has been used to describe variabilities, including discrete count data. Because a normal distribution is continuous and can take negative values, it is inappropriate for count data, which are discrete and can only take zero and positive integers, such as bacterial cell numbers. A discrete probability distribution integrated into the GLM would be suitable for expressing biological count data instead of a continuous distribution such as a normal distribution. The Poisson distribution is often used to describe death events at certain time intervals in survival analyses (Dickman et al., 2004; Dickman and Coviello, 2015). A negative binomial distribution is used for over dispersal count data in the field of ecology (Ver Hoef and Boveng, 2007). The GLM can be handled by both frequentist statistics and Bayesian inference. A GLM with Bayesian inference is often used to avoid over fitting (Dey et al., 2000). A Bayesian GLM can flexibly integrate various probability distributions as model residuals and parameter uncertainty.

Another problem in the current frequentist statistical fitting procedure is the point estimation of a model parameter. The model parameters in frequentist methods, such as the least-squares method and maximum likelihood, are often estimated by fitting the model to the data. The parameters are determined at one point in the estimation. However, because the experimental data are uncertain in a real situation, the obtained parameters are also uncertain (Garre et al., 2020; van Boekel, 2020). Therefore, the estimated parameters exhibit unexplained fluctuations (van Boekel, 2020), and parameter estimation requires considering parameter errors (Dolan and Mishra, 2013). Furthermore, many types of uncertainties exist, such as model uncertainty and parameter uncertainty (FAO/WHO, 2008). In previous studies, model parameters were estimated using Bayesian inference (Jaloustre et al., 2011; Koyama et al., 2019; van Boekel, 2020). Bayesian inference has been used as a means to quantitatively estimate parameter uncertainty (Pouillot et al., 2003; Crépet et al., 2009; Koyama et al., 2019).

In the present study, a Bayesian GLM was introduced to fit observed bacterial inactivation data and growth data, and simulate bacterial behavior considering variability and uncertainty. Two types of bacteria were investigated to show applicability of the model to spoilage and pathogenic bacteria. For the inactivation data, we used datasets published in literature pertaining to the thermal inactivation of *Bacillus simplex*. As the growth data, the data obtained by investigating the growth of *Listeria monocytogenes* at 25°C were used. The data used contained three observed colony count replications for developing kinetic models, and over 50 observed colony count replications for validating bacterial behavior with small initial cell numbers. Individual cell heterogeneity and initial cell numbers were considered as variability and described using several probability distributions integrated into the model residual. The parameter uncertainty was obtained by Bayesian inference. From fitting to prediction, we consistently consider the variability in bacterial behavior. The modeling procedure considering the variability and uncertainty can contribute to improving risk-based processing design and exposure assessment.

MATERIALS AND METHODS

Dataset

Inactivation Dataset

The data reported by Abe et al. (2019) were used in this study. In their study, *Bacillus simplex,* which is a psychrophilic spore-forming bacterium, originating from pasteurized milk acquired from Hokkaido Research Organization (Japan). The strain was cultured in Nutrient Agar (Eiken, Tokyo, Japan) with some components and then in Nutrient Broth (Merck) with some components at 30°C for 24 h, respectively. *Bacillus simplex* spores were obtained by culturing in Spo8-agar (Faille et al., 2007; Helmond et al., 2017). The *Bacillus simplex* in the suspension with 10^5 cells was thermally inactivated at 94°C for kinetic evaluation. Viable counts were estimated by plating onto nutrient agar (Eiken, Tokyo, Japan) at 30°C after 2 days. Three independent trials were conducted. Furthermore, 60 replications of bacterial inactivation with an initial cell number of 10^n ($n = 1–3$) were used to observe the variation in bacterial inactivation.

Growth Dataset

Bacterial Strain and Inoculum Preparation

Listeria monocytogenes (ATCC 19118) was used in the present study. The bacteria was maintained at –80°C in tryptic soy broth (TSB; Merck, Darmstadt, Germany) containing 10 vol/vol% glycerol. The strain was activated by incubating the cells at 37°C

for 24 h on tryptic soy agar (TSA; Merck) and twice at 37°C for 24 h in 5 mL of TSB to obtain a homogeneous and stable cell population. The cells were then collected by centrifugation (3,000 × *g* for 10 min). The resulting pellet was washed twice with TSB and re-suspended in 5 mL of TSB before the experiments.

Kinetic Evaluation of Bacterial Growth

Bacterial growth was investigated by colony counting methods. The inoculum [1×10^5 colony-forming units (CFU)/mL] was prepared by series 10-fold dilutions in TSB. Aliquots (100 μL) were dispensed into the wells of 8-well polymerase chain reaction (PCR) microplates for cell concentration of 10^4 CFU/100 μL per well. The high initial cell concentration was investigated for kinetic evaluation to avoid interference of variability derived from low cell concentrations. The microplates were incubated at 25°C. Samples were withdrawn at regular intervals to obtain kinetic data of microbial growth. At each sampling time, 8-well PCR microplates were incubated at 5°C to prevent further bacterial growth. The entire sample (100 μL) from each well was diluted by serial 10-fold dilution in TSB. The bacterial cell number was determined by plating 100 μL of the diluted suspensions on TSA plates, which were then incubated at 37°C for 24 h. The experiment was repeated independently three times.

Stochastic Evaluation of Bacterial Growth

Bacterial growth with a small number of initial cells ($n = 50$) were examined to evaluate the variation in cell growth. Suspensions with average of 10^n ($n = -1-1$) CFU/100 μL were prepared by 10-fold dilution in TSB. Aliquots (100 μL) from the same inoculum culture were dispensed into wells of an 8-well PCR microplate by using an 8-channel micropipette. Cell growth ($n = 50$ replicates) was independently assessed in 50 wells of multiple 8-well PCR microplates. The microplates were incubated at 25°C. Samples were withdrawn at regular intervals to obtain probabilistic data of microbial growth. At each sampling time, the 8-well PCR microplates were incubated at 5°C to prevent further bacterial growth. The bacterial cell numbers were determined by direct plating of 100 μL of the culture onto TSA plates without dilution (average of initial cell numbers of 0.1: examined after 0–10 h; 1: 0–6 h; and 10: 0–4 h) or after diluting (1 cells: 8 and 10 h; 10 cells: 6, 8, and 10 h). The plates were incubated at 37°C for 24 h. Fifty independent replicates were analyzed.

Modeling

We introduced a Bayesian GLM instead of the currently used least-squares method. The Bayesian GLM can flexibly integrate various probability distributions as model residuals and parameter uncertainties, unlike the least-squares method. **Figure 1** shows a conceptual diagram of the fitting procedure. Because the number of bacteria is count data, we used the Poisson distribution and negative binomial distribution as model residuals instead of the normal distribution.

Bayesian GLM for Inactivation Dataset

Figure 2A shows the conceptual diagram of the inactivation model. In the least-squares method used in frequentist statistics, the error in the logarithmic number of cells is assumed to follow a normal distribution (**Figure 2A**). In contrast, the error is assumed to follow a Poisson distribution in the inactivation process when using the GLM (**Figure 2B**).

First, we show a kinetic model based on the least-squares method. The data with 10^5 inactivated cells were fitted to the Weibull model. The Weibull model was fitted to the inactivation data, and the Weibull model is described in Equation (1):

$$log_{10}\frac{N_t}{N_0} = -\left(\frac{t}{\delta}\right)^p \tag{1}$$

where t, N_t, N_0, p, and δ denote the inactivation time, bacterial population at time t, initial number of cells, shape parameter, and scale parameter, respectively. Curve regression to the Weibull model was conducted using a non-linear least-squares method.

Next, we construct the GLM. Equation (1) can be transformed into Equation (2):

$$N_t = N_0 \times 10^{-(t/\delta)^p} \tag{2}$$

Here, the bacterial cell number experimentally obtained via a dilution series was assumed to follow a Poisson distribution (Koyama et al., 2016). Therefore, it can be assumed that the initial cell data follow a Poisson distribution. In addition, we assumed that the inactivation rate of each cell was equal and that a cell inactivation event was independent of another event. The number of surviving cells can also follow a Poisson distribution under the assumption that the initial cells (which follow the Poisson distribution) die at random (Aguirre et al., 2009). Therefore, it can be assumed that the observed values of the number of surviving bacteria obtained at each time are taken from a Poisson distribution with an average of $N_0 \times 10^{-(t/\delta)^p}$, and the bacterial population at time t (N_t) can be described as in Equation (3):

$$N_t \sim Poisson\left(N_0 \times 10^{-(t/\delta)^p}\right) \tag{3}$$

In this study, the parameters (δ and p) and the initial bacterial count (N_0) were estimated from the heating time (t) and the number of surviving bacteria at each time (N_t). The random variable in the number of cells is Poisson-distributed, which is equivalent to the model residual of the dependent variable in the GLM. The Bayesian GLM is constructed using Equation (3).

Bayesian GLM for the Growth Dataset

Figure 3 shows a conceptual diagram of the growth model. In the least-squares method used in frequentist statistics, the error in the logarithmic number of cells is assumed to follow a normal distribution (**Figure 3A**). In contrast, the error in the initial cell number is assumed to follow a Poisson distribution, and the error in the number of divisions during the exponential phase is assumed to follow a negative binomial distribution (**Figure 3B**).

First, we show a kinetic model based on the least-squares method. The growth model used in this study was based on a three-phase linear model (Buchanan et al., 1997; McKellar and Lu, 2003) without a stationary phase. In this study, to simplify the calculation, the stationary phase was not included in the data

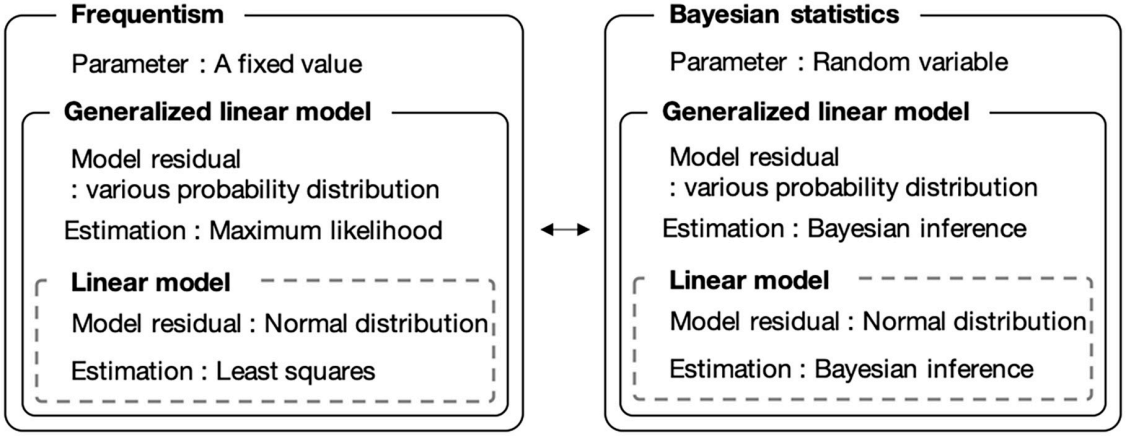

FIGURE 1 | Comparison of frequentist and Bayesian statistical modeling. Bayesian statistics allows the use of parameters as random variables. The generalized linear model allows to use model residuals with various probability distributions.

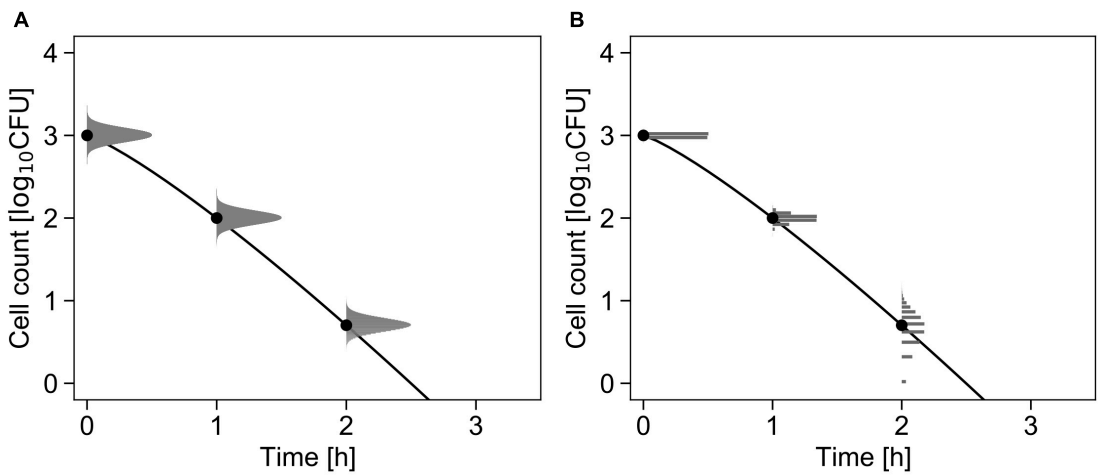

FIGURE 2 | Comparison of the differences in the probability distributions assumed to represent bacterial variation during the inactivation process. Each graph shows changes in the probability density of the survival cell number with $\delta = 1$, $p = 1.2$, and $N_0 = 10^3$ cells (Equations 1 and 3). The solid line and points represent the inactivation kinetic and mean value of the probability distribution, respectively. The logarithmic survival cell number is assumed to follow a normal distribution **(A)**, whereas the survival cell number is assumed to follow a Poisson distribution **(B)**.

used for the analysis. The kinetic model is described in Equation (4):

$$\log_{10} N_t = \log_{10}\left(N_0 \times exp\left(\mu \times (t - \lambda)\right)\right)(t > \lambda) \quad (4)$$

$$\log_{10} N_t = \log_{10} N_0 \ (t \leq \lambda)$$

where t, N_0, N_t, μ, and λ denote the incubation time, initial cell number, number of bacteria, maximum growth rate, and lag time, respectively. Curve regression to the growth data was conducted using the least-squares method, and μ and λ were estimated.

Next, we construct the GLM. Here, as with the inactivation model, since the initial cells were experimentally obtained using a dilution series, the initial cells were assumed to follow a Poisson distribution. In addition, we assumed that the exponential growth rate of the individual cells is equal and that cell division is independent of another event (Coleman and Marks, 1999). Under these assumptions, a pure birth process is used to calculate the stochastic growth of bacteria (Renshaw, 1993; Coleman and Marks, 1999). In the pure birth process, the number of divisions can be described as a negative binomial distribution, as in Equation (5):

$$D_t \sim Negbin\left(N_0,\ exp\left(-\mu \times (t - \lambda)\right)\right)(t > \lambda) \quad (5)$$

$$N_0 \sim Poisson\,(N_0)$$

$$D_t = 0 \ (t \leq \lambda)$$

$$N_t = N_0 + D_t$$

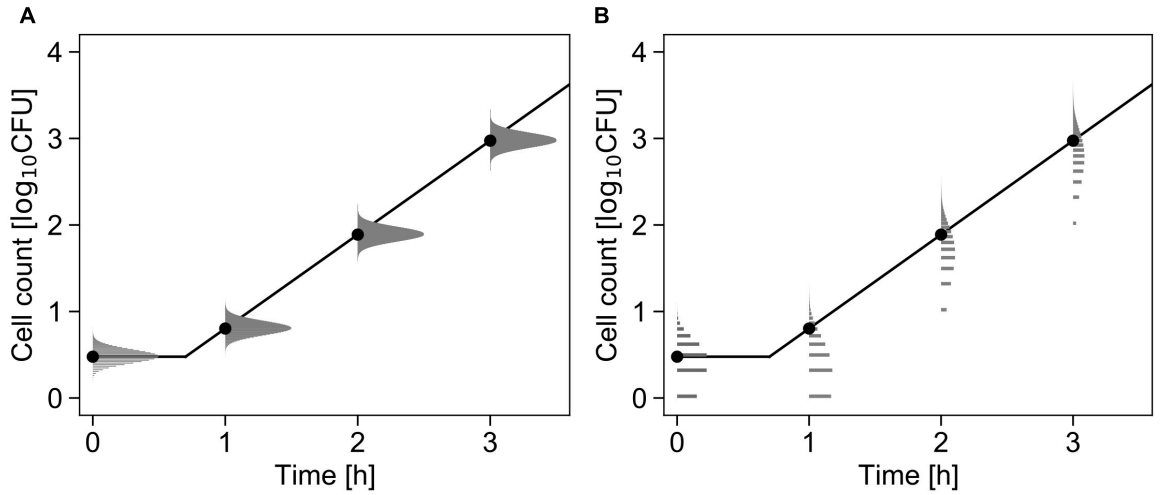

FIGURE 3 | Comparison of the differences in the probability distributions assumed to represent bacterial variation during the growth process. Each graph shows changes in the probability density of the cell number with $\mu = 2.5$, $\lambda = 0.7$, and $N_0 = 3$ cells (Equations 4 and 5). The solid line and points represent the growth kinetics and mean value of the probability distribution, respectively. The logarithmic cell number is assumed to follow a normal distribution at all times **(A)**. The initial cell number is assumed to follow a Poisson distribution, and the growth number of divisions is assumed to follow a negative binomial distribution **(B)**.

where t, D_t, N_0, N_t, μ, and λ denote the incubation time, a total number of cell divisions in bacterial population up to time t, number of initial cells, number of bacteria, maximum growth rate, and lag time, respectively. In this study, Bayesian inference was conducted using the growth dataset in both the lag and exponential phases. The parameters (μ and λ) were estimated from the incubation time (t) and the number of bacteria at each time point (N_t). The Bayesian GLM is constructed using Equation (5).

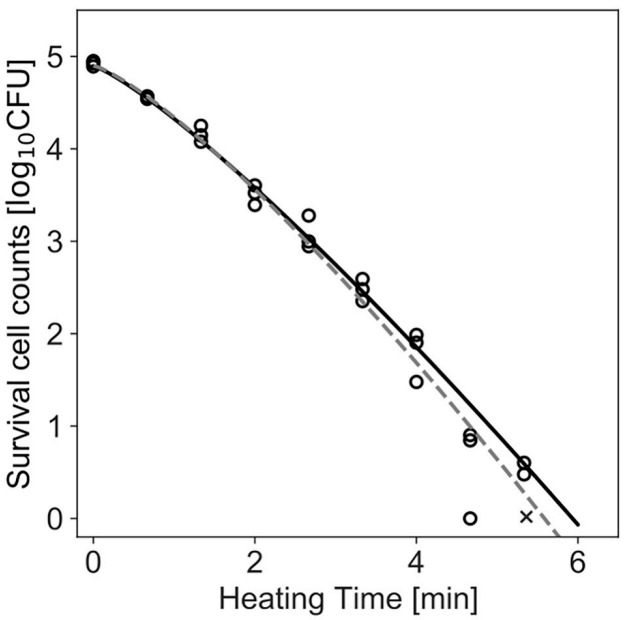

FIGURE 4 | Survival kinetics of *Bacillus simplex* with a population of 10^5 cells, heated at 94°C. Each time has three replications. No colonies are detected at the time indicated by a cross (×). The dashed line indicates the fitted Weibull model by the least-squares method. The solid line indicates the median of the fitting by Bayesian inference.

Computation

In this study, the parameters were estimated using Bayesian inference. In Bayesian inference, the obtained data were considered to have been generated from a probability distribution, and all the parameters were estimated as a probability distribution. Bayesian inference can combine priors, even if no prior information is available. In this study, we used a uniform distribution as a non-informative prior distribution because there was no prior information. For each model, inferences were made on 10^4 iterations with four independent chains. The first 5,000 iterations of 10^4 iterations were removed as a warm up period and the rest 5,000 iterations were used as posterior parameters estimation. Convergence was verified by both visually checking the Markov Chain Monte Carlo chain traces and examining the Gelman and Rubin diagnostic called R-hat. The R-hat value should be close to 1.0. Computations were performed using PyStan and Python (version 3.7.7).

Simulation

Inactivation Dataset

Two parameters (δ and p) were obtained in pairs, and 2×10^4 sets (5,000 iterations × 4 chains) were obtained by conducting Bayesian inference. We simulated the inactivation behavior with average of initial cell numbers of 10^n ($n = 1$–3) using 2×10^4 sets of parameters. We assumed that the initial cell number and the survival cell number at each time followed a Poisson distribution. The time t (min) was set from 0 to 6 at 0.05 (min) intervals. The time and parameter values were substituted into Equation (2), and the survival cell numbers (N_t) were calculated corresponding

to each time and each parameter. We generated random numbers as many as 2×10^4 sets from the Poisson distribution with mean $N_0 \times 10^{-(t/\delta)^p}$. The number obtained here was defined as the number of surviving cells at that time. The 2×10^4 predicted results were arranged in an ascending order, and the points corresponding to the top 2.5% and the bottom 2.5% were plotted. These lines were set as the 95% predicted interval, and the predicted results were compared with the observed values for 10^n (n = 1–3) cell inactivation. The procedure for evaluating the predicted results was mostly based on a previous study (Hiura et al., 2020). The 2×10^4 prediction results at each time points were arranged in ascending order. If observed colony count was greater than the prediction corresponding to the lower 2.5% and less than the prediction corresponding to the upper 2.5%, the observed colony count was considered to be within the prediction range. The ratio of the number in the 95% prediction interval among the 60 observed values was calculated as the accuracy.

Growth Dataset

The parameters obtained in section "Computation" were used to predict the growth behavior with average of initial cell numbers of 10^n ($n = -1-1$). We predicted the growth behavior at 10^n ($n = -1-1$) initial cells using 2×10^4 sets of parameters.

(1) Simulation of initial bacterial number

The initial number of bacteria was assumed to follow a Poisson distribution. We generated random numbers as many as 2×10^4 sets from the Poisson distribution with mean N_0. The number obtained here was set as the number of initial cells.

(2) Simulation of the growth number of cells

The estimated parameters (μ and λ), the initial number of bacteria, and the time (t_i) to predict the number of bacteria were substituted into Equation (5), and the random number following a negative binomial distribution was generated. At the desired time (t_i), if $t_i \leq \lambda$, the bacterial population could not grow. When $t_i > \lambda$, we generated a random number following a negative binomial distribution. The obtained value was the division number at each time. The number of bacteria at each time point was predicted by adding this division number and the initial cell number.

The 2×10^4 simulated results obtained by the above procedure were arranged in an ascending order, and the points corresponding to the top 2.5% and the bottom 2.5% were plotted at each time. These lines were set at 95% predicted intervals, and the simulated results were compared with the observed values for 10^n ($n = -1-1$) cell growth behavior. The procedure for evaluating the predicted results was as with section "Inactivation Dataset." The ratio of the number in the 95% prediction interval among the 50 observed values was calculated as the accuracy.

RESULTS

Bayesian Inference and Prediction of Bacterial Behavior in the Inactivation Process

Figure 4 shows the dataset of the inactivation of *B. simplex* with 10^5 cells, and the fitted results by the least-squares method and Bayesian inference. Both kinetic and Bayesian fitting yielded similar results. As a regression to the Weibull model using the least-squares method in frequentist statistics, δ and p were 1.58 (standard deviation was 0.12) and 1.26 (standard deviation was 0.09), respectively. The root-mean-square error as a goodness-of-fit index was 0.18, which indicates a good fit. **Figure 5** shows the posterior distributions of the parameters δ and p with Bayesian inference. Bayesian inference was conducted using data with a survival cell count of 0 colony forming unit (CFU). The R-hat value was 1.0 for each parameter, which indicates a good convergence. The mean values of δ and p were 1.59 (standard deviation was 0.11) and 1.21 (standard deviation was 0.15), respectively. The correlation coefficient between parameters δ and p was 0.18, indicating a poor positive correlation. The average values of the parameters estimated by Bayesian inference were comparable to the results estimated by the least-squares method used in frequentist statistics. However, the parameters were narrowed down to one point in the least-squares method, whereas the parameters were estimated as probability distributions in Bayesian inference.

Figure 6 shows a comparison between the observed data and the simulated results by the model. The rates of validity of the

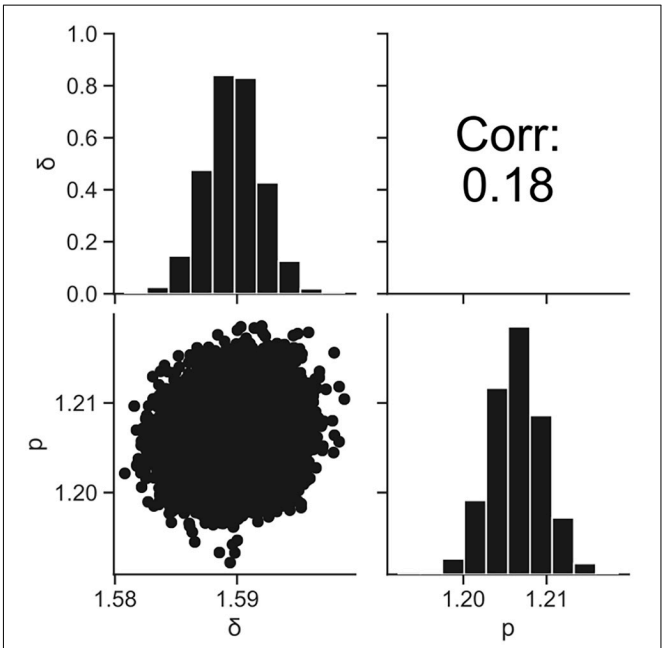

FIGURE 5 | Histograms (on the diagonal), correlation plots (under the diagonal), and correlation coefficients (over the diagonal) of the estimated parameters δ and p resulting from Bayesian inference.

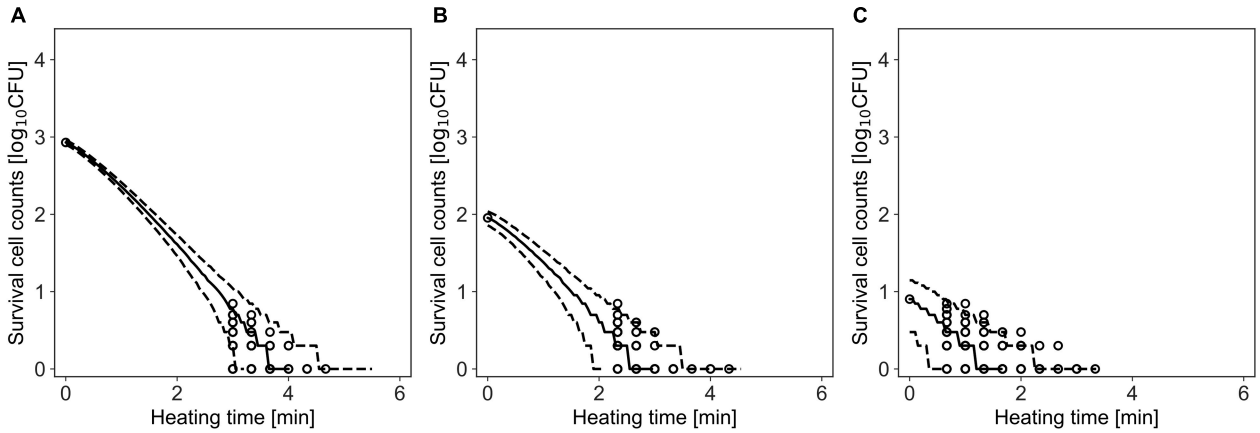

FIGURE 6 | Comparison between observed and simulated Inactivation of *Bacillus simplex* with initial cell numbers of 10^3 **(A)**, 10^2 **(B)**, and 10 cells **(C)**. The solid and dashed lines indicate the median of the prediction and the 95% predicted interval, respectively. Observed data are indicated by a circle.

number of cells within the 95% prediction band were 96, 99, and 96% for initial cell numbers of 850, 90, and 8, respectively. This result indicates that the simulation by this model covers almost the entire variation in the inactivation behavior.

Bayesian Inference and Simulation of Bacterial Behavior in the Growth Process

Figure 7 shows the dataset of the growth behavior of *L. monocytogenes* with a population of 10^4 cells incubated at 25°C, and the fitted results by the least-squares method and Bayesian inference. Both kinetic and Bayesian fitting yielded similar results. As a regression to the kinetic model using the least-squares method, μ and λ were 0.68 (standard deviation was 0.01) and 2.18 (standard deviation was 0.15), respectively. The RMSE was 0.05. **Figure 8** shows the posterior distributions of the parameters μ and λ with Bayesian inference. The R-hat value was 1.0 for each parameter, which indicates a good convergence. The mean values of μ and λ were 0.71 (standard deviation was 0.14) and 2.72 (standard deviation was 0.01), respectively. The correlation coefficient between the parameters μ and λ was 0.69, indicating a positive correlation. The average values of the parameters estimated by Bayesian inference were comparable to the results estimated by the least-squares method used in frequentist statistics.

Figure 9 shows a comparison between the observed data and the results simulated by the model. The rates of validity of the number of cells within the 95% predicted interval were 80, 94, and 96% for average of initial cell numbers of 24, 2, and 0.3 cell, respectively. For 0.3 and 2 cell, the accuracy was calculated for observed values greater than 0 CFU. This result indicates that the model simulation covers almost the entire variation in the growth behavior of the small initial cell number.

DISCUSSION

In the present study, we introduced Bayesian GLM to incorporate the variability and uncertainty into a predictive model. The estimated results of the parameter uncertainty by both the inactivation and growth models were represented in the form of a probability distribution (**Figures 5**, **8**), which has not been considered in the conventional least-squares method. The estimated parameters enabled to predict the inactivation behavior at various initial cell numbers, such as 10^3, 10^2, and 10 cells, with an accuracy of over 90% (**Figure 6**). The estimated parameters of the growth model enabled to predict the growth behavior at various

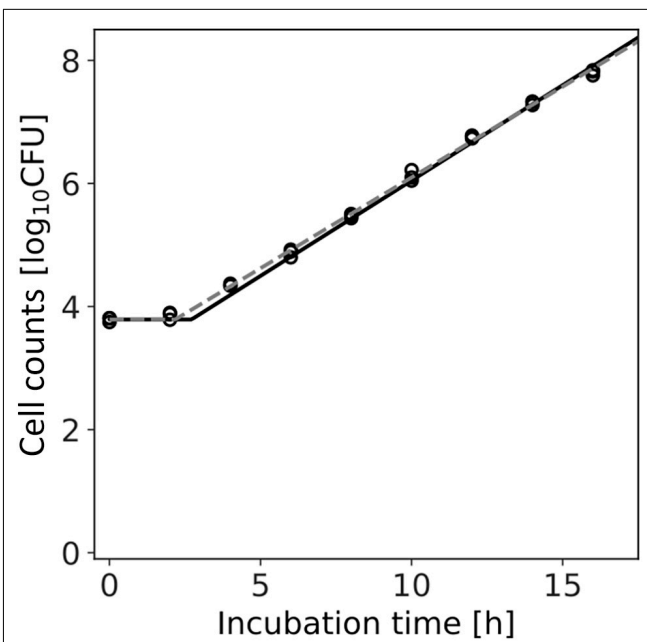

FIGURE 7 | Growth kinetics of *Listeria monocytogenes* with a population of 10^4 cells incubated at 25°C. Each time has three replications. The dashed line indicates the growth kinetics fitted by the least-squares method used in frequentist statistics. The solid line indicates the median of the fitting by Bayesian inference.

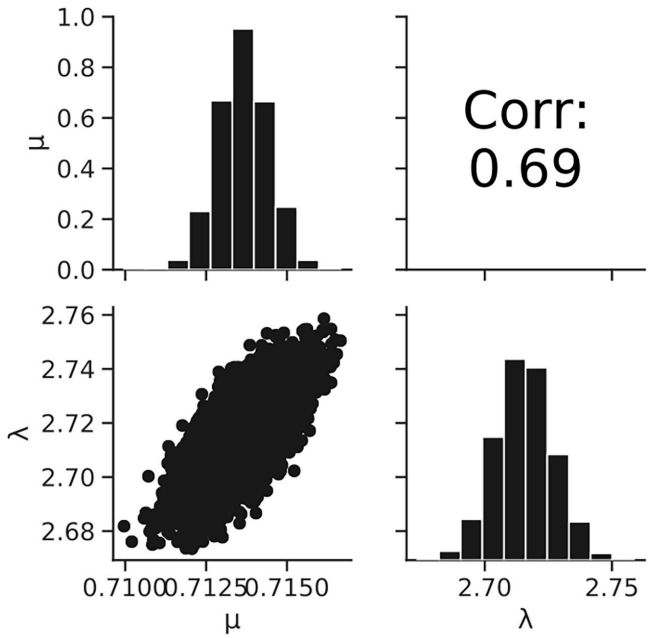

FIGURE 8 | Histograms (on the diagonal), correlation plots (under the diagonal), and correlation coefficients (over the diagonal) of the estimated parameters μ and λ resulting from Bayesian inference.

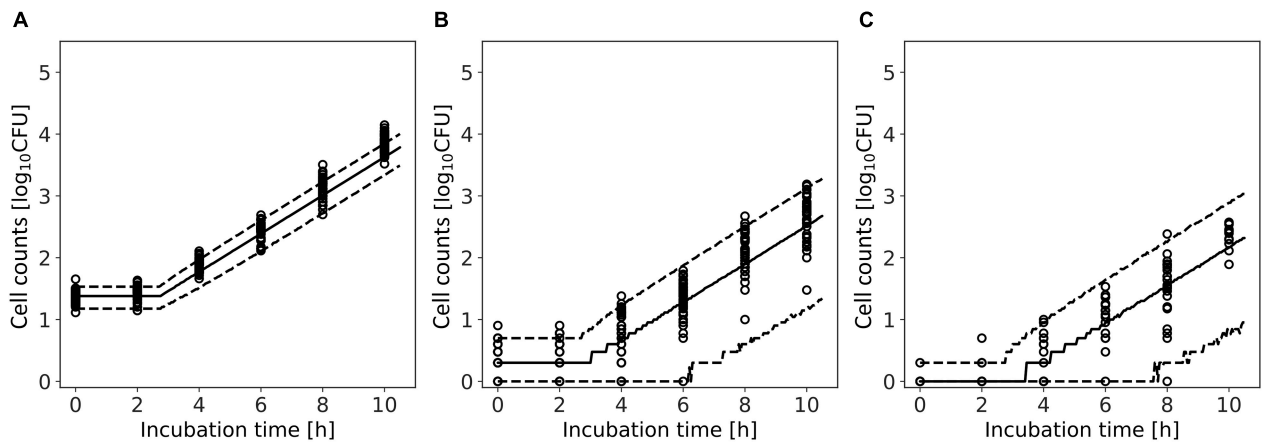

FIGURE 9 | Comparison between observed and simulated growths of *Listeria monocytogenes* with average of initial cell numbers of 10 **(A)**, 1 **(B)**, and 10^{-1} cell **(C)**. The solid and dashed lines indicate the median of the simulation and the 95% predicted interval, respectively. Observed data are indicated by a circle.

initial cell numbers, such as 24, 2, and 0.3 cell (**Figure 9**). In particular, for less than 2 cells, the growth behavior was predicted with a high accuracy of over 90%. The present model expresses the variation in the bacterial behavior at low cell concentrations, which is remarkable given the individual cell heterogeneity (Koutsoumanis and Lianou, 2013; Aspridou and Koutsoumanis, 2015). The Bayesian GLM was able to fit the inactivation and growth of the bacterial population and predict the bacterial behavior considering variability and uncertainty. This modeling procedure allows to consistently consider the variations in the actual bacterial behavior, from fitting to prediction.

As a means of expressing the variation in bacterial behavior, a stochastic model has been developed, that expresses the variability in bacterial behavior with a probability distribution (FAO/WHO, 2008). Several models that can represent variability in bacterial behavior have been developed. Previous studies have clarified that variability due to individual cell heterogeneity can be expressed using a probability distribution and Monte Carlo simulation (Poschet, 2003; Aspridou and Koutsoumanis, 2015). Others have suggested combining kinetic models with computer simulations to demonstrate variability in bacterial behavior (Abe et al., 2019; Hiura et al., 2020). Even if the variability is expressed by a Monte Carlo simulation after fitting the model, such

a method is mathematically inappropriate because there are discrepancies in the model residuals during and after fitting. Therefore, in the present study, a consistent procedure, from fitting to prediction, was implemented by introducing the GLM and model fitting to the data considering the variability due to individual cell heterogeneity. The model fitting to the data and the bacterial behavior simulation can be conducted under the assumption of the same probability distribution in the process of fitting the model to the data and the simulation (Equations 3 and 5). It is reasonable to consider variability and uncertainty while fitting to the data instead of doing so after the fitting.

In the least-squares method, the logarithmic number of bacterial populations is treated as a continuous number because a normal distribution is used as the error distribution. The cell count is logarithmically analyzed in data analyses in the field of microbiology. Because the logarithm cannot be taken for 0 CFU, the count of 0 CFU is omitted from the dataset. O'Hara and Kotze (2010) suggested that distributions designed to deal with counts, such as the Poisson distribution or negative binomial distribution, should be used to fit count data instead of using a continuous distribution such as a normal distribution. O'Hara and Kotze (2010) also insisted that a log-transformation of count data should be considered when dealing with zero observations. With a discrete distribution, it is possible to make fitting and predictions, including for data with a cell number of 0 CFU. Therefore, in the present study, the number of bacteria was treated as a discrete number when fitting using the GLM (Equations 3 and 5). We expressed the variability in the bacterial cell number by introducing a discrete distribution, i.e., a Poisson distribution (Equations 3 and 5), and a negative binomial distribution (Equation 5). We were able to use data with a survival cell count of 0 CFU for parameter estimation (**Figure 4**) and prediction, since the Poisson distribution was used as the error distribution of the cell count. With the use of discrete distributions, the data of bacterial counts, including 0 CFU, can be used for analyses. Thus, data loss during analysis can be prevented. A discrete probability distribution is useful for expressing the number of bacteria counts, particularly in the case of a low dose, including zero.

Variability and uncertainty simultaneously appear experimentally (Poschet, 2003; Park and Lee, 2008). It is necessary to consider both these factors when conducting exposure assessments (FAO/WHO, 2008). Bacterial behavior is characterized by variability and uncertainty, and the need to consider both has been pointed out (Nauta, 2000). It is relatively easier to define variability using an equation than uncertainty, since variability is derived from some exact factors such as individual cell inactivation time as individual cell heterogeneity (Aspridou and Koutsoumanis, 2015). Therefore, the definition of variability such as individual cell inactivation time and between-strains is an important first step, since understanding variability can help determine the degree of uncertainty. The better we know the variability, the clearer the uncertainty. We defined the variability in the number of bacteria during the inactivation and growth processes using the Poisson distribution and negative binomial distribution (Equations 3 and 5), which can be a fundamental assumption for the further analysis of the variability and uncertainty in bacterial behavior.

Some other distributions such as Poisson-lognormal and Poisson-gamma distributions were used to describe number of cells in food production, where many factors affect the heterogeneity of microbial numbers among food units (Gonzales-Barron and Butler, 2011). Poisson-lognormal and Poisson-gamma distributions are used to describe over dispersion of count data (Congdon, 2006). These probability distributions may be possible choice to predict bacterial population behavior in food.

Only colony count data have been used for constructing kinetic models in Bayesian GLM that considers variability and uncertainty in bacterial behavior. Colony count data can be found not only in literature but also in databases such as ComBase[1]. So far, risk related to food borne pathogens has been assessed using these accumulated data. The model proposed in the present study can help represent the variability and uncertainty in bacterial behavior using existing published data, providing a more realistic quantitative exposure assessment compared to using the conventional least-squares method. The proposed modeling procedure can help account for the variability and uncertainty in risk-based modeling.

CONCLUSION

The present study illustrated the construction of a Bayesian GLM considering the variability and uncertainty in bacterial inactivation and growth behavior. This modeling procedure allowed to consistently assume a probability distribution representing the variation in bacterial behavior throughout the fitting process for simulating bacterial behavior. The developed models enable a more explicit illustration of the variation in bacterial behavior via probability distributions, because the models are based on probabilistic theory. For example, the variation in bacterial numbers following a Poisson distribution was derived from experimentally prepared bacterial cells via a dilution process. In addition, the probability distributions of the growth or inactivation processes were assumed to be independent of other biological events. Thus, the models developed in the present study provide a reliable foundation for representing the variability and uncertainty. The Bayesian GLM can separately describe the variability and uncertainty, which cannot be done using the conventional least-squares methods used in frequentist statistics.

DATA AVAILABILITY STATEMENT

The datasets and codes in this article can be found online at: https://github.com/Satoko-Hiura/Bayesian-generalized-linear-model-for-simulating-bacterial-inactivation-growth.git.

AUTHOR CONTRIBUTIONS

SH, HA, KK, and SK designed the study and wrote the manuscript. SH performed the study and analyzed the data.

[1] www.combase.cc

All authors contributed to the article and approved the submitted version.

FUNDING

This study was supported by a grant from the Food Safety Commission, Cabinet Office, Government of Japan (Research Program for Risk Assessment Study on Food Safety, number 2004). This work was also supported by JSPS KAKENHI (Grant No. 19K23655).

ACKNOWLEDGMENTS

We would like to thank Editage for the English language editing (https://www.editage.jp).

REFERENCES

Abe, H., Koyama, K., Kawamura, S., and Koseki, S. (2019). Stochastic modeling of variability in survival behavior of *Bacillus simplex* spore population during isothermal inactivation at the single cell level using a Monte Carlo simulation. *Food Microbiol.* 82, 436–444. doi: 10.1016/j.fm.2019.03.005

Aguirre, J. S., Pin, C., Rodríguez, M. R., and de Fernando, G. D. G. (2009). Analysis of the variability in the number of viable bacteria after mild heat treatment of food. *Appl. Environ. Microbiol.* 75, 6992–6997. doi: 10.1128/AEM.00452-09

Aspridou, Z., and Koutsoumanis, K. P. (2015). Individual cell heterogeneity as variability source in population dynamics of microbial inactivation. *Food Microbiol.* 45, 216–221. doi: 10.1016/j.fm.2014.04.008

Buchanan, R. L., Whiting, R. C., and Damert, W. C. (1997). When is simple good enough: a comparison of the Gompertz, Baranyi, and three-phase linear models for fitting bacterial growth curves. *Food Microbiol.* 14, 313–326. doi: 10.1006/fmic.1997.0125

Coleman, M. E., and Marks, H. M. (1999). Qualitative and quantitative risk assessment. *Food Control* 10, 289–297. doi: 10.1016/S0956-7135(99)00052-3

Congdon, P. (2006). *Bayesian Statistical Modelling*. Chichester: John Wiley & Sons Ltd, doi: 10.1002/9780470035948

Crépet, A., Stahl, V., and Carlin, F. (2009). Development of a hierarchical Bayesian model to estimate the growth parameters of *Listeria monocytogenes* in minimally processed fresh leafy salads. *Int. J. Food Microbiol.* 131, 112–119. doi: 10.1016/j.ijfoodmicro.2009.01.028

Dey, D. K., Ghosh, S. K., and Mallick, B. K. (2000). *Generalized Linear Models: A Bayesian Perspective*. Boca Raton, FL: CRC Press.

Dickman, P. W., and Coviello, E. (2015). Estimating and modeling relative survival. *Stata J.* 15, 186–215. doi: 10.1177/1536867X1501500112

Dickman, P. W., Sloggett, A., Hills, M., and Hakulinen, T. (2004). Regression models for relative survival. *Stat. Med.* 23, 51–64. doi: 10.1002/sim.1597

Dolan, K. D., and Mishra, D. K. (2013). Parameter estimation in food science. *Annu. Rev. Food Sci. Technol.* 4, 401–422. doi: 10.1146/annurev-food-022811-101247

Faille, C., Tauveron, G., Le Gentil-Lelièvre, C., and Slomianny, C. (2007). Occurrence of *Bacillus cereus* spores with a damaged exosporium: consequences on the spore adhesion on surfaces of food processing lines. *J. Food Prot.* 70, 2346–2353. doi: 10.4315/0362-028x-70.10.2346

FAO/WHO. (2008). *Exposure Assessment of Microbiological Hazards in Food*. Rome: FAO.

Garre, A., Zwietering, M. H., and Besten den, H. M. W. (2020). Multilevel modelling as a tool to include variability and uncertainty in quantitative microbiology and risk assessment. Thermal inactivation of *Listeria monocytogenes* as proof of concept. *Food Res. Int.* 137, 109374. doi: 10.1016/j.foodres.2020.109374

Gil, M. M., Miller, F. A., Brandão, T. R. S., and Silva, C. L. M. (2017). Mathematical models for prediction of temperature effects on kinetic parameters of microorganisms' inactivation: tools for model comparison and adequacy in data fitting. *Food Bioprocess. Technol.* 10, 2208–2225. doi: 10.1007/s11947-017-1989-x

Gonzales-Barron, U., and Butler, F. (2011). A comparison between the discrete Poisson-gamma and Poisson-lognormal distributions to characterise microbial counts in foods. *Food Control* 22, 1279–1286. doi: 10.1016/j.foodcont.2011.01.029

Helmond, M., Nierop Groot, M. N., and van Bokhorst-van de Veen, H. (2017). Characterization of four *Paenibacillus* species isolated from pasteurized, chilled ready-to-eat meals. *Int. J. Food Microbiol.* 252, 35–41. doi: 10.1016/j.ijfoodmicro.2017.04.008

Hiura, S., Abe, H., Koyama, K., and Koseki, S. (2020). Transforming kinetic model into a stochastic inactivation model: statistical evaluation of stochastic inactivation of individual cells in a bacterial population. *Food Microbiol.* 91:103508. doi: 10.1016/j.fm.2020.103508

Jaloustre, S., Cornu, M., Morelli, E., Noël, V., and Delignette-Muller, M. L. (2011). Bayesian modeling of *Clostridium perfringens* growth in beef-in-sauce products. *Food Microbiol.* 28, 311–320. doi: 10.1016/j.fm.2010.04.002

Koutsoumanis, K. P., and Lianou, A. (2013). Stochasticity in colonial growth dynamics of individual bacterial cells. *Appl. Environ. Microbiol.* 79, 2294–2301. doi: 10.1128/AEM.03629-12

Koyama, K., Aspridou, Z., Koseki, S., and Koutsoumanis, K. (2019). Describing uncertainty in *Salmonella* thermal inactivation using Bayesian statistical modeling. *Front. Microbiol.* 10:2239. doi: 10.3389/fmicb.2019.02239

Koyama, K., Hokunan, H., Hasegawa, M., Kawamura, S., and Koseki, S. (2016). Do bacterial cell numbers follow a theoretical Poisson distribution? Comparison of experimentally obtained numbers of single cells with random number generation via computer simulation. *Food* Microbiol. 60, 49–53. doi: 10.1016/j.fm.2016.05.019

Lammerding, A. M., and Fazil, A. (2000). Hazard identification and exposure assessment for microbial food safety risk assessment. *Int. J. Food Microbiol.* 58, 147–157. doi: 10.1016/s0168-1605(00)00269-5

McKellar, R. C., and Lu, X. (2003). *Modeling Microbial Responses in Food*. New York, NY: CRC Press.

Nauta, M. J. (2000). Separation of uncertainty and variability in quantitative microbial risk assessment models. *Int. J. Food Microbiol.* 57, 9–18. doi: 10.1016/S0168-1605(00)00225-7

Nelder, J. A., and Wedderburn, R. W. M. (1972). Generalized linear models. *J. R. Stat. Soc. Ser. A* 135, 370–384. doi: 10.2307/2344614

O'Hara, R. B., and Kotze, D. J. (2010). Do not log-transform count data. *Methods Ecol. Evol.* 1, 118–122. doi: 10.1111/j.2041-210X.2010.00021.x

Park, J.-P., and Lee, D.-S. (2008). Analysis of temperature effects on microbial growth parameters and estimation of food shelf life with confidence band. *J. Food Sci. Nutr.* 13, 104–111. doi: 10.3746/jfn.2008.13.2.104

Poschet, F. (2003). Monte Carlo analysis as a tool to incorporate variation on experimental data in predictive microbiology. *Food Microbiol.* 20, 285–295. doi: 10.1016/S0740-0020(02)00156-9

Pouillot, R., Albert, I., Cornu, M., and Denis, J. B. (2003). Estimation of uncertainty and variability in bacterial growth using Bayesian inference. Application to *Listeria monocytogenes*. *Int. J. Food Microbiol.* 81, 87–104. doi: 10.1016/s0168-1605(02)00192-7

Ratkowsky, D. A., Ross, T., Macario, N., Dommett, T. W., and Kamperman, L. (1996). Choosing probability distributions for modelling generation time variability. *J. Appl. Bacteriol.* 80, 131–137.

Renshaw, E. (1993). *Modelling Biological Populations in Space and Time*. New York, NY: Cambridge University Press.

van Boekel, M. A. J. S. (2020). On the pros and cons of Bayesian kinetic modeling in food science. *Trends Food Sci. Technol.* 99, 181–193.

Ver Hoef, J. M., and Boveng, P. L. (2007). Quasi-Poisson vs. negative binomial regression: how should we model overdispersed count data? *Ecology* 88, 2766–2772. doi: 10.1890/07-0043.1

Conflict of Interest: The authors declare that the research was conducted in the absence of any commercial or financial relationships that could be construed as a potential conflict of interest.

frontiers in Microbiology

ORIGINAL RESEARCH
published: 04 August 2021
doi: 10.3389/fmicb.2021.704302

Complete Replacement of Nitrite With a *Lactobacillus fermentum* on the Quality and Safety of Chinese Fermented Sausages

Yuning Xu[1] *and Yinglian Zhu*[1,2]*

[1] College of Food Science and Engineering, Qingdao Agricultural University, Qingdao, China, [2] Qingdao Special Food Research Institute, Qingdao, China

This study investigated the positive effects of complete replacement of nitrite with a *Lactobacillus fermentum* on the quality and safety of Chinese fermented sausages, and evaluated the risk of this strain. The effects of the strain on pH, color, nitrite, thiobarbituric acid reactive substances (TBARS), total volatile basenitrogen (TVB-N), metmyoglobin (Met-Mb), biological amines, free amino acid content, and sensory index have been studied. The results revealed that the strain reduced the pH of the sausages, which reduced the risk of food-borne pathogens, and accelerated the acidification and gelation process. The inoculation of the strain produced pink color similar to 50 mg/kg nitrite, significantly reducing the residual risk of nitrite in the sausages. In addition, the strain effectively improved quality and nutrition of the sausages through preventing fat oxidation, protein decomposition, and myoglobin oxidation and increasing free amino acid content. The harmful biogenic amines species of the treated sample were reduced, although the tyramine contents were higher than the control, and the contents of the two groups were all far below the specified limit (800 mg/kg). The sensory analysis showed that the strain enhanced the taste, flavor, sourness, and overall acceptability of the sample sausages. Therefore, replacing nitrite completely with the strain *L. fermentum* could be a potential strategy to produce healthier and safer acceptable sausages through decreasing the risk of nitrite and improving nutrition and quality of the sausages.

Keywords: nitrite, *Lactobacillus fermentum*, fermented sausages, biological amines, thiobarbituric acid reactive substances, total volatile basenitrogen, metmyoglobin

OPEN ACCESS

Edited by:
Gongliang Zhang,
Dalian Polytechnic University, China

Reviewed by:
Małgorzata Karwowska,
University of Life Sciences of Lublin, Poland
Hatice Yazgan,
Cukurova University, Turkey

***Correspondence:**
Yinglian Zhu
cjs52002@163.com

Specialty section:
This article was submitted to Food Microbiology, a section of the journal Frontiers in Microbiology

Received: *02 May 2021*
Accepted: *12 July 2021*
Published: *04 August 2021*

Citation:
Xu Y and Zhu Y (2021) Complete Replacement of Nitrite With a Lactobacillus fermentum on the Quality and Safety of Chinese Fermented Sausages. Front. Microbiol. 12:704302. doi: 10.3389/fmicb.2021.704302

INTRODUCTION

In food process, specific food additives are often added to prevent corruption and extend the shelf life of the foods. However, the residual of some chemical additives will threaten human health, and they might also form toxic compounds due to the chemical reaction between the reactants (Mologni et al., 2019). Hence, the development of natural and harmless food additives has become research hotspots in food industry. The natural biopreservatives are ideal natural food preservatives, which are safe, nontoxic, and efficient and have no negative effects. However, there are fewer natural microbial preservatives that can be used in the meat industry, and in-depth explorations are needed.

Chinese fermented sausages have unique flavor and rich nutrition, so they are very popular among people. However, naturally fermented sausages are easily contaminated by bacteria and have a short shelf life. Usually, certain food additives are added in the process of naturally fermented sausages to extend the shelf life. Among them, nitrite is often used in the process because it has color development ability, antioxidant activity, and antibacterial effects. However, the products of protein degradation during meat storage would react with nitrite to produce N-nitrosamine (Drabik-Markiewicz et al., 2011), which has carcinogenic effects to humans. As people pay more and more attention to health, it is very urgent to develop natural preservatives that are harmless to human health in the meat industry.

Lactic acid bacteria (LAB), as a kind of probiotics, are often used as starters for foods, such as sausages and yogurts. A previous report indicated that the LAB inoculated in the meat products could degrade nitrite and scavenge free radicals, and exhibited antioxidant activity and antibacterial effects (Ren et al., 2014). A previous report indicated that the *Lactobacillus plantarum* P2 isolated from traditional fermented sauerkraut had the ability to scavenge hydroxyl free radicals and superoxide free radicals and could degradate nitrite effectively (Chen et al., 2019). Zhang et al. (2020) found that the *L. plantarum* LPL-1 inhibited the growth of spoilage bacteria during fermentation and significantly reduced the content of histamine, putrescine, and cadaverine, and the total amount of biogenic amines of sausages. Guimarães et al. (2018) showed that the *L. plantarum* UM55 CFS could produce lactic acid along with other organic acids during fermentation, which has been confirmed to inhibit the growth of *Aspergillus flavus*. In addition, the *Lactobacillus fermentum* R6 was found to have antibacterial ability against the growth of *Clostridium perfringens* and its spores in chicken meat, so the strain could be used as a potential biopreservatives to prevent the contamination by *C. perfringens* in meat products (Li et al., 2017).

Some other studies pointed that the LAB had the effect of improving color in fermented sausages. The effect of different concentrations of *L. fermentum* on the color development of fermented sausages was studied, and the results showed that the strain contributed to the production of nitrosomyoglobin (Mb-NO) and 10^8 CFU/g meat of the strain could produce the pink color similar to 60 mg/kg nitrite (Zhang et al., 2007). The research of Kawahara et al. (2006) showed that *Lactobacillus sakei* M32 could produce the red color with high redness (a^* value) and low yellowness (b^* value), and the color of the sample was similar to that of the control with nitrite added. Chen et al. (2016) isolated two strains of *L. plantarum* CMRC6 and *L. sakei* CMRC15 from traditional fermented pork and found that the two strains promoted nitrosation of myoglobin and produced the pink color in the sausages due to their nitrite reductase activity. In addition, LAB is usually used to improve the flavor and texture of fermented foods as a starter due to its acid production capacity. Moreover, LAB have many other functions, including regulating the intestinal flora, improving immunity, lowering cholesterol, etc. (Khalique et al., 2020; Saravanakumar et al., 2020). Therefore, the inoculation of LAB in foods has great value to improve food nutrition and protect human health (Sharafedtinov et al., 2013; Tu et al., 2018).

The above reports indicated that LAB have color development and antibacterial activity, so they might have the potential to replace nitrite in meat processing. However, no practical LAB strains have yet been found for industrial application as a complete substitute for nitrite. Therefore, the replacement for nitrite with LAB in meat products still requires in-depth exploration. The target of this study was to evaluate the positive effects of complete replacement of nitrite with the *L. fermentum* (CICC 21828) on the quality and safety of Chinese fermented sausages. The effects of the strain on pH, color, nitrite, thiobarbituric acid reactive substances (TBARS), total volatile basenitrogen (TVB-N), metmyoglobin (Met-Mb), tyramine, free amino acid content, and sensory index have been studied.

MATERIALS AND METHODS

Strains

The LAB used in this experiment were *L. fermentum* (CICC 21828), which was provided by China Center of Industrial Culture Collection and preserved in the fermentation engineering laboratory, Qingdao Agricultural University.

Sausage Manufacture

The formulation of the sausages includes 75% lean pork meat, 25% pork back fat, 2.3% NaCl, 3% sucrose, and 1% D-sodium erythorbate. The pork and pork casings were obtained from a local retailer in Qingdao (China). In addition, the 0.005% (50 mg/kg) $NaNO_2$ was added in the control (Yoo et al., 2015), and 10^{10} CFU/g meat of the strain *L. fermentum* was inoculated in the sample to substrate 50 mg/kg $NaNO_2$. All the raw materials were chopped, mixed, and marinated at 4°C for 24 h. The mixture was then stuffed in natural pork casings, fermented at 37°C in an incubator for 3 h with relative humidity (RH) of 90%, and then hung and dehydrated at 10°C for 20 days, with an RH of 70% according to our previous report (Zhu et al., 2020). Finally, the sausages were baked at 80°C for 1 h, at 65°C for 8 h, and then steamed at 100°C for 30 min.

pH and Chroma

The sausages were minced to small pieces and were homogenized in 90 ml of sterilized saline (0.85%, w/v) in a BagMixer for 90 s, and then the pH was detected using a pH meter (FiveEasy Plus 28, Mettler Toledo, Shanghai, China) with a solid electrode. The sausages were sliced into slices about 2 cm and wrapped with a layer of film, and the chroma measurement was carried out with a Chroma Meter (CR-400, Konica Minolta Co., Tokyo, Japan). The values of lightness (L^* value), a^* value, and b^* value were recorded from different pieces of each sample.

Nitrite Residual

The nitrite residual was measured with the method of hydrochloride naphthodiamide according to a previous report (Zhang et al., 2007) with minor modification. The sausages were minced to small pieces and were pounded with mortar

in 25 ml of saturated borax solution. The volume was adjusted to 100 ml with distilled water and boiled in a water bath for 15 min, and then cooled to room temperature. After being filtered, the filtrate (25 ml) was taken out and mixed with 4-aminobenzenesulfonic acid (2 ml, 4 g/L) and N-naphthyl-ethylenediamine dihydrochloride (1 ml, 2 g/L) and set aside for 15 min. The absorbance was measured at the wavelength of 538 nm, and the nitrite residual was expressed with the following formula: $NaNO_2 = (C \cdot 2000)/(M \cdot V)$. Here, C is the sodium nitrite concentration of the sample obtained from the calibration curve, M is the sample weight, and V is the volume of the extraction solution.

TBARS

According to the method of Geeta and Yadav (2017) with slight modification, minced sausages (10 g) were homogenized with 50 ml of trichloroacetic acid solution (7.5% of trichloroacetic acid, 0.1% of EDTA, w/v), and then were filtered twice with three layers of filter paper. The filtrate was heated, and the distillate was collected. Then, 5 ml of the distillate and 5 ml of the TBA reagent (0.02 mol/L, thiobarbituric acid) were mixed and boiled in a water bath for 35 min. After being cooled, the absorbance was detected at 530 nm with a spectrophotometer (UV-1,200, MAPADA, Shanghai, China), and the TBA value was expressed with the formula below:

$$\text{TBA value} = \frac{50 \times (A - B)}{m}$$

Here, A is the absorbance value of the sample solution, and B is the absorbance value of the blank.

TVB-N

The measurement of the TVB-N content was carried out according to the method of Wang et al. (2016) with some modifications. The sausages were minced to small pieces and were homogenized in 90 ml of distilled water in a BagMixer for 90 s, stirred for 30 min, and filtered with three layers of filter paper. Then, 10 ml of the filtrate was mixed with 10 ml of MgO solution (10 g/L) and distilled for 5 min in semimicro Kjeldahl bottle. The distillate was mixed with 10 ml of boric acid solution (10 g/L) and titrated with 0.01 mol/L HCl. The content of the TVB-N was determined according to the consumption of hydrochloric acid.

Amino Acid

The measurement of amino acid content was carried out by the ninhydrin colorimetric method. The sausages were minced to small pieces and homogenized in 90 ml of distilled water in a BagMixer for 90 s, boiled in a water bath for 10 min, cooled, and filtered. Then, 1 ml of the filtrate was mixed with 1 ml of citric acid buffer solution (0.2 mol/L, pH 6.86) and 1 ml of ninhydrin coloring solution in a test tube, and then the distilled water was added to make the total volume to 5.0 ml, shaken well, capped, and boiled in a water bath for 15 min. After being cooled, the absorbance was measured at 568 nm. Then, the content of amino acid was acquired by the standard curve. The standard curve was established through a series of concentrations of glycine standard solution (10, 20, 30, 40, and 50 μg/ml), and the processing steps were same as above.

Met-Mb

The Met-Mb measurement was carried out according to our previous report (Zhu et al., 2020). Sausage samples (10 g) were homogenized in 25 ml of ice-cold phosphate buffer (0.01 mol/L, pH 6.8), placed in the dark at 4°C for 1 h, and then centrifuged at 4,000 g for 5 min at 4°C. Finally, the supernatant was filtered with a 0.45-μm nitrocellulose filter membrane. The Met-Mb content was determined by measuring the absorbance at 572, 562, 545, and 525 nm, respectively, using a spectrophotometer. The percentage of Met-Mb was determined with the formula below:

$$\text{Met}-\text{Mb}\% = \left\{-2.51\left(\frac{A_{572}}{A_{525}}\right) + 0.777\left(\frac{A_{562}}{A_{525}}\right) + 0.8\left(\frac{A_{545}}{A_{525}}\right) + 1.098\right\} \times 100.$$

Biogenic Amine

Sausage samples (1 g) were homogenized with 10 ml of trichloroacetic acid solution (5%, v/v) and extracted by ultrasonic extraction for 30 min. After centrifugation, the extraction (1 ml) was taken out and reacted with 0.2 ml of NaOH (2 mol/L) and 100 μl of benzoyl chloride at 40°C for 30 min. Then, the mixture was terminated with methanol and filtered with the membrane (0.22 μm) for high-performance liquid chromatography (HPLC) to determine the biogenic amine content. HPLC analysis was carried out with Syncronis C18 column according to our previous report (Zhu et al., 2020). The temperature of the column was set as 35°C with the injection volume of 20 μl and the UV detection wavelength of 254 nm. The gradient mobile phase contained solvent A and solvent B, and the procedure was started at a ratio of 70:30 (A:B) with a flow rate of 0.8 ml/min; subsequently, solvent B increased gradually to 70% within 38 min, and then maintained for 4 min.

Sensory Analysis

Texture, flavor, slice, color, taste, sourness, and overall acceptability of the samples were evaluated according to a 10-point scale from 1 to 10 (Nassu et al., 2003). The evaluation was performed by 10 people who had experience in sensory evaluation of fermented sausages. The samples were sliced to 5-mm thickness and marked with three-digit random numbers. Then, the numbered slices were placed on white plates, and each sample was evaluated three times. Water and unsalted crackers were supplied to the panel to purify their palate between different samples.

Statistical Analysis

All measurements were performed in triplicate, respectively. The data analysis was carried out using IBM SPSS Statistics 23.0 (IBM, New York, NY, United States). For multiple comparisons between more than three sample groups, the one-way analysis of variance (ANOVA) was applied and the significant difference between the groups were analyzed with Duncan's multiple range tests. For the

comparison between two sample groups, independent-sample *t*-test was employed. For both analysis methods, the significance was set at the level of $p < 0.05$.

RESULTS

pH

pH is an important indicator to monitor the fermentation process of fermented sausages. In **Figure 1**, pH of the control and the sample showed very little decrease at the beginning of the fermentation (within 0.5 h). It might be because *L. fermentum* was in the growth phase of adapting to the new environment, resulting in low amount of lactic acid production. In the subsequent phase, the pH of the sample decreased sharply, which was much lower than that of the control. The sharp drop of the pH reflected that the anaerobic glycolysis increased and large amounts of lactic acid were produced in the growth of LAB (Chen et al., 2016). However, the pH of the sample was lower than the control during the whole fermentation process. For the sample sausages, when the pH dropped below 5.5, the speed of the pH decrease became slow. The phenomena might be attributed to the generation of non-protein nitrogen in the meat by proteolytic process, which would inhibit the decrease in pH through buffering the lactic acid (Chen et al., 2016). For the cathepsins will be activated and at pH 5.0–5.5 and accelerate the proteolysis (Visessanguan et al., 2003).

Color Analysis

According to **Table 1**, the L^* value of the sample and the control all decreased throughout the ripening process, and the value of the sample was lower than that of the control at the end of the 20th day. The a^* value of the sample and the control was also affected by ripening time and declined over time. However, at the 20th day, no significant difference ($p < 0.05$) in a^* value was found between the sample and the control, indicating that the strain inoculation could produce the pink color in the sausages nitrite-free and could make the color stable. This further indicated that the strain had a similar color development ability to nitrite. Another study also reported that LAB had the color formation ability in meat products nitrite-free (Gao et al., 2014). In addition, LAB application level was important for color development, and 10^8 CFU/g inoculation of *L. fermentum* might develop the pink color similar to that produced by 60 mg/kg of nitrite (Zhang et al., 2007). The b^* value of the sample and the control both increased during the ripening process, which indicated the oxidation of the sausages increased (Xiang et al., 2019). However, the value of the sample was much lower than that of the control in the whole ripening process, which indicated that the sample had good color and could inhibit lipid peroxidation (Xiang et al., 2019).

TABLE 1 | The color of the sausages during ripening period.

	Control		Sample	
	X	SD	X	SD
L*				
0d	59.78^{aA}	2.15	54.23^{bA}	1.78
5d	54.34^{aB}	1.73	50.45^{aB}	3.12
10d	53.33^{aB}	2.37	47.61^{bBC}	2.16
15d	48.42^{aC}	2.09	48.55^{aBC}	1.40
20d	47.27^{aC}	1.03	44.50^{bC}	1.14
a*				
0d	12.34^{aA}	1.14	10.71^{aA}	0.67
5d	13.67^{aA}	0.83	9.89^{bA}	0.85
10d	7.63^{aB}	0.45	6.38^{aB}	0.83
15d	4.79^{aC}	1.15	5.18^{aBC}	0.48
20d	5.26^{aC}	0.84	4.87^{aC}	0.56
b*				
0d	1.25^{aD}	0.31	0.44^{bC}	0.08
5d	3.49^{aC}	0.56	0.56^{bBC}	0.11
10d	4.12^{aC}	0.43	1.40^{bB}	0.67
15d	5.25^{aB}	0.21	3.16^{bA}	0.78
20d	6.22^{aA}	0.47	3.85^{bA}	0.32

The superscripted letters a b c represent significantly different ($p < 0.05$) in the same line, and A B C represent significantly different ($p < 0.05$) in the same column.

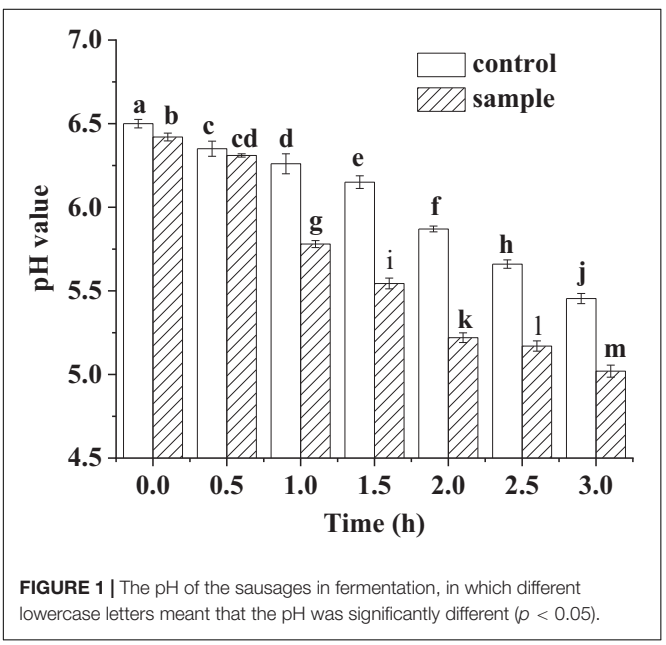

FIGURE 1 | The pH of the sausages in fermentation, in which different lowercase letters meant that the pH was significantly different ($p < 0.05$).

The Nitrite Content

In **Figure 2**, although no nitrite was added to the sample, small amounts (3.22–2.07 mg/kg) of nitrite were detected in the sample sausages during the ripening process. In other study, small amounts of nitrite were also detected in the sausages with *L. fermentum* inoculation and nitrite free (Zhang et al., 2007). The source of nitrite in the sample was not clear, which might be derived from the curing process of meat. Zhang et al. (2007) regarded that the source of nitrite might be tap water, because it was very difficult to produce tap water of nitrite free. The nitrite content of the two groups decreased during the ripening process. The reduction in nitrite content in the control attributed to the reaction between the nitrite and myoglobin, which resulted in

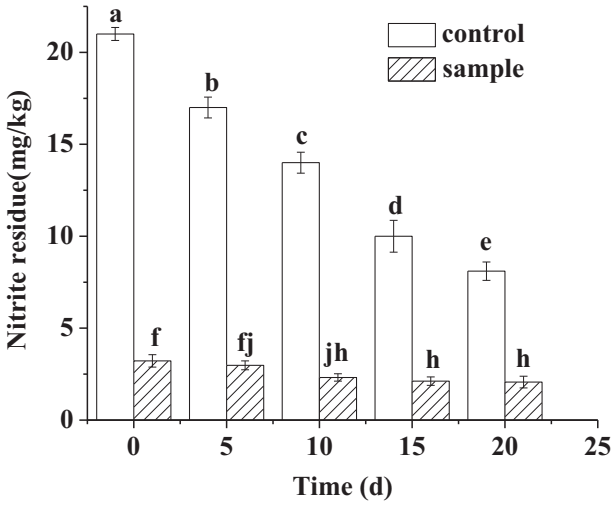

FIGURE 2 | The nitrite content of the sausages during ripening period, in which different lowercase letters meant that nitrite content was significantly different ($p < 0.05$).

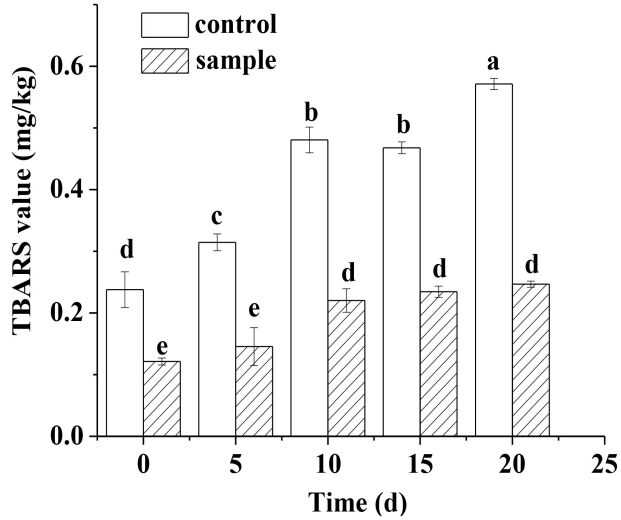

FIGURE 3 | The TBARS content of the sausages during ripening period, in which different lowercase letters meant that TBARS content was significantly different ($p < 0.05$).

the production of nitrosomyoglobin (Mb-NO). For the sample, it might be that the strain had nitrite degradation ability according to the previous report (Yoo et al., 2015). However, the content of the sample was always significantly lower ($p < 0.05$) than that of the control during all the ripening process. On the 30th day, the content of the sample was 2.07 mg/kg, and that of the control was 8.1 mg/kg.

TBARS

The TBA value reflects the extent of oxidation and rancidity of lipids in meat products. The TBA value of the two groups both increased constantly with extending ripening time (**Figure 3**). However, the TBA value of the control remained significantly higher ($p < 0.05$) than that of the sample during the whole ripening process (**Figure 3**). A previous study also had the similar result that the strain *Lactobacillus pentosus* inoculated in sausages had significantly inhibited the oxidation of lipids compared to the control (Sun et al., 2017). Although a previous report pointed out that nitrite could restrain the oxidation of lipids through different channels (Berardo et al., 2016), the result showed that the strain *L. fermentum* had stronger antioxidant capacity against lipids compared to the nitrite.

TVB-N Content

It could be seen from **Figure 4** that the TVB-N content of the two groups increased continuously with time. TVB-N mainly reflects the degree of protein decomposition of meat products by microorganisms (Dabadé et al., 2015). Another study also regarded that TVB-N production might be due to the action of spoilage bacteria and endogenous enzymes (Song et al., 2011). There had been no significant difference ($p < 0.05$) between the sample and the control at the 20th day, indicating that the strain had a similar ability with that of nitrite in preventing protein decomposition from microorganisms and endogenous enzymes.

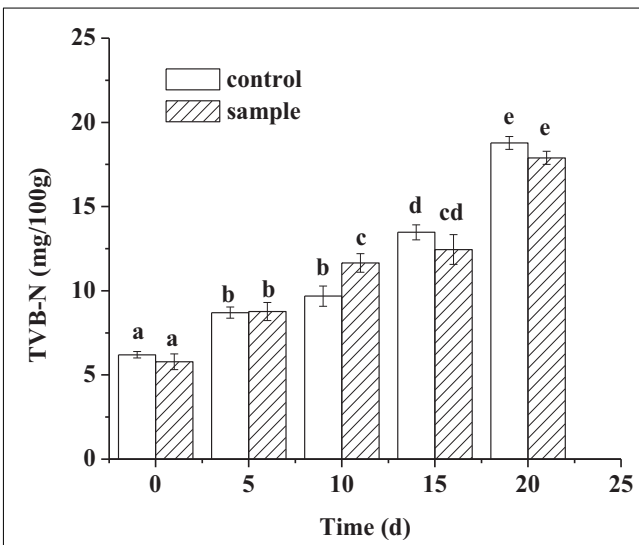

FIGURE 4 | The TVB-N content of the sausages during ripening period, in which different lowercase letters meant that TVB-N content was significantly different ($p < 0.05$).

Hence, the strain had a similar ability as nitrite to reduce protein decomposition and microbial risks.

Free Amino Acid and Met-Mb

In **Figure 5A**, the content of total amino acids in the control was 18.38 mg/100 g, while that of the sample was 53.19 mg/100 g. In fermented sausages, meat proteins are first hydrolyzed into polypeptides by endogenous proteases, and further hydrolyzed into amino acids by microbial protease (Hu et al., 2021). The higher total amino acid contents in the sample inoculated with LAB might due to the proteolytic activity of the strain

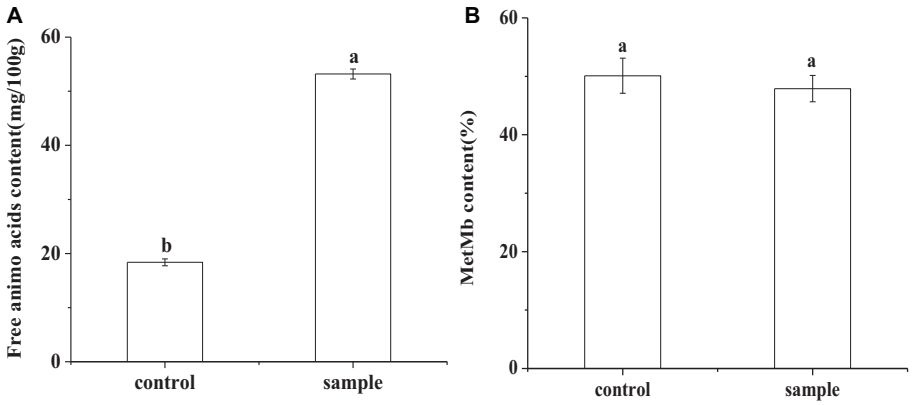

FIGURE 5 | The free amino acid content **(A)** and the Met-Mb content **(B)** of the sausages at the end of ripening period, in which different lowercase letters meant that amino acid content or Met-Mb content was significantly different ($p < 0.05$).

(Hu et al., 2021). The highest total amino acid concentration was also observed in a previous study of the sausages inoculated with *L. plantarum* MLK 14-2 (Yoo et al., 2015). Met-Mb was the oxidation product of myoglobin in meat products, which had a negative effect on color (Howes et al., 2019). There had been no significant difference ($p < 0.05$) in the content of Met-Mb between the control and the sample (**Figure 5B**), which indicated that replacing nitrite with *L. fermentum* did not cause an increase in Met-Mb content.

The Content of Biogenic Amines

Biogenic amines are usually found in a wide range of fermented foods and can bring health risks, in which histamine, tyramine, and phenethylamine are the primary cause of food poisoning. The European Union has established certain regulations on histamine with the maximum levels of 100 mg/kg (Sun et al., 2016). According to a previous report, the established maximum limits were 800 mg/kg for tyramine (Ercan et al., 2019) and 30 mg/kg for phenethylamine, respectively (Kandasamy et al., 2021). Seven kinds of biogenic amines including tyramine, putrescine, cadaverine, spermidine, tryptamine, phenylethylamine, and spermine were detected in the control (**Table 2**). For the sample, only tyramine, putrescine, cadaverine, spermidine, tryptamine, and spermine were detected, and no phenylethylamine was found. A previous report had suggested that the LAB used in the sausages might not contain phenylalanine decarboxylase activities, which resulted in no phenylethylamine produced (Pircher et al., 2007). Although the tyramine contents of sample was higher than the control, the contents of the two groups were all far below the specified limit (800 mg/kg). No histamine was detected both in the sample and the control, so the two group sausages had no histamine risk. In addition, the contents of spermidine and tryptamine decreased, and the contents of putrescine and cadaverine increased in the sample compared to the control. Hence, it is necessary to add other food additives together with the strain to inhibit the production of putrescine and cadaverine in future studies.

Sensory Analysis

Sensory analysis was performed by evaluating the texture, flavor, slice, color, taste, sourness, and overall acceptability of the sausages. **Figure 6** shows that the scores of the sample were similar to the control in the texture, slice, and color. The scores of taste, flavor, and sourness of the sample were better than those of the control. The relatively high acidity might be attributed to the production of lactic acid during fermentation of the LAB, which brought better and proper sourness (Odutayo et al., 2020). The better taste and flavor of the sample might be because the fermentation of the LAB could produce a variety of flavor components (Hu et al., 2019). Moreover, the inoculation of LAB could inhibit the lipid oxidation of the sausages, which prevents the unfavorite flavor (Hu et al., 2019). The result was consistent with the TBARS analysis (**Figure 3**) that the *L. fermentum* had stronger antioxidant capacity against lipid oxidation compared to the nitrite. Therefore, the overall acceptability of the sausages was better than the control, which was similar to a previous report that the LAB inoculation could make sausage quality better (Bachtarzi et al., 2020).

TABLE 2 | The biogenic amine content of the sausages at the end of ripening period.

Biogenic amine (mg/kg)	Sausage	
	Control	Sample
Tyramine	78.24^{b}	116.62^{a}
Putrescine	6.60^{b}	85.27^{a}
Cadaverine	163.30^{b}	462.13^{a}
Spermidine	4.53^{a}	2.50^{b}
Tryptamine	5.88^{a}	0.19^{b}
Phenylethylamine	6.15	ND
Spermine	28.68^{a}	31.21^{a}
Histamine	ND	ND

The superscripted letters a b c represent significantly different ($p < 0.05$) in the same line.

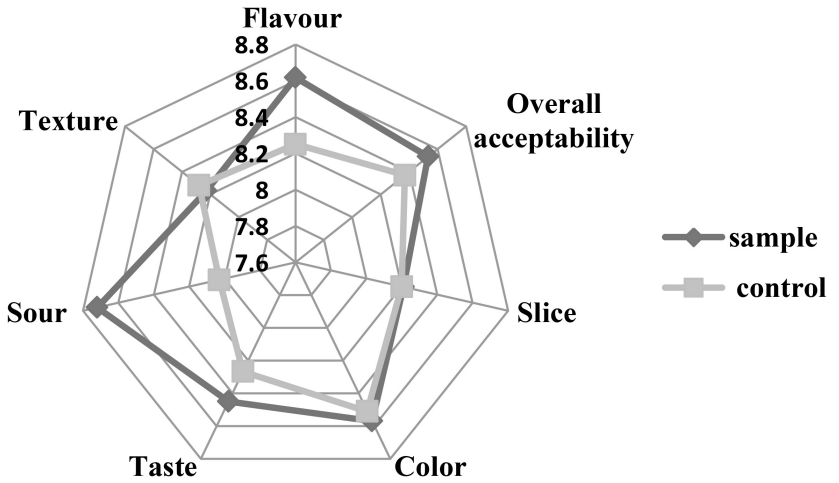

FIGURE 6 | The sensory analysis of the sausages.

DISCUSSION

The low pH of the sample sausages fermented by *L. fermentum* (**Figure 1**) signified that the acidification of the sample was much stronger than that of the control fermented spontaneously (Wang et al., 2013). The pH sharp drop of the samples might induce conformational changes of proteins and result in acid-induced gelation (Zeng et al., 2013). In addition, low pH might decrease the risk of food-borne pathogens and improve the safety of the sausages (Gao et al., 2014), which would extend shelf life of the sausages (Sun et al., 2017). Because the growth of food borne pathogens and spoilage bacteria would be inhibited under acidic conditions, the spoilage of the sausage might be suppressed.

There had no significance in a^* value ($p > 0.05$) between the sample and the control at the 20th day, which indicated that the *L. fermentum* had the color formation ability in meat products nitrite-free. The color formation ability might be because some LAB had nitric oxide synthase (NOS) activity, resulting in the production of NO, which reacted with myoglobin (Mb) in the inoculated sausages and generated the pink product of Mb-NO (Zhu et al., 2019). Compared to the control, the much lower b^* value of the sample reflected that the strain inoculation could inhibit lipid peroxidation. The oxidation might result in the oxidation of Fe^{2+}, which would cause the color of the sausages to appear brown (Ganhão et al., 2010). The color formation capacity and the antilipid oxidation ability of the strain indicated that the strain had the potential to replace nitrite for color development. In addition, nitrite can react with secondary amines to form nitrosamines (Sun et al., 2017), which has carcinogenic effects to humans. In this study, replacing nitrite with the *L. fermentum* significantly reduced the content of nitrite compared to the control (**Figure 2**). Therefore, replacing nitrite with the strain of *L. fermentum* decreased the residual of nitrite from the source and eliminate the carcinogenic risk of nitrite.

Lipid peroxidation will produce some harmful substances; therefore, the antioxidant function of the additives and the reduction of TBA value are very important (Gao et al., 2014). The strong antioxidant capacity of the strain *L. fermentum* against lipid oxidation (**Figure 3**) might be because the strain could scavenge free radical effectively (Chen et al., 2019). The sausage quality could be improved by preventing fat oxidation (Hu et al., 2019). In addition, the strain could inhibit the production of TVB-N (**Figure 4**), which is probably because the acidification process inhibited the growth of bacteriaceae and other bacteria (Sun et al., 2017). Because some microorganisms could secrete proteases, which might hydrolyze protein to produce nitrogen compounds including TVB-N (Sun et al., 2017).

The highest total amino acid concentration in the sample (**Figure 5A**) might be attributed to the strain hydrolyzed proteins forming the necessary amino acids required for growth (Hou et al., 2015). Amino acids play a key role in enhancing the flavor and increasing the nutrition of the sausages. The similar Met-Mb content in the control and the sample (**Figure 5B**) indicated that the strain *L. fermentum* had a similar ability as nitrite against Mb oxidation and avoided excessive production of Met-Mb. This ability might be due to the presence of Met-Mb reductase in the strain, which reduced Met-Mb to Mb and further produced Mb-NO (Zhu et al., 2019).

Small amounts of biogenic amines have important physiological effects on the human body, but if accumulated excessively, it would be life-threatening (Silla Santos, 1996). The results showed that substituting nitrite with the strain reduced the species of harmful biological amines and no phenylethylamine was detected in the sample (**Table 2**). Histamine is the most harmful amine and is closely related to human health problems (Nie et al., 2014). No histamine was detected in the sample, which might be because LAB could inhibit the growth of Enterobacteriaceae, which have been proven to be able to produce large amounts of histamine (Pircher et al., 2007). Even so, if other additives together with the strain were added to inhibit the production of tyramine, putrescine, and cadaverine, the biogenic amines risk could be reduced thoroughly, and the quality and safety of sausages would be greatly improved.

The quality of meat products depends on consumer' appreciation and acceptance. Therefore, sensory analysis is very important for meat products according to the sensory evaluation test. The inoculation of the *L. fermentum* enhanced the taste, flavor, sourness, and overall acceptability of the sample sausages (**Figure 6**). The higher acidification of the sample could inhibit the growth of the pathogens and spoilage bacteria and make the LAB dominate the microflora (Xiao et al., 2020), which further enhanced the flavor of the sausages. On the other hand, the previous report indicated that there was a synergistic effect between sourness and saltiness, and the sourness enhanced the salty taste of the sausages, thereby giving the sausages a better taste (Hu et al., 2021). In addition, the strain has strong antioxidant capacity against lipid oxidation (**Figure 3**), which might prevent the rancid flavor of lipids oxidation.

CONCLUSION

This study explored the positive effects of complete replacement of nitrite with the strain *L. fermentum* on the quality and safety of Chinese fermented sausages and evaluated the risk of this strain. The results revealed that the strain reduced the pH and the food-borne pathogens risk, and accelerated the acidification process and gelation formation of the sausages. In addition, the strain could produce the pink color similar to 50 mg/kg nitrite, significantly reducing the residual risk of nitrite in the sausages. In addition, the strain prevented fat oxidation, protein decomposition, and Mb oxidation and increased the free amino acid content. The strain reduced species of biogenic amines, and decreased the phenylethylamine, spermidine, and tryptamine risk. Some other additives that can inhibit the production of tyramine, putrescine, and cadaverine are necessary to replace nitrite with the strain *L. fermentum* together in the future research. Therefore, the strain has the potential to replace nitrite to produce healthier sausages.

DATA AVAILABILITY STATEMENT

The original contributions presented in the study are included in the article/supplementary material, further inquiries can be directed to the corresponding author/s.

AUTHOR CONTRIBUTIONS

YX was responsible for the method, data acquisition, curation, and analysis. YZ designed the study and drafted the original manuscript. Both authors contributed to the article and approved the submitted version.

FUNDING

The research was financially supported by the National Natural Science Foundation of China (No. 31501512) and the Shandong Province Key Research and Development Plan-Special Plan for Medical Food (No. 2019YYSP023).

REFERENCES

Bachtarzi, N., Speciale, I., Kharroub, K., Castro, C. D., Ruiz, L., and Ruas-Madiedo, P. (2020). Selection of exopolysaccharide-producing *Lactobacillus plantarum* (lactiplantibacillus plantarum) isolated from algerian fermented foods for the manufacture of skim-milk fermented products. *Microorganisms* 8:1101. doi: 10.3390/microorganisms8081101

Berardo, A., De Maere, H., Stavropoulou, D. A., Rysman, T., Leroy, F., and De Smet, S. (2016). Effect of sodium ascorbate and sodium nitrite on protein and lipid oxidation in dry fermented sausages. *Meat Sci.* 121, 359–364. doi: 10.1016/j.meatsci.2016.07.003

Chen, X., Li, J., Zhou, T., Li, J., Yang, J., Chen, W., et al. (2016). Two efficient nitrite-reducing *Lactobacillus* strains isolated from traditional fermented pork (Nanx Wudl) as competitive starter cultures for Chinese fermented dry sausage. *Meat Sci.* 121, 302–309. doi: 10.1016/j.meatsci.2016.06.007

Chen, Y., Li, Q., Xia, C., Yang, F., Xu, N., Wu, Q., et al. (2019). Effect of selenium supplements on the antioxidant activity and nitrite degradation of lactic acid bacteria. *World J. Microb. Bio.* 35, 1–13. doi: 10.1007/s11274-019-2609-x

Dabadé, D. S., den Besten, H. M. W., Azokpota, P., Nout, M. J. R., Hounhouigan, D. J., and Zwietering, M. H. (2015). Spoilage evaluation, shelf-life prediction, and potential spoilage organisms of tropical brackish water shrimp (Penaeus notialis) at different storage temperatures. *Food Microbiol.* 48, 8–16. doi: 10.1016/j.fm.2014.11.005

Drabik-Markiewicz, G., Dejaegher, B., De Mey, E., Kowalska, T., Paelinck, H., and Vander Heyden, Y. (2011). Influence of putrescine, cadaverine, spermidine or spermine on the formation of N-nitrosamine in heated cured pork meat. *Food Chem.* 126, 1539–1545. doi: 10.1016/j.foodchem.2010.11.149

Ercan, S. Ş, Soysal, Ç, and Bozkurt, H. (2019). Biogenic amine contents of fresh and mature kashar cheeses during refrigerated storage. *Food Health* 5, 19–29. doi: 10.3153/FH19003

Ganhão, R., Morcuende, D., and Estévez, M. (2010). Protein oxidation in emulsified cooked burger patties with added fruit extracts: influence on colour and texture deterioration during chill storage. *Meat Sci.* 85, 402–409. doi: 10.1016/j.meatsci.2010.02.008

Gao, Y. R., Li, D. P., and Liu, X. Y. (2014). Bacteriocin-producing *Lactobacillus sakei* C2 as starter culture in fermented sausages. *Food Control* 35, 1–6. doi: 10.1016/j.foodcont.2013.06.055

Geeta, and Yadav, A. S. (2017). Antioxidant and antimicrobial profile of chicken sausages prepared after fermentation of minced chicken meat with *Lactobacillus plantarum* and with additional dextrose and starch. *LWT Technol.* 77, 249–258. doi: 10.1016/j.lwt.2016.11.050

Guimarães, A., Santiago, A., Teixeira, J. A., Venâncio, A., and Abrunhosa, L. (2018). Anti-aflatoxigenic effect of organic acids produced by *Lactobacillus plantarum*. *Int. J. Food Microbiol.* 264, 31–38. doi: 10.1016/j.ijfoodmicro.10.025

Hou, J. C., Liu, F., Ren, D. X., Han, W. W., and Du, Y. O. (2015). Effect of culturing conditions on the expression of key enzymes in the proteolytic system of lactobacillus bulgaricus. *J. Zhejiang Univ. Sci. B* 16, 317–326. doi: 10.1631/jzus.B1400230

Howes, B. D., Milazzo, L., Droghetti, E., Nocentini, M., and Smulevich, G. (2019). Addition of sodium ascorbate to extend the shelf-life of tuna meat fish: a risk or a benefit for consumers? *J. Inorg. Biochem.* 200:110813. doi: 10.1016/j.jinorgbio.2019.110813

Hu, Y. Y., Chen, Q., Wen, R. X., Wang, Y., Qin, L. G., and Kong, B. (2019). Quality characteristics and flavor profile of Harbin dry sausages inoculated with lactic acid bacteria and *Staphylococcus xylosus*. *LWT Technol.* 114:108392. doi: 10.1016/j.lwt.2019.108392

Hu, Y. Y., Li, Y. J., Zhu, J. M., Kong, B. H., Liu, Q., and Chen, Q. (2021). Improving the taste profile of reduced-salt dry sausage by inoculating different lactic acid bacteria. *Food Res. Int.* 145:110391. doi: 10.1016/j.foodres.2021.110391

Kandasamy, S., Yoo, J., Yun, J., Kang, H. B., and Ham, J. S. (2021). Quantitative analysis of biogenic amines in different cheese varieties obtained from the korean domestic and retail markets. *Metabolites* 11:31. doi: 10.3390/metabo11010031

Kawahara, Y., Nakamura, M., Sakagami, I., and Suzuki, Y. (2006). Bright red color formation of cooked pork loin cured with lactic acid bacteria starter culture without adding nitrite during low-temperature storage. *Food Sci. Tech. Res.* 12, 101–107. doi: 10.3136/fstr.12.101

Khalique, A., Zeng, D., Shoaib, M., Wang, H., and Ni, X. (2020). Probiotics mitigating subclinical necrotic enteritis (sne) as potential alternatives to antibiotics in poultry. *AMB Express* 10:50. doi: 10.1186/s13568-020-00989-6

Li, P., Jia, S., Zhou, C., Fang, H., and Chen, C. (2017). Protective role of *Lactobacillus fermentum* R6 against *Clostridium perfringens* in vitro and in chicken breast meat under temperature abuse conditions. *Innov. Food Sci. Emerg.* 41, 117–123. doi: 10.1016/j.ifset.2017.03.001

Mologni, L., Daguer, H., Motta, G. E., Merlo, T. C., and Lindner, J. D. D. (2019). Interactions of preservatives in meat processing: formation of carcinogenic compounds, analytical methods, and inhibitory agents. *Food Res. Int.* 125:108608. doi: 10.1016/j.foodres.2019.108608

Nassu, R. T., Goncalves, L. A. G., Silva, M., and Beserra, F. J. (2003). Oxidative stability of fermented goat meat sausage with different levels of natural antioxidant. *Meat Sci.* 63, 43–49. doi: 10.1016/S0309-1740(02)00051-7

Nie, X., Zhang, Q., and Lin, S. (2014). Biogenic amine accumulation in silver carp sausage inoculated with *Lactobacillus plantarum* plus *Saccharomyces cerevisiae*. *Food Chem.* 153, 432–436. doi: 10.1016/j.foodchem.2013.12.093

Odutayo, O. E., Omonigbehin, E. A., Olawole, T. D., Ogunlana, O. O., and Afolabi, I. S. (2020). Fermentation enhanced biotransformation of compounds in the kernel of *Chrysophyllum albidum*. *Molecules* 25:6021. doi: 10.3390/molecules25246021

Pircher, A., Bauer, F., and Paulsen, P. (2007). Formation of cadaverine, histamine, putrescine and tyramine by bacteria isolated from meat, fermented sausages and cheeses. *Eur. Food Res. Technol.* 226, 225–231. doi: 10.1007/s00217-006-0530-7

Ren, D., Li, C., Qin, Y., Yin, R., Du, S., Ye, F., et al. (2014). In vitro evaluation of the probiotic and functional potential of *Lactobacillus* strains isolated from fermented food and human intestine. *Anaerobe* 30, 1–10. doi: 10.1016/j.anaerobe.2014.07.004

Silla Santos, M. H. (1996). Biogenic amines: their importance in foods. *Int. J. Food Microbiol.* 29, 213–231. doi: 10.1016/0168-1605(95)00032-1

Saravanakumar, K., Sathiyaseelan, A., Mariadoss, A., Chelliah, R., and Wang, M. H. (2020). *Lactobacillus rhamnosus* GG and biochemical agents enrich the shelf life of fresh-cut bell pepper (capsicum annuum l. var. grossum (l.) sendt). *Foods* 9:1252. doi: 10.3390/foods9091252

Sharafedtinov, K. K., Plotnikova, O. A., Alexeeva, R. I., Sentsova, T. B., and Mikelsaar, M. (2013). Hypocaloric diet supplemented with probiotic cheese improves body mass index and blood pressure indices of obese hypertensive patients-a randomized double-blind placebo-controlled pilot study. *Nutr. J.* 12:138. doi: 10.1186/1475-2891-12-138

Song, Y., Liu, L., Shen, H., You, J., and Luo, Y. (2011). Effect of sodium alginate-based edible coating containing different anti-oxidants on quality and shelf life of refrigerated bream (Megalobrama amblycephala). *Food Control* 22, 608–615. doi: 10.1016/j.foodcont.2010.10.012

Sun, F., Kong, B., Chen, Q., Han, Q., and Diao, X. (2017). N-nitrosoamine inhibition and quality preservation of Harbin dry sausages by inoculated with *Lactobacillus pentosus*, *Lactobacillus curvatus* and *Lactobacillus sake*. *Food Control* 73, 1514–1521. doi: 10.1016/j.foodcont.2016.11.018

Sun, X., Zhou, K., Gong, Y., Zhang, N., Yang, M., Qing, D. D., et al. (2016). Determination of biogenic amines in Sichuan-style spontaneously fermented sausages. *Food Anal. Methods* 9, 2299–2307. doi: 10.1007/s12161-016-0417-6

Tu, P., Bian, X., Liang, C., Gao, B., Ru, H., Knobloch, T. J., et al. (2018). Characterization of the functional changes in mouse gut microbiome associated with increased *Akkermansia muciniphila* population modulated by dietary black raspberries. *ACS Omega* 3, 10927–10937. doi: 10.1021/acsomega.8b00064

Visessanguan, W., Benjakul, S., and An, H. (2003). Purification and characterization of cathepsin L in arrowtooth flounder (Atheresthes stomias) muscle. *Comp. Biochem. Physiol. B Biochem. Mol. Biol.* 134, 477–487. doi: 10.1016/S1096-4959(02)00293-2

Wang, X. H., Ren, H. Y., Liu, D. Y., Zhu, W. Y., and Wang, W. (2013). Effects of inoculating *Lactobacillus sakei* starter cultures on the microbiological quality and nitrite depletion of Chinese fermented sausages. *Food Control* 32, 591–596. doi: 10.1016/j.foodchem.2016.04.036

Wang, X. H., Ren, H. Y., Wang, W., and Xie, Z. J. (2016). Effects of a starter culture on histamine reduction, nitrite depletion and oxidative stability of fermented sausages. *J. Food Saf.* 36, 195–202. doi: 10.1111/jfs.12227

Xiang, R., Cheng, J. R., Zhu, M. J., and Liu, X. M. (2019). Effect of mulberry (Morus alba) polyphenols as antioxidant on physiochemical properties, oxidation and bio-safety in Cantonese sausages. *LWT Food Sci. Technol.* 116:108504. doi: 10.1016/j.lwt.2019.108504

Xiao, Y., Liu, Y., Chen, C., Xie, T., and Li, P. (2020). Effect of *Lactobacillus plantarum* and staphylococcus xylosus on flavour development and bacterial communities in chinese dry fermented sausages. *Food Res. Int.* 135:109247. doi: 10.1016/j.foodres.2020.109247

Yoo, S. A., Na, C. S., Park, S. E., Seo, S. H., and Son, H. S. (2015). Characterization of fermented sausages using *Lactobacillus plantarum* MLK 14-2 as starter culture. *J. Korean Soc. Appl. Biol. Chem.* 58, 349–358. doi: 10.1007/s13765-015-0052-8

Zeng, X. F., Xia, W. S., Jiang, Q. X., and Yang, F. (2013). Effect of autochthonous starter cultures on microbiological and physico-chemical characteristics of Suan yu, a traditional Chinese low salt fermented fish. *Food Control* 33, 344–351. doi: 10.1016/j.foodcont.2013.03.001

Zhang, X., Kong, B., and Xiong, Y. L. (2007). Production of cured meat color in nitrite-free Harbin red sausage by *Lactobacillus fermentum* fermentation. *Meat Sci.* 77, 593–598. doi: 10.1016/j.meatsci.2007.05.010

Zhang, Y., Qin, Y., Wang, Y., Huang, Y., Li, P., and Li, P. (2020). *Lactobacillus plantarum* LPL-1, a bacteriocin producing strain, changed the bacterial community composition and improved the safety of low-salt fermented sausages. *LWT Food Sci. Technol.* 128:109385. doi: 10.1016/j.lwt.2020.109385

Zhu, Y., Wang, P., Guo, L., Wang, J., Han, R., Sun, J., et al. (2019). Effects of partial replacement of sodium nitrite with *Lactobacillus pentosus* inoculation on quality of fermented sausages. *J. Food Process. Preserv.* 43:e13932. doi: 10.1111/jfpp.13932

Zhu, Y. L., Guo, L. P., and Yang, Q. L. (2020). Partial replacement of nitrite with a novel probiotic *Lactobacillus plantarum* on nitrate, color, biogenic amines and gel properties of Chinese fermented sausages. *Food Res. Int.* 137:109351. doi: 10.1016/j.foodres.2020.109351

Conflict of Interest: The authors declare that the research was conducted in the absence of any commercial or financial relationships that could be construed as a potential conflict of interest.

Publisher's Note: All claims expressed in this article are solely those of the authors and do not necessarily represent those of their affiliated organizations, or those of the publisher, the editors and the reviewers. Any product that may be evaluated in this article, or claim that may be made by its manufacturer, is not guaranteed or endorsed by the publisher.

frontiers in Microbiology

ORIGINAL RESEARCH
published: 04 August 2021
doi: 10.3389/fmicb.2021.702725

Heavy Metal Resistance in *Salmonella* Typhimurium and Its Association With Disinfectant and Antibiotic Resistance

*Ghulam Raza Mustafa[1†], Ke Zhao[1†], Xueping He[1], Shujuan Chen[2], Shuliang Liu[2], Ahsan Mustafa[3], Li He[2], Yong Yang[2], Xiumei Yu[1], Petri Penttinen[1], Xiaolin Ao[2], Aiping Liu[2], Muhammad Zubair Shabbir[4], Xuebin Xu[5] and Likou Zou[1]**

[1] College of Resources, Sichuan Agricultural University, Chengdu, China, [2] College of Food Science, Sichuan Agricultural University, Ya'an, China, [3] Key Laboratory for Animal Disease-Resistance Nutrition of China, Ministry of Education, Institute of Animal Nutrition, Sichuan Agricultural University, Chengdu, China, [4] Institute of Microbiology, University of Veterinary and Animal Sciences, Lahore, Pakistan, [5] Shanghai Municipal Center for Disease Control and Prevention, Shanghai, China

OPEN ACCESS

Edited by:
Fereidoun Forghani, IEH Laboratories and Consulting Group, United States

Reviewed by:
Govindaraj Dev Kumar, University of Georgia Griffin Campus, United States
Jianmin Zhang, South China Agricultural University, China

***Correspondence:**
Likou Zou
zoulikou@sicau.edu.cn

† These authors have contributed equally to this work

Specialty section:
This article was submitted to Food Microbiology, a section of the journal Frontiers in Microbiology

Received: *29 April 2021*
Accepted: *05 July 2021*
Published: *04 August 2021*

Citation:
Mustafa GR, Zhao K, He X, Chen S, Liu S, Mustafa A, He L, Yang Y, Yu X, Penttinen P, Ao X, Liu A, Shabbir MZ, Xu X and Zou L (2021) Heavy Metal Resistance in SalmonellaTyphimurium and Its Association With Disinfectant and Antibiotic Resistance. Front. Microbiol. 12:702725. doi: 10.3389/fmicb.2021.702725

Metals are widely used in animal feed for their growth-stimulating and antimicrobial effects, yet their use may potentially promote the proliferation of antibiotic resistance through co-selection. We studied the prevalence and associations of metal, antibiotic, and disinfectant resistances of 300 *Salmonella* Typhimurium isolates from pig meat, pig manure, chicken meat, poultry manure, and human stool from Sichuan, China. Seventy four percent of the 300 *Salmonella* Typhimurium isolates were considered resistant to Cu, almost 50% to Zn and Cr, over 25% to Mn and Cd, and almost 10% to Co. Most of the isolates carried at least one heavy metal resistance gene (HMRG). The Cr-Zn-Cd-resistance gene *czcD* was carried by 254 isolates and the Cu-resistance genes *pcoR* and *pcoC* by 196 and 179 isolates, respectively. Most of the isolates were resistant to at least one antibiotic and almost 80% were multidrug-resistant. The prevalence of resistance to six antibiotics was higher among the pig meat and manure isolates than among other isolates, and that of streptomycin and ampicillin were highest among the pig meat isolates and that of ciprofloxacin and ofloxacin among the pig manure isolates. From 55 to 79% of the isolates were considered resistant to disinfectants triclosan, trichloroisocyanuric acid, or benzalkonium chloride. The metal resistances and HMRGs were associated with resistance to antibiotics and disinfectants. Especially, Cu-resistance genes were associated with resistance to several antibiotics and disinfectants. The transfer of the Cr-Zn-Cd-resistance gene *czcD*, Cu-resistance gene *pcoC,* and Co-Ni-resistance gene *cnrA* into *Escherichia coli* and the increased Cu-resistance of the transconjugants implied that the resistance genes were located on conjugative plasmids. Thus, the excessive use of metals and disinfectants as feed additives and in animal care may have the potential to promote antibiotic resistance through co-selection and maintain and promote antibiotic resistance even in the absence of antibiotics.

Keywords: *Salmonella* Typhimurium, heavy metal resistance, disinfectant resistance, antibiotic resistance, heavy metal resistance gene, conjugation

INTRODUCTION

Salmonella infections are a major public health concern worldwide (Sodagari et al., 2020). *Salmonella* is the second most common cause of food-borne diseases worldwide and is associated with more deaths than any other food-borne disease in the developed countries (WHO, 2020). Food-borne Disease Active Surveillance Network (Foodnet) reported *Salmonella* as the leading cause of food-borne disease-related deaths in the United States (Barton Behravesh et al., 2011). Among the food-borne infections caused by a single etiologic agent in the United States in 2015, *Salmonella* was responsible for 34% of the outbreaks, 39% of the illnesses, 64% of the hospitalizations, and 60% of the deaths (Dewey-Mattia et al., 2018). The European Food Safety Authority (EFSA) confirmed salmonellosis as the second most common zoonosis with over 90,000 confirmed cases in 2017 (EFSA and ECDC, 2018). The food-borne surveillance system in China suggested that *Salmonella* was the second most common bacteria causing food-borne outbreaks during 2000–2014 (Luo et al., 2017). Thus, the *Salmonella* infection-related mortality and morbidity burden societies worldwide (Majowicz et al., 2010). For example, in England, the *Salmonella* infections, characterized by diarrhea, fever, and abdominal cramps, leading to over 11,000 annual GP consultations (Tam et al., 2012; Barr and Smith, 2014).

More than 2,600 serotypes of *Salmonella* have been identified (Takaya et al., 2020). *Salmonella* Typhimurium is one of the predominant serotypes in many countries, including China (Ceyssens et al., 2015; Wang Y. et al., 2017; Simpson et al., 2018) and it has held first or second place in China for many years (Ran et al., 2011; Wang Y. et al., 2017). *Salmonella* Typhimurium was also reported as the most frequently isolated serotype of non-typhoidal *Salmonella* from food-borne illnesses in different provinces of China (Liang et al., 2015), which represented 25.5, 29.44, and 39.7%, of the isolates obtained from diarrheal disease surveillance between 2006-2010 in Shanghai, 2010–2014 and 2013–2018 in Shenzhen, China (Zhang et al., 2014; Li W. et al., 2017; Shen et al., 2020). *Salmonella* is associated with a wide variety of foods, yet animal products, especially pig and poultry, are the main source of *Salmonella* (Hugas and Beloeil, 2014; Antunes et al., 2016; Demirbilek, 2017; Heredia and García, 2018). The routes of transmission for *Salmonella* Typhimurium include contaminated meat, eggs, and manure (Antunes et al., 2016; Chousalkar et al., 2018; Kumar et al., 2019). With the development of China, the average intake of meat, especially pig increased from 37.1 g/day in 1992 to 64.3 g/day per person in 2012 and was expected to surpass 100 g/day people by 2020 which has indirectly increased the risk of food-borne zoonoses, including salmonellosis (He et al., 2016; CIIN, 2018a,b; Pan et al., 2018, 2019). In China, *Salmonella* Typhimurium strains are commonly isolated from retail meat, particularly pig, suggesting a link between human infections with this serotype and pig products.

Antibiotics have commonly been used to treat animal diseases and as growth promoters (Allen et al., 2013). However, a substantial amount of the antibiotics are excreted in feces and enter soil via manure (Kumar et al., 2005). Due to food safety and health issues, many countries, e.g., in the European Union, have banned the use of antibiotics in the feed of animals as growth promoters (Burch, 2006). Both WHO and individual countries have introduced guidelines to withdraw medicated feed additives to combat antimicrobial resistance from animal resources (Hu and Cowling, 2020). Metal-containing compounds are also widely used animal feed additives (Cavaco et al., 2011; Argudín et al., 2016). Metals, e.g., copper, zinc, cobalt, chromium, and manganese, are widely used in animal feed for their growth-stimulating and antimicrobial effects; copper and silver are commonly used as disinfectants and preservatives, and mercury, lead, arsenic, and cadmium can be found as contaminants in animal feed (Seiler and Berendonk, 2012; Korish and Attia, 2020). However, the use of heavy metals at high concentrations causes problems due to their toxicity, bioaccumulation, and biomagnification in the food chain (**Figure 1**; Eisler, 1993). Heavy metal contamination in meat and the prevalence of these pollutants in the environment is a risk for both food safety and human health (Khan et al., 2008; Bamuwamye et al., 2015; Lu et al., 2015). Notably, the use of metals may potentially promote the proliferation of antibiotic resistance through co-selection; the metal and antibiotic resistance are often linked either due to co-location of the resistance genes, a shared resistance mechanism, or co-regulation of resistance pathways (Baker-Austin et al., 2006; Deng et al., 2017; Pal et al., 2017; Yang et al., 2020). The disinfectant resistance genes and heavy metal resistance genes (HMRGs) are commonly located in mobile genetic elements (MGEs) (Frost et al., 2005). The role of metals, antibiotics, and disinfectants in the development and spread of antimicrobial resistance has raised concerns (Bragg et al., 2014; Roosa et al., 2014; Zou et al., 2014; Di Cesare et al., 2016). However, the co-occurrence of heavy metal, antibiotic and disinfectant resistance in *Salmonella* Typhimurium isolates from retail foods, animal manure, and human stool has not been widely investigated. Therefore, we studied the prevalence and associations of resistances of *Salmonella* Typhimurium isolates from pig meat, pig manure, chicken meat, poultry manure, and human stool from Sichuan, China.

MATERIALS AND METHODS

Bacterial Strains

The 300 *Salmonella* Typhimurium strains analyzed in this study were isolated from January 2016 to December 2018 in Sichuan, China, from pig meat (n = 182), pig manure (n = 23), chicken meat (n = 30), poultry manure (n = 27), and stool of hospitalized diarrhea patients (n = 38). The details of sampling and location of the strains are available in **Supplementary Tables 4A,B**.

Isolates and Serotyping

Collected specimens were tested for *Salmonella* using the following protocol. Stool samples from diarrhea patients were enriched in Selenite Brilliant Green broth (SBG, CHROMagar, Paris, France) for 16–22 h at 37°C. For the isolation of *Salmonella* from pig and chicken meat and manure samples, the method described by the United States Department of Agriculture Food

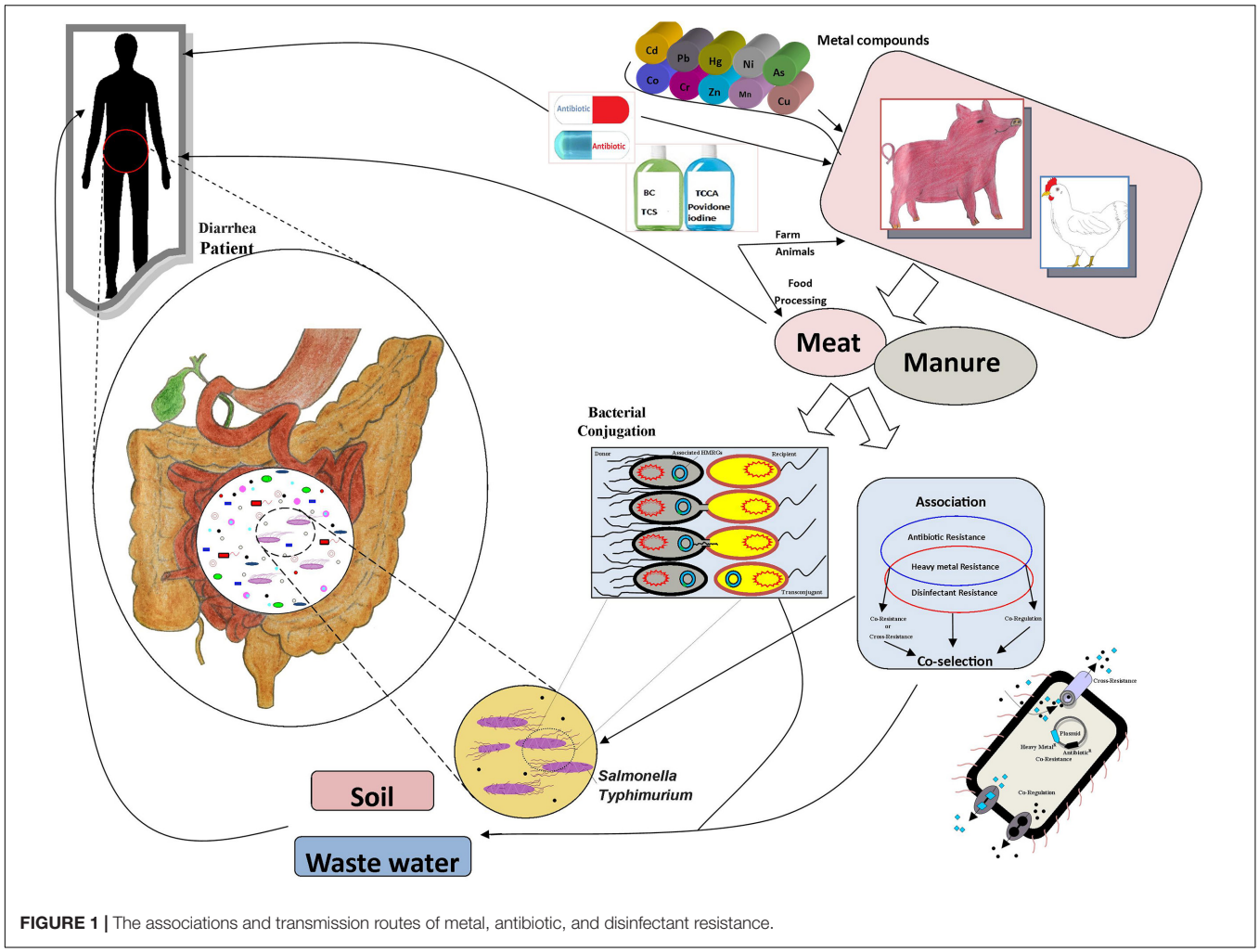

FIGURE 1 | The associations and transmission routes of metal, antibiotic, and disinfectant resistance.

Safety and Inspection Service was used (Cui et al., 2006; Guo et al., 2011). Twenty five g portions of meat were used for enrichment and each sample was placed in separate sterile Erlenmeyer flasks with 225 mL buffered peptone water then incubated at 37°C in a water bath with shaking at 120 rpm for 6 h. After pre-enrichment, 1 and 10 mL of pre-enriched solutions were transferred to 100 mL each of the Rappaport-Vassiliadis (RV; Beijing Land Bridge Technology Co., Ltd.) and tetrathionate (TT; Beijing Land Bridge Technology Co., Ltd., Beijing, China) broths, respectively, and incubated at 42°C in a water bath with shaking at 160 rpm for 24 h. One loopful of TT broth and RV broth were streaked onto xylose lysine tergitol agar plates (Beijing Land Bridge Technology Co., Ltd.), and onto agar of xylose lysine deoxycholate (Beijing Land Bridge Technology Co., Ltd.) respectively, and incubated at 37°C for 24 h. Three plausible *Salmonella* colonies from each plate were inoculated onto urea agar slants (Beijing Land Bridge Technology Co., Ltd.) and triple sugar iron (Beijing Land Bridge Technology Co., Ltd.), and incubated at 35°C for 24 h. Further, typical *Salmonella* phenotypes were confirmed by polymerase chain reaction (PCR) as described previously (Cui et al., 2006). A 284 bp PCR product targeting *invA* was amplified using the primers *invA* 139 (5′-GTGAAATTATCGCCA CGTTCGGGCAA-3′) and *invA* 141 (5′-TCATCGCACCGT CAAAGGAACC-3′) (Deng et al., 2017). Only one isolate from each *Salmonella* positive sample was randomly selected and included in this study (Vo et al., 2006). Confirmed isolates were stored in Tryptone Soya Broth (Hangzhou Microbial Reagent Co., Ltd.) containing 20% glycerol at −80°C until use. Confirmed *Salmonella* isolates were further serotyped according to the Kauffmann-White scheme, by slides using a microtiter agglutination test for O and H antigens, as described in the manufacturer's instructions (SSI, Copenhagen, Denmark).

PCR Amplification of Heavy Metal Resistance Genes

The total DNA from *Salmonella* Typhimurium strains was extracted using TIANamp bacteria DNA kit (TIANGEN Biotect (Beijing) Co., Ltd.) according to the manufacturer's instructions. DNA extractions were stored at −20°C for further analysis. HMRGs *cnrA, nccA, pbrA, pcoA, pcoC, pcoR, chrB, czcB, czcD, arsB, merA,* and *cadD* were amplified using previously published primers (**Supplementary Table 1**). PCR amplification was carried

TABLE 1 | Incidence of metal resistance among 300 *Salmonella* Typhimurium strains isolated from pig meat, pig manure, poultry manure, chicken meat, and human stool samples.

	MIC									Resistance
	12.5	**25**	**50**	**100**	**200**	**400**	**800**	**1600**	**3200**	**%**
Cu				1	1	76	**222**			74
Zn			4			152	**143**			47.7
Mn			1				216	**83**		27.7
Cd	5	207	**88**							29.3
Co		1		2	270	**27**				9
Cr						163	**137**			45.7

The strains with MIC higher than that of control strains E. coli ATCC 10536 and Salmonella H9812 were considered resistant. The numbers of resistant strains are in bold.

out in a 25 μL reaction volume, comprising 10 μL of 2 × T5 Super PCR Mix, 2 μL of 5 × Enhancer Buffer, 1 μL of each forward and reverse primer, 2U of Taq-polymerase (Promega, Madison, WI, United States) and 2 μL of template DNA or 2 μL of sterile deionized water as a negative control. The thermal program included initial denaturation at 98°C for 3 min, followed by 34 cycles of denaturation at 98°C for 10 s, annealing at the Tm of primer pair (**Supplementary Table 1**) for 10 s and extension at 72°C for 20 s, and a final extension at 72°C for 2 min. The success of amplification was verified using electrophoresis in 0.8% agarose gel (GENEI, Bengaluru, India) with a 2,000 bp DNA molecular weight marker as reference (Fermentas, Waltham, MA, United States) and visualized using a gel documentation system (BIO-RAD, Hercules, CA, United States). Appropriate positive controls for amplification were selected from retail meat *Salmonella* Typhimurium isolates. The positive controls were confirmed by sequencing the amplicons (GENEWIZ, Inc., Germantown, MD, United States). All results were confirmed by at least two independent assays.

Determination of Minimal Inhibitory Concentrations (MICs)

The minimal inhibitory concentrations (MICs) of metal ions, disinfectants, and antibiotics for *Salmonella* Typhimurium were determined using the agar microdilution method as described by the Clinical and Laboratory Standards Institute (CLSI) (Weinstein and Lewis, 2020). Mueller-Hinton agar plates were inoculated with bacteria suspended in 0.85% NaCl to a turbidity equivalent to a 0.5 McFarland using a multipoint inoculator (Oxoid, Lenexa, KS, United States) with approximately 10^4 CFU per spot. The plates were incubated at 37°C for 18–24 h. The MICs were determined as the lowest concentration of the metal that inhibited the growth of strains completely after 18–24 h of culture at 37°C. All experiments were run in triplicate.

The MICs of copper ($CuCl_2.2H_2O$), chromium ($CrCl_3.6H_2O$), cobalt ($CoCl_2$), cadmium ($CdCl_2$), zinc ($ZnSO_4$), and manganese Mn ($MnCl_2$) (Alfa Aesar, Shanghai, China) were determined. Doubling dilutions of the heavy metal stock solutions were incorporated into Mueller-Hinton agar plates with final concentrations ranging from 0.25 to 3200 mg L^{-1}. *Escherichia coli* ATCC 10536 and *Salmonella* H9812 were used as the quality control strain in the tests (Zou et al., 2014; Deng et al., 2017; Yang et al., 2020). The MICs of benzalkonium chloride (BC), Trichloroisocyanuric acid (TCCA), (Chengdu Best-Reagent Company, Chengdu, China; > 98% purity), Triclosan (TCS) (J&K Chemical; > 98% purity), were determined at concentration ranges of 0.125-1024 mg L^{-1} for BC and TCCA and 0.03125–1.0 mg L^{-1} for TCS. *Escherichia coli* ATCC 10536 and *Salmonella* H9812 were used as the quality control strain in the tests (Zou et al., 2014; Deng et al., 2017; Yang et al., 2020). In the MIC assays of streptomycin (S), sulfonamides (S3), tetracycline (TET), ampicillin (AMP), nalidixic acid (NA), chloramphenicol (C), sulfamethoxazole (SXT), trimethoprim (TMP), gentamicin (CN), amoxicillin/clavulanic acid (AMC), ciprofloxacin (CIP), ofloxacin (OFX), ceftazidime (CAZ) and cefotaxime (CTX) (Hangzhou Microbial Reagent Co., Ltd., China), the breakpoints for antibiotic resistance and/or susceptibility were determined as recommended by the Clinical and Laboratory Standards Institute (CLSI). *Escherichia coli* ATCC 25922 and 35218 strain were used for quality control (Wang J. et al., 2017).

Conjugation Experiment

The transfer of HMRGs was determined in a conjugation experiment using mixed broth cultures as previously described

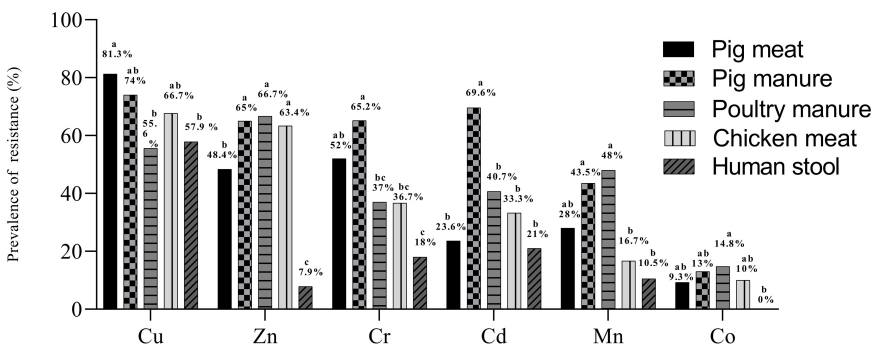

FIGURE 2 | Prevalence of resistance to Cu, Zn, Mn, Cd, Co, and Cr among *Salmonella* Typhimurium isolates from pig meat, pig manure, poultry manure, chicken meat, and human stool. Different lowercase letters indicate statistically significant differences between groups ($P < 0.05$).

TABLE 2 | Prevalence of heavy metal resistance genes among 300 *Salmonella* Typhimurium isolates.

Heavy metal resistance gene	Number of isolates (n)	Prevalence (%)
czcD	254	84.7
pcoR	196	65.3
pcoC	179	59.7
cnrA	155	51.7
nccA	153	51
cadD	131	43.7
merA	104	34.7
pbrA	63	21
pcoA	61	20.3
chrB	18	6
czcB	17	5.7
arsB	15	5

(Cai et al., 2008). Isolates with the highest resistance against copper and other metals were chosen as donors. Plasmid-free *Escherichia coli* J53 strain resistant to sodium azide and sensitive to the metals used in this study was selected as a recipient. Donor and recipient strains were grown on trypticase soy agar (TSA) plates overnight, single colonies of donor and recipient were inoculated into 30 mL of Mueller Hinton Broth (MHB) and grown at 37°C for 18 h, after which the recipient and donor strains were mixed at 10:1 (v = v) proportion. Subsequently, 1 mL of the mixture was inoculated onto a sterilized membrane on Mueller Hinton Agar (MHA) and incubated at 37°C for 18 h. The trans-conjugant bacteria were suspended into 3 mL of 0.9% NaCl, and serial dilutions were spread on MHA plates containing 200–400 μg/mL copper and 100 μg/mL sodium azide (Wang et al., 2003; Xu et al., 2007). Plates were incubated at 37°C and inspected at 24 and 48 h. The transfer of heavy metal resistance determinants was determined by amplifying the Cr-Zn-Cd-resistance gene *czcD*, Cu-resistance gene *pcoC,* and Co-Ni-resistance gene *cnrA* using DNA from trans-conjugant bacteria as a template. The MIC of copper ($CuCl_2.2H_2O$) for the trans-conjugants were determined with final concentrations ranging from 100 to 800 μg L^{-1}. The conjugation experiment was repeated at least twice.

Statistical Analysis

Association of the metal resistances and HMRGs with antibiotic and disinfectant resistance in *Salmonella* Typhimurium were determined using the χ^2-test of independence or Fisher's exact test was performed to analyze data using SPSS v. 21. *P*-value less than 0.05 was considered statistically significant.

The data about prevalence were analyzed using one-way analysis of variance (ANOVA) and Duncan's multiple range tests in SAS statistical software (SAS Institute; Cary, NC, United States). Differences were considered statistically significant at $P \leq 0.05$. The results were visualized using GraphPad prism 8.0.1. (GraphPad Software, San Diego, CA, United States).

RESULTS

Metal Resistance

Over 98% of the 300 *Salmonella* Typhimurium isolates had MICs of 400–800 mg L^{-1} for Cu, 400–800 mg L^{-1} for Zn, 800–1600 mg L^{-1} for Mn, 25–50 mg L^{-1} for Cd, 200–400 mg L^{-1} for Co and 400–800 mg L^{-1} for Cr (**Table 1**). Compared to *E. coli* ATCC 10536 and *Salmonella* H9812, 74% (n = 222), 47.7% (n = 143), 45.7% (n = 137), 27.7% (n = 83), 29.3% (n = 88), and 9% (n = 27) of the isolates had higher MIC for Cu, Zn, Cr, Mn, Cd and Co, respectively, and were considered resistant. The prevalence of Cu resistance was higher among the isolates from pig meat than among the human stool and poultry manure isolates ($P < 0.05$) (**Figure 2**). The prevalence of Zn resistance was highest among the isolates from pig manure, poultry manure, and chicken meat, second highest among the pig meat isolates, and lowest among the human stool isolates ($P < 0.05$).

The prevalence of Cr resistance was highest among the isolates from pig manure and lowest among the human stool isolates ($P < 0.05$). The prevalence of Cd resistance was higher among the isolates from pig manure than among the other isolates ($P < 0.05$). The prevalence of Mn resistance was highest among the isolates from pig and poultry manure and lowest among the chicken meat and human stool isolates ($P < 0.05$). None of the human stool isolates showed Co resistance and among the other isolates, the prevalence of resistance was on the same level.

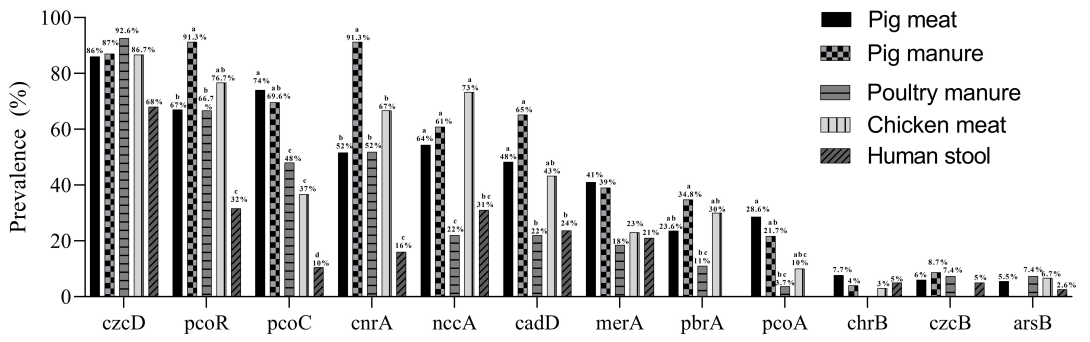

FIGURE 3 | Prevalence of heavy metal resistance genes among *Salmonella* Typhimurium isolates from pig meat, pig manure, poultry manure, chicken meat, and human stool. Different lowercase letters indicate statistically significant differences between groups ($P < 0.05$).

TABLE 3 | Prevalence of antibiotic resistance among 300 *Salmonella* Typhimurium isolates.

Antibiotic resistance	Number of isolates	Prevalence (%)
S	237	79
S3	234	78
TET	228	76
AMP	216	72
NA	194	64
C	180	60
SXT	171	57
TMP	165	55
CN	123	41
AMC	54	18
CIP	27	9
OFX	18	6
CAZ	3	1
CTX	3	1

In total, 97% (n = 291) of the isolates carried at least one heavy metal resistance gene (HMRG). A total of 132 gene combinations were found (**Supplementary Table 2**). The Cr-Zn-Cd-resistance gene *czcD* was carried by 254 isolates. The Cu-resistance genes *pcoR* and *pcoC* were found in 196 and 179 isolates, respectively. The Co-Ni-resistance gene *cnrA,* Ni-Cr-Cd-resistance gene *nccA,* and Cd-resistance gene *cadD* were carried by 155, 153, and 131 the isolates, respectively. The Hg-resistance gene *merA,* Pb-resistance gene *pbrA,* Cu-resistance gene *pcoA,* and Cr-resistance gene *chrB* were carried by 104, 63, 61, and 18 isolates, respectively. The Cr-Zn-Cd-resistance gene *czcB* and As-resistance gene *arsB* were carried by 17 and 15 isolates (**Table 2**).

The prevalence of *pcoR* and *cnrA* were highest among the pig manure isolates and lowest among the human stool isolates ($P < 0.05$) (**Figure 3**). The prevalence of *pcoC* was highest among the pig meat and manure isolates and lowest among the human stool isolates ($P < 0.05$). The prevalence of *nccA* was highest among the chicken meat isolates and lowest among the poultry manure isolates ($P < 0.05$). The prevalence of *cadD* was higher among the pig meat, pig manure, and chicken meat isolates than among the poultry manure and human stool isolates ($P < 0.05$). The prevalence of *pbrA* was higher among the pig manure isolates than among the poultry manure isolates ($P < 0.05$). The prevalence of *pcoA* was higher among the pig meat isolates than among the poultry manure isolates ($P < 0.05$).

Antibiotic Resistance

A total of 287 *Salmonella* Typhimurium isolates were resistant to at least one antibiotic; all the 23 pig manure isolates, 98.4% of the pig meat isolates (n = 179), 97.4% of the human stool isolates (n = 37), 86.7% of the chicken meat isolates (n = 26) and 81.5% of the poultry manure isolates (n = 22). Over 200 isolates were resistant to streptomycin (S), sulfonamides (S3), tetracycline (TET), or ampicillin (AMP), over 120 isolates to nalidixic acid (NA), chloramphenicol (C), sulfamethoxazole (SXT), trimethoprim (TMP) or gentamicin (CN), and less than 55 to amoxicillin/clavulanic acid (AMC), ciprofloxacin (CIP), ofloxacin (OFX), ceftazidime (CAZ) or cefotaxime (CTX) (**Table 3**).

The prevalence of resistance to S and AMP was higher among the pig meat isolates than among the poultry manure, chicken meat, and human stool isolates ($P < 0.05$) (**Figure 4**). The prevalence of resistance to S3, TET, C, SXT, TMP, and CN was highest among the pig meat and manure isolates ($P < 0.05$). The prevalence of resistance to CIP and OFX was highest among the pig manure isolates ($P < 0.05$). The prevalence of resistance to AMC was higher among the pig meat and manure isolates than among the human stool isolates ($P < 0.05$). The prevalence of resistance to NA was higher among the pig and chicken meat isolates than among the poultry manure isolates ($P < 0.05$). None of the pig and chicken meat and poultry manure isolates were resistant to CAZ, and none of the pig meat and pig and poultry manure isolates were resistant to CTX.

A total of 77 resistance profiles were observed among the isolates. A multiple resistance profile TET-AMP-SXT-C-NA-TMP-CN-S3-S was carried by 36 isolates, TET-AMP-SXT-C-TMP-S3-S by 25 isolates,

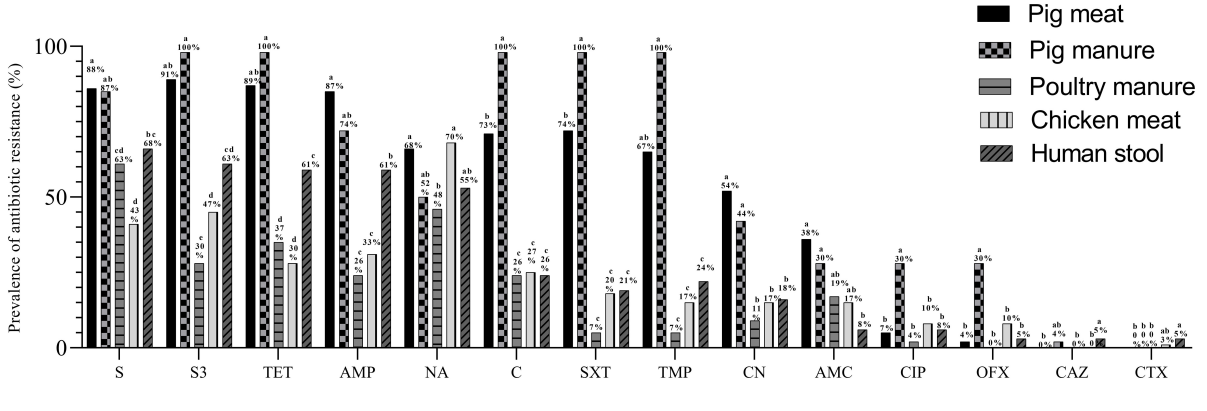

FIGURE 4 | Prevalence of antibiotic resistance among *Salmonella* Typhimurium isolates from pig meat, pig manure, poultry manure, chicken meat, and human stool. Different lowercase letters indicate statistically significant differences between groups ($P < 0.05$).

TABLE 4 | Incidence of disinfectants among 300 *Salmonella* Typhimurium strains isolated from pig meat, pig manure, poultry manure, chicken meat, and human stool samples.

	MIC										Resistance
	2	**4**	**8**	**16**	**32**	**64**	**128**	**256**	**512**	**1024**	**%**
BC	17	3	42	**181**	**18**	**39**					79.3
TCCA					33		4	45	**149**	**69**	72.7
	MIC										**Resistance**
	0.0313		**0.0625**		**0.125**		**0.25**		**0.5**	**1**	
Triclosan (TCS)	112		24		**46**		**77**		**39**	**2**	55

The strains with MIC higher than that of control strain E. coli ATCC 10536 and Salmonella H9812 were considered resistant. The numbers of resistant strains are in bold.

TET-AMC-AMP-SXT-C-NA-TMP-CN-S3-S by 23 isolates, and TET-AMP-S3-S by 16 isolates (**Supplementary Table 3**).

A total of 238 isolates were multidrug-resistant (MDR) with resistance to at least three classes of antibiotics. The prevalence of MDR was highest among pig manure isolates (100%, $n = 23$) followed by pig meat isolates (92.3%, $n = 168$), human stool isolates (68.4%, $n = 26$), poultry manure isolates (40.7%, $n = 11$) and chicken meat isolates (36.6%, $n = 11$).

Disinfectant Resistance

The MICs of *E. coli* ATCC 10536 and *Salmonella* H9812 for benzalkonium chloride (BC), trichloroisocyanuric acid (TCCA), and triclosan (TCS) were 8, 256, and 0.0625, mg L^{-1}, respectively. A total of 238, 218, and 164 of the *Salmonella* Typhimurium isolates had higher MICs for BC, TCCA, and TCS, respectively, than *E. coli* ATCC 10536 and *Salmonella* H9812 (**Table 4**) and were considered resistant. The prevalence of BC and TCS resistance was lowest among the human stool isolates ($P < 0.05$) (**Figure 5**). The prevalence of BC resistance was higher among the pig manure isolates than among the chicken meat isolates ($P < 0.05$), whereas the prevalence of TCS resistance was lower among the pig manure isolates than among the poultry manure isolates ($P < 0.05$).

Association of Metal Resistance and Heavy Metal Resistance Genes With Antibiotic and Disinfectant Resistance

All the six metal resistances were associated with resistance to at least one antibiotic (**Table 5** and **Supplementary Table 5A**). Cr-resistance was associated with resistance to eight antibiotics and to two disinfectants, Cu-resistance was associated with resistance to eight antibiotics, and Zn-resistance was associated with resistance to six antibiotics and to two disinfectants.

All the 12 HMRGs were associated with resistance to at least two antibiotics (**Table 6** and **Supplementary Table 5B**). The Hg-resistance gene *merA* was associated with resistance to 12 antibiotics and to three disinfectants, the Cu-resistance gene *pcoA* with resistance to ten antibiotics and to two disinfectants, the Pb-resistance gene *pbrA* with resistance to seven antibiotics and to two disinfectants, and the Ni-Cr-Cd-resistance gene *nccA* and the Cu-resistance gene *pcoC* with resistance to seven antibiotics and to one disinfectant ($P < 0.05$).

Transfer of Heavy Metal Resistance Genes

A conjugation experiment was carried out to determine the transferability of HMRGs. The genes *cnrA, pcoC,* and *czcD* were successfully transferred from *Salmonella* Typhimurium isolates S15 and S24 to *Escherichia coli* J53 (**Figure 6**). The transfer rate was 1×10^{-3} per donor. The MIC of Cu was 100 μg L^{-1} for the *Escherichia coli* J53, 800 μg L^{-1} for the isolates S15 and S24, 200 μg L^{-1} for the J53 with genes transferred from S15 and 300 μg L^{-1} for J53 with genes transferred from S24 (**Table 7**).

DISCUSSION

The increasing resistance of *Salmonella* strains to antimicrobial agents has become a major public health concern worldwide. However, little information is available on the resistance and co-resistance to heavy metals, disinfectants, and antibiotics among *Salmonella* Typhimurium from retail meat and manure. Thus, we studied the prevalence and associations of resistances of *Salmonella* Typhimurium isolate from pig meat,

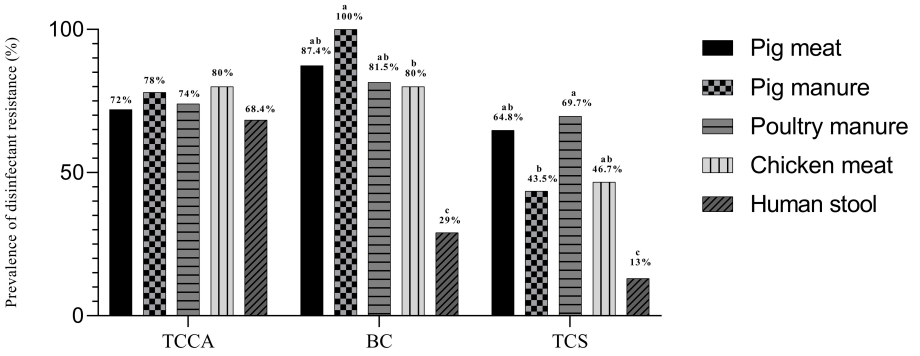

FIGURE 5 | Prevalence of disinfectant resistance among *Salmonella* Typhimurium isolates from pig meat, pig manure, poultry manure, chicken meat, and human stool. Different lowercase letters indicate statistically significant differences between groups ($P < 0.05$).

TABLE 5 | The association of metal resistances with antibiotic and disinfectant resistance in *Salmonella* Typhimurium.

Metal	Antibiotic/Disinfectant	*P*-value
	Antibiotic	
Cd	CIP	< 0.00001
	OFX	< 0.00001
	CAZ	0.0003
Co	AMP	0.0229
Cr	AMP	0.0019
	SXT	< 0.00001
	CIP	< 0.05
	C	0.0329
	OFX	0.0002
	TMP	< 0.05
	CN	0.0028
	S3	0.0167
Cu	TET	< 0.00001
	AMP	0.0001
	SXT	< 0.00001
	C	0.0007
	TMP	< 0.00001
	CN	0.0002
	S3	0.0022
	S	< 0.00001
Mn	AMP	0.044
	SXT	0.004
	TMP	0.0279
	CN	0.0013
Zn	SXT	0.0036
	CIP	0.0019
	C	0.0249
	OFX	0.0007
	TMP	0.0037
	CN	0.0062
	Disinfectant	
Cd	BC	0.0397
Co	BC	0.0227
Cr	BC	0.0303
	TCCA	< 0.00001
Mn	BC	0.0012
Zn	BC	< 0.00001
	TCCA	< 0.05

TABLE 6 | The association of HMRGs with antibiotic and disinfectant resistance in *Salmonella* Typhimurium.

HMRG	Antibiotic/Disinfectant	*P*-value
	Antibiotic	
cadD	AMP	0.0064
	SXT	< 0.00001
	S3	0.0106
	TMP	0.0002
chrB	AMP	0.0293
	TMP	0.0135
cnrA	SXT	0.0003
	CIP	0.0075
	OFX	0.0101
	TMP	0.0001
merA	TET	< 0.00001
	AMC	0.0044
	AMP	< 0.00001
	SXT	0.0033
	CIP	0.0003
	C	0.0063
	OFX	0.0001
	NA	0.0079
	TMP	0.0286
	CN	< 0.00001
	S3	< 0.00001
	S	0.011
nccA	TET	0.0313
	AMP	0.0144
	SXT	0.0072
	OFX	0.0356
	NA	0.0119
	TMP	0.0106
	CN	0.001
pbrA	SXT	0.0009
	CIP	0.0005
	C	0.044
	OFX	0.0001
	NA	0.0012
	TMP	0.0069
	CN	0.0005
pcoA	TET	0.0002
	AMC	0.0083
	AMP	0.000114
	SXT	< 0.00001
	CIP	0.0375
	C	0.0081
	NA	0.0369
	TMP	0.0003
	CN	0.0002
	S3	0.0002
pcoC	TET	0.000012
	AMP	< 0.00001
	SXT	< 0.00001
	C	< 0.00001
	TMP	< 0.00001
	CN	0.000025
	S3	0.000024
pcoR	SXT	0.0098
	CIP	0.0002
	OFX	0.0027
	TMP	0.0104

(Continued)

pig manure, chicken meat, poultry manure, and human stool from Sichuan, China.

In our study, 74% of the 300 *Salmonella* Typhimurium isolates were considered resistant to Cu, almost 50% to Zn and Cr, over 25% to Mn and Cd, and almost 10% to Co. Approximately similar prevalence of Cu resistant isolates has been detected among *Salmonella enterica* isolates from meat and meat-based products (Figueiredo et al., 2019). The high prevalences of Cu and Zn resistant isolates may have been due to selection by heavy metal micronutrients in the feed; the use of heavy metal micronutrients resulted in high concentrations of Cu and Zn in pig feces in the U.S. (Medardus et al., 2014). Alarmingly, the resistant strains in the feces may contaminate the meat, as suggested by the high Cu resistance prevalence among the pig and chicken meat isolates. The high prevalence of resistant manure isolates suggested that the resistance may spread further by the use of manure as a soil amendment in agriculture. Further studies are needed to

TABLE 6 | Continued

HMRG	Antibiotic/Disinfectant	*P*-value
	Disinfectant	
cnrA	BC	0.0066
merA	BC	0.0349
	TCS	0.000027
	TCCA	0.0007
nccA	BC	0.0016
pbrA	BC	0.0013
	TCCA	<0.00001
pcoA	BC	0.0072
	TCCA	0.000045
pcoC	BC	0.0004
pcoR	BC	0.0005
	TCCA	0.0214

TABLE 7 | Transconjugation of metal resistance genes from *Salmonella* Typhimurium to *Escherichia coli* J53.

Strain number		Genes	MIC of Cu (μg L^{-1})				
			100	200	300	400	800
Recipient	*Escherichia coli*						
	J53		100				
Donor	*Salmonella* Typhimurium						
	ST-24	*cnrA, pcoC, czcD*					800
	ST-15	*CnrA, pcoC, czcD*					800
Transconjugant	*Escherichia coli*						
	J53-ST-24	*cnrA, pcoC, czcD*			300		
	J53-ST-15	*cnrA, pcoC, czcD*		200			

ascertain whether the high prevalence of Cu resistance among human stool isolates had resulted from meat products.

In line with the prevalence of metal resistances, most of the isolates carried at least one heavy metal resistance gene (HMRG), and the prevalences of the Cu-resistance genes *pcoR* and *pcoC* and Cu resistance were at the same level. HMRGs are found in a wide variety of bacteria from various environments (Li L.-G. et al., 2017; Pal et al., 2017). The *czcD* gene is involved in the regulation of an efflux system that mediates the resistance to metal ions (Anton et al., 1999). Almost 70% of the *Salmonella* Typhimurium isolates from pig feed and feces carried *czcD* (Medardus et al., 2014). In our study, the prevalence of the Cr-Zn-Cd-resistance gene *czcD* was 85%, higher than that of resistances to those metals. Possibly the gene was not effectively expressed under the test conditions. However, ascertaining this necessitates further analyses.

The metal resistant isolates are often also antibiotic and disinfectant resistant; the resistance genes may be co-located, e.g., on a plasmid, or the resistance mechanism, e.g., an efflux pump, may provide resistance against both metals, and antibiotics (Deng et al., 2017; Pal et al., 2017). In our study, most of the *Salmonella* Typhimurium isolates were resistant to at least one antibiotic and almost 80% were multidrug-resistant. Similarly, among *Salmonella* isolates from retail food of animal origin in Romania and China, over 90% were resistant to at least one antibiotic, and from 43 to over 80% were multidrug-resistant (Mihaiu et al., 2014; Deng et al., 2017). The prevalence of resistance to

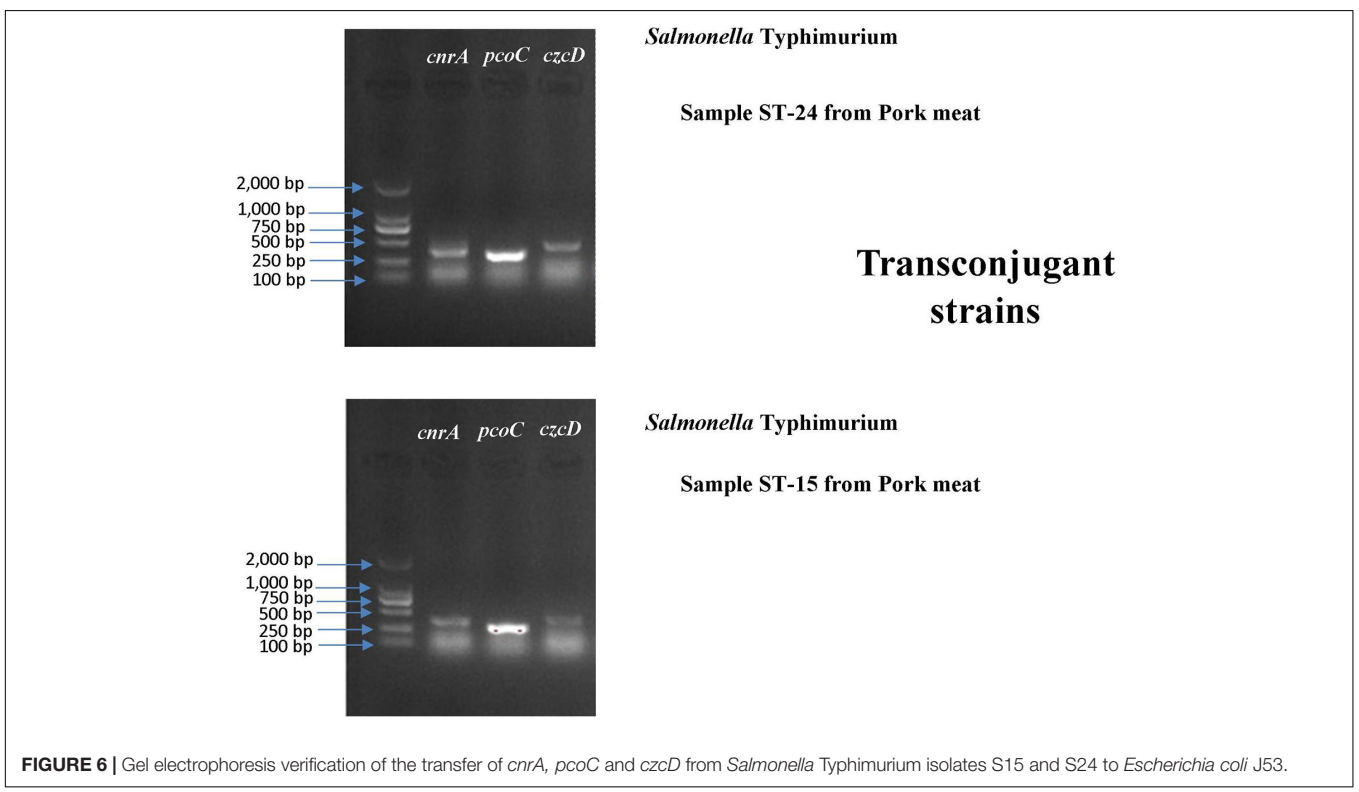

FIGURE 6 | Gel electrophoresis verification of the transfer of *cnrA, pcoC* and *czcD* from *Salmonella* Typhimurium isolates S15 and S24 to *Escherichia coli* J53.

streptomycin, sulfonamides, tetracycline, and ampicillin were all over 70% among our isolates. In agreement with Deng et al. (2017), pigs were a major source of antibiotic-resistant isolates. The prevalence of resistance to six antibiotics was higher among the pig meat and manure isolates than among other isolates, and that of streptomycin and ampicillin were highest among the pig meat isolates and that of ciprofloxacin and ofloxacin among the pig manure isolates. In our study, from 55 to 79% of the isolates were considered resistant to disinfectants triclosan (TCS), trichloroisocyanuric acid (TCCA), or benzalkonium chloride (BC). The MICs for BC resistance were lower than those of the meat *Salmonella* isolates, among which almost 60% had a MIC of 128 mg L^{-1} for BC (Deng et al., 2017). For three of the disinfectants, the prevalence of resistance was lowest among the human stool isolates, suggesting that the resistance had not been passed on in the food chain.

Due to the genes and mechanisms shared between metal, antibiotic, and disinfectant resistance, the development of resistance against metals may be associated with the development of antibiotic and disinfectant resistance (Deng et al., 2017; Pal et al., 2017). Similar to previous studies (Deng et al., 2017; Di Cesare et al., 2016; Yang et al., 2018), in our study, the metal resistances and HMRGs were associated with resistance to antibiotics and disinfectants. Especially, Cu-resistance genes were associated with resistance to several antibiotics and disinfectants. Thus, the excessive use of metals and disinfectants as feed additives and in animal care may have the potential to promote antibiotic resistance through co-selection. Alarmingly, this co-selection can maintain and promote antibiotic resistance even in the absence of antibiotics, and e.g., Cu may co-select for resistance to last-resort antibiotics such as colistin (Pal et al., 2017).

Knowing the genetic linkage of resistance genes and their association with MGEs is critical to fully understand the risks of horizontal transfer of resistance genes between bacteria (Martínez et al., 2015; Pal et al., 2015). The operons encoding resistance against different metals have been confirmed to be located on the same plasmid (Fang et al., 2016). In our study, the transfer of the Cr-Zn-Cd-resistance gene *czcD*, Cu-resistance gene *pcoC,* and Co-Ni-resistance gene *cnrA* into *Escherichia coli* and the increased Cu-resistance of the transconjugants implied that the resistance genes were located on conjugative plasmids and may be expressed in a receiving strain. Similarly, Hasman and Aarestrup (2002) and Amachawadi et al. (2013) reported that the copper resistance gene *tcrB* is horizontally transferable and linked to macrolide and glycopeptide resistance. Thus, the metal resistance genes may spread between bacteria and, due to the connection between metal and antibiotic resistance, further increase the prevalence of antibiotic resistance in the environment.

The study had the few limitations. Firstly, *Salmonella* Typhimurium, as a control strain, was not available and therefore we used standard control strains like *Escherichia coli* ATCC 25922, *Escherichia coli* ATCC 10536 and *Salmonella* H9812 as some previous studies who did the same in a scenario where the control strain was not available due to the reason such as faced by us.

Secondly, understanding differences in metal tolerances among pig feces isolates is certainly worthwhile and could have been done. However, group-wise comparison has previously been performed by a few researchers before with some limitations. In the current study, we made group-wise comparison and tried answering some of the limitations that were found in those previous studies. Since our group is constantly working on this particular aspect, future study will certainly be conducted in the subject manner as proposed.

CONCLUSION

We found a co-occurrence of heavy metal, antibiotic and disinfectant resistance in *Salmonella* Typhimurium isolates originating from retail foods, animal manure, and human stool. Such an increased prevalence of metal resistance and its corresponding genes among *Salmonella* Typhimurium isolates has not been reported previously and therefore provides a baseline study to further investigate the subject matter. Further, a prevalence of resistance and its genes indicates that meat and manure could be potential sources of human exposure to multiple strains of resistant *Salmonella* and other food-borne diseases. An excessive as well as an irrational use of metals and disinfectants either as feed additives or in an animal care setting may promote antibiotic resistance through co-selection and the transfer of the resistance genes through MGEs.

DATA AVAILABILITY STATEMENT

The original contributions presented in the study are included in the article/**Supplementary Material**, further inquiries can be directed to the corresponding author/s.

AUTHOR CONTRIBUTIONS

GM and KZ wrote the manuscript under the supervision of LZ. GM, KZ, XH, SC, SL, AM, LH, YY, XY, XA, AL, and XX performed sample collection and research work. GM and KZ performed data analysis. GM, KZ, LZ, MS, PP, and AM revised the manuscript. LZ was correspond to the author furthest up on the author list. All authors approved the manuscript's final version.

FUNDING

This work was supported by the Department of Science and Technology of Sichuan Province (21GJHZ0113 and 2020YJ0338).

SUPPLEMENTARY MATERIAL

The Supplementary Material for this article can be found online at: https://www.frontiersin.org/articles/10.3389/fmicb.2021.702725/full#supplementary-material

REFERENCES

Allen, H. K., Levine, U. Y., Looft, T., Bandrick, M., and Casey, T. A. (2013). Treatment, promotion, commotion: antibiotic alternatives in food-producing animals. *Trends Microbiol.* 21, 114–119. doi: 10.1016/j.tim.2012.11.001

Amachawadi, R. G., Scott, H. M., Alvarado, C. A., Mainini, T. R., Vinasco, J., Drouillard, J. S., et al. (2013). Occurrence of the transferable copper resistance Gene tcrB among fecal enterococci of U.S. feedlot cattle fed copper-supplemented diets. *Appl. Environ. Microbiol.* 79, 4369–4375. doi: 10.1128/aem.00503-13

Anton, A., Große, C., Reißmann, J., Pribyl, T., and Nies, D. H. (1999). CzcD is a heavy metal ion transporter involved in regulation of heavy metal resistance in Ralstonia sp. strain CH34. *J. Bacteriol.* 181, 6876–6881. doi: 10.1128/jb.181.22.6876-6881.1999

Antunes, P., Mourão, J., Campos, J., and Peixe, L. (2016). Salmonellosis: the role of poultry meat. *Clin. Microbiol. Infect.* 22, 110–121. doi: 10.1016/j.cmi.2015.12.004

Argudín, M. A., Lauzat, B., Kraushaar, B., Alba, P., Agerso, Y., Cavaco, L., et al. (2016). Heavy metal and disinfectant resistance genes among livestock-associated methicillin-resistant *Staphylococcus aureus* isolates. *Vet. Microbiol.* 191, 88–95. doi: 10.1016/j.vetmic.2016.06.004

Baker-Austin, C., Wright, M. S., Stepanauskas, R., and McArthur, J. V. (2006). Co-selection of antibiotic and metal resistance. *Trends Microbiol.* 14, 176–182. doi: 10.1016/j.tim.2006.02.006

Bamuwamye, M., Ogwok, P., and Tumuhairwe, V. (2015). Cancer and non-cancer risks associated with heavy metal exposures from street foods: evaluation of roasted meats in an urban setting. *J. Environ. Pollut. Hum. Health* 3, 24–30.

Barr, W., and Smith, A. (2014). Acute diarrhea in adults. *Am. Fam. Physician* 89, 180–189.

Barton Behravesh, C., Jones, T. F., Vugia, D. J., Long, C., Marcus, R., Smith, K., et al. (2011). Deaths associated with bacterial pathogens transmitted commonly through food: foodborne diseases active surveillance network (FoodNet), 1996–2005. *J. Infect. Dis.* 204, 263–267. doi: 10.1093/infdis/jir263

Bragg, R., Jansen, A., Coetzee, M., van der Westhuizen, W., and Boucher, C. (2014). "Bacterial resistance to quaternary ammonium compounds (QAC) disinfectants," in *Infectious Diseases and Nanomedicine II Advances in Experimental Medicine and Biology*, eds R. Adhikari and S. Thapa (New Delhi: Springer), 1–13. doi: 10.1007/978-81-322-1774-9_1

Burch, D. (2006). Anticipated Effects of the Withdrawal of Antibiotic Growth Promoters (AGPs) From Pigs in the European Union on 1st January 2006. Available online at: http://www.octagon-services.co.uk/articles/withdrawalAGP.htm

Cai, J. C., Zhou, H. W., Zhang, R., and Chen, G.-X. (2008). Emergence of *Serratia marcescens*, *Klebsiella pneumoniae*, and *Escherichia coli* Isolates possessing the plasmid-mediated carbapenem-hydrolyzing beta-lactamase KPC-2 in intensive care units of a Chinese hospital. *Antimicrob. Agents Chemother.* 52, 2014–2018. doi: 10.1128/aac.01539-07

Cavaco, L. M., Hasman, H., Aarestrup, F. M., Wagenaar, J. A., Graveland, H., Veldman, K., et al. (2011). Zinc resistance of Staphylococcus aureus of animal origin is strongly associated with methicillin resistance. *Vet. Microbiol.* 150, 344–348.

Ceyssens, P.-J., Mattheus, W., Vanhoof, R., and Bertrand, S. (2015). Trends in serotype distribution and antimicrobial susceptibility in *Salmonella enterica* isolates from humans in Belgium, 2009 to 2013. *Antimicrob. Agents Chemother.* 59, 544–552. doi: 10.1128/aac.04203-14

Chousalkar, K., Gast, R., Martelli, F., and Pande, V. (2018). Review of egg-related salmonellosis and reduction strategies in United States, Australia, United Kingdom and New Zealand. *Crit. Rev. Microbiol.* 44, 290–303. doi: 10.1080/1040841x.2017.1368998

CIIN (2018a). *Analysis of the Development Status and Development Trend of China's pig Breeding Industry in 2018* [图]_中国工业信息网. Available Online at: https://www.chyxx.com/industry/201801/603323.html (accessed June 3, 2021)

CIIN (2018b). *Analysis of the Scale of Pig Breeding in China and the Development Potential of Pig Production Areas in Henan Province in 2017 (Figure)*_中国工业信息网. Available Online at: https://www.chyxx.com/industry/201808/667438.html (accessed June 3, 2021)

Cui, S., Zheng, J., and Meng, J. (2006). An improved method for rapid isolation of Salmonella against Proteus in chicken carcasses. *J. Food Saf.* 26, 49–61. doi: 10.1111/j.1745-4565.2005.00032.x

Demirbilek, S. K. (2017). Salmonellosis in animals. *Salmonella Re-Emerg. Pathog.* doi: 10.5772/intechopen.72192 Available online at: https://www.intechopen.com/books/salmonella-a-re-emerging-pathogen/salmonellosis-in-animals

Deng, W., Quan, Y., Yang, S., Guo, L., Zhang, X., Liu, S., et al. (2017). Antibiotic resistance in salmonella from retail foods of animal origin and its association with disinfectant and heavy metal resistance. *Microb. Drug Resist.* 24, 782–791. doi: 10.1089/mdr.2017.0127

Dewey-Mattia, D., Manikonda, K., Chen, J., Kisselburgh, H., Pilewski, C., Sundararaman, P., et al. (2018). *Surveillance for Foodborne Disease Outbreaks–United States, 2016: Annual Report*. U.S. Centers for Disease Control and Prevention (CDC), Atlanta, Georgia.

Di Cesare, A., Eckert, E. M., D'Urso, S., Bertoni, R., Gillan, D. C., Wattiez, R., et al. (2016). Co-occurrence of integrase 1, antibiotic and heavy metal resistance genes in municipal wastewater treatment plants. *Water Res.* 94, 208–214. doi: 10.1016/j.watres.2016.02.049

EFSA and ECDC (2018). The European Union summary report on trends and sources of zoonoses, zoonotic agents and food-borne outbreaks in 2017. *EFSa J.* 16:e05500.

Eisler, R. (1993). *Zinc Hazards to Fish, Wildlife, and Invertebrates: a Synoptic Review*. Washington, DC: US Department of the Interior.

Fang, L., Li, X., Li, L., Li, S., Liao, X., Sun, J., et al. (2016). Co-spread of metal and antibiotic resistance within ST3-IncHI2 plasmids from E. coli isolates of food-producing animals. *Sci. Rep.* 6:25312.

Figueiredo, R., Card, R. M., Nunez-Garcia, J., Mendonça, N., da Silva, G. J., and Anjum, M. F. (2019). Multidrug-resistant *Salmonella enterica* isolated from food animal and foodstuff may also be less susceptible to heavy metals. *Foodborne Pathog. Dis.* 16, 166–172. doi: 10.1089/fpd.2017.2418

Frost, L. S., Leplae, R., Summers, A. O., and Toussaint, A. (2005). Mobile genetic elements: the agents of open source evolution. *Nat. Rev. Microbiol.* 3, 722–732. doi: 10.1038/nrmicro1235

Guo, C., Hoekstra, R. M., Schroeder, C. M., Pires, S. M., Ong, K. L., Hartnett, E., et al. (2011). Application of Bayesian techniques to model the burden of human salmonellosis attributable to U.S. food commodities at the point of processing: adaptation of a Danish model. *Foodborne Pathog. Dis.* 8, 509–516. doi: 10.1089/fpd.2010.0714

Hasman, H., and Aarestrup, F. M. (2002). tcrB, a gene conferring transferable copper resistance in *Enterococcus faecium*: occurrence, transferability, and linkage to macrolide and glycopeptide resistance. *Antimicrob. Agents Chemother.* 46, 1410–1416. doi: 10.1128/aac.46.5.1410-1416.2002

He, Y., Yang, X., Xia, J., Zhao, L., and Yang, Y. (2016). Consumption of meat and dairy products in China: a review. *Proc. Nutr. Soc.* 75, 385–391. doi: 10.1017/s0029665116000641

Heredia, N., and García, S. (2018). Animals as sources of food-borne pathogens: a review. *Anim. Nutr.* 4, 250–255. doi: 10.1016/j.aninu.2018.04.006

Hu, Y. J., and Cowling, B. J. (2020). Reducing antibiotic use in livestock, China. *Bull. World Health Organ.* 98, 360–361. doi: 10.2471/blt.19.243501

Hugas, M., and Beloeil, P. A. (2014). Controlling Salmonella along the food chain in the European Union - progress over the last ten years. *Eurosurveillance* 19:20804.

Khan, S., Cao, Q., Zheng, Y. M., Huang, Y. Z., and Zhu, Y. G. (2008). Health risks of heavy metals in contaminated soils and food crops irrigated with wastewater in Beijing, China. *Environ. Pollut.* 152, 686–692. doi: 10.1016/j.envpol.2007.06.056

Korish, M. A., and Attia, Y. A. (2020). Evaluation of heavy metal content in feed, litter, meat, meat products, liver, and table eggs of chickens. *Animals* 10:727. doi: 10.3390/ani10040727

Kumar, D., Pornsukarom, S., and Thakur, S. (2019). "Antibiotic usage in poultry production and antimicrobial-resistant Salmonella in poultry," in *Food Safety in Poultry Meat Production Food Microbiology and Food Safety*, eds K. Venkitanarayanan, S. Thakur, and S. C. Ricke (Cham: Springer), 47–66. doi: 10.1007/978-3-030-05011-5_3

Kumar, K., Gupta, S. C., Baidoo, S. K., Chander, Y., and Rosen, C. J. (2005). Antibiotic uptake by plants from soil fertilized with animal manure. *J. Environ. Qual.* 34, 2082–2085. doi: 10.2134/jeq2005.0026

Li, L.-G., Xia, Y., and Zhang, T. (2017). Co-occurrence of antibiotic and metal resistance genes revealed in complete genome collection. *ISME J.* 11, 651–662. doi: 10.1038/ismej.2016.155

Li, W., Li, Y., Liu, Y., Shi, X., Jiang, M., Lin, Y., et al. (2017). Clonal expansion of biofilm-forming *Salmonella typhimurium* ST34 with multidrug-resistance phenotype in the southern coastal region of China. *Front. Microbiol.* 8:2090.

Liang, Z., Ke, B., Deng, X., Liang, J., Ran, L., Lu, L., et al. (2015). Serotypes, seasonal trends, and antibiotic resistance of non-typhoidal Salmonella from human patients in Guangdong Province, China, 2009–2012. *BMC Infect. Dis.* 15:53.

Lu, Y., Song, S., Wang, R., Liu, Z., Meng, J., Sweetman, A. J., et al. (2015). Impacts of soil and water pollution on food safety and health risks in China. *Environ. Int.* 77, 5–15. doi: 10.1016/j.envint.2014.12.010

Luo, Q., Li, S., Liu, S., and Tan, H. (2017). Foodborne illness outbreaks in China, 2000–2014. *Int. J. Clin. Exp. Med.* 10, 5821–5831.

Majowicz, S. E., Musto, J., Scallan, E., Angulo, F. J., Kirk, M., O'Brien, S. J., et al. (2010). The global burden of nontyphoidal Salmonella gastroenteritis. *Clin. Infect. Dis.* 50, 882–889.

Martínez, J. L., Coque, T. M., and Baquero, F. (2015). What is a resistance gene? ranking risk in resistomes. *Nat. Rev. Microbiol.* 13, 116–123. doi: 10.1038/nrmicro3399

Medardus, J. J., Molla, B. Z., Nicol, M., Morrow, W. M., Rajala-Schultz, P. J., Kazwala, R., et al. (2014). In-feed use of heavy metal micronutrients in US swine production systems and its role in persistence of multidrug-resistant salmonellae. *Appl. Environ. Microbiol.* 80, 2317–2325. doi: 10.1128/aem.04283-13

Mihaiu, L., Lapusan, A., Tanasuica, R., Sobolu, R., Mihaiu, R., Oniga, O., et al. (2014). First study of Salmonella in meat in Romania. *J. Infect. Dev. Ctries.* 8, 050–058. doi: 10.3855/jidc.3715

Pal, C., Asiani, K., Arya, S., Rensing, C., Stekel, D. J., Larsson, D. J., et al. (2017). Metal resistance and its association with antibiotic resistance. *Adv. Microb. Physiol.* 70, 261–313. doi: 10.1016/bs.ampbs.2017.02.001

Pal, C., Bengtsson-Palme, J., Kristiansson, E., and Larsson, D. J. (2015). Co-occurrence of resistance genes to antibiotics, biocides and metals reveals novel insights into their co-selection potential. *BMC Genomics* 16:964.

Pan, H., Li, X., Fang, W., and Yue, M. (2018). Analysis of major human and foodborne pathogens and their resistance to antimicrobials in the USA in the past two decades: implications for surveillance and control of antimicrobial resistance in China. *J. Zhejiang Univ. Agric. Life Sci.* 44, 237–246.

Pan, H., Zhou, X., Chai, W., Paudyal, N., Li, S., Zhou, X., et al. (2019). Diversified sources for human infections by *Salmonella enterica* serovar newport. *Transbound. Emerg. Dis.* 66, 1044–1048. doi: 10.1111/tbed.13099

Ran, L., Wu, S., Gao, Y., Zhang, X., Feng, Z., Wang, Z., et al. (2011). Laboratory-based surveillance of nontyphoidal Salmonella infections in China. *Foodborne Pathog. Dis.* 8, 921–927.

Roosa, S., Wattiez, R., Prygiel, E., Lesven, L., Billon, G., and Gillan, D. C. (2014). Bacterial metal resistance genes and metal bioavailability in contaminated sediments. *Environ. Pollut.* 189, 143–151. doi: 10.1016/j.envpol.2014.02.031

Seiler, C., and Berendonk, T. U. (2012). Heavy metal driven co-selection of antibiotic resistance in soil and water bodies impacted by agriculture and aquaculture. *Front. Microbiol.* 3:399.

Shen, H., Chen, H., Ou, Y., Huang, T., Chen, S., Zhou, L., et al. (2020). Prevalence, serotypes, and antimicrobial resistance of Salmonella isolates from patients with diarrhea in Shenzhen, China. *BMC Microbiol.* 20:197.

Simpson, K. M., Hill-Cawthorne, G. A., Ward, M. P., and Mor, S. M. (2018). Diversity of Salmonella serotypes from humans, food, domestic animals and wildlife in New South Wales. Australia. *BMC Infect. Dis.* 18:623.

Sodagari, H. R., Wang, P., Robertson, I., Habib, I., and Sahibzada, S. (2020). Non-Typhoidal Salmonella at the human-food-of-animal-origin interface in Australia. *Animals* 10:1192. doi: 10.3390/ani10071192

Takaya, A., Yamamoto, T., and Tokoyoda, K. (2020). Humoral immunity vs. Salmonella. *Front. Immunol.* 10:3155.

Tam, C. C., Rodrigues, L. C., Viviani, L., Dodds, J. P., Evans, M. R., Hunter, P. R., et al. (2012). Longitudinal study of infectious intestinal disease in the UK (IID2 study): incidence in the community and presenting to general practice. *Gut* 61, 69–77. doi: 10.1136/gut.2011.238386

Vo, A. T., Van Duijkeren, E., Fluit, A. C., Heck, M. E., Verbruggen, A., Maas, H. M., et al. (2006). Distribution of *Salmonella enterica* serovars from humans, livestock and meat in Vietnam and the dominance of Salmonella Typhimurium phage type 90. *Vet. Microbiol.* 113, 153–158. doi: 10.1016/j.vetmic.2005.10.034

Wang, J., Li, Y., Xu, X., Liang, B., Wu, F., Yang, X., et al. (2017). Antimicrobial resistance of *Salmonella enterica* serovar Typhimurium in Shanghai, China. *Front. Microbiol.* 8:510.

Wang, M., Tran, J. H., Jacoby, G. A., Zhang, Y., Wang, F., and Hooper, D. C. (2003). Plasmid-mediated quinolone resistance in clinical isolates of *Escherichia coli* from Shanghai, China. *Antimicrob. Agents Chemother.* 47, 2242–2248. doi: 10.1128/aac.47.7.2242-2248.2003

Wang, Y., Cao, C., Alali, W. Q., Cui, S., Li, F., Zhu, J., et al. (2017). Distribution and antimicrobial susceptibility of foodborne Salmonella serovars in eight provinces in China from 2007 to 2012 (except 2009). *Foodborne Pathog. Dis.* 14, 393–399. doi: 10.1089/fpd.2016.2237

Weinstein, M. P., and Lewis, J. S. (2020). The clinical and laboratory standards institute subcommittee on antimicrobial susceptibility testing: background, organization, functions, and processes. *J. Clin. Microbiol.* 58:e1864-19.

WHO (2020). *Food Safety*. Geneva: WHO.

Xu, X., Wu, S., Ye, X., Liu, Y., Shi, W., Zhang, Y., et al. (2007). Prevalence and expression of the plasmid-mediated quinolone resistance determinant qnrA1. *Antimicrob. Agents Chemother.* 51, 4105–4110. doi: 10.1128/aac.00616-07

Yang, Q. E., Agouri, S. R., Tyrrell, J. M., and Walsh, T. R. (2018). Heavy metal resistance genes are associated with blaNDM-1-and blaCTX-M-15-carrying Enterobacteriaceae. *Antimicrob. Agents Chemother.* 62:e2642-17.

Yang, S., Deng, W., Liu, S., Yu, X., Mustafa, G. R., Chen, S., et al. (2020). Presence of heavy metal resistance genes in *Escherichia coli* and Salmonella isolates and analysis of resistance gene structure in E. coli E308. *J. Glob. Antimicrob. Resist.* 21, 420–426. doi: 10.1016/j.jgar.2020.01.009

Zhang, J., Jin, H., Hu, J., Yuan, Z., Shi, W., Ran, L., et al. (2014). Serovars and antimicrobial resistance of non-typhoidal Salmonella from human patients in Shanghai, China, 2006–2010. *Epidemiol. Infect.* 142, 826–832. doi: 10.1017/s0950268813001659

Zou, L., Meng, J., McDermott, P. F., Wang, F., Yang, Q., and Cao, G. (2014). Presence of disinfectant resistance genes in *Escherichia coli* isolated from retail meats in the USA. *J. Antimicrob. Chemother.* 69, 2644–2649. doi: 10.1093/jac/dku197

Conflict of Interest: The authors declare that the research was conducted in the absence of any commercial or financial relationships that could be construed as a potential conflict of interest.

Publisher's Note: All claims expressed in this article are solely those of the authors and do not necessarily represent those of their affiliated organizations, or those of the publisher, the editors and the reviewers. Any product that may be evaluated in this article, or claim that may be made by its manufacturer, is not guaranteed or endorsed by the publisher.

frontiers in Microbiology

REVIEW
published: 16 September 2021
doi: 10.3389/fmicb.2021.714265

Aptasensors for *Staphylococcus aureus* Risk Assessment in Food

Ziqian Huang[1], Xin Yu[2], Qingli Yang[1], Ying Zhao[3]* and Wei Wu[1]**

[1] College of Food Science and Engineering, Qingdao Agricultural University, Qingdao, China, [2] Qingdao Municipal Hospital, Qingdao, China, [3] Department of Anesthesiology, Qilu Hospital, Cheeloo College of Medicine, Shandong University, Qingdao, China

Staphylococcus aureus (*S. aureus*) is the top ordinary pathogen causing epidemic and food poisoning. The authentication of *S. aureus* has great significance for pathologic diagnosis and food hygiene supervision. Various biosensor methods have been established for identification. This paper reviews the research progress of aptasensors for *S. aureus* detection, focusing on the classification of aptamer technologies, including optical aptasensors and electrochemical aptasensors. Furthermore, the feasibility and future challenges of *S. aureus* detection for aptamer assays are discussed. Combining aptasensors with nanomaterials appears to be the developing trend in aptasensors.

Keywords: *Staphylococcus aureus*, detection, aptamers, biosensors, aptasensors

OPEN ACCESS

Edited by:
Biao Suo,
Henan Agricultural University, China

Reviewed by:
Matthew D. Moore,
University of Massachusetts Amherst, United States
Shijia Wu,
Jiangnan University, China

****Correspondence:***
Qingli Yang
rice407@163.com
Ying Zhao
18561812656@163.com
Wei Wu
wuweiouc@126.com

Specialty section:
This article was submitted to Food Microbiology, a section of the journal Frontiers in Microbiology

Received: *25 May 2021*
Accepted: *17 August 2021*
Published: *16 September 2021*

Citation:
Huang Z, Yu X, Yang Q, Zhao Y and Wu W (2021) Aptasensors for Staphylococcus aureus Risk Assessment in Food. Front. Microbiol. 12:714265. doi: 10.3389/fmicb.2021.714265

INTRODUCTION

Foodborne pathogens caused by microorganisms are the main problem of food safety. *Staphylococcus aureus* (*S. aureus*), an anaerobic Gram-positive bacterium, is a common cause of foodborne intoxications (Hulme, 2017), with strong adaptability and the ability to tolerate a wide range of pH, temperature, and humidity. *S. aureus* strains produce one or more extracellular proteins, called staphylococcal enterotoxin (SE), which are composed of staphylococcal enterotoxin A (SEA), staphylococcal enterotoxin B (SEB), staphylococcal enterotoxin C (SEC), etc. (Principato and Qian, 2014). These extracellular proteins may inhibit the host's immune response to *S. aureus*; hence, SE is thought to be the typical cause of food poisoning in humans after eating contaminated food. Infected people frequently develop gastrointestinal symptoms such as feeling sick, emesis, and diarrhea within hours. The disease is generally mild and usually resolves within 24–48 h of the onset of symptoms and rarely requires hospitalization. Foods susceptible to staphylococcal intoxication are usually meat, meat and egg products, milk (especially if animals are affected by mastitis), and baked goods (McMillan et al., 2016; Johler et al., 2018). In Spain, 21% of 940 food samples (milk, cheese, meat, baked goods, etc.) were reported to be positive for *Staphylococcus* spp. in 2016 (European Food Safety Authority and European Centre for Disease Prevention and Control, 2017). In 2017, a total of 4,600 animal specimens were collected in Italy; 28.8% of them were positive. Among these data, the incidence of sheep (37.4%) was significantly high (European Food Safety Authority and European Centre for Disease Prevention and Control, 2018). Salty foods such as ham are also implicated by the ability of *S. aureus* that grew with low moisture activity (Qi and Miller, 2000). It is critical to detect efficiently and to prevent the occurrence of the disease since *S. aureus* has become a kind of pathogenic bacteria that caused serious harm to food safety. The risk assessment of foodborne pathogens can quickly and effectively assess the pathogenic factors of different types of foodborne diseases, such as bacterial food poisoning, by constructing early outbreak prediction model. Food safety risk assessment, especially microbial risk assessment

(MRA), plays an important role in ensuring food safety and controlling foodborne diseases. An accurate and reliable risk assessment process is essential for people's health and safety.

Staphylococcus aureus biofilms can form physical barriers that affect the spread and distribution of antibiotics; bacteria are encapsulated in the extracellular biofilm matrix and arranged in multiple layers, which can develop resistance to antimicrobial agents and host immune systems by damaging the action of phagocytes (Prenafeta et al., 2014). The occurrence of the methicillin-resistant *Staphylococcus aureus* (MRSA) is on account of the excellent capacity of *S. aureus* to suit antibiotics. Enterotoxin-producing MRSA can also act as a foodborne pathogen under growth conditions favorable for enterotoxin production. MRSA has long been recognized as a major pathogenic factor in human healthcare-related infections (HA-MRSA) (Sergelidis and Angelidis, 2017). MRSA strains have been implicated in community-associated infections (CA-MRSA) in many countries (Deurenberg et al., 2007). It has been reported that MRSA transported on poultries and domestic animals are called LA-MRSA (Macori et al., 2017). Up to now, the presence of LA-MRSA in live domestic animals, wild animals, fresh foods, and ready-to-eat foods has been demonstrated in a number of studies (Sieber et al., 2018; da Silva et al., 2020). A study in Greece examined 367 samples (36 bulk tank milk, 19 milk dairy products, 72 humans, 185 animals, and 55 pieces of equipment), of which 57.8% of the samples tested positive for *S. aureus* (Papadopoulos et al., 2018). Identical conclusions were obtained from studies that people, animals, and the surrounding environment may be related to MRSA contamination in the dairy production chain (Tegegne et al., 2019).

Tuerk and Gold (1990) established SELEX technology, which successfully screened synthetic oligonucleotides with high affinity and specificity from RNA library. The SELEX process is implemented in DNA library, and single-stranded DNA (ssDNA) was prepared by thermal deformation of DNA library. Generally, the target is fixed on the magnetic beads as the selection object, and then the ssDNA aptamer of the target is selected *in vitro*. The magnetic beads modified with the target are co-incubated with the DNA library, and the unbound or weakly bound ssDNA is discarded after magnetic separation. The ssDNA combined with the magnetic beads is eluted and collected as the template for polymerase chain reaction (PCR) amplification. After PCR amplification, a new ssDNA library is formed, which will be SSco-incubated with magnetic beads in the next round of screening. In the screening process, negative selection and inverse selection are combined to reduce the enrichment of non-specific ssDNA during selection. The incubation, elution, and amplification steps are repeated continuously, with the increase of screening times, the incubation time will be shorter; ultimately, the ssDNA aptamer of the target will be finally obtained. Multiple SELEX screenings give the aptamer a higher specificity with more stable affinity than antibodies. The concept of aptamer was first proposed by Ellington and Szostak (1990). So far, many aptamers have been developed for *S. aureus* and its toxins (DeGrasse, 2012; Baumstummler et al., 2014; Huang et al., 2014, 2015).

By virtue of its three-dimensional structure, aptamer is highly selective in binding to targets and has high affinity and strength specificity similar to antigen–antibody reaction, which can detect targeted pathogens in complex food samples. Biosensors consist of recognition elements and sensors. The signal of the sample is amplified by the biometric element, and the sensor transforms the biometric signals into measurable signals. Aptamer-based multi-class materials can be used as signal amplifiers to establish aptasensors, which can obtain higher sensitivity and is more suitable for rapid detection of pathogens in the field, and have become a new method for risk assessment of pathogens.

AVAILABLE METHODS FOR DETECTING *S. aureus*

In the past two decades, foodborne pathogen detection by conventional ways mostly relies on the culture and identification of microorganisms, which are accurate and reliable; however, it remains challenging due to laborious duty and a long period of experimental operation. With the development of molecular detection technology, PCR has been gradually applied to foodborne pathogenic bacteria detection. However, owing to its inability to distinguish between dead and alive bacteria as well as the fact that the experiment is prone to interference, it is difficult to satisfy the requirements of actual detection (Tao et al., 2020). Compared with traditional antibodies, aptamers, which act as a new molecular recognition element, have the advantages of a wide range of target molecules, fabulous stability, long storage life, and high specificity (Gopinath et al., 2016). Biosensors based on nucleic acid aptamer have proved promising for detecting foodborne pathogens. The aptamer biosensor made by combining the biosensor technology not only has the characteristics of high specificity, strong affinity, easy modification, and good stability but also maintains the advantages of rapid response, simple operation, and low cost of the biosensor. **Figure 1** shows a diagram of representative components and techniques that can be integrated into a biosensor in order to detect the pathogens.

Conventionally, the detection methods of foodborne pathogens will be further discussed below, which can be systematized by culture-based, nucleic acid-based and immune-based methods. The culture method is currently the most widespread and sophisticated test method and is generally recognized as the gold standard for microbiological analysis of foodborne pathogens. The culture-based method relies on the cultivation of microorganisms on Agar plates to form visible colonies; next, the colonies are subjected to a standard biochemical identification that provides qualitative or quantitative analysis of pathogen bacteria in food samples. This method remains the preferred method for numerous food testing laboratories since it is 10-cent and easy to use. However, preliminary results can take 2–3 days, while identification of specific pathogenic microorganisms can take more than a week (Zhao et al., 2014). Because of this, it is incapable to handle food safety emergencies.

Nucleic acid-based methods manipulate the DNA or RNA sequence of a target pathogen by detecting specificity. In

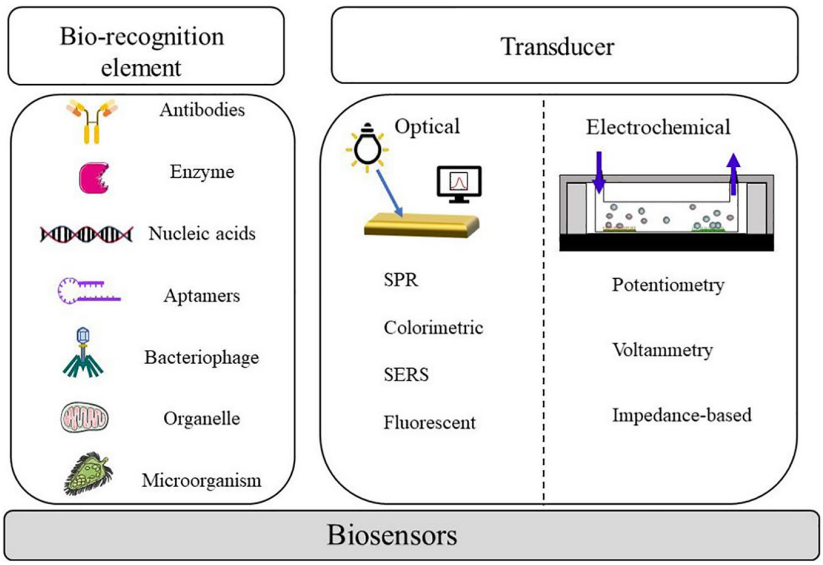

FIGURE 1 | Components and measurement methods associated with biosensors for pathogen detection.

recent years, it is generally accepted that nucleic acid-based methods are divided into several categories, including simple PCR, multiplex polymerase chain reaction (MPCR), quantitative polymerase chain reaction (qPCR), and loop-mediated isothermal amplification (LAMP). The most widely used nucleic acid amplification method to detect pathogens is PCR. This technique was first reported by Saiki et al. (1985). The principle is that two nucleic acid chains from different sources have complementary base sequences, which can specifically bind to form molecular hybridization chains (Ramesh et al., 1992).

Polymerase chain reaction can detect many toxin genes of *S. aureus* in a short time. The very first time PCR was utilized to detect *S. aureus* was reported in 1991 (Wilson et al., 1991). After adding the total DNA of the object to be tested, the sequence of the target gene of SEB is amplified by PCR or real-time fluorescence PCR, and quantitative monitoring can be conducted by electrophoresis bands or fluorescence intensity. Martinon and Wilkinson (2011) established a low-cost, SYBR Green based double-chain real-time PCR for simultaneous detection of *Listeria monocytogenes* and *S. aureus* in food. Detection limit was 2 CFU/g in raw meat containing *S. aureus* (Martinon and Wilkinson, 2011). However, PCR-based tests used alone are unable to provide any indication of the cell viability being examined because they do not distinguish DNA from living and dead cells (Foddai and Grant, 2020). The specificity of the PCR technology depends on the specificity of the primer and template DNA binding; without increasing the fungus, it can detect *S. aureus* directly from the gene level, and more accurate, rapid, and more sensitive (Smith and Osborn, 2009) detection has been successfully carried out in a variety of pathogens, but the price is higher.

Multiplex PCR provides faster detection by simultaneously amplifying multiple gene targets compared to simple PCR. Tao et al. (2020) established a common primer-mediated MPCR technique for non-qualitative screening of 11 common foodborne pathogens. Park et al. (2006) used MPCR to detect *S. aureus* in kimchi, and the detection limit was 260 CFU/ml. qPCR, also known as real-time PCR, is a way that continuously monitors the production of PCR products throughout the reaction process, providing rapid, simultaneous amplification and gene detection (Valderrama et al., 2016). LAMP is a DNA isothermal amplification technique proposed by Notomi et al. (2000). This research employed a DNA polymerase and a set of primers specially designed to identify six different sequences in the target DNA and does not require a cyclic process such as transgenesis during the whole process. It is a new DNA amplification method, which is simple, quick, and highly specific (Srividya et al., 2019), and has the possibility of replacing the PCR method. At the same time, in the actual detection work, it was found that PCR technology has high requirements for primers, system establishment, and annealing temperature screening; high requirements for target fragment screening; and high sampling standards. Immunoassay method for detecting foodborne pathogens is based on the antigen–antibody union. It is used to quickly detect pathogens, which have not yet been realized by other conventional methods. The most frequently used immunoassay method is enzyme-linked immunosorbent assay (ELISA), which is widely applied to the detection of foodborne pathogens, fungal toxins, and bacterial toxins. While short detection time and high sensitivity are required compared to traditional culture-based methods, ELISA falls short of being able to detect pathogens in real time (Umesha and Manukumar, 2018). Sandwich ELISA is a modified ELISA that uses two antibodies against a single antigen (Priyanka et al., 2016). The usage of sandwich ELISA for rapid foodborne pathogen detection has been studied, and the sensitivity and specificity of sandwich structure are much higher than before. The presence of the bacteria can also be proved by testing for enterotoxins.

Immunoassay has become the main tool for rapid detection of harmful toxigenic bacteria due to its high specificity for toxicity. Nouri et al. (2018) designed a new kit for the detection of SEA in milk, with a detection time of about 15 min and a sensitivity of 15.6 ng of toxin. For instance, Sun et al. (2020) developed a sandwich chemiluminescent immunoassay (CLIA) to detect SEB, an anti-SEB monoclonal antibody was used as the capture antibody, and Nb37-ALP was used as the detector antibody; the detection limit was 1.44 ng/ml. In another sandwich ELISA assay, nano-antibodies acted as capturing antibodies, and the detection antibodies were acted by phage nanoantibodies with amplified signal properties. Under the optimal cases, the quantitative range of this method was 1–512 ng/ml, and the detection limit was 0.3 ng/ml (Ji et al., 2020). In actual detection, this method is highly dependent on equipment; secondly, antibody preparation is difficult and it is prone to false positives; finally, the experiment has certain requirements such as the professional level of the experimenter. Obviously, the methods mentioned above are not sufficient, and most of them are longstanding and laborious jobs. To a large extent, aptasensor detection can alleviate the problems of the above methods. **Table 1** summarizes the advantages of conventional methods and aptasensors for *S. aureus* detection.

PRINCIPLES OF APTASENSORS FOR *S. aureus* DETECTION

Nucleic acid-based aptamers are a ssDNA fragment or short RNA sequences that are obtained by separation of nucleotides synthesized *in vitro* in libraries using SELEX. They have characteristics that can be easily synthesized *in vitro*, simple to modify, and can be designed flexibly in a sequence. Compared with traditional antibodies, aptamers have more advantages. As a new molecular recognition element, aptamers can recognize not only single molecules like protein and nucleic acid but also large molecular complexes such as cells, bacteria, microorganisms, and viruses. It has a wider range of target molecules (proteins, nucleic acids, parasites, bacteria, cells, viruses, etc.) and a higher affinity than antigen–antibody reaction; the molecular weight is about 20–100 bp, which makes it easier to enter the cell; the preparation process does not require antibody immunity; and animal experiments can be synthesized *in vitro* for subsequent experiments. Stable properties and longer storage life make aptamers the ideal experimental material. Massive aptasensors have been logically designed and miscellaneous techniques, including optical and electrochemical aptasensors, have been used and combined to acquire gratifyingly detectable signals. After screening the nucleic acid of foodborne pathogens, the detected signals should be further converted into recognizable output signals. The nucleic acid aptamer can perform signal output through the biosensor, fix the nucleic acid aptamer on the substrate of the biosensor, and transform the chemical, physical, electrical, or optical changes in the adsorption process into detectable signals through sensing technology. This paper introduces the application of these sensors in the detection of nucleic acid aptamer in foodborne pathogenic bacteria.

Optical Aptasensors

With the advantages of high sensitivity, speediness, and specificity, the optical sensor has been widely used in *S. aureus* detection. It is commonly known that optical aptasensors are classified into surface plasmon resonance (SPR), colorimetric aptasensors, surface-enhanced Raman spectroscopy (SERS), and fluorescence (Rubab et al., 2018). Optical biosensors consist of a biological recognition layer, a transducer, and amplification. Various optical-based aptamer sensors that have emerged in recent years are summarized in **Table 2**.

SPR Aptasensors

Surface plasmon resonance has the benefits of no mark detection, real-time supervision of the dynamic process of biological reaction, and non-destructive detection. SPR is the surface

TABLE 1 | Comparison of conventional methods and aptasensors for detection of *S. aureus*.

Detection methods	Basic principle	Advantages	Limitations	Detection limit (CFU/ml)	Assay time
Culture-based methods	Traditional culture is the growth of pathogens in the culture medium and the formation of visible colonies	Gold standard Cost-effective Simple	Time-consuming Complex operation	$>10^4$	7 days
Nucleic acid-based methods	DNA or RNA sequences of target pathogens were manipulated by specific detection	Rapid Specific Sensitive	CostStandardized material Specialized experiment	10^3–10^4	10–24 h
ELISA	The basic principle is the combination of the antibody with the antigen followed by the detection of the antigen–antibody complex	Highly specific Rapid Cost-effective Automatic machine application	Poor stability Existing cross-contamination Equipment required	10^3–10^5	3–10 h
Aptasensors	The detection is based on the high-affinity and high-specificity binding of the secondary or tertiary structures formed by single nucleotides	Wide target range High affinity and specificity Good thermal stability Long storage life Stable properties Flexible Low molecular weight	Limited conformational diversity Time-consuming and low success rate of SELEX process	10^1–10^5	0.5–3 h

plasma produced by light at the interface of two kinds of dielectric constant materials to reduce the intensity of reflected light. Kinetic and equilibrium analysis of the presence of SPR provides access to characterize molecular interactions, for instance, the aptasensor binds to the analyte, the mutual effect between the antibody and the antigen, and the characterization of the receptor (Damborsky et al., 2016). The limit of detection (LOD) of SPR is based on several factors, such as the molecular weight of the target probe, optical properties, and the affinity of the probe (Nguyen et al., 2015). However, the size of pathogenic bacteria can interfere with some measurements, and the detection limit is often too high. Wang's group assembled aptamers on a gold substrate mediated by polyadenine. The designed aptasensors can only show an SPR signal at concentrations of *S. aureus* greater than 1×10^6 CFU/ml (Wang et al., 2019). The aptamer was applied to detect *S. aureus* in milk by resonance combination with localized surface plasmon resonance (LSPR). It should be pointed out that the LOD of aptasensors was 10^3 CFU/ml, and the analysis time was only 120 s (Khateb et al., 2020).

Colorimetry has been widely used due to the following reasons: low cost, simple, practical, fast, and portable diagnosis. There is no need for an analytical device to easily and immediately verify the presence of pathogens in samples based on color variations (Song et al., 2011). Metal nanoparticles, such as gold and silver, are the subject of attention in aptasensors because of their optical properties related to size and distance. Chang et al. (2016) reported a duplex detection method based on aptamer and gold nanoparticles (AuNPs), which can accurately identify *S. aureus* from common pathogens. Using AuNPs as an indicator, the bacteria were first incubated with antagonistic *S. aureus* aptamers, and then aptamers were inserted into AuNPs to avoid the interaction between bacteria and AuNPs. When salt was added, AuNPs that were bound to the bacteria remained red, while those that were not turned blue (Chang et al., 2016). Yuan and coworkers developed colorimetric aptasensors for *S. aureus* based on AuNPs using tyramine signal amplification (TSA) technology. The method has a detection sensitivity of up to 9 CFU/ml, with a linear range of 10–10^6 CFU/ml (Yuan et al., 2014). A colorimetric immunoassay is adopted based on immuno-magnetic and signal amplification of AuNPs etching to enhance the activity of peroxidase for *S. aureus* detection. IgY-Fe_3O_4/Au nanocomposite was regarded as the capture probe; at the same time, aptamer-AuNPs were used as the signal amplifier, and the *S. aureus* can be lightly caught by the naked eye at 10 CFU/ml and a linear range of 10–10^6 CFU/ml (Yao et al., 2020). Yu et al. (2020) developed a colorimetric aptasensor for high-throughput detection of *S. aureus* catalyzed by aptamers and the dsDNA–SYBR Green I (Sg I) complex. In addition, this method can directly detect *S. aureus*, and the LOD in PBS buffer was 81 CFU/ml and the detection time was 5.5 h (Yu et al., 2020).

Surface-Enhanced Raman Spectroscopy Aptasensors

Surface-enhanced Raman spectroscopy is a kind of common sensing technology, which involves resonance Raman effect excited by plasmon. When molecules are attached to metallic surfaces, like silver nanoparticles and AuNPs, the light scatter of molecules increases. The mechanism of SERS can be divided into electromagnetic field enhancement and chemical mechanism (CM), which is due to the particular interaction of adsorbed substances between metal surfaces and molecules (Langer et al., 2019). It is generally believed that the electromagnetic field on the metal surface can be expressively raised due to plasma excitation because the electromagnetic mechanism provides most of the enhancement (Payton et al., 2014). Zhu et al. (2021) assembled a *S. aureus* aptasensor using SERS technology based on an aptamer functionalized polydimethylsiloxane (PDMS) membrane. The aptamer was fixed on the AuNPS-PDMS membrane by Au-S. The gold-core silver-shell nanoflower (Au@AgNFS) revised by mercaptobenzoic acid (4-MBA) and aptamer was used as the

TABLE 2 | Optical-based aptasensors for detect *S. aureus*.

Advantages	Limitations	Detection methods	Detection limit	Linear range	References
Worthy sensitivity Label-free detection Quantification	Limited detection of the whole cell Requires a relatively large equipment Complex analysis system	SPR	10^6 CFU/ml	10^5–10^8 CFU/ml	Wang et al., 2019
Simple and rapid Portability Cost-effective	Low sensitivity Limited quantification	Colorimetry	9 CFU/ml	10–10^6 CFU/ml	Yuan et al., 2014
		Colorimetry	10 CFU/ml	10–10^6 CFU/ml	Yao et al., 2020
		Colorimetry	81 CFU/ml in PBS	10^2–10^7 CFU/ml	Yu et al., 2020
		Colorimetry	1.5×10^7 cells/ml	1.5×10^7–5.3×10^7 cells/ml	Lim et al., 2021
Superior sensitivity Able to characterize more details Label-free detection	Finite quantification capability Complicated analysis spectrum	SERS	13 CFU/ml	$4.3 \times$ 10–4.3×10^7 CFU/ml	Zhu et al., 2021
		SERS	35 CFU/ml	10^2–10^7 CFU/ml	Zhang et al., 2015
		SERS	3 cells/ml	10^2–10^7 cells/ml	Pang et al., 2019
		SERS	1.5 CFU/ml	10–10^7 CFU/ml	Gao et al., 2017
High sensitivity, stable Simultaneous detection Nanomaterials applications	Requires pretreatment Complex operation steps	Fluorescence	1.7 CFU/ml	7–7×10^7 CFU/ml	Yu et al., 2017
		Fluorescence	64 CFU/ml	10^2–10^7 CFU/ml	Lu et al., 2020
		Fluorescence	7.6×10^2 cells/ml	6.0×10^2–6.0×10^5 cells/ml	He et al., 2014

signal probe. A sandwich structure used is for taking substrate target-signal molecular probes. Under optimized experimental conditions, LOD is 13 CFU/ml. The linear range of this experiment was 4.3 × 10 to 4.3 × 10^7 CFU/ml (Zhu et al., 2021). Zhang et al. (2015) used Raman molecule-modified AuNPs and aptamers as signal probes. Fe_3O_4 magnetic AuNPS (Au-MNP) immobilized with aptamers were designed to capture *S. aureus*. Under optimal conditions, the LOD was 35 CFU/ml (Zhang et al., 2015). A magnet SERS biosensor was proposed based on the double recognition of pathogens by aptamers and antibiotics. Fe_3O_4@Au magnetic nanoparticles (Au-MNPs) modified with aptamers were compounded by bacteria-specific magnetism and SERS active substrates, and vancomycin-labeled SERS (Au@MBA) was intended for sensitive quantification of pathogens. *S. aureus* in real samples, such as milk and orange juice, were detected; the LOD was 3 cells/ml, and the detection of the aptasensor reported ranged from 10 to 10^7 cells/ml (Pang et al., 2019). Zhang et al. (2018) first reported a dual vancomycin and aptamer identification of a sensitive SERS platform, with *Escherichia coli* (*E. coli*) and *S. aureus* as target bacteria, and, at the same time, detected 20 kinds of pathogenic bacteria. To sum up, the LOD was shown to be 20 cells/ml, and *S. aureus* was in the range of 20–10^5 cells/ml (Zhang et al., 2018). It is generally accepted that SERS has overcome the shortcomings of Raman spectroscopy, such as flat Raman signal, poor LOD, and photobleaching (Smolsky et al., 2017).

Fluorescent-Based Aptasensors

Fluorescence has become one of the most commonly used sensing ways for the analysis and detection of low-concentration analytes because of its high sensitivity, high efficiency, and simple and rapid analysis. Fluorescence can be classified as labeled and unlabeled. Labeled fluorescence requires at least one chromophore or fluorescent cluster, and the typically labeled fluorescence assay is Förster (fluorescence) resonance energy transfer (FRET) detection. The realization of fluorescence signal mainly depends on the interaction between a non-radiative energy long-range dipole and a dipole used to transfer from the donor to the recipient, called FRET; there are generally two sensing strategies, namely, a signal on and signal off. Yu et al. (2017) proposed a dual recognition of *S. aureus* using vancomycin and aptamer nucleic acid based on a bimolecular affinity FRET platform. The donors and the receptors are, respectively, gold nanoclusters that function with vancomycin and aptamer-modified AuNPs, under optimal detection conditions; using this approach, the linear range for monitoring *S. aureus* was 20–10^8 CFU/ml, with the LOD as low as 10 CFU/ml (Yu et al., 2017). Tao et al. (2021) designed a one-step FRET assay for *S. aureus* detection. With aptamer-modified quantum dots (QDs) as donors and antibiotics-modified AuNPs playing the role of acceptors, the detection time was 1 h, and the detection linear range was 10–5 × 10^8 CFU/ml; the LOD in food samples (milk and orange juice) was 100 CFU/ml (Tao et al., 2021). Lu et al. (2020) introduced the protective binding influence between aptamers and targets, to construct the aptasensors, thus avoiding the optimization of the aptamer probe sequence. Sensitive detection of *S. aureus* was achieved (LOD was 64 CFU/ml, and the dynamic range was 10^2–10^7 CFU/ml). The method mentioned above can be used for high-precision quantification of *S. aureus* in tap water, milk, and pork (Lu et al., 2020). He et al. (2014) designed to immobilize the aptamer of *S. aureus* on fluorescent silica nanoparticles to generate Aptamer/FSiNPs. The experiment is described as follows, in a nutshell. Firstly, the sample is grown with the self-assembly, and then the sample was stained with DNA dye and finally detected by two-color flow cytometry. Using this approach, the aptasensor had a LOD of 1.5 × 10^2 cells/ml in buffer and 7.6 × 10^2 cells/ml in spiked milk (He et al., 2014). Based on carbon dots (CDs) and gold nanoparticles, Yao et al. (2021) established a one-step fluorescence method for *S. aureus* detection. When *S. aureus* occurs, the fluorescence signal is turned off according to the aptamer that preferentially binds to the pathogen phenomenon. The LOD of this unlabeled method was 10 CFU/ml, and the linear range was 10–10^6 CFU/ml (Yao et al., 2021).

Molecules capable of fluorescing sensing are usually carried by structures called fluorophores and receptors, and in some systems, these two structures can be combined. A method for the detection of *S. aureus* fluorescence based on a molecular beacon (MB) and chain displacement target cycle has been developed by Cai et al. (2019). The results revealed that the detection range of *S. aureus* was 80–8 × 10^6 CFU/ml, and the LOD was 39 CFU/ml (Cai et al., 2019). Hundreds of studies heretofore have focused on nanomaterials; a large number of nanomaterials such as QDs, up-conversion nanoparticles (UCNPs), CDs, AuNPs, graphene oxide (GO), and carbon nanotubes (CNTs) have been applied in fluorescence biosensors. High-sensitivity and multiplex methods have been established to detect simultaneously and specifically three pathogens, using polychromatic UCNPs as markers and aptamers as molecular recognition elements. Under optimum conditions, the bacterial concentration was linearly correlated with the luminescent signal in the range of 50–10^6 CFU/ml. The LOD of this work was found to be 25 CFU/ml for *S. aureus* (Wu et al., 2014). Shrivastava et al. (2018) demonstrated a culture-free, rapid, quantitative method to detect *S. aureus* based on a smartphone. Marked *S. aureus* are captured by a magnet in a box where light-emitting diodes act as a source of excitement and then smartphone cameras are used to create a fluorescent image. The method allows the detection of *S. aureus* directly from peanut milk samples for 10 min, with a minimum detection concentration of 10 CFU/ml (Shrivastava et al., 2018).

Electrochemical Aptasensors

Electrochemical biosensors can be widely used in pathogen detection for the safety of food and drinking water, medical diagnosis, environmental monitoring, and biological threats due to their wide variety (Yang et al., 2018). Electrochemical biosensors that can be used for real-time detection, with high specificity and no contamination, have become a bioanalytical method for clinical diagnosis of proteins in point-of-care systems (Chikkaveeraiah et al., 2012). As can be seen from **Figure 2**, the principle of electrochemical detection is expressed. Electrochemical aptasensors combined with a

variety of nanomaterials (CNTs, graphene, GO, etc.) have been widely popularized in food and clinic (Ravalli et al., 2016; Wang et al., 2016; Pourakbari et al., 2019). Electrochemical aptasensors utilize electrodes as the transduction element and aptamers as the biometric identification element to convert signals into electrochemical signals. Ceramic electrodes, metal electrodes [Au and platinum (Pt)], polymer materials electrodes, and carbon electrodes have been widely used as electrodes (Amiri et al., 2020). The following three methods representing electrochemical transducer detection will be introduced: potentiometry, voltammetry, and impedimetry. **Table 3** compares the electrochemical detection of *S. aureus* based on aptasensors.

Aptasensor Detection Based on Potentiometry

Potentiometry, also known as amperometry, measures the potential by applying a current. One advantage of this method is the ability to use a low-cost measuring instrument. Hernández et al. (2014) synthesized a potentiometric aptasensor using graphene electrodes modified on carbon rods and an aptamer attached to graphene, which can catch a single CFU/ml of *S. aureus*. Lian et al. (2015) have developed a new piezoelectric sensor that connects *S. aureus* aptamers with gold electrodes, using aptamers as a recognition element. Using 4-mercaptobenzene-diazonium tetrafluoroborate (MBDT) as a molecular crosslinking agent, graphene was chemically bonded to the interdigital gold electrode (IDE) of a series of electrode piezoelectric quartz crystals (SPQC). At the time when *S. aureus* appears, the aptamer falls off the surface of graphene (Lian et al., 2015). Cai et al. (2021) designed an electrochemical method for *S. aureus* detection of three-helix molecular switches. An aptamer modified on the magnetic bead was used to capture the pathogens and release the complementary strand cDNA. In the next step, the gold electrode that modified the triple helix structure controls the release and shutdown of the signal. The system was able to detect water and honey samples, the LOD was 8 CFU/ml, and the linear range was from 30 to 3×10^8 CFU/ml (Cai et al., 2021).

Aptasensor Detection Based on Voltammetry

Voltammetry is a method of measuring current by controlling potential. Recently, Abbaspour et al. (2015) employed a sandwich structure modified with silver nanoparticles and aptamers to detect *S. aureus*. The primary aptamer was securely fixed to the magnetic bead in order to catch *S. aureus*, while the secondary aptamer is combined with silver nanoparticles to improve the specific electrochemical properties. In addition, the LOD of this voltammetry was shown to be 1.0 CFU/ml, and the dynamic range was 10–1×10^6 CFU/ml (Abbaspour et al., 2015). **Figure 3** shows the schematic of the classical two-aptamer sandwich method for the electrochemical detection of *S. aureus*. The construction of electrochemical aptasensors is not only applied to the risk assessment of *S. aureus* in food, but also has a good application in the risk assessment of toxins. Mousavi Nodoushan et al. (2019) detected SEB on screen-printed electrodes modified with graphene oxide (rGO) and nano-gold sea urchins (Aunus). DNA chain probes were connected to aptamers and probes were connected to Aunus electrodes. When the SEB appeared, the aptamer disconnected from the electrode and the peak current is recorded using an electrochemical signal generator. The electrochemical aptasensor developed is highly sensitive in milk, meat, and serum samples. The aptasensor had a LOD of 0.21 fM, with a wide linear range of 5.0–500.0 fM (Mousavi Nodoushan et al., 2019).

Aptasensor Detection Based on Impedimetry

Electrochemical impedance spectroscopy (EIS) is a technique used to study electrode systems and to conclude the quantification of electrochemical processes. Despite the complexity of EIS, it has high commercial potential, and has been widely used in environmental monitoring, disease monitoring, and other fields. One of its advantages is small-amplitude

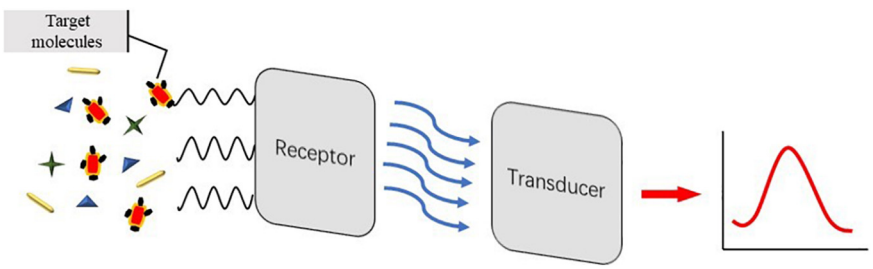

FIGURE 2 | Schematic illustration of detection principle of electrochemical aptasensors.

TABLE 3 | Comparison of analytical features of electrochemically related aptasensors for *S. aureus* detection.

Detection methods	Working electrode	Detection limit	Linear range	References
Potentiometry	GO/rGO aptasensor electrode	1 CFU/ml		Hernández et al., 2014
Potentiometry	Aptamer/graphene interdigitated gold electrode	41 CFU/ml	4.1×10–4.1×10^5 CFU/ml	Lian et al., 2015
Impedimetry	Glassy carbon electrode	1 CFU/ml	1.2×10^1–1.2×10^8 CFU/ml	Ranjbar and Shahrokhian, 2018
Voltammetry	Carbon electrode	0.21 fM	5.0–500.0 fM	Mousavi Nodoushan et al., 2019
Chronocoulometry	Modified gold electrode	3 pg/ml	0.05–100 ng/ml	Chen et al., 2019

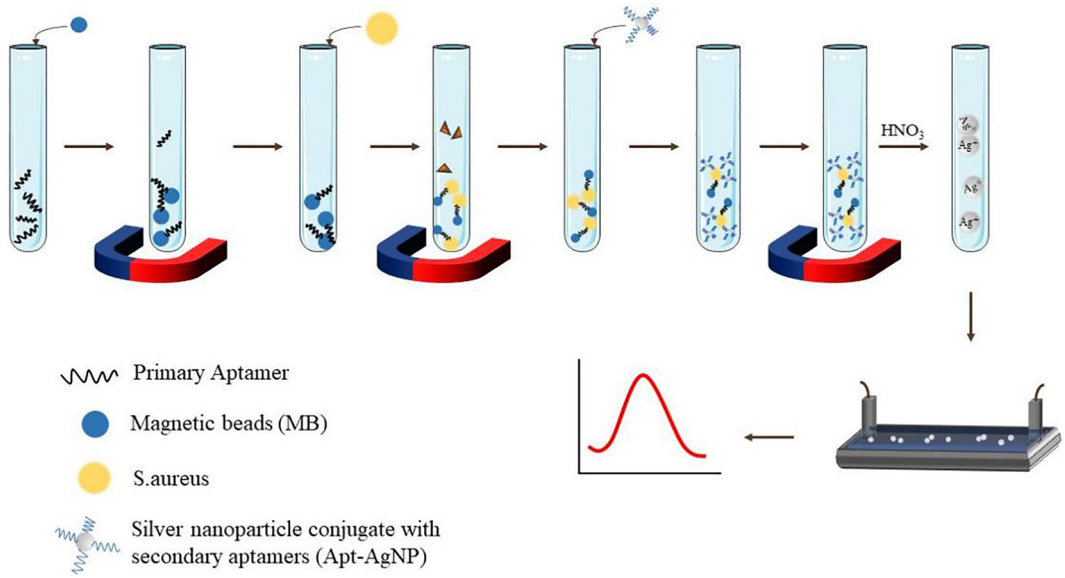

FIGURE 3 | Schematic display electrochemical dual aptamer sandwich detection of *S. aureus*.

homeostatic disturbance, such that it can be realized without damaging the detection of the case. It may also measure, in case of uncertainty, the presence of REDOX pairs (Bahadır and Sezgintürk, 2014). The precision and operation procedure of the instrument has a certain influence on subsequent results. Zhang et al. (2019) used aptamer-magnetic separation in the resistivity method to detect *S. aureus*. The linear ranges of *S. aureus* were 4.1×10^3 to 4.1×10^8 CFU/ml, and LOD was 4.0×10^3 CFU/ml in pure water (Zhang et al., 2019). Reich et al. (2017), who combined EIS use with aptamers to detect *S. aureus*, showed a LOD of 10 CFU/ml. EIS aptasensors also have many applications in the risk assessment of toxins in food. Combining induced release strategy with amplification of HCR signals, Chen et al. (2019) developed an electrochemically competitive nanoprobe for ultrasensitive specificity SEB detection measured with chronocoulometry. Three classical electrodes were used for this experiment, namely, a modified gold electrode, an Ag/AgCl reference electrode, and an auxiliary platinum wire electrode. Under the first-rank conditions, the charge difference of SEB increased linearly with the logarithmic increase of SEB concentration in the range of 5 pg/ml to 100 ng/ml, and the detection limit was as low as 3 pg/ml (Chen et al., 2019).

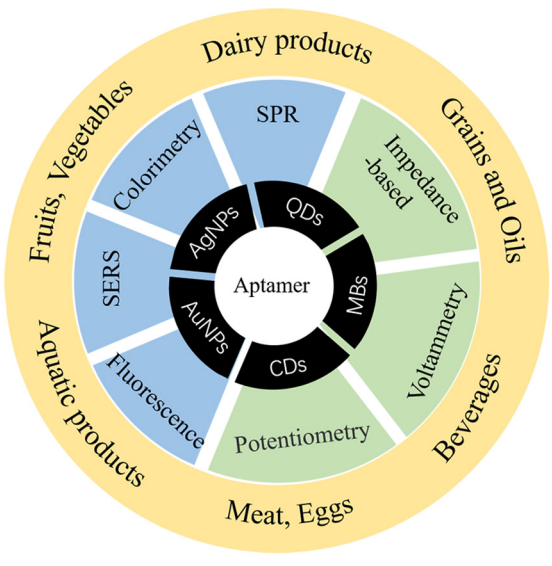

FIGURE 4 | Applicable materials, methods, and applications of aptamers for *S. aureus* risk assessment.

CONCLUSION

This article reviews how aptasensors have been applied to risk assessment in food, especially for foodborne pathogens such as *S. aureus*. As a tool of risk assessment of foodborne pathogens, aptasensors have good competitiveness in terms of time, sensitivity, specificity, and cost.

Staphylococcus aureus produces enterotoxin (especially in animal-derived food such as milk and cream, which are easily infected) to cause food poisoning and has become a worldwide foodborne pathogenic factor. It is necessary to establish a method with less time and high sensitivity for *S. aureus*. It is commonly known that aptasensor detection has been widely applied to foodborne pathogens. However, the sensibility is limited, and it is still the focus of future research to improve the sensitivity and shorten the detection time of foodborne pathogens. In the practical application of aptasensors, there are many problems that need to be solved, for example, finite configuration of aptamers, aptamers with a high negative charge are difficult to combine with a negatively charged target, time-consuming process, and

low success rate of SELEX. In the next step, how to quickly obtain excellent aptamers, shorten the specific aptamer screening cycle, improve the success rate of SELEX, and save cost and investment will become a research focus, so as to further promote the application of aptamer technology in the detection of pathogens. In the future, it is hoped that aptamers combined with a variety of nanomaterials to form simpler and faster aptasensors for detection will not only improve the success rate of detection but also provide a variety of data processing methods in different types of food. **Figure 4** shows the applications of materials for *S. aureus* aptasensor detection in food risk assessment. By virtue of its remarkable detection characteristics, simultaneously solving the above-mentioned issues, detection methods are prone to false-positive results and other defects, and there is thus room for the further development of aptamers. New technologies have also been mentioned in the paper, including new applications of signal transduction and the combination of signal transduction and enhancement of signal amplification mode. With these advances, the sensitivity and time of detection have greatly improved. It is predicted that aptamers will be further combined with nanomaterials, and portable detection instruments will be developed.

AUTHOR CONTRIBUTIONS

ZH and XY drafted the manuscript. WW, QY, and YZ designed the concept and revised the manuscript. All authors contributed to the article and approved the submitted version.

FUNDING

This work was financially supported by the Breeding Plan of Shandong Provincial Qingchuang Research Team (2019), the China Postdoctoral Science Foundation under Grant No. 2019M652320, and the National Natural Science Foundation of China under Grant No. 81703228.

REFERENCES

Abbaspour, A., Norouz-Sarvestani, F., Noori, A., and Soltani, N. (2015). Aptamer-conjugated silver nanoparticles for electrochemical dual-aptamer-based sandwich detection of staphylococcus aureus. *Biosens. Bioelectron.* 68, 149–155. doi: 10.1016/j.bios.2014.12.040

Amiri, M., Nekoueian, K., and Saberi, R. S. (2020). Graphene-family materials in electrochemical aptasensors. *Anal. Bioanal. Chem.* 413, 673–699. doi: 10.1007/s00216-020-02915-y

Bahadır, E. B., and Sezgintürk, M. K. (2014). A review on impedimetric biosensors. *Artif. Cells Nanomed. Biotechnol.* 44, 248–262. doi: 10.3109/21691401.2014.942456

Baumstummler, A., Lehmann, D., Janjic, N., and Ochsner, U. A. (2014). Specific capture and detection of *Staphylococcus aureus* with high-affinity modified aptamers to cell surface components. *Lett. Appl. Microbiol.* 59, 422–431. doi: 10.1111/lam.12295

Cai, R., Yin, F., Zhang, Z., Tian, Y., and Zhou, N. (2019). Functional chimera aptamer and molecular beacon based fluorescent detection of *Staphylococcus aureus* with strand displacement-target recycling amplification. *Anal. Chim. Acta* 1075, 128–136. doi: 10.1016/j.aca.2019.05.014

Cai, R., Zhang, Z., Chen, H., Tian, Y., and Zhou, N. (2021). A versatile signal-on electrochemical biosensor for *Staphylococcus aureus* based on triple-helix molecular switch. *Sens. Act. Chem.* 326:128842. doi: 10.1016/j.snb.2020.128842

Chang, T., Wang, L., Zhao, K., Ge, Y., He, M., and Li, G. (2016). Duplex identification of *Staphylococcus aureus* by aptamer and gold nanoparticles. *J. Nanosci. Nanotechnol.* 16, 5513–5519. doi: 10.1166/jnn.2016.11656

Chen, X., Liu, Y., Lu, Y., Xiong, X., Li, Y., Liu, Y., et al. (2019). Chronocoulometric aptamer based assay for staphylococcal enterotoxin B by target-triggered assembly of nanostructured dendritic nucleic acids on a gold electrode. *Mikrochim. Acta* 186, 109. doi: 10.1007/s00604-019-3236-9

Chikkaveeraiah, B. V., Bhirde, A. A., Morgan, N. Y., Eden, H. S., and Chen, X. (2012). Electrochemical immunosensors for detection of cancer protein biomarkers. *ACS Nano* 6, 6546–6561. doi: 10.1021/nn3023969

da Silva, A. C., Rodrigues, M. X., and Silva, N. C. C. (2020). Methicillin-resistant Staphylococcus aureus in food and the prevalence in Brazil: a review. *Braz. J. Microbiol.* 51, 347–356. doi: 10.1007/s42770-019-00168-1

Damborsky, P., Svitel, J., and Katrlik, J. (2016). Optical biosensors. *Essays Biochem.* 60, 91–100. doi: 10.1042/EBC20150010

DeGrasse, J. A. (2012). A single-stranded DNA aptamer that selectively binds to *Staphylococcus aureus* enterotoxin B. *PLoS One* 7:e33410. doi: 10.1371/journal.pone.0033410

Deurenberg, R. H., Vink, C., Kalenic, S., Friedrich, A. W., Bruggeman, C. A., and Stobberingh, E. E. (2007). The molecular evolution of methicillin-resistant *Staphylococcus aureus*. *Clin. Microbiol. Infect.* 13, 222–235. doi: 10.1111/j.1469-0691.2006.01573.x

Ellington, A. D., and Szostak, J. W. (1990). In vitro selection of RNA molecules that bind specific ligands. *Nature* 346, 818–822. doi: 10.1038/346818a0

European Food Safety Authority, and European Centre for Disease Prevention and Control (2017). The European Union summary report on trends and sources of zoonoses, zoonotic agents and food-borne outbreaks in 2016. *EFSA J.* 15:e05077. doi: 10.2903/j.efsa.2017.5077

European Food Safety Authority, and European Centre for Disease Prevention and Control (2018). The European Union summary report on trends and sources of zoonoses, zoonotic agents and food-borne outbreaks in 2017. *EFSA J.* 16:e05500. doi: 10.2903/j.efsa.2018.5500

Foddai, A. C. G., and Grant, I. R. (2020). Methods for detection of viable foodborne pathogens: current state-of-art and future prospects. *Appl. Microbiol. Biotechnol.* 104, 4281–4288. doi: 10.1007/s00253-020-10542-x

Gao, W., Li, B., Yao, R., Li, Z., Wang, X., Dong, X., et al. (2017). Intuitive label-Free SERS detection of bacteria using aptamer-based in situ silver nanoparticles synthesis. *Anal. Chem.* 89, 9836–9842. doi: 10.1021/acs.analchem.7b01813

Gopinath, S. C., Lakshmipriya, T., Chen, Y., Phang, W. M., and Hashim, U. (2016). Aptamer-based 'point-of-care testing'. *Biotechnol. Adv.* 34, 198–208. doi: 10.1016/j.biotechadv.2016.02.003

He, X., Li, Y., He, D., Wang, K., Shangguan, J., and Shi, H. (2014). Aptamer-fluorescent silica nanoparticles bioconjugates based dual-color flow cytometry for specific detection of *Staphylococcus aureus*. *J. Biomed. Nanotechnol.* 10, 1359–1368. doi: 10.1166/jbn.2014.1828

Hernández, R., Vallés, C., Benito, A. M., Maser, W. K., Xavier Rius, F., and Riu, J. (2014). Graphene-based potentiometric biosensor for the immediate detection of living bacteria. *Biosens. Bioelectron.* 54, 553–557. doi: 10.1016/j.bios.2013.11.053

Huang, Y., Chen, X., Duan, N., Wu, S., Wang, Z., Wei, X., et al. (2015). Selection and characterization of DNA aptamers against *Staphylococcus aureus* enterotoxin C1. *Food Chem.* 166, 623–629. doi: 10.1016/j.foodchem.2014.06.039

Huang, Y., Chen, X., Xia, Y., Wu, S., Duan, N., Ma, X., et al. (2014). Selection, identification and application of a DNA aptamer against *Staphylococcus aureus* enterotoxin A. *Anal. Methods* 6, 690–697. doi: 10.1039/c3ay41576g

Hulme, J. (2017). Recent advances in the detection of methicillin resistant *Staphylococcus aureus* (MRSA). *BioChip J.* 11, 89–100. doi: 10.1007/s13206-016-1201-9

Ji, Y., Li, X., Lu, Y., Guo, P., Zhang, G., Wang, Y., et al. (2020). Nanobodies based on a sandwich immunoassay for the detection of staphylococcal enterotoxin B free from interference by protein A. *J. Agric. Food Chem.* 68, 5959–5968. doi: 10.1021/acs.jafc.0c00422

Johler, S., Macori, G., Bellio, A., Acutis, P. L., Gallina, S., and Decastelli, L. (2018). Short communication: characterization of *Staphylococcus aureus* isolated along the raw milk cheese production process in artisan dairies in Italy. *J. Dairy Sci.* 101, 2915–2920. doi: 10.3168/jds.2017-13815

Khateb, H., Klös, G., Meyer, R. L., and Sutherland, D. S. (2020). Development of a Label-Free LSPR-Apta sensor for *Staphylococcus aureus* detection. *ACS Appl. Bio Mater.* 3, 3066–3077. doi: 10.1021/acsabm.0c00110

Langer, J., Jimenez de Aberasturi, D., Aizpurua, J., Alvarez-Puebla, R. A., Auguié, B., Baumberg, J. J., et al. (2019). Present and future of surface-enhanced raman scattering. *ACS Nano* 14, 28–117. doi: 10.1021/acsnano.9b04224

Lian, Y., He, F., Wang, H., and Tong, F. (2015). A new aptamer/graphene interdigitated gold electrode piezoelectric sensor for rapid and specific detection of *Staphylococcus aureus*. *Biosens. Bioelectron.* 65, 314–319. doi: 10.1016/j.bios.2014.10.017

Lim, S. H., Ryu, Y. C., and Hwang, B. H. (2021). Aptamer-immobilized gold nanoparticles enable facile and on-site detection of *Staphylococcus aureus*. *Biotechnol. Bioprocess Eng.* 26, 107–113. doi: 10.1007/s12257-020-0161-z

Lu, Y., Yuan, Z., Bai, J., Lin, Q., Deng, R., Luo, A., et al. (2020). Directly profiling intact *Staphylococcus aureus* in water and foods via enzymatic cleavage aptasensor. *Anal. Chim. Acta* 1132, 28–35. doi: 10.1016/j.aca.2020.07.058

Macori, G., Giacinti, G., Bellio, A., Gallina, S., Bianchi, D. M., Sagrafoli, D., et al. (2017). Molecular epidemiology of methicillin-resistant and methicillin-susceptible *Staphylococcus aureus* in the ovine dairy chain and in farm-related humans. *Toxins (Basel)* 9:161. doi: 10.3390/toxins9050161

Martinon, A., and Wilkinson, M. G. (2011). Selection of optimal primer sets for use in a duplex sybr green-based, real-time polymerase chain reaction protocol for the detection of listeria monocytogenes and *Staphyloccocus aureus* in foods. *J. Food Saf.* 31, 297–312. doi: 10.1111/j.1745-4565.2011.00301.x

McMillan, K., Moore, S. C., McAuley, C. M., Fegan, N., and Fox, E. M. (2016). Characterization of *Staphylococcus aureus* isolates from raw milk sources in Victoria, Australia. *BMC Microbiol.* 16:169. doi: 10.1186/s12866-016-0789-1

Mousavi Nodoushan, S., Nasirizadeh, N., Amani, J., Halabian, R., and Imani Fooladi, A. A. (2019). An electrochemical aptasensor for staphylococcal enterotoxin B detection based on reduced graphene oxide and gold nano-urchins. *Biosens. Bioelectron.* 127, 221–228. doi: 10.1016/j.bios.2018.12.021

Nguyen, H. H., Park, J., Kang, S., and Kim, M. (2015). Surface plasmon resonance: a versatile technique for biosensor applications. *Sensors (Basel)* 15, 10481–10510. doi: 10.3390/s150510481

Notomi, T., Okayama, H., Masubuchi, H., Yonekawa, T., Watanabe, K., Amino, N., et al. (2000). Loop-mediated isothermal amplification of DNA. *Nucleic Acids Res.* 28:E63.

Nouri, A., Ahari, H., and Shahbazzadeh, D. (2018). Designing a direct ELISA kit for the detection of *Staphylococcus aureus* enterotoxin A in raw milk samples. *Int. J. Biol. Macromol.* 107(Pt B), 1732–1737. doi: 10.1016/j.ijbiomac.2017.10.052

Pang, Y., Wan, N., Shi, L., Wang, C., Sun, Z., Xiao, R., et al. (2019). Dual-recognition surface-enhanced Raman scattering(SERS)biosensor for pathogenic bacteria detection by using vancomycin-SERS tags and aptamer-Fe3O4@Au. *Anal. Chim. Acta* 1077, 288–296. doi: 10.1016/j.aca.2019.05.059

Papadopoulos, P., Papadopoulos, T., Angelidis, A. S., Boukouvala, E., Zdragas, A., Papa, A., et al. (2018). Prevalence of *Staphylococcus aureus* and of methicillin-resistant *S. aureus* (MRSA) along the production chain of dairy products in north-western Greece. *Food Microbiol.* 69, 43–50. doi: 10.1016/j.fm.2017.07.016

Park, Y. S., Lee, S. R., and Kim, Y. G. (2006). Detection of *Escherichia coli* O157:H7, *Salmonella* spp., *Staphylococcus aureus* and *Listeria monocytogenes* in kimchi by multiplex polymerase chain reaction (mPCR). *J. Microbiol. (Seoul, Korea)* 44, 92–97.

Payton, J. L., Morton, S. M., Moore, J. E., and Jens, L. (2014). A hybrid atomistic electrodynamics–quantum mechanical approach for simulating surface-enhanced Raman scattering. *Acc. Chem. Res.* 47, 88–99.

Pourakbari, R., Shadjou, N., Yousefi, H., Isildak, I., Yousefi, M., Rashidi, M. R., et al. (2019). Recent progress in nanomaterial-based electrochemical biosensors for pathogenic bacteria. *Mikrochim. Acta* 186:820. doi: 10.1007/s00604-019-3966-8

Prenafeta, A., Sitjà, M., Holmes, M. A., and Paterson, G. K. (2014). Short communication: biofilm production characterization of mecA and mecC methicillin-resistant *Staphylococcus aureus* isolated from bovine milk in Great Britain. *J. Dairy Sci.* 97, 4838–4841. doi: 10.3168/jds.2014-7986

Principato, M., and Qian, B. F. (2014). Staphylococcal enterotoxins in the etiopathogenesis of mucosal autoimmunity within the gastrointestinal tract. *Toxins (Basel)* 6, 1471–1489. doi: 10.3390/toxins6051471

Priyanka, B., Patil, R. K., and Dwarakanath, S. (2016). A review on detection methods used for foodborne pathogens. *Indian J. Med. Res.* 144, 327–338. doi: 10.4103/0971-5916.198677

Qi, Y., and Miller, K. J. (2000). Effect of low water activity on staphylococcal enterotoxin A and B biosynthesis. *J. Food Protect.* 63, 473–478. doi: 10.4315/0362-028X-63.4.473

Ramesh, R., Munshi, A., and Panda, S. K. (1992). Polymerase chain reaction. *Natl. Med. J. India* 5, 115–119.

Saiki, R. K., Scharf, S., Faloona, F., Mullis, K. B., Horn, G. T., Erlich, H. A., et al. (1985). Enzymatic amplification of beta-globin genomic sequences and restriction site analysis for diagnosis of sickle cell anemia. *Science* 230, 1350–1354.

Ranjbar, S., and Shahrokhian, S. (2018). Design and fabrication of an electrochemical aptasensor using Au nanoparticles/carbon nanoparticles/cellulose nanofibers nanocomposite for rapid and sensitive detection of S*taphylococcus aureus*. *Bioelectrochemistry* 123, 70–76.

Ravalli, A., Voccia, D., Palchetti, I., and Marrazza, G. (2016). Electrochemical, electrochemiluminescence, and photoelectrochemical aptamer-based nanostructured sensors for biomarker analysis. *Biosensors* 6:39. doi: 10.3390/bios6030039

Reich, P., Stoltenburg, R., Strehlitz, B., Frense, D., and Beckmann, D. (2017). Development of an impedimetric aptasensor for the detection of *Staphylococcus aureus*. *Int. J. Mol. Sci.* 18:2484. doi: 10.3390/ijms18112484

Rubab, M., Shahbaz, H. M., Olaimat, A. N., and Oh, D. H. (2018). Biosensors for rapid and sensitive detection of *Staphylococcus aureus* in food. *Biosens. Bioelectron.* 105, 49–57. doi: 10.1016/j.bios.2018.01.023

Sergelidis, D., and Angelidis, A. S. (2017). Methicillin-resistant *Staphylococcus aureus*: a controversial food-borne pathogen. *Lett. Appl. Microbiol.* 64, 409–418. doi: 10.1111/lam.12735

Shrivastava, S., Lee, W. I., and Lee, N. E. (2018). Culture-free, highly sensitive, quantitative detection of bacteria from minimally processed samples using fluorescence imaging by smartphone. *Biosens. Bioelectron.* 109, 90–97. doi: 10.1016/j.bios.2018.03.006

Sieber, R. N., Skov, R. L., Nielsen, J., Schulz, J., Price, L. B., Aarestrup, F. M., et al. (2018). Drivers and dynamics of methicillin-resistant livestock-associated *Staphylococcus aureus* CC398 in pigs and humans in Denmark. *mBio* 9:e02459-18. doi: 10.1128/mBio.02142-18

Smith, C. J., and Osborn, A. M. (2009). Advantages and limitations of quantitative PCR (Q-PCR)-based approaches in microbial ecology. *FEMS Microbiol. Ecol.* 67, 6–20. doi: 10.1111/j.1574-6941.2008.00629.x

Smolsky, J., Kaur, S., Hayashi, C., Batra, S., and Krasnoslobodtsev, A. (2017). Surface-enhanced Raman scattering-based immunoassay technologies for detection of disease biomarkers. *Biosensors* 7:7. doi: 10.3390/bios7010007

Song, Y., Wei, W., and Qu, X. (2011). Colorimetric biosensing using smart materials. *Adv. Mater.* 23, 4215–4236. doi: 10.1002/adma.201101853

Srividya, A., Maiti, B., Chakraborty, A., and Chakraborty, G. (2019). Loop mediated isothermal amplification: a promising tool for screening genetic mutations. *Mol. Diagn. Ther.* 23, 723–733. doi: 10.1007/s40291-019-00422-0

Sun, T., Zhao, Z., Liu, W., Xu, Z., He, H., Ning, B., et al. (2020). Development of sandwich chemiluminescent immunoassay based on an anti-staphylococcal enterotoxin B Nanobody-Alkaline phosphatase fusion protein for detection of staphylococcal enterotoxin B. *Anal. Chim. Acta* 1108, 28–36. doi: 10.1016/j.aca.2020.01.032

Tao, J., Liu, W., Ding, W., Han, R., Shen, Q., Xia, Y., et al. (2020). A multiplex PCR assay with a common primer for the detection of eleven foodborne pathogens. *J. Food Sci.* 85, 744–754. doi: 10.1111/1750-3841.15033

Tao, X., Liao, Z., Zhang, Y., Fu, F., Hao, M., Song, Y., et al. (2021). Aptamer-quantum dots and teicoplanin-gold nanoparticles constructed FRET sensor for sensitive detection of *Staphylococcus aureus*. *Chin. Chem. Lett.* 32, 791–795. doi: 10.1016/j.cclet.2020.07.020

Tegegne, H. A., Florianova, M., Gelbicova, T., Karpiskova, R., and Kolackova, I. (2019). Detection and molecular characterization of methicillin-resistant *Staphylococcus aureus* isolated from bulk tank milk of cows, sheep, and goats. *Foodborne Pathog. Dis.* 16, 68–73. doi: 10.1089/fpd.2018.2511

Tuerk, C., and Gold, L. (1990). Systematic evolution of ligands by exponential enrichment: RNA ligands to bacteriophage T4 DNA polymerase. *Science* 249, 505–510.

Umesha, S., and Manukumar, H. M. (2018). Advanced molecular diagnostic techniques for detection of food-borne pathogens: current applications and future challenges. *Crit. Rev. Food Sci. Nutr.* 58, 84–104. doi: 10.1080/10408398.2015.1126701

Valderrama, W. B., Dudley, E. G., Doores, S., and Cutter, C. N. (2016). Commercially available rapid methods for detection of selected food-borne pathogens. *Crit. Rev. Food Sci. Nutr.* 56, 1519–1531. doi: 10.1080/10408398.2013.775567

Wang, W. W., Han, X., and Chu, L. Q. (2019). Polyadenine-mediated immobilization of aptamers on a gold substrate for the direct detection of bacterial pathogens. *Anal. Sci.* 35, 967–972.

Wang, Z., Yu, J., Gui, R., Jin, H., and Xia, Y. (2016). Carbon nanomaterials-based electrochemical aptasensors. *Biosens. Bioelectron.* 79, 136–149. doi: 10.1016/j.bios.2015.11.093

Wilson, I. G., Cooper, J. E., and Gilmour, A. (1991). Detection of enterotoxigenic *Staphylococcus aureus* in dried skimmed milk: use of the polymerase chain reaction for amplification and detection of staphylococcal enterotoxin genes entB and entC1 and the thermonuclease gene nuc. *Appl. Environ. Microbiol.* 57, 1793–1798. doi: 10.1128/AEM.57.6.1793-1798.1991

Wu, S., Duan, N., Shi, Z., Fang, C., and Wang, Z. (2014). Simultaneous aptasensor for multiplex pathogenic bacteria detection based on multicolor upconversion nanoparticles labels. *Anal. Chem.* 86, 3100–3107. doi: 10.1021/ac404205c

Yang, Y., Yang, X., Yang, Y., and Yuan, Q. (2018). Aptamer-functionalized carbon nanomaterials electrochemical sensors for detecting cancer relevant biomolecules. *Carbon* 129, 380–395. doi: 10.1016/j.carbon.2017.12.013

Yao, S., Li, J., Pang, B., Wang, X., Shi, Y., Song, X., et al. (2020). Colorimetric immunoassay for rapid detection of *Staphylococcus aureus* based on etching-enhanced peroxidase-like catalytic activity of gold nanoparticles. *Mikrochim. Acta* 187:504. doi: 10.1007/s00604-020-04473-7

Yao, S., Zhao, C., Shang, M., Li, J., and Wang, J. (2021). Enzyme-free and label-free detection of *Staphylococcus aureus* based on target-inhibited fluorescence signal recovery. *Food Chem. Toxicol.* 150:112071. doi: 10.1016/j.fct.2021.112071

Yu, M., Wang, H., Fu, F., Li, L., Li, J., Li, G., et al. (2017). Dual-recognition forster resonance energy transfer based platform for one-step sensitive detection of pathogenic bacteria using fluorescent vancomycin-gold nanoclusters and aptamer-gold nanoparticles. *Anal. Chem.* 89, 4085–4090. doi: 10.1021/acs.analchem.6b04958

Yu, T., Xu, H., Zhao, Y., Han, Y., Zhang, Y., Zhang, J., et al. (2020). Aptamer based high throughput colorimetric biosensor for detection of *Staphylococcus aureus*. *Sci. Rep.* 10:9190. doi: 10.1038/s41598-020-66105-7

Yuan, J., Wu, S., Duan, N., Ma, X., Xia, Y., Chen, J., et al. (2014). A sensitive gold nanoparticle-based colorimetric aptasensor for *Staphylococcus aureus*. *Talanta* 127, 163–168. doi: 10.1016/j.talanta.2014.04.013

Zhang, C., Wang, C., Xiao, R., Tang, L., Huang, J., Wu, D., et al. (2018). Sensitive and specific detection of clinical bacteria via vancomycin-modified Fe3O4@Au nanoparticles and aptamer-functionalized SERS tags. *J. Mater. Chem. B* 6, 3751–3761. doi: 10.1039/c8tb00504d

Zhang, H., Ma, X., Liu, Y., Duan, N., Wu, S., Wang, Z., et al. (2015). Gold nanoparticles enhanced SERS aptasensor for the simultaneous detection of *Salmonella* typhimurium and *Staphylococcus aureus*. *Biosens. Bioelectron.* 74, 872–877. doi: 10.1016/j.bios.2015.07.033

Zhang, X., Wang, X., Yang, Q., Jiang, X., Li, Y., Zhao, J., et al. (2019). Conductometric sensor for viable *Escherichia coli* and *Staphylococcus aureus* based on magnetic analyte separation via aptamer. *Mikrochim. Acta* 187:43. doi: 10.1007/s00604-019-3880-0

Zhao, X., Lin, C. W., Wang, J., and Oh, D. H. (2014). Advances in rapid detection methods for foodborne pathogens. *J. Microbiol. Biotechnol.* 24, 297–312. doi: 10.4014/jmb.1310.10013

Zhu, A., Ali, S., Xu, Y., Ouyang, Q., and Chen, Q. (2021). A SERS aptasensor based on AuNPs functionalized PDMS film for selective and sensitive detection of *Staphylococcus aureus*. *Biosens. Bioelectron.* 172:112806. doi: 10.1016/j.bios.2020.112806

Conflict of Interest: The authors declare that the research was conducted in the absence of any commercial or financial relationships that could be construed as a potential conflict of interest.

Publisher's Note: All claims expressed in this article are solely those of the authors and do not necessarily represent those of their affiliated organizations, or those of the publisher, the editors and the reviewers. Any product that may be evaluated in this article, or claim that may be made by its manufacturer, is not guaranteed or endorsed by the publisher.

frontiers in Microbiology

ORIGINAL RESEARCH
published: 16 September 2021
doi: 10.3389/fmicb.2021.688614

Serotyping, MLST, and Core Genome MLST Analysis of *Salmonella enterica* From Different Sources in China During 2004–2019

Shigan Yan[1†], Wencheng Zhang[1†], Chengyu Li[1], Xu Liu[1], Liping Zhu[1], Leilei Chen[2]* and Baowei Yang[3]*

[1] Shandong Provincial Key Laboratory of Bioengineering, School of Bioengineering, Qilu University of Technology, Shandong Academy of Sciences, Jinan, China, [2] Institute of Agro-Food Sciences and Technology, Shandong Academy of Agricultural Sciences, Jinan, China, [3] College of Food Science and Engineering, Northwest A&F University, Yangling, China

OPEN ACCESS

Edited by:
Jun Wang,
Qingdao Agricultural University, China

Reviewed by:
Guojie Cao,
Center for Food Safety and Applied Nutrition, United States Food and Drug Administration, United States
Xihong Zhao,
Wuhan Institute of Technology, China

***Correspondence:**
Liping Zhu
zhuliping2012@aliyun.com.cn
Leilei Chen
chenleilei8210@163.com

[†] These authors have contributed equally to this work

Specialty section:
This article was submitted to Food Microbiology, a section of the journal Frontiers in Microbiology

Received: 31 March 2021
Accepted: 11 August 2021
Published: 16 September 2021

Citation:
Yan S, Zhang W, Li C, Liu X, Zhu L, Chen L and Yang B (2021) Serotyping, MLST, and Core Genome MLST Analysis of Salmonella enterica From Different Sources in China During 2004–2019. Front. Microbiol. 12:688614. doi: 10.3389/fmicb.2021.688614

Salmonella enterica (*S. enterica*) is an important foodborne pathogen, causing food poisoning and human infection, and critically threatening food safety and public health. *Salmonella* typing is essential for bacterial identification, tracing, epidemiological investigation, and monitoring. Serotyping and multilocus sequence typing (MLST) analysis are standard bacterial typing methods despite the low resolution. Core genome MLST (cgMLST) is a high-resolution molecular typing method based on whole genomic sequencing for accurate bacterial tracing. We investigated 250 *S. enterica* isolates from poultry, livestock, food, and human sources in nine provinces of China from 2004 to 2019 using serotyping, MLST, and cgMLST analysis. All *S. enterica* isolates were divided into 36 serovars using slide agglutination. The major serovars in order were Enteritidis (31 isolates), Typhimurium (29 isolates), Mbandaka (23 isolates), and Indiana (22 isolates). All strains were assigned into 43 sequence types (STs) by MLST. Among them, ST11 (31 isolates) was the primary ST. Besides this, a novel ST, ST8016, was identified, and it was different from ST40 by position 317 C → T in *dnaN*. Furthermore, these 250 isolates were grouped into 185 cgMLST sequence types (cgSTs) by cgMLST. The major cgST was cgST235530 (11 isolates), and only three cgSTs contained isolates from human and other sources, indicating a possibility of cross-species infection. Phylogenetic analysis indicated that most of the same serovar strains were putatively homologous except Saintpaul and Derby due to their multilineage characteristics. In addition, serovar I 4,[5],12:i:- and Typhimurium isolates have similar genomic relatedness on the phylogenetic tree. In conclusion, we sorted out the phenotyping and genotyping diversity of *S. enterica* isolates in China during 2004–2019 and clarified the temporal and spatial distribution characteristics of *Salmonella* from different hosts in China in the recent 16 years. These results greatly supplement *Salmonella* strain resources, genetic information, and traceability typing data; facilitate the typing, traceability, identification, and genetic evolution analysis of *Salmonella*; and therefore, improve the level of analysis, monitoring, and controlling of foodborne microorganisms in China.

Keywords: *Salmonella enterica*, whole genome sequencing, serotype, MLST, cgMLST

INTRODUCTION

Salmonella enterica (*S. enterica*) is one of the primary foodborne pathogens to cause food poisoning and human infection (Zhang et al., 2015). Foodborne salmonellosis is an important public health concern worldwide, and it annually causes about 115 million infections and 370,000 deaths globally (Seif et al., 2018). The primary sources of *S. enterica* foodborne infection include poultry eggs, meats, and their derived products (Arthur et al., 2008). Therefore, it is crucial to monitor *Salmonella* from animal food, especially poultry eggs, and their derived food products (Mezal et al., 2014).

Accurate typing and tracing are essential for microbial epidemiological investigation, food safety, and public health. Bacterial typing methods include phenotyping and genotyping. Among them, serotyping and multilocus sequence typing (MLST) are the most frequently used.

Serotyping identification has become the general standard method for *Salmonella* traceability and phenotypic classification for nearly 100 years. Serotype classification is based on serum agglutination tests of bacterial O and H antigens using the White–Kauffmann–Le Minor (WKL) scheme, which is adopted worldwide by public health organizations (Mezal et al., 2014). Up to now, more than 2610 serovars (also serotypes) of *Salmonella* have been documented globally (Monte et al., 2021). Moreover, *Salmonella* serotypes usually relate to their host adaptation and virulence, and the change in serotype proportion could reflect the epidemic status, so serotyping plays an essential role in *Salmonella* surveillance and outbreak investigations (Fierer and Guiney, 2001; Kumar et al., 2009; Dera-tomaszewska, 2012; Barbour et al., 2015). In the past, more attention has been paid to serovars Typhimurium and Enteritidis (Almeida et al., 2018).

In recent years, gene sequencing-based typing assays have been rapidly developed for bacterial tracing with vigorous vitality, including pulsed-field gel electrophoresis, MLST, core genome MLST (cgMLST), whole genome multilocus sequence typing (wgMLST), and whole gene single nucleotide polymorphism (wgSNP) (Liu et al., 2016, 2019; Radomski et al., 2019; Tiba-Casas et al., 2019). Among these molecular typing methods, MLST was developed to establish analytical microorganism typing (Maiden et al., 1998), recognize evolutionary relationships of *Salmonella* (Achtman et al., 2012; Ashton et al., 2016; Mairi et al., 2020; Zhang et al., 2020), and determine clonal isolate distributions across various environments and hosts (Wang M. et al., 2020; Zhao et al., 2020). In addition, there is a strong correlation between serotypes and sequence types (STs) of *Salmonella* (Wang X. et al., 2020). However, MLST cannot obtain accurate traceability of Typhimurium and I 4,[5],12:i:- because *Salmonella* isolates of these two serovars are often divided into the same STs (Possebon et al., 2020).

With the widespread extension of whole genomic sequencing (WGS), WGS-based high-resolution molecular subtyping methods have become popularized in outbreak investigation and bacterial tracing. As a kind of WGS-based subtyping method, cgMLST has high accuracy and can divide strains with minor sequence differences into different cgMLST sequence types (cgSTs), providing a powerful typing approach for molecular epidemiologic investigations. It is most commonly applied for foodborne disease surveillance in the public health area (Yoshida et al., 2016; Vincent et al., 2018; Ben Hassena et al., 2021). cgMLST is proven to be an adequate tool for cluster definition and has become a routine means in many countries and laboratories (Mellmann et al., 2011; Sabat et al., 2017; Simon et al., 2018; Robertson et al., 2019; Wang Y. J. et al., 2020; Hyeon et al., 2021).

In this article, we examine the serotypes, MLST, and cgMLST of *S. enterica* isolates from different sources in nine provinces in China from 2004 to 2019 to investigate their phenotyping and genotyping diversities and genetic relationships.

MATERIALS AND METHODS

Salmonella enterica Isolates

A total of 250 *S. enterica* isolates tested were from different sources in nine provinces in China from 2004 to 2019 except for 2005 and 2013 (**Figure 1**). The nine provinces, including Guangdong, Guangxi, Fujian, Sichuan, Shaanxi, Henan, Shandong, Shanghai, and Beijing, were major animal-breeding regions in China. The numbers of *S. enterica* isolates from different sources, years, or provinces were not equivalent. The details of these *S. enterica* isolates are shown in **Supplementary Table 1**. Out of these 250 isolates, 197 were from poultry-derived products, 31 from human, 15 from livestock meat, and 7 from infant nutrition rice formula (food); 16 were isolated in 2004, 9 in 2006, 4 in 2007, 11 in 2008, 31 in 2009, 105 in 2010, 27 in 2011, 13 in 2012, 1 in 2014, 10 in 2015, 5 in 2016, 5 in 2017, 7 in 2018, and 5 in 2019; 13 were separated in Guangdong, 19 in Guangxi, 11 in Fujian, 28 in Sichuan, 67 in Shaanxi, 18 in Henan, 10 in Shandong, 29 in Shanghai, and 55 in Beijing.

Among the 250 *S. enterica* isolates, 219 strains were isolated from animal products or nutrition rice formula samples. All food samples were immediately homogenized and subjected to *Salmonella* isolation following the standard protocol as previously described (World Health Organization (WHO), 2003). In short, the sample homogenates were added into selenite cysteine broth and incubated at 35°C for 24 h to selectively enrich *Salmonella*. Each enriched broth was streaked onto *Salmonella Shigella* and xylose lysine deoxycholate agar plates and incubated at 37°C for 24 h. Presumptive *Salmonella* colonies were picked and cultured in triple sugar iron agar media and then systematically identified by microbiological, biochemistry, and 16S rDNA sequencing analysis to confirm *Salmonella* strains. Thirty-one *Salmonella* isolates from humans were isolated and identified by the Beijing Center for Disease Prevention and Control. All identified *Salmonella* isolates were stored in 25% (v/v) glycerol at −80°C in our lab and reproduced periodically.

Serotyping by Slide Agglutination and Prediction by Genome

Salmonella enterica isolates were cultured in nutrient broth at 37°C overnight. A drop of fermentation broth was taken on glass slides to test somatic O antigen by slide agglutination. Meanwhile, each strain was grown on Swarm agar plates

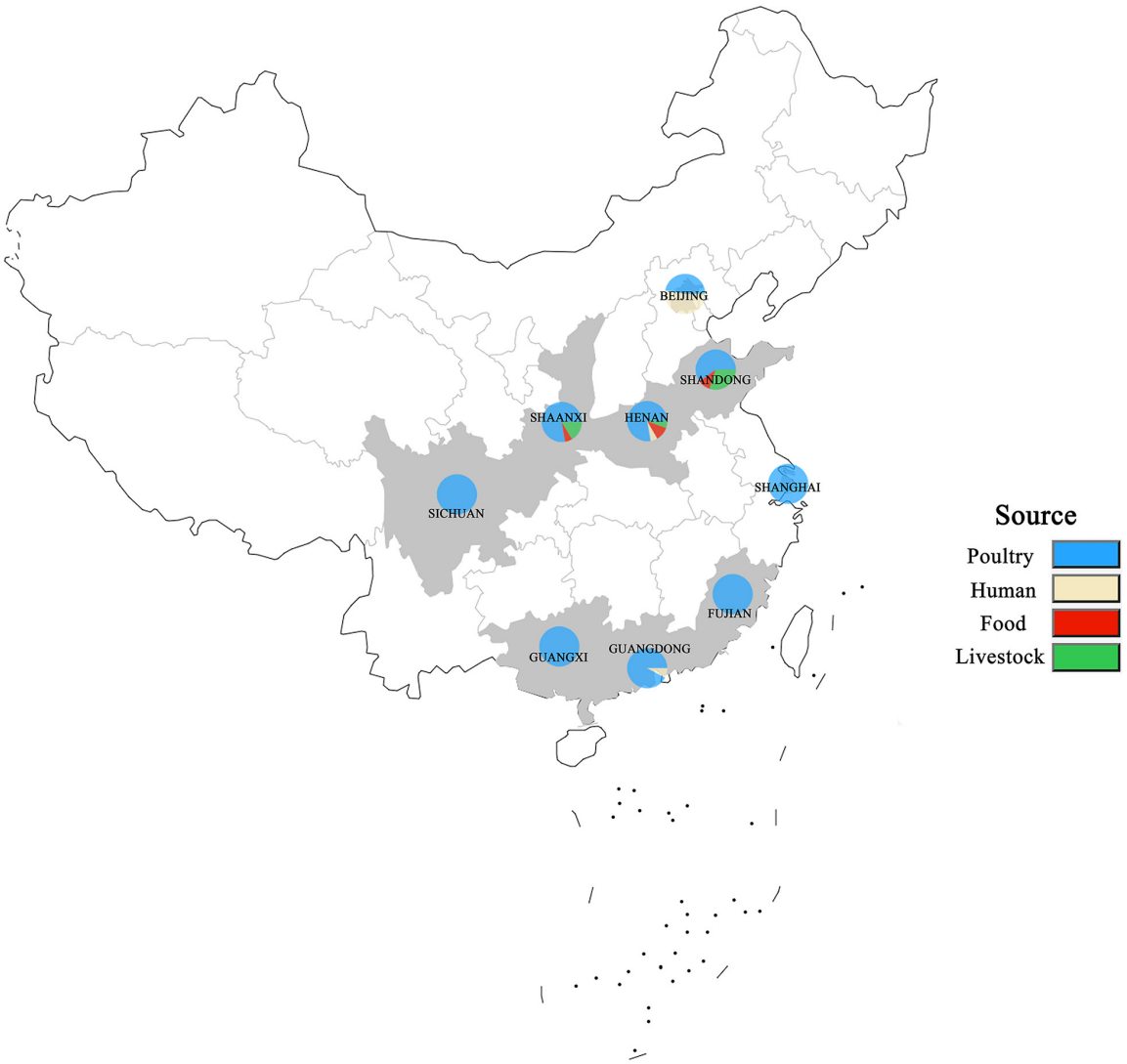

FIGURE 1 | Distribution of *S. enterica* isolates in China from 2004 to 2019. The locations where the strains were isolated are shown on the map. The isolates obtained from humans, poultry, livestock, and food are labeled in different colors.

at 37°C overnight, and single colonies were picked to test phases 1 and 2 of H antigens by slide agglutination. Diagnostic sera for *Salmonella* antigens were purchased from Tianrun Bio-Pharmaceutical Co. (Ningbo, China) and SandA Reagents Lab Ltd. (Bangkok, Thailand). *Salmonella* serotyping was classified by the WKL scheme. Additionally, O antigen, H antigen, and serovars were predicted based on *Salmonella* genomes using *Salmonella In Silico* Typing Resource (SISTR[1]).

Bacterial Genome Sequencing and Genomic Assembly

The genomic DNA of each *S. enterica* isolate was extracted with the sodium dodecyl sulfate method using the TIANamp Bacteria DNA Kit DP302-02 (TIANGEN, China) following the manufacturer's instructions. The extracted genomic DNA quality and integrity were evaluated on 0.5–1% agarose gels, concentration was measured using a fluorimeter (MD2000H, Biofuture), and purity was determined with a spectrophotometer based on the ratio of OD_{260} to OD_{280} ($OD_{260}/OD_{280} \geq 1.8$). The sequence libraries were constructed using Illumina's Nebnext Ultra DNA Library Prep Kit (NEB, United States). According to different attribute sequences, each sample was assigned with an index code. In brief, the DNA sample was first broken into approximately 350 bp fragments by sonication. After end repair, DNA fragments were ligated head-to-tail to a full-length adaptor for further PCR amplification. The PCR products were purified by the AMPure XP system, the size distribution of the libraries was analyzed by the Agilent bioanalyzer, and quantitative analysis was performed by real-time PCR.

[1]https://lfz.corefacility.ca/sistr-app/

The genomic DNA of 250 *S. enterica* isolates was sequenced using the Illumina NovaSeq PE150 platform at Beijing Novogene Bioinformatics Technology Co., Ltd. Considering the influence of low-quality data in the obtained raw sequencing data on the accuracy and reliability of subsequent information analysis, the original data were filtered to obtain the clean data. The specific processing steps included (1) removal of the reads containing low-quality bases (mass value ≤20) over a certain percentage (the default was 40%), (2) removal of reads containing a higher proportion of N (the default was 10%), (3) removal of sequences overlapping with adapters exceeding a certain threshold (the default was 15 bp) and with fewer than three mismatches, and (4) removal of data that might originate from the host after BLASTing against the host database.

The specific processing steps for genome assembly with clean data included (1) assembling with SOAP *de novo* software (Li et al., 2008) with different *K*-mers (the default was 107) first and then with the optimal *K*-mer after adjusting other parameters (-d -u -R -F, etc.) according to the project type, and the least scaffolds were chosen as the preliminary assembly result; (2) assembling with SPAdes software (Bankevich et al., 2012) with different *K*-mers (the default was 127) and then with the optimal *K*-mer according to the project type, and the assembly results as the least scaffolds were obtained; (3) assembling with Abyss software (Simpson et al., 2009) with the 64 nt *K*-mer to obtain the assembly results; (4) using the CISA software to integrate the above three assembly results, and only the assembly results with the least scaffolds were selected; (5) using GapCloser software to fill the gap of preliminary assembly results and remove the same lane pollution by filtering the reads with low sequencing depth (less than 0.35 of the average depth) to obtain the final assembly results; and (6) counting the final assembly result (without fragments below 500 bp) for gene prediction by GeneMarkS software (Besemer et al., 2001).

MLST, cgMLST, and Phylogenetic Analysis

Salmonella enterica isolates were analyzed based on genomic sequences (clean data) using *in silico* MLST and cgMLST analysis on the EnteroBase online platform[2] for *Salmonella*. Seven housekeeping gene loci, including *aroC*, *dnaN*, *hemD*, *hisD*, *purE*, *sucA*, and *thrA*, were chosen for MLST analysis of *Salmonella*. The neighbor-joining tree of *S. enterica* was established based on MLST information.

A *Salmonella* cgMLST v2 scheme comprising 3002 target loci of *Salmonella* was employed to analyze cgMLST based on genomic sequences, and neighbor-joining was used to make the dendrograms based on cgMLST information. *Salmonella* GrapeTree was constructed based on the above cgMLST scheme by EnteroBase GreepTree using NINJA neighbor-joining algorithm.

The tanglegram algorithm was applied to compare the MLST and cgMLST phylogenetic trees by placing trees side by side and drawing a straight line (or connector) between corresponding taxa (Scornavacca et al., 2011; Huson and Scornavacca, 2012). Although the algorithm can effectively reduce the number of intersections between connectors, the change of nodes in the evolution of these two types of phylogenetic trees are in the same direction and can lead to multiple short-distance intersections between connectors. If the two types of trees were identical and no connectors crossed, the cluster of phylogenetic tips remains unchanged.

[2]http://enterobase.warwick.ac.uk

RESULTS

Serotyping Classification of *S. enterica* in China During 2004–2019

The 250 *S. enterica* strains tested in the study were divided into 36 serotypes by slide agglutination (**Figure 2A**). *Salmonella* serovar Enteritidis (*n* = 31) was the most common serotype in China from 2004 to 2019, followed by Typhimurium (*n* = 29), Mbandaka (*n* = 23), Indiana (*n* = 22), Derby (*n* = 21), Thompson (*n* = 17), Agona (*n* = 12), and I 4,[5],12:i:- (*n* = 9). Senftenberg, Rissen, and Albany accounted for 3.2% (*n* = 8), respectively. Braenderup and Schwarzengrund possessed seven and six isolates, respectively. Cerro and Corvallis both had five isolates. Blockley, Hadar, Infantis, Meleagridis, Newport, and Saintpaul each encompassed four isolates. Havana and Kentucky both had three isolates. Bovismorbificans, Hvittingfoss, Kottbus, and Stanley each contained two isolates. Anatum, Litchfield, London, Pomona, Potsdam, Tennessee, and Uganda each included one isolate. There were 19 serotypes observed in more than two provinces. Albany, Mbandaka, Enteritidis, I 4,[5],12:i:-, and Typhimurium appeared in three provinces.

The 250 *S. enterica* isolates were divided into different serotypes based on their sources (**Supplementary Table 1**). The 197 isolates from poultry belonged to 34 serotypes, among which Typhimurium had the most isolates (*n* = 24), followed in turn by Indiana (*n* = 20), Enteritidis (*n* = 20), Mbandaka (*n* = 18), Derby (*n* = 17), and Thompson (*n* = 16). The 31 isolates from humans belonged to 13 serotypes with Enteritidis accounting for the largest percentage with 32.26% (*n* = 10). The 15 isolates from livestock contained nine serotypes, among which Derby and Mbandaka each included four stereotypes. In addition, the seven isolates from foods belonged to seven different serotypes.

According to statistics of the isolation years, the number of isolates was different in each year with Typhimurium, Enteritidis, or I 4,[5],12:i:- being the most abundant ones during 2012–2019. Our investigations are similar to those recently reported; Enteritidis and Typhimurium are still major serovars of *Salmonella* from animal food or humans (Greig and Ravel, 2009; Hendriksen et al., 2011; Yang et al., 2019; Perry et al., 2020; Shen et al., 2020; Xin et al., 2021).

Comparative serotyping analysis of the 250 isolates showed that the serotypes of 245 (98%) isolates based on slide agglutination were consistent with the genome-based prediction, and only five isolates, QLULP2, QLUY902, QLUY914, QLUY931, and QLUY933, were different. Among them, serotype Typhimurium of QLULP2, QLUY902, QLUY914, and QLUY933 based on slide agglutination was wrongly predicted as I 4,[5],12:i:-, and the serotype I 4,[5],12:i:- of QLUY931 based

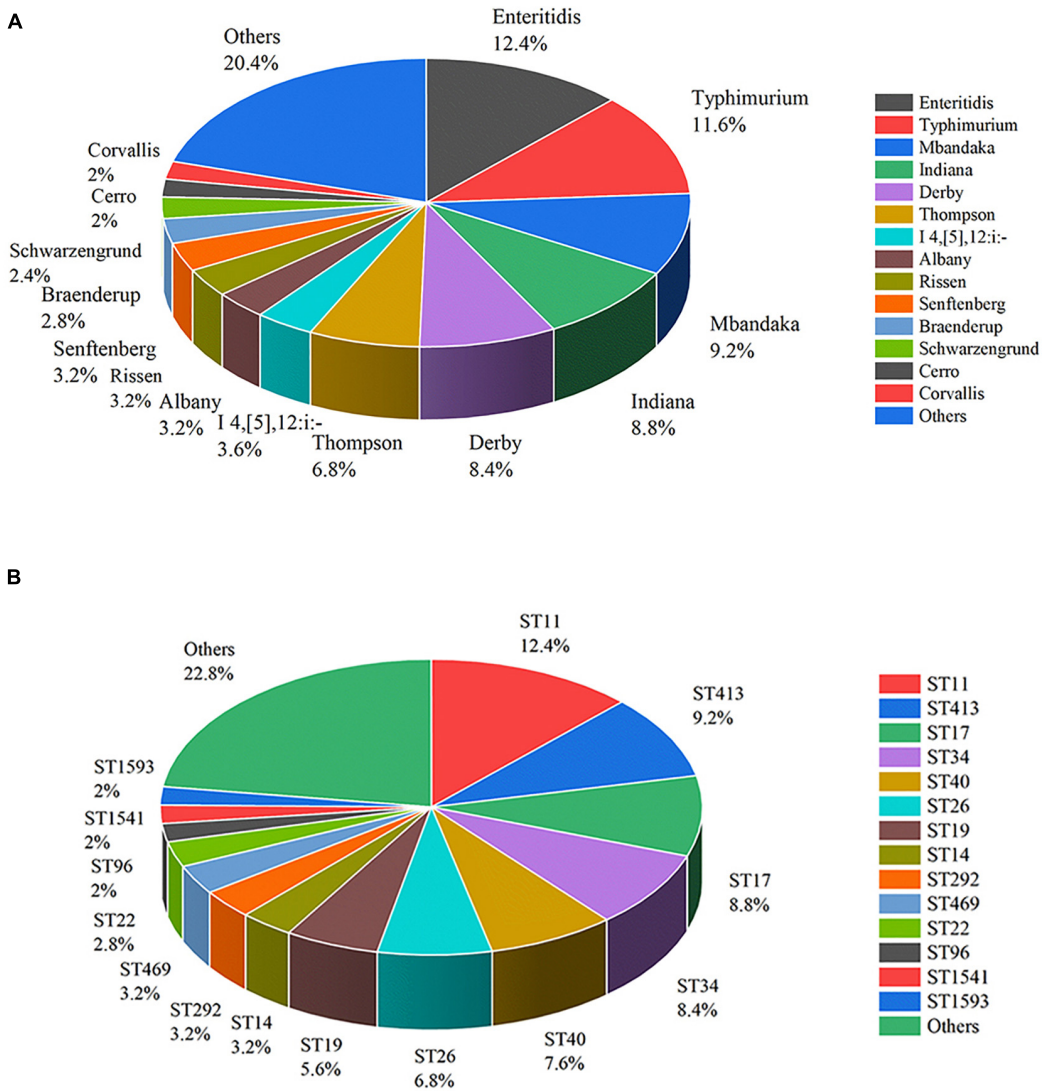

FIGURE 2 | Distribution of *Salmonella enterica* isolates of serotypes **(A)** and STs **(B)**.

on slide agglutination was wrongly predicted as Typhimurium. It is worth noting that Typhimurium and I 4,[5],12:i:- were rare in genome-based prediction by SISTR in our study. The results proved once again that *Salmonella* serotype prediction based on the genome is concordant with serovar by the serum agglutination test except Typhimurium and I 4,[5],12:i:-, so WGS-derived serotyping can replace the agglutination assay to some extent and be applied in the typing, traceability, and identification of *Salmonella*.

Salmonella Draft Genome Analysis

The genomic reads of 250 *S. enterica* isolates were stored in the Sequence Read Archive (SRA) of the National Center for Biotechnology Information (NCBI). SRA serial numbers of the submitted 250 strains are shown in **Supplementary Table 1**.

A total of 9656 (≥500 bp) contigs varying from 9 to 92 with an average of 38.62 per genome were generated. The average draft genome size was 4.88 Mb, ranging from 4.35 to 5.48 MB. Likewise, the average G + C content observed was 52.04%. Functional annotation of all draft genomes predicted an average of 4692 genes, ranging from 4173 to 5334.

In silico MLST Analysis of *S. enterica*

The 250 *Salmonella* isolates were divided into 43 STs and 37 eBurst groups (eBGs) using *in silico* MLST. However, ST3134 belonged to neither eBG. ST11 was the most common (n = 31), followed in turn by ST413 (n = 23), ST17 (n = 22), ST34 (n = 21), ST40 (n = 19), ST26 (n = 17), ST19 (n = 14), ST14 (n = 8), ST292 (n = 8), and ST469 (n = 8). ST distribution is shown in **Figure 2B**.

In addition, among the 43 STs identified, a novel ST named ST8016 (QLUY608) was obtained, and it differed from ST40 by 1 SNP in the *dnaN* locus at position 317 (C → T, named *dnaN*1076, compared to *dnaN*20). Compared with the ST40 *dnaN* locus, this mutation occurred in the second codon position, resulting

in a non-synonymous change from C to Y. Our findings enrich MLST data of *Salmonella*, facilitating the typing, traceability, and identification of *Salmonella*.

Among the 43 STs, 25 STs were observed in more than two provinces and 18 STs in one province. ST17 and ST40 appeared in seven provinces. The results indicate that these two STs were prevalent and had the possibility of transregional infection.

Statistics of the isolation sources revealed that (1) the 31 isolates from humans consisted of 13 different STs, among which ST11 had the highest number of 10 isolates, followed by ST34 (n = 6); (2) the 197 isolates from poultry belonged to 37 STs, among which ST11 had the highest number (n = 22), followed in turn by ST413 (n = 21), ST17 (n = 16), ST40 (n = 16), and ST26 (n = 15); (3) the 15 isolates from livestock contained 9 STs, among which ST413 had the highest number (n = 4); and (4) the 7 isolates from food belonged to 7 different STs.

Statistics of isolation years found that the major ST of every year was different during 2004–2011. ST413 was the major ST in 2004, 2007, and 2011; ST11 was the major ST during 2012–2019 except 2014; and ST34 was the major ST from 2014 to 2019 except 2018. The results showed that the major ST of *Salmonella* was not constant in every year.

Comparison of MLST and serotyping showed that each ST only comprised one serotype except ST34. Nine isolates of I 4,[5],12:i:- and 12 isolates of Typhimurium belonged to ST34. In addition, four serovars included more than one ST: 29 isolates with serotype Typhimurium contained four STs (ST19, ST34, ST128, and ST1544), 21 isolates of Derby contained three STs (ST40, ST8016, and ST71), 4 isolates of Newport contained 2 STs (ST50 and ST3134), and 6 isolates of Schwarzengrund contained two STs (ST96 and ST241). The results represent that the accuracy of MLST was higher than that of serotyping.

TABLE 1 | *Salmonella enterica* cgSTs from different years, provinces, or sources of isolation.

cgST	Numbers	Source	Province	Years
cgST42868	5	Poultry	Shaanxi, Fujian	2010, 2011
cgST217495	6	Poultry	Beijing, Shaanxi	2010, 2012
cgST234925	3	Poultry	Sichuan, Fujian	2010
cgST234927	3	Poultry	Sichuan, Shaanxi	2006, 2010
cgST234930	6	Poultry, food	Sichuan, Shaanxi	2006, 2007, 2010, 2012
cgST234932	3	Poultry	Sichuan, Fujian	2010
cgST235529	2	Poultry, food	Sichuan, Shaanxi	2006, 2010
cgST235530	11	Poultry	Shaanxi, Guangdong	2010, 2011
cgST235678	2	Poultry	Sichuan, Shaanxi	2010, 2011
cgST235686	2	Poultry	Guangxi, Shaanxi	2010, 2011
cgST235712	2	Poultry	Shaanxi, Shanghai	2006
cgST235797	2	Poultry	Guangdong, Shaanxi	2007, 2011
cgST236211	2	Poultry, human	Guangdong	2010
cgST236321	2	Poultry, human	Beijing	2008, 2012
cgST236324	2	Poultry, human	Beijing	2009, 2012

cgMLST Analysis of *Salmonella* Based on Genomic Sequences

A total of 3002 target genes were identified from the *S. enterica* genome using the EnteroBase cgMLST module. The cgMLST analysis of *S. enterica* isolates is shown in **Supplementary Table 1**. The cgMLST analysis revealed that the 250 *Salmonella* isolates were grouped into 185 cgSTs, all of which contained only one serotype. Among them, 243 isolates belonged to 182 novel cgSTs, and 7 belonged to three known cgSTs. Among the 185 cgSTs, cgST235530 contained the most abundant isolates, followed by cgST217495 (n = 6) and cgST234930 (n = 6). We comprehensively analyzed the WGS-based genotypes of *Salmonella* in China in the past 16 years and found many novel cgSTs, which enriched the genotype data resources and promoted the development of traceability level of *Salmonella*.

The relationship of cgST with the years, regions, and sources of isolation is shown in **Table 1**. Among the 185 cgSTs, 33 cgSTs contained more than two isolates, and 15 cgSTs contained strains from different years, provinces, or sources of isolation. In detail, 12 cgSTs isolates were from multiple provinces, 12 cgSTs from different years, and 5 cgSTs from different sources, representing the possibility of cross-outbreaking in different locations, hosts, or years. cgST236211, cgST236321, and cgST236324 contained multiple isolates from human and other sources, indicating a possibility of cross-species infection. In addition, 152 strains had unique cgSTs in this study.

A neighbor-joining tree was generated based on the 250 strains' cgMLST information (**Figure 3**). Many serovars formed serovar-specific clades in this tree, suggesting that the same serovars were putatively homologous except that isolates of Saintpaul, Derby, and I 4,[5],12:i:- were heterologous. To further investigate the relationship of Saintpaul, Derby, and I 4,[5],12:i:- isolates, the GrapeTrees of each serovar were constructed based on cgMLST information (**Figure 4**). In the GrapeTrees, Saintpaul contained four isolates belonging to two clades with a long genetic distance, representing that Saintpaul was putatively polyphyletic (**Figure 4A**). Similarly, Derby contained 21 isolates that did not wholly cluster together. QLUY614 (cgST236253) had a long genetic distance to the other 20 isolates, suggesting Derby was putatively polyphyletic, too (**Figure 4B**). Differently, the nine isolates of serovar I 4,[5],12:i:- had close genetic distances in the GrapeTree even though they did not completely cluster together (**Figure 4C**). In a word, isolates of Saintpaul and Derby were putatively polyphyletic and characterized by multilineages (Yin et al., 2020).

Additionally, I 4,[5],12:i:- and Typhimurium in a similar genetic distance may have a near genetic relationship (**Figure 3**). To further investigate the relatedness of I 4,[5],12:i:- and Typhimurium, their GrapeTree was constructed based on cgMLST information of serovar I 4,[5],12:i:- (n = 9) and Typhimurium (n = 28) (**Figure 5**). In the GrapeTree, Typhimurium isolates were clustered into eight highly clonal clades and four highly clonal clusters (clusters 1–4), and nine isolates of I 4,[5],12:i:- and 12 isolates of Typhimurium were clustered into cluster 4. The low homologous diversity within I 4,[5],12:i:- and Typhimurium in combination with the above cgST tree on coherent clades indicate that these two serovars might have similar genomic sequences.

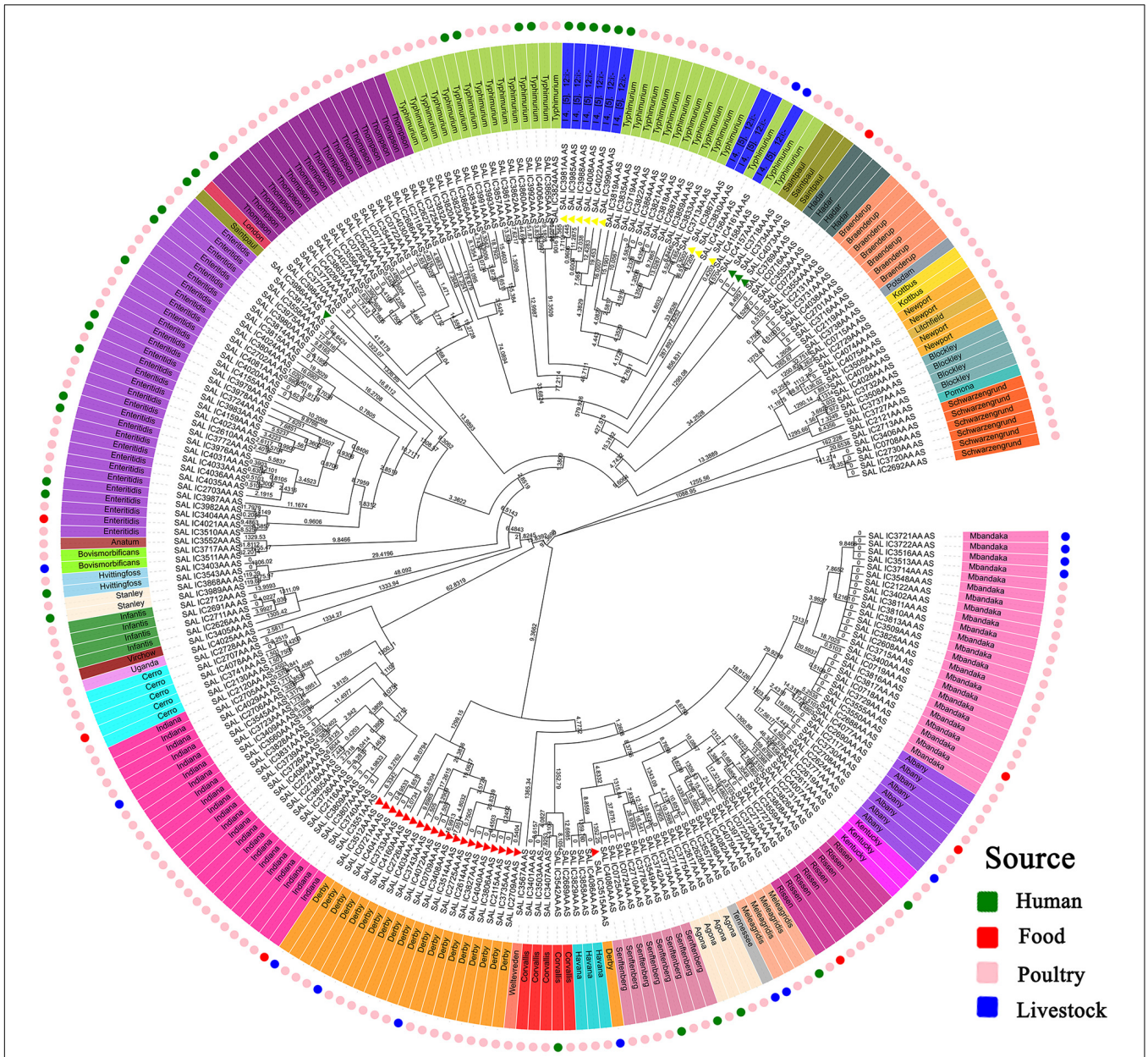

FIGURE 3 | Core genome MLST-based phylogenetic tree of *S. enterica* isolates. The neighbor-joining algorithm phylogenetic tree was created by EnteroBase based on cgMLST information and visualized using Evolview. The numbers stand for Branchlength values. The isolates' serotypes are labeled in color, and most serovars forms serovar-specific clades except Saintpaul, Derby, and I 4,[5],12:i:-, which are signaled by the same color triangles. I 4,[5],12:i:- and Typhimurium may have a close genetic and evolutionary relationship. Further determination of the evolutionary relationship between the abovementioned serovars will be furtherly carried out. Different colors are used in the outermost ring to indicate the separation source to distinguish the specificities of different isolates.

In addition, only three isolates from patients were in the same genetic position with other strains in the evolutionary tree. As mentioned, isolates of cgST236211, cgST236321, and cgST236324 were in the same genetic position in the tree: QLULY5 (human, Beijing, 2009) with QLULR4 (poultry, Beijing, 2012) of Thompson; QLULY1 (human, Beijing, 2008) with QLULR2 (poultry, Beijing, 2012) of Senftenberg; and QLULN4 (human, Guangdong, 2010) with QLUY510 (poultry, Guangdong, 2010) of Hvittingfoss. There was a strong homology among these isolates and a possibility of cross-species infection in patients although significant differences existed in some isolates from different years of isolation.

Analysis of isolates' clustering position in the evolutionary tree showed isolates of Hadar, I 4,[5],12:i:-, Saintpaul, Kentucky, and Mbandaka had a strong correlation between genetic position and source (**Figure 3**). Among the three Kentucky isolates, QLULA8 (Guangxi, 2010) and QLULA5 (Beijing, 2010) isolates from poultry were putatively homologous and had a long genetic

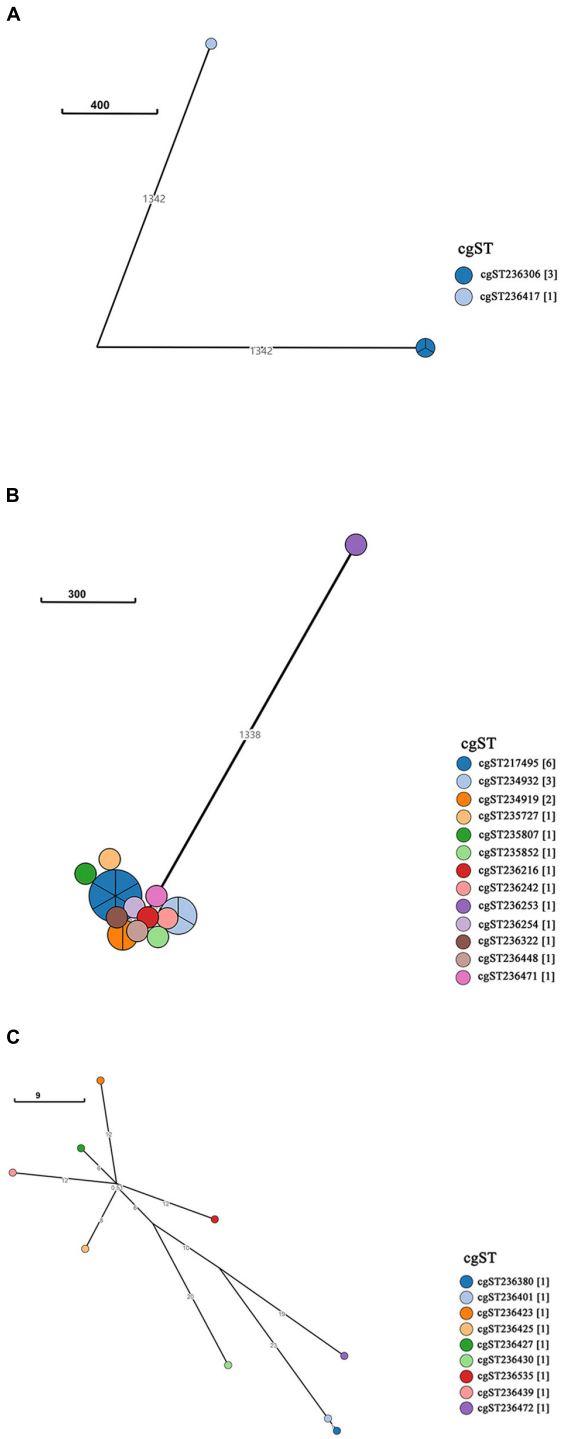

FIGURE 4 | GrapeTree of *Salmonella* serovar Saintpaul, Derby, and I 4,[5],12:i:- isolates. GrapeTree constructed based on the 3002 core genes by EnteroBase GrapeTree using NINJA neighbor-joining algorithm. **(A)** GrapeTree among the four serovar Saintpaul isolates, where every node means different cgST and the line between two nodes indicates a long distance (≥1000); **(B)** GrapeTree of the 21 Derby and 1 cgST (cgST236253) isolates with a long genetic distance (≥1000) to other cgSTs; **(C)** GrapeTree of the nine serovar I 4,[5],12:i:- and nine cgST isolates with nodes indicating they all have a relatively close genetic distance (≤100).

distance to the isolate QLUF123 (Beijing, 2018) from patients. What is more, among the 13 Mbandaka isolates, four from livestock were in the same genetic position in the evolutionary tree with high homology and had a long genetic distance to other isolates of different sources. Obviously, serovar I 4,[5],12:i:- isolates from the same hosts were at an adjacent genetic position in the evolutionary tree.

Major Serovars and cgSTs of *Salmonella* Isolates From Different Sources, Years, and Provinces

A total of 25 major cgSTs and 26 major serovars appeared among the 250 *Salmonella* isolates from different sources in nine provinces during 2004–2019. Among them, four major serovars from livestock in Fujian province in 2007 and 2011 were clustered in major cgSTs. In detail, 11 major cgSTs belonged to major serovars. For example, four isolates of cgST236240 in 2004 belonged to Mbandaka, and the major serovars in 2004 were Derby (n = 4) and Mbandaka (n = 4). Obviously, the major serovar Typhimurium clustered with 19 isolates in 2009, but the major cgST was cgST236385 (n = 3, Havana). Meanwhile, the major serovar from poultry was Typhimurium (n = 28), and the major cgST was cgST235530 (n = 11, Mbandaka). The 28 Typhimurium isolates were divided into 26 different cgSTs and seven isolates from food belonged to seven serovars and seven cgSTs. The major serotype was always Typhimurium, Enteritidis, or I 4,[5],12:i:- during 2015–2019. However, these three serovar isolates possessed different cgSTs. Major cgSTs and major serovars of *Salmonella* isolates from different sources in different years and provinces are shown in **Table 2**.

Comparative Analysis of MLST and cgMLST Within *S. enterica* Isolates

Identification of all loci present within *Salmonella* isolates was performed using MLST and cgMLST schemes. The 250 *S. enterica* isolates in China from 2004 to 2019 were used to generate a tanglegram for a visual comparison of cgMLST and MLST (**Figure 6**). Most of the straight lines were parallel, and only some minor straight lines crossed with others, indicating that the majority of STs were parallel to cgSTs. This phenomenon may give rise by differences between the located deeper internal nodes within these two phylogenies. By comparison, most of the isolates were grouped into the same clusters by MLST and cgMLST.

Further analysis shows that the crosslines were mainly due to the differences in the genetic relationships between some different serovar isolates in the evolutionary tree established by MLST and cgMLST. By comparison, the following serovar isolates had close genetic relationships in the MLST-based neighbor-joining tree but not in the cgMLST-based neighbor-joining tree: (1) 1 isolate of Virchow (QLUY603) with 5 Corvallis isolates, (2) 1 isolate of Weltevreden (QLULO6) with all 23 Mbandaka isolates and 8 Albany isolates, (3) 3 isolates of Kentucky with all 8 Rissen isolates, (4) f isolates of Cero with 1 Saintpaul isolate (QLUF115), and (5) 5 isolates of Saintpaul and all 31 Enteritidis isolates. Although MLST and cgMLST clustered two isolates of Stanley (QLUF119, QLUZ101) and

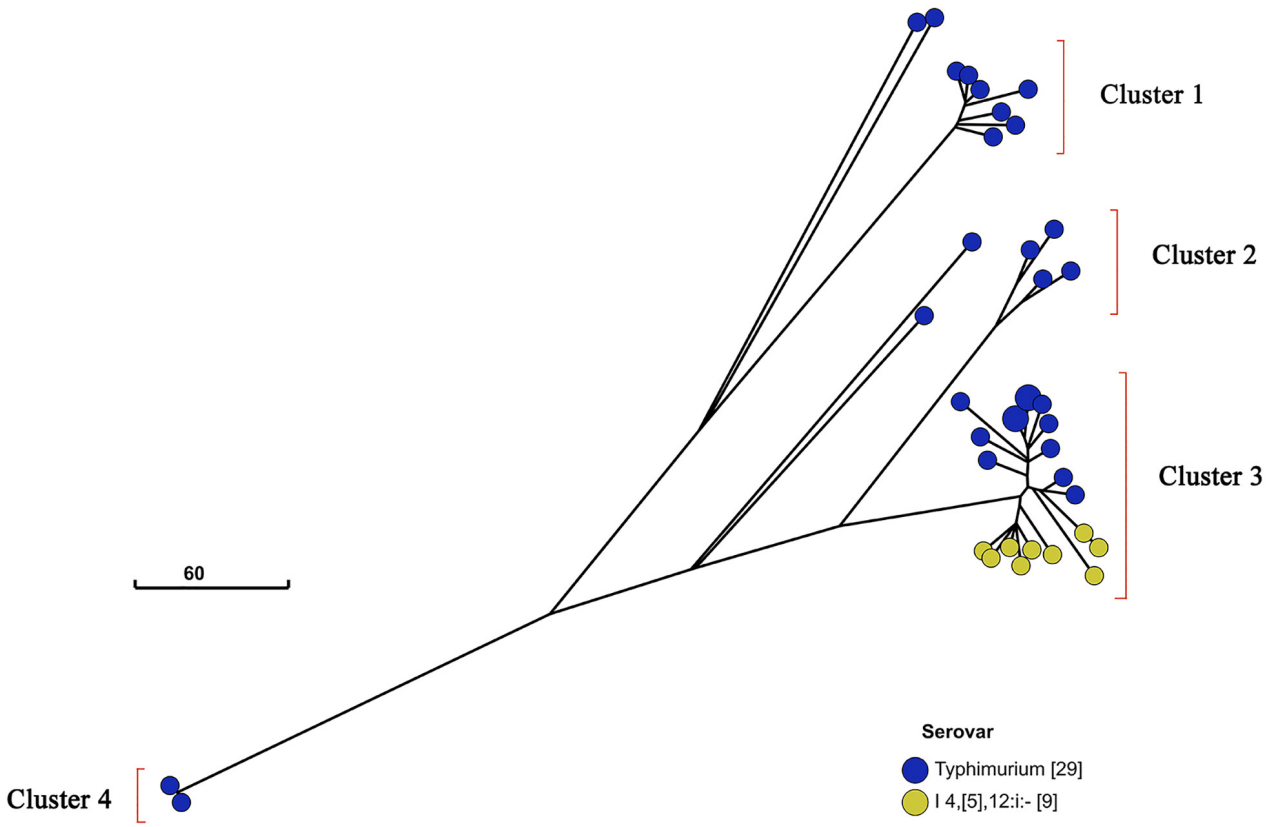

FIGURE 5 | GrapeTree of *Salmonella* serovar I 4,[5],12:i:- and Typhimurium isolates. GrapeTree of nine serovar I 4,[5],12:i:- isolates and 29 serovar Typhimurium isolates constructed based on cgMLST information by EnteroBase GrapeTree function and neighbor-joining algorithm. These 38 isolates belong to four clusters in the tree, and all nine serovar I 4,[5],12:i:- isolates belong to cluster 3 with 12 serovar Typhimurium isolates, showing that *Salmonella* serovar I 4,[5],12:i:- and Typhimurium have a closer genetic relationship.

two isolates of Hvittingfoss (QLULN4, QLUY510) together, the MLST-based neighbor-joining tree indicated one Virchow isolate (QLUY603) is closely related with five Corvallis isolates, and the cgMLST-based neighbor-joining tree placed them at a longer genetic distance. However, the majority of *Salmonella* isolates were grouped into the same clusters by both MLST and cgMLST. Obviously, the evolutionary tree by cgMLST was more detailed than that by MLST.

DISCUSSION

In recent years, with increasing demand for food safety, the detection of foodborne *Salmonella* becomes greatly important, and *Salmonella* from food is tested more intensively worldwide (Yang et al., 2019). *Salmonella* typing is essential for microbial determination, epidemiological investigation, and outbreak tracing. Serotyping and MLST are the gold standard bacterial typing methods. However, they both could not accurately trace because they are relatively low-resolution. Thus, it is significant to establish high-resolution and reliable subtyping methods for tracing epidemic strains in pathogenic outbreaks (Jolley et al., 2012).

Serotyping by slide agglutination has been widely adopted for *Salmonella* classification for nearly 100 years. In this study, we serotyped 250 *Salmonella* isolates from different sources in China in the past 16 years, and the results show all strains tested in the study were divided into 36 serotypes, and *Salmonella* serovars Enteritidis and Typhimurium were still the major serovars, which is similar to a recent report (Perry et al., 2020; Shen et al., 2020). Enteritidis is frequently isolated from animal food globally and is one of the most common serovars associated with human salmonellosis (Greig and Ravel, 2009; Hendriksen et al., 2011; Yang et al., 2019).

However, serotyping by slide agglutination has some shortcomings, such as being low-resolution, expensive, and time-consuming. In addition, this serological test requires well-trained personnel to operate it as well as high-quality sera; otherwise, it is prone to error in serotype determination because of artificial discrimination of differences in agglutination profiles and the incomplete phenomenon of H antigen expression (Zhou et al., 2020). However, it does not mean that serotyping will be rapidly replaced because it has become a traditional microbial phenotyping classification method by microorganists and public health organizations. Therefore, it will still play a fundamental role in bacterial tracing in the near future.

TABLE 2 | Major cgSTs and major serovars of *S. enterica* isolates.

	Number of strains	Major cgSTs (no., serovar)	Major serovars (no.)
Year			
2004	16	cgST236240 (4, Mbandaka)	Derby (4), Mbandaka (4)
2006	9	cgST235712 (2, Infantis)	Infantis (2), Thompson (2)
2007	4	cgST234930 (2, Mbandaka)	Mbandaka (2)
2008	11	cgST236457 (2, Meleagridis)	Corvallis (3)
2009	32	cgST236385 (3, Havana)	Typhimurium (19)
2010	105	cgST42868 (4, Braenderup)	Indiana (12)
		cgST234918 (4, Schwarzengrund)	
		cgST234928 (4, Senftenberg)	
2011	27	cgST235530 (9, Mbandaka)	Mbandaka (9)
2012	13	cgST217495 (4, Derby)	Enteritidis (6)
2014	1	–	–
2015	10	–	Typhimurium (4)
2016	5	–	Enteritidis (2), I 4,[5],12:i:- (2)
2017	5	–	Enteritidis (2), I 4,[5],12:i:- (2)
2018	7	–	Enteritidis (2), Typhimurium (2)
2019	5	–	Enteritidis (2), I 4,[5],12:i:- (2)
Province			
Beijing	55	cgST217495 (3, Derby)	Enteritidis (15)
Fujian	11	cgST234918 (4, Schwarzengrund)	Schwarzengrund (4)
Guangdong	13	cgST236218 (2, Corvallis)	Mbandaka (3)
		cgST236211 (2, Hvittingfoss)	
		cgST235530 (2, Mbandaka)	
Guangxi	19	cgST235719 (2, Cerro)	Albany (3)
		cgST234919 (2, Derby)	Cerro (3)
		cgST236457 (2, Meleagridis)	Newport (3)
		cgST236458 (2, Newport)	
Henan	18	–	Enteritidis (3)
Shandong	10	cgST236436 (2, Enteritidis)	Enteritidis (5)
Shanghai	29	cgST236385 (3, Havana)	Typhimurium (19)
Shaanxi	67	cgST234930 (9, Mbandaka)	Mbandaka (18)
Sichuan	28	cgST234928 (4, Senftenberg)	Thompson (5)
Source			
Food	7	–	–
Human	31	–	Enteritidis (10)
Livestock	15	cgST236240 (4, Mbandaka)	Mbandaka (4)
Poultry	197	cgST235530 (11, Mbandaka)	Typhimurium (28)

"–" means no major serovars or major cgSTs.

We also validated the serotyping by agglutination assay using SISTR prediction based on genomic sequences. The two methods are highly consistent with a consistency rate of 98%, which is similar to recent reports (Robertson et al., 2018; Uelze et al., 2019; Lyu et al., 2021). However, SISTR has a low identification for Typhimurium and I 4,[5],12:i:- in our research. This situation may be because SISTR only predicts serotypes based on related coding genes, and the results of slide agglutination tests are affected by many factors, such as gene mutation or inexpression.

Facing potential food safety risks, serological misidentification may endanger underestimating the occurrence of certain *Salmonella* serotypes outbreaks. The serotype prediction based on nucleic acid sequences plays an essential role in serotype validation. Therefore, it is essential to validate the slide agglutination assay. Several methods have been developed to predict serotypes based on nucleic acid sequences (Achtman et al., 2012; Inouye et al., 2014; Zhang et al., 2019). MLST is attractive because of being generated with easily replicated protocols and correlated well with the majority of lineages and serovars by means of eBGs. The advantages of MLST are more uniform, well relative with serotypes, and convenient to communicate by databases (Kimura, 2018).

The 250 *Salmonella* isolates were divided into 43 STs using *in silico* MLST with ST11 being the most abundant ST ($n = 31$). Among the 43 STs identified, a novel ST, ST8016 (QLUY608), differs from ST40 by 1 SNP in the *dnaN* locus at position 317 (C → T, named *dnaN*1076, compared with *dnaN*20). According to MLST typing, ST34 contains I 4, [5],12:i:- and

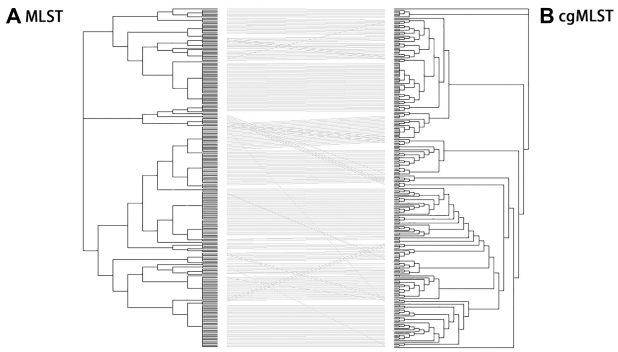

FIGURE 6 | Comparison of phylogenies by MLST **(A)** and cgMLST **(B)** based on genomic sequences of 250 *Salmonella* isolates. Tanglegram linking tips with the same label to each other *via* a straight line produced within dendroscope 3 of 250 *Salmonella* isolates. By comparing of N-J trees by MLST and cgMLST, clustering in the two trees was mostly congruent although a few sections show several inversions. This led to some isolates being clustered at the edge of one tree, moving to the center of the other. In addition, the tree by cgMLST was more detailed than that by MLST.

Typhimurium. The method cannot distinguish I 4,[5],12:i:- from Typhimurium with the same STs because of similar genomic sequences. Furthermore, a GrapeTree was constructed using the genomic sequences of all isolates of I 4,[5],12:i:- (n = 9) and Typhimurium (n = 29). The results show that the isolates of the two serovars could not be completely clustered together: only nine isolates of I 4,[5],12:i:- and 12 isolates of Typhimurium belong to the same cluster and are in similar genetic positions on the evolutionary tree (**Figure 5**). However, the MLST approach may cause two main issues to predict serotype using SISTR: (1) a few STs do not have a serovar designation in the MLST database and (2) the unexpected identification of novel STs.

Molecular typing for *Salmonella* of the same serovars is essential in outbreak investigation and bacterial epidemiology. The increasing availability of analytical approaches for whole genome-based subtyping will continue to fuel the adoption of genomics in the context of epidemiological investigations. With the reduction of sequencing cost and the promotion of genome sequencing, a large amount of bacterial genome data has been generated, and it has become routine to trace microorganisms based on bacterial genomic sequences. Molecular typing methods based on WGS with high resolution and outstanding accuracy are used as routine bacterial trace analysis methods. Each has different advantages and drawbacks that determine its applicability and limitations. In recent years, cgMLST, wgMLST, and SNP have become innovative tracing tools (García-Soto et al., 2020; Gu et al., 2020; Monte et al., 2021). cgMLST well correlates with time and regions of bacterial isolates. Microorganism epidemiological investigation results found that the main pathogens may probably change during outbreaking, and these will be largely muted by conventional low-resolution typing methods (Quick et al., 2015). In this study, cgMLST can distinguish the differences and confirm the extremely minute association of these strains of major serotypes. Although they have been grouped into Enteritidis, Typhimurium, and I 4,[5],12:i:- since 2015, we judged the prevalent *Salmonella* was not due to continuous spread of individual strains.

It is worth noting that the traceability is influenced by the use of different cgMLST classification schemes (Li et al., 2008). In several cgMLST scheme protocols, 3002 core loci cgMLST schemes of *Salmonella* promoted in EnteroBase have been widely accepted because of applying the default settings of loci and alleles most likely to be used by many microbiologists to obtain accordant and accurate applications across laboratories and jurisdictions. EnteroBase is well adopted because it covers a large number of isolates' genomic sequences, and the fixed typing scheme makes the cgMLST results truly comparable among different researchers. EnteroBase covers more than 270,000 *Salmonella* genomic sequences globally and facilitates cgMLST analysis of *Salmonella*. The convenience and pertinence of data collection and collation provide strong data support for pathogen evolution analysis. The fixed typing scheme makes it easy to explore the homologous relationship of individual isolates in the database and to invoke more isolates with certain characteristics. Only by retrieving the isolate information, including time, country or region of isolation, serotype, and MLST and cgMLST typing results of the isolate, could the isolate's relevant information be obtained. The availability of a web-based analysis platform enables users to conduct cgMLST analysis with minimal local hardware requirements. cgMLST analysis based on thousands of genomic alleles has a higher typing accuracy than MLST. The former was verified to be a more realistic reflection of the evolutionary relationship within the species (Ruppitsch et al., 2015).

High-resolution molecular methods for *Salmonella* typing are not replacing MLST because MLST is relatively convenient for establishing a good relationship with serovars (Kimura, 2018). Comparing evolutionary trees by MLST and cgMLST, the two methods have similar clustering results. However, cgMLST can further distinguish even minor differences between isolates, and the clustering is more detailed. Compared with cgMLST, MLST is generally more discriminatory, but it cannot provide a satisfactory resolution for public health surveillance. Our study also indicates cgMLST is significantly more accurate than MLST, no cgST contains two or more serovars, even I 4,[5],12:i:- and Typhimurium.

According to the evolutionary analysis, the isolates representing the most serovars formed serovar-specific clades in our established neighbor-joining tree except Saintpaul, I 4,[5],12:i:-, and Derby. To explore the genetic and evolutionary relationship among these three serotypes, we further constructed a GrapeTree of the isolates of the three serovars (**Figure 4**). Only Saintpaul and Derby have multilineages (Yin et al., 2020).

Among the three typing methods, serotyping showed the lowest resolution, and cgMLST had the highest accuracy. Serotyping was based on reactions of antisera to the lipopolysaccharide and flagellar antigens; otherwise, it did not reflect the genetic relatedness between serovars; MLST, based on seven housekeeping genes, was an accurate, reliable typing method, well suited to routine microbial surveillance; WGS-based cgMLST could greatly improve the accuracy of typing and was convenient to share or compare across international

labs, so it should be developed in the traceability typing of microorganisms with vitality in the future.

CONCLUSION

We investigated 250 *S. enterica* isolates from China during 2004–2019 using serotyping, MLST, and cgMLST. All the *Salmonella* strains were divided into 36 serovars, 43 STs by MLST, and 185 cgSTs by cgMLST. We found the prevalent serovars, STs, and cgSTs of *Salmonella* from different years, regions, and host sources. In addition, we also discovered a novel ST and 182 novel cgSTs. This article clarifies the temporal and spatial distribution characteristics of phenotyping and genotyping diversity of *S. enterica* isolates in China in the recent 16 years. Our results supplement the strain resources, genetic information, and typing data of *Salmonella*; benefit the typing, traceability, determination, and genetic evolution analysis of *Salmonella*; and therefore, promote the level of analysis, monitoring, and prevention and controlling of *Salmonella* in China.

DATA AVAILABILITY STATEMENT

The datasets presented in this study can be found in online repositories. The names of the repository/repositories and accession number(s) can be found in the article/ **Supplementary Material**.

AUTHOR CONTRIBUTIONS

SY, WZ, and LZ were major contributors in writing the manuscript, and conceived and designed the study. SY, LC, and BY contributed materials and resources. CL and XL worked for slide agglutination. All authors read and approved the final manuscript.

FUNDING

This work was funded by the National Key Research and Development Program of China (Grant Number 2017YFC1601400), the Natural Science Foundation of Shandong province (ZR2018LC003), and the Key Research and Development Program of Shandong Province (Grant Numbers 2019GNC106154 and 2014GSF120006).

ACKNOWLEDGMENTS

We thank Qian Chen and Yuanyuan Zhang of Beijing Center for Diseases Prevention and Control for collecting many *Salmonella enterica* isolates from humans.

SUPPLEMENTARY MATERIAL

The Supplementary Material for this article can be found online at: https://www.frontiersin.org/articles/10.3389/fmicb.2021.688614/full#supplementary-material

Supplementary Table 1 | Background information, draft genome, serovars, and genotypes of 250 *Salmonella enterica* isolates. Comment: assembly barcode was obtained by submitting the raw genome data into EnteroBase, and the replacement strain name played an identification role in the established evolutionary tree. SRA numbers were obtained from the NCBI SRA. It is important to note that prefixes such as "QLUL" were added to the strain's name after submission to EnteroBase in order to obviously distinguish it, so there may be some bias from the SRA database strain names.

REFERENCES

Achtman, M., Wain, J., Weill, F. X., Nair, S., Zhou, Z., Sangal, V., et al. (2012). Multilocus sequence typing as a replacement for serotyping in *Salmonella enterica*. *PLoS Pathog.* 8:e1002776. doi: 10.1371/journal.ppat.1002776

Almeida, F., Amanda, A. S., Marta, I. C. M., Dália dos, P. R., Alessandro De, M. V., Yan, L., et al. (2018). Phylogenetic and antimicrobial resistance gene analysis of *Salmonella* Typhimurium strains isolated in Brazil by whole genome sequencing. *PLoS One* 13:e0201882. doi: 10.1371/journal.pone.0201882

Arthur, T. M., Brichta-harhay, D. M., Bosilevac, J. M., Guerini, M. N., Kalchayanand, N., Wells, J. E., et al. (2008). Prevalence and characterization of *Salmonella* in bovine lymph nodes potentially destined for use in ground beef. *J. Food Prot.* 71, 1685–1688. doi: 10.4315/0362-028x-71.8.1685

Ashton, P. M., Nair, S., Peters, T. M., Bale, J. A., Powell, D. G., Painset, A., et al. (2016). Identification of *Salmonella* for public health surveillance using whole genome sequencing. *PeerJ.* 4:e1752. doi: 10.7717/peerj.1752

Bankevich, A., Nurk, S., Antipov, D., Gurevich, A. A., Dvorkin, M., Kulikov, A. S., et al. (2012). SPAdes: a new genome assembly algorithm and its applications to single-cell sequencing. *J. Comput. Biol.* 19, 455–477. doi: 10.1089/cmb.2012.0021

Barbour, E. K., Ayyash, D. B., Alturkistni, W., Alyahiby, A., Yaghmoor, S., Yousef, J., et al. (2015). Impact of sporadic reporting of poultry *Salmonella* serovars from selected developing countries. *J. Infect.Dev. Ctries.* 9, 1–7. doi: 10.3855/jidc.5065

Ben Hassena, A., Haendiges, J., Zormati, S., Guermazi, S., Gdoura, R., Gonzalez-Escalona, N., et al. (2021). Virulence and resistance genes profiles and clonal relationships of non-typhoidal food-borne *Salmonella* strains isolated in Tunisia by whole genome sequencing. *Int. J. Food Microbiol.* 337:108941. doi: 10.1016/j.ijfoodmicro.2020.108941

Besemer, J., Alexandre, L., and Mark, B. (2001). GeneMarkS: a self-training method for prediction of gene starts in microbial genomes. Implications for finding sequence motifs in regulatory regions. *Nucleic Acids Res.* 29, 2607–2618. doi: 10.1093/nar/29.12.2607

Dera-tomaszewska, B. (2012). *Salmonella* serovars isolated for the first time in poland 1995-2007. *Int. J. Occup. Med. Environ. Health* 25, 294–303. doi: 10.2478/S13382-012-0038-2

Fierer, J., and Guiney, D. G. (2001). Diverse virulence traits underlying different clinical outcomes of *Salmonella* infection. *J. Clin. Invest.* 107, 775–780. doi: 10.1172/JCI12561

García-Soto, S., Abdel-Glil, M. Y., Tomaso, H., Linde, J., and Methner, U. (2020). Emergence of multidrug-resistant *Salmonella enterica* subspecies *enterica* serovar infantis of multilocus sequence type 2283 in German broiler farms. *Front. Microbiol.* 11:1741. doi: 10.3389/fmicb.2020.01741

Greig, J. D., and Ravel, A. (2009). Analysis of foodborne outbreak data reported internationally for source attribution. *Int. J. Food Microbiol.* 130, 77–87. doi: 10.1016/j.ijfoodmicro.2008.12.031

Gu, D., Wang, Z., Tian, Y., Kang, X., Meng, C., Chen, X., et al. (2020). Prevalence of *Salmonella* isolates and their distribution based on whole-genome sequence in

a chicken slaughterhouse in Jiangsu, China. *Front. Vet. Sci*. 7:29. doi: 10.3389/fvets.2020.00029

Hendriksen, R. S., Vieira, A. R., Karlsmose, S., Lo Fo Wong, D. M. A., Jensen, A. B., Wegener, H. C., et al. (2011). Global monitoring of *Salmonella* serovar distribution from the world health organization global foodborne infections network country data bank: results of quality assured laboratories from 2001 to 2007. *Foodborne Pathog. Dis*. 8, 887–900. doi: 10.1089/fpd.2010.0787

Huson, D. H., and Scornavacca, C. (2012). Dendroscope 3: an interactive tool for rooted phylogenetic trees and networks. *Syst. Biol*. 61, 1061–1067. doi: 10.1093/sysbio/sys062

Hyeon, J. Y., Li, S. T., Mann, D. A., Zhang, S. K., Kim, K. J., Lee, D. H., et al. (2021). Whole-genome sequencing analysis of *Salmonella enterica* serotype enteritidis isolated from poultry sources in South Korea, 2010–2017. *Pathogens* 10:45. doi: 10.3390/pathogens10010045

Inouye, M., Dashnow, H., Raven, L. A., Schultz, M. B., Pope, B. J., Tomita, T., et al. (2014). SRST2: rapid genomic surveillance for public health and hospital microbiology labs. *Genome Med*. 6:90. doi: 10.1186/s13073-014-0090-6

Jolley, K. A., Bliss, C. M., Bennett, J. S., Bratcher, H. B., Brehony, C., Colles, F. M., et al. (2012). Ribosomal multilocus sequence typing: universal characterization of bacteria from domain to strain. *Microbiology* 158(Pt 4), 1005–1015. doi: 10.1099/mic.0.055459-0

Kimura, B. (2018). Will the emergence of core genome MLST end the role of in silico MLST? *Food Microbiol*. 75, 28–36.

Kumar, Y., Sharma, A., Sehgal, R., Kumar, S., Paratyphi, S. C., Worthington, S., et al. (2009). Distribution trends of *Salmonella* serovars in India (2001–2005). *Trans. R. Soc. Trop. Med. Hyg*. 103, 390–394. doi: 10.1016/j.trstmh.2008.09.009

Li, R., Li, Y., Kristiansen, K., and Wang, J. (2008). SOAP: short oligonucleotide alignment program. *Bioinformatics* 24, 713–714. doi: 10.1093/bioinformatics/btn025

Liu, Y. Y., Chen, C. C., and Chiou, C. S. (2016). Construction of a pan-genome allele database of *Salmonella enterica* serovar enteritidis for molecular subtyping and disease cluster identification. *Front. Microbiol*. 7:2010. doi: 10.3389/fmicb.2016.02010

Liu, Y. Y., Lin, J. W., and Chen, C. C. (2019). Cano-wgMLST_BacCompare: a bacterial genome analysis platform for epidemiological investigation and comparative genomic analysis. *Front. microbiol*. 10:1687. doi: 10.3389/fmicb.2019.01687

Lyu, N., Feng, Y. Q., Pan, Y. L., Huang, H., Liu, Y., Xue, C., et al. (2021). Genomic characterization of *Salmonella enterica* isolates from retail meat in Beijing, China. *Front. Microbiol*. 12:636332. doi: 10.3389/fmicb.2021.636332

Maiden, M. C. J., Bygraves, J. A., Feil, E., Morelli, G., Russell, J. E., Urwin, R., et al. (1998). Multilocus sequence typing: a portable approach to the identification of clones within populations of pathogenic microorganisms. *Proc. Natl. Acad. Sci. U.S.A*. 95, 3140–3145. doi: 10.1073/pnas.95.6.3140

Mairi, A., Barraud, O., Muggeo, A., de Champs, C., and Touati, A. (2020). Genomic analysis of a multidrug-resistant *Klebsiella pneumoniae* ST11 strain recovered from Barbary deer (*Cervus elaphus barbarus*) in Akfadou Forest, Algeria. *J. Glob. Antimicrob. Resist*. 22, 515–518. doi: 10.1016/j.jgar.2020.04.027

Mellmann, A., Dag, H., Craig, A., Cummings, E. B., Zentz, S. R., Leopold, A. R., et al. (2011). Prospective genomic characterization of the German enterohemorrhagic *escherichia coli* O104:H4 outbreak by rapid next generation sequencing technology. *PLoS One* 6:e22751. doi: 10.1371/journal.pone.0022751

Mezal, E. H., Sabol, A., Khan, M. A., Ali, N., Stefanova, R., and Khan, A. A. (2014). Isolation and molecular characterization of *Salmonella enterica* serovar Enteritidis from poultry house and clinical samples during 2010. *Food Microbiol*. 38, 67–74. doi: 10.1016/j.fm.2013.08.003

Monte, D. F. M., Nethery, M. A., Barrangou, R., Landgraf, M., and Fedorka-Cray, P. J. (2021). Whole-genome sequencing analysis and CRISPR genotyping of rare antibiotic-resistant *Salmonella enterica* serovars isolated from food and related sources. *Food Microbiol*. 93:103601. doi: 10.1016/j.fm.2020.103601

Perry, F., Casey, J., Bridget, A., and Ryan, J. A. (2020). The differential phosphorylation-dependent signaling and glucose immunometabolic responses induced during infection by *Salmonella enteritidis* and *Salmonella* heidelberg in chicken macrophage-like cells. *Microorganisms* 8:1041. doi: 10.3390/microorganisms8071041

Possebon, F. S., Tiba Casas, M. R., Nero, L. A., Yamatogi, R. S., Araújo, J. P., Pinto, J. P., et al. (2020). Prevalence, antibiotic resistance, PFGE and MLST characterization of *Salmonella* in swine mesenteric lymph nodes. *Prev. Vet. Med*. 179:105024. doi: 10.1016/j.prevetmed.2020.105024

Quick, J., Ashton, P., Calus, S., Chatt, C., Gossain, S., Hawker, J., et al. (2015). Rapid draft sequencing and real-time nanopore sequencing in a hospital outbreak of *Salmonella*. *Genome Biol*. 16:114. doi: 10.1186/s13059-015-0677-2

Radomski, N., Sabrina, C., Emeline, C., Arnaud, F., Pauline, B., Federica, P., et al. (2019). A simple and robust statistical method to define genetic relatedness of samples related to outbreaks at the genomic scale–application to retrospective *Salmonella* foodborne outbreak investigations. *Front. Microbiol*. 10:2413. doi: 10.3389/fmicb.2019.02413

Robertson, J., Yoshida, C., Kruczkiewicz, P., Nadon, C., Nichani, A., Taboada, E. N., et al. (2018). Comprehensive assessment of the quality of *Salmonella* whole genome sequence data available in public sequence databases using the *Salmonella* in silico Typing Resource (SISTR). *Microb. Genom*. 4:e000151. doi: 10.1099/mgen.0.000151

Robertson, S. A., Sidge, J. L., Koski, L., Hardy, M. C., Stevenson, L., Signs, K., et al. (2019). Onsite investigation at a mail-order hatchery following a multistate *Salmonella* illness outbreak linked to live poultry–United States, 2018. *Poult. Sci*. 98, 6964–6972. doi: 10.3382/ps/pez529

Ruppitsch, W., Ariane, P., Karola, P., Stefan, B., Haizpea, L. F., Franz, A., et al. (2015). Defining and evaluating a core genome multilocus sequence typing scheme for whole-genome sequence-based typing of *Listeria monocytogenes*. *J. Clin. Microbiol*. 53, 2869–2876. doi: 10.1128/JCM.01193-15

Sabat, A. J., Sandra, M. H., Viktoria, A., Amadu, J., John, E. D., Hajo, G., et al. (2017). Complete-genome sequencing elucidates outbreak dynamics of ca-mrsa usa300 (st8-spa t008) in an academic hospital of Paramaribo, Republic of Suriname. *Sci. Rep*. 7:41050. doi: 10.1038/srep41050

Scornavacca, C., Zickmann, F., and Huson, D. H. (2011). Tanglegrams for rooted phylogenetic trees and networks. *Bioinformatics* 27, i248–i256. doi: 10.1093/bioinformatics/btr210

Seif, Y., Kavvas, E., Lachance, J. C., Yurkovich, J. T., Nuccio, S. P., Fang, X., et al. (2018). Genome-scale metabolic reconstructions of multiple *Salmonella* strains reveal serovar-specific metabolic traits. *Nat. Commun*. 9:3771. doi: 10.1038/s41467-018-06112-5

Shen, H., Chen, H., Ou, Y., Huang, T., Chen, S., Zhou, L., et al. (2020). Prevalence, serotypes, and antimicrobial resistance of *Salmonella* isolates from patients with diarrhea in Shenzhen, China. *BMC Microbiol*. 20:197. doi: 10.1186/s12866-020-01886-5

Simon, S., Trost, E., Bender, J., Fuchs, S., Malorny, B., Rabsch, W., et al. (2018). Evaluation of WGS based approaches for investigating a food-borne outbreak caused by *Salmonella enterica* serovar Derby in Germany. *Food Microbiol*. 71, 46–54. doi: 10.1016/j.fm.2017.08.017

Simpson, J. T., Wong, K., Jackman, S. D., Schein, J. E., Jones, S. J. M., and Birol, I. (2009). ABySS: a parallel assembler for short read sequence data. *Genome Res*. 19, 1117–1123. doi: 10.1101/gr.089532.108

Tiba-Casas, M. R., Cláudio, T. S., Cláudia, R. G., Elisabete, A. A., Flávia, B. S., Amanda Maria de, J. B., et al. (2019). Molecular analysis of clonally related *Salmonella* Typhi recovered from epidemiologically unrelated cases of typhoid fever, Brazil. *Int. J. Infect. Dis*. 81, 191–195. doi: 10.1016/j.ijid.2019.02.009

Uelze, L., Borowiak, M., Deneke, C., Szabó, I., Fischer, J., Tausch, S. H., et al. (2019). Comparative assessment of the performance and accuracy of four open-source tools for in silico serotyping of *Salmonella spp.* based on whole-genome short read sequencing data. *Appl. Environ. Microbiol*. 86:e2265-19. doi: 10.1128/AEM.02265-19

Vincent, C., Usongo, V., Berry, C., Tremblay, D. M., Moineau, S., Yous, K., et al. (2018). Comparison of advanced whole genome sequence-based methods to distinguish strains of *Salmonella enterica* serovar Heidelberg involved in foodborne outbreaks in Québec. *Food Microbiol*. 73, 99–110. doi: 10.1016/j.fm.2018.01.004

Wang, M., Zhang, M., Lu, Y., Kang, X., Meng, C., Zhou, L., et al. (2020). Analyses of prevalence and molecular typing of *Salmonella* in the goose production chain. *Poult. Sci*. 99, 2136–2145. doi: 10.1016/j.psj.2019.12.008

Wang, X., Wang, H., Li, T., Liu, F., Cheng, Y., Guo, X., et al. (2020). Characterization of *Salmonella* spp. isolated from chickens in Central China. *BMC Vet. Res*. 16:299. doi: 10.1186/s12917-020-02513-1

Wang, Y. J., Zhang, L. H., Niu, T., and Feng, Y. (2020). Genomic characterization of a multidrug-resistant *Salmonella enterica* serovar goldcoast sequence type 358 strain in China. *J. Glob. Antimicrob. Resist.* 23, 181–183. doi: 10.1016/j.jgar.2020.09.007

World Health Organization (WHO). (2003). *Basic Laboratory Procedures in Clinical Bacteriology*, 2nd Edn. Geneva: World Health Organization, 37–50.

Xin, Y., Zhu, H. W., Bo, Y. H., Li, Y. Z., Zhang, Y., Liu, Y., et al. (2021). Prevalence and antimicrobial resistance of *Salmonella enterica* subspecies *enterica* serovar Enteritidis isolated from broiler chickens in shandong province. China, 2013–2018. *Poult. Sci.* 100, 1016–1023. doi: 10.1016/j.psj.2020.09.079

Yang, X., Wu, Q., Zhang, J., Huang, J., Chen, L., Wu, S., et al. (2019). Prevalence, bacterial load, and antimicrobial resistance of *Salmonella* serovars isolated from retail meat and meat products in China. *Front. Microbiol.* 10:2121. doi: 10.3389/fmicb.2019.02121

Yin, Z., Liu, J., Du, B., Ruan, H. H., Huo, Y. X., Du, Y., et al. (2020). Whole-genome-based survey for polyphyletic serovars of *Salmonella enterica* subsp. *enterica* provides new insights into public health surveillance. *Int. J. Mol. Sci.* 21:5226. doi: 10.3390/ijms21155226

Yoshida, C. E., Kruczkiewicz, P., Laing, C. R., Lingohr, E. J., Gannon, V. P. J., Nash, J. H. E., et al. (2016). The *Salmonella* in silico typing resource (SISTR): an open web-accessible tool for rapidly typing and subtyping draft *Salmonella* genome assemblies. *PLoS One* 11:e0147101. doi: 10.1371/journal.pone.0147101

Zhang, S., den Bakker, H. C., Li, S., Chen, J., Dinsmore, B. A., Lane, C., et al. (2019). SeqSero2: rapid and improved *Salmonella* serotype determination using whole-genome sequencing data. *Appl. Environ. Microbiol.* 85:e01746-19. doi: 10.1128/AEM.01746-19

Zhang, S., Yin, Y., Jones, M. B., Zhang, Z., Kaiser, B. L. D., Dinsmore, B. A., et al. (2015). *Salmonella* serotype determination utilizing high-throughput genome sequencing data. *J. Clin. Microbiol.* 53, 1685–1692. doi: 10.1128/JCM.00323-15

Zhang, Z., Yang, J., Xu, X., Zhou, X., Shi, C., Zhao, X., et al. (2020). Co-existence of mphA, oqxAB and blaCTX-M-65 on the IncHI2 Plasmid in highly drug-resistant *Salmonella enterica* serovar Indiana ST17 isolated from retail foods and humans in China. *Food Control* 118:107269. doi: 10.1016/j.foodcont.2020.107269

Zhao, X., Hu, M., Zhang, Q., Zhao, C., Zhang, Y., Li, L., et al. (2020). Characterization of integrons and antimicrobial resistance in *Salmonella* from broilers in Shandong, China. *Poult. Sci.* 99, 7046–7054. doi: 10.1016/j.psj.2020.09.071

Zhou, Z., Alikhan, N. F., Mohamed, K., Fan, Y., and Achtman, M. (2020). The EnteroBase user's guide, with case studies on *Salmonella* transmissions, *Yersinia* pestis phylogeny, and *Escherichia* core genomic diversity. *Genome Res.* 30, 138–152. doi: 10.1101/gr.251678.119

Conflict of Interest: The authors declare that the research was conducted in the absence of any commercial or financial relationships that could be construed as a potential conflict of interest.

Publisher's Note: All claims expressed in this article are solely those of the authors and do not necessarily represent those of their affiliated organizations, or those of the publisher, the editors and the reviewers. Any product that may be evaluated in this article, or claim that may be made by its manufacturer, is not guaranteed or endorsed by the publisher.

frontiers in Microbiology

ORIGINAL RESEARCH
published: 24 September 2021
doi: 10.3389/fmicb.2021.730656

Prevalence, Antimicrobial Susceptibility, and Molecular Characterization of *Escherichia coli* Isolated From Raw Milk in Dairy Herds in Northern China

Huimin Liu[1,2†], *Lu Meng*[1,2†], *Lei Dong*[1,2†], *Yangdong Zhang*[1,2], *Jiaqi Wang*[1,2] *and Nan Zheng*[1,2*]

[1]*Laboratory of Quality and Safety Risk Assessment for Dairy Products of Ministry of Agriculture and Rural Affairs, Institute of Animal Sciences, Chinese Academy of Agricultural Sciences, Beijing, China,* [2]*Key Laboratory of Quality & Safety Control for Milk and Dairy Products of Ministry of Agriculture and Rural Affairs, Institute of Animal Sciences, Chinese Academy of Agricultural Sciences, Beijing, China*

OPEN ACCESS

Edited by:
Fereidoun Forghani, IEH Laboratories and Consulting Group, United States

Reviewed by:
Jinxin Liu, Nanjing Agricultural University, China
Kai Deng, IEH Laboratories and Consulting Group, United States

***Correspondence:**
Nan Zheng
zhengnan_1980@126.com

†These authors have contributed equally to this work and share first authorship

Specialty section:
This article was submitted to Food Microbiology, a section of the journal Frontiers in Microbiology

Received: *25 June 2021*
Accepted: *26 August 2021*
Published: *24 September 2021*

Citation:
Liu H, Meng L, Dong L, Zhang Y, Wang J and Zheng N (2021) Prevalence, Antimicrobial Susceptibility, and Molecular Characterization of Escherichia coli Isolated From Raw Milk in Dairy Herds in Northern China. Front. Microbiol. 12:730656. doi: 10.3389/fmicb.2021.730656

Escherichia coli is a common bacterium in the intestines of animals, and it is also the major important cause of toxic mastitis, which is an acute or peracute disease that causes a higher incidence of death and culling of cattle. The purpose of this study was to investigate *E. coli* strains isolated from the raw milk of dairy cattle in Northern China, and the antibacterial susceptibility of these strains and essential virulence genes. From May to September 2015, 195 raw milk samples were collected from 195 dairy farms located in Northern China. Among the samples, 67 (34.4%) samples were positive for *E. coli*. About 67 *E. coli* strains were isolated from these 67 samples. The prevalence of Shiga toxin-producing *E. coli* (STEC), enterotoxigenic *E. coli* (ETEC), enteropathogenic *E. coli* (EPEC), and enteroinvasive *E. coli* (EIEC) were 9, 6, 4.5, and 1.5%, respectively. Among the virulence genes detected, *stx*1 was the most prevalent (6/67, 9%) gene, followed by *eae* (3/67, 4.5%), and *est*B (2/67, 3%). Moreover, the strains exhibited different resistance levels to ampicillin (46.3%), amoxicillin-clavulanic acid (16.4%), trimethoprim-sulfamethoxazole (13.4%), tetracycline (13.4%), cefoxitin (11.9%), chloramphenicol (7.5%), kanamycin (7.5%), streptomycin (6.0%), tobramycin (4.5%), azithromycin (4.5%), and ciprofloxacin (1.5%). All of the *E. coli* isolates were susceptible to gentamicin. The prevalence of β-lactamase-encoding genes was 34.3% in 67 *E. coli* isolates and 45% in 40 β-lactam-resistance *E. coli* isolates. The overall prevalence of bla_{SHV}, bla_{TEM}, bla_{CMY}, and bla_{CTX-M} genes were 1.5, 20.9, 10.4, and 1.5%, respectively. Nine non-pathogenic *E. coli* isolates also carried β-lactamase resistance genes, which may transfer to other pathogenic *E. coli* and pose a threat to the farm's mastitis management projects. Our results showed that most of *E. coli* were multidrug resistant and possessed multiple virulence genes, which may have a huge potential hazard with public health, and antibiotic resistance of *E. coli* was prevalent in dairy herds in Northern China, and ampicillin should be used cautiously for mastitis caused by *E. coli* in Northern China.

Keywords: *Escherichia coli*, virulence, antimicrobial resistance, raw milk, Northern China

INTRODUCTION

Escherichia coli was a common inhabitant of the intestine of animals (Tark et al., 2016). During parturition and early lactation period, *E. coli* was found to usually infect mammary gland of cows, which may cause acute and local mastitis (Hinthong et al., 2017). *Escherichia coli* is the main cause of bacterial mastitis in cows. It is usually short-lived, causing the infection that lasts 2–3 days. However, *E. coli* has been displayed to cause persistent infections in a few cases (Lippolis et al., 2017). Pathogenic *E. coli* can cause disease in animals and humans due to virious virulence (Ntuli et al., 2016). Based on the epidemiological, clinical, and pathogenic characteristics, *E. coli* is classified into different pathotypes: Shiga toxin-producing *E. coli* (STEC), enteroaggregative *E. coli* (EAEC), enterotoxigenic *E. coli* (ETEC), enteropathogenic *E. coli* (EPEC), and enteroinvasive *E. coli* (EIEC; Rugeles et al., 2010). Numerous outbreaks associated with *E. coli* in milk and other foods have been reported recently (EFSA-ECDC, 2012; EFSA, 2015; Ombarak et al., 2016). For example, STEC can generate two types of Shiga toxins (*stx*1 and *stx*2), and EPEC can produce *bfp* gene, which were involved in pathogenicity of gastrointestinal tract (Hernandes et al., 2009; Douellou et al., 2016). ETEC can express heat-stable *est* genes that can cause severe diarrhea. EAEC can produce *aggR* gene, which were associated with the generation of biofilm (Medeiros et al., 2013). The *ipa*H gene from EIEC can lead to the occurrence of fever, vomiting, and dehydration in infected children. The higher prevalence of *E. coli* is closely associated with hygiene in raw milk (Radostits et al., 2007). Therefore, the study on *E. coli* in raw milk is significant.

Escherichia coli is not only with the potential occurrence, but also with the rapid development of antibiotic resistance bacteria (Ntuli et al., 2016). Inappropriate selection and abuse of antibiotics could lead to antibiotic resistance in bacteria (Da Silva and Mendonça, 2012). Moreover, *E. coli* may develop acquired resistance to other antibiotics by carrying various resistance characteristics on mutation, plasmids, or transposons (Gonggrijp et al., 2016). For example, extended-spectrum β-lactamases *E. coli*, resistant to β-lactam antibiotics including third- and fourth-generation cephalosporins, acquires ESBL by mutation or plasmid-mediated horizontal gene transfer (Freitag et al., 2016). Acquired antibiotic resistance also has a transmission potential to humans and other animals (Ruegg et al., 2014). Raw milk can also facilitate the transmission of antibiotic resistance genes to the human gastrointestinal tract, In addition to the presence of pathogenic bacteria. A better understanding on the resistance profile of *E. coli* isolates will improve our understanding of appropriate treatments for pathogen-related management (Tark et al., 2016). Therefore, monitoring the antibiotic resistance of *E. coli* in raw milk may show the trend or specific characteristics of antibiotic resistance and help to better prevent or more effectively treat mastitis on dairy farm.

Antimicrobial resistance and virulence types in *E. coli* have been studied on raw milk of healthy dairy cattle and of bovine mastitis in a variety of countries, including Northern Italy, Romania, Brazil, Egypt, South Korea, and Thailand (Trevisani et al., 2014; Ombarak et al., 2016; Ribeiro et al., 2016; Tark et al., 2016; Hinthong et al., 2017; Tabaran et al., 2017). However, incidence on antibiotic resistance of *E. coli* from raw milk in Northern China were very limited. Continuous monitoring of the antibiotic resistance and virulence type of *E. coli* could be necessary to evaluate *E. coli* risk in raw milk. Therefore, the objective of the work was to investigate the rate of *E. coli* strains isolated from raw milk in Northern China, and to characterize the antimicrobial susceptibility and key virulence genes of these strains.

MATERIALS AND METHODS

Collection of Samples

In total, 195 raw milk were collected from 195 dairy farms from four cities, which was the major dairy-production cities of Northern China (herd size ≥300, no clinical mastitis cow, milking frequency two or three times per day), from May to September in 2015 (average daily temperature >20°C). There were 30 raw milk samples from Jinan, 40 samples from Harbin, 50 samples from Beijing, and 75 samples from Hohhot (**Figure 1**). The raw milk samples were collected from the top, middle, and bottom of bulk tank, mixed well, and then transferred into sterile bottles and transported to laboratory at 4°C immediately.

Isolation and Identification of *E. coli*

Aliquots (25 ml) of each sample were added to 225 ml tryptic soy broth, and then incubated at 37°C for 16 h with shaking for *E. coli* detection. The samples were placed onto Eosin Methylene Blue agar plates (Beijing Land Bridge Technology Ltd., Beijing, China). The agar plates were incubated at 37°C for 18–24 h. The presumptive colonies (typical blue-black appearance with a metallic green sheen) were picked. All the colonies were sub-cultured onto nutrient agar slants at 37°C for 16 h, and then used for biochemical identification. The colonies initially identified as *E. coli* were examined by Voges-Proskauer negative, methyl-red positive and citrate negative. All isolates were stored at −80°C until use.

All the presumptive colonies were confirmed by PCR on 16S rRNA gene detection (**Supplementary Table S1**). Genomic DNA was extracted with the InstaGene Matrix DNA extraction kit (Bio-Rad Laboratories), based on the manufacturer's instruction. PCR were performed with the EmeraldAmp Max PCR Master Mix kit (Takara, Dalian, China) followed the instructions of manufacturer. The primers were synthesized by GeneCreate Biological Engineering Co., Ltd. (Wuhan, China). Briefly, 25 μl reactions, which contains 12.5 μl of 2 × EmeraldAmp Max PCR Master Mix kit, 10 pmol of each primer, 1 μl of extracted DNA and ultrapure water, were prepared. The amplification conditions were as follows: 94°C for 3 min; 30 cycles of 94°C for 30 s, 55°C for 30 s, and 72°C for 1 min; and 72°C for 10 min for a final extension step. Without genomic DNA as negative control and *E. coli* ATCC 25922 as positive control were included in all the PCR assays.

FIGURE 1 | Map of sampling locations. In total, 195 samples were collected from Hohhot, Beijing, Harbin, and Jinan.

Detection of Virulence Determinants

Seven virulence genes for each diarrheagenic *E. coli* were detected by PCR method: *stx*1 and *stx*2 for STEC, *est*A, *est*B, and *elt*B for ETEC, *agg*R for EAEC, *bfp* and *eae* for EPEC, and *ipa*H for EIEC. Amplified products were analyzed by agarose gel electrophoresis, and then visualized by SYBR Safe DNA Stain gel staining. All the primers were shown in **Supplementary Table S1**.

Antimicrobial Susceptibility Patterns

Antimicrobial patterns for recovered *E. coli* were determined by agar disk diffusion method (CLSI, 2012). Gentamicin (10 μg), tobramycin (10 μg), streptomycin (10 μg), amoxicillin-clavulanic acid (20/10 μg), ampicillin (10 μg), ciprofloxacin (5 μg), azithromycin (15 μg), cefoxitin (30 μg), chloramphenicol (30 μg), tetracycline (30 μg), kanamycin (30 μg), and trimethoprim-sulfamethoxazole (1.25/23.75 μg) were used as antibiotic agents (Oxoid, Basingstoke, United Kingdom). *Escherichia coli* ATCC 25922 and *Staphylococcus aureus* ATCC 6538 were used as quality controls. The experiment was repeated three times.

Antimicrobial Resistance Genes

Four β-lactamase resistance related genes (bla_{CMY}, bla_{SHV}, bla_{CTX-M}, and bla_{TEM}) and two tetracycline genes (*tet*A and *tet*B) were detected by multiplex PCR in *E. coli* strains (**Supplementary Table S1**). The amplification conditions were as follows: 95°C for 5 min, 30 cycles of 94°C for 30 s, 63°C for 90 s, and 72°C for 90 s, and 72°C for 7 min for a final extension step (Ribeiro et al., 2016). *Escherichia coli* strains ATCC 25922 was used as a positive control in each run.

RESULTS

Prevalence of *E. coli*

Out of 195 samples, 67 (34.4%) raw milk samples were positive for *E. coli*. Among these 67 raw milk samples, 67 *E. coli* strains were isolated, including 11 strains (36.7%) of 30 Jinan samples, 23 strains (30.7%) of 75 Hohhot samples, 16 strains (40.0%) of 40 Harbin samples, and 17 strains (34.0%) of 50 Beijing samples.

Virulence Genes

About 20.9% of the isolates (14/67) harbored more than one virulence gene, as shown in **Table 1**. The prevalence of EAEC, EIEC, EPEC, ETEC, and STEC was 0, 1.5, 4.5, 6, and 9%. Among the virulence genes detected, *stx*1 was the most prevalent gene (6/67, 9%), followed by *eae* (3/67, 4.5%), *est*B (2/67, 3%), *stx2* (1/67, 1.5%), *est*A (1/67, 1.5%), *elt* (1/67, 1.5%), and *ipa*H (1/67, 1.5%). The *aggR* and *bfp* were not discovered in any

TABLE 1 | Virulence genes in *Escherichia coli* from raw cow milk samples.

Tapes of samples	No. of strains	STEC (%)				ETEC (%)				EPEC (%)			EAEC (%)	EIEC (%)	Total (%)
		stx1	*stx2*	*stx1&stx2*	Total	*estA*	*estB*	*elt*	Total	*eae*	*bfp*	Total	*aggR*	*ipaH*	
Hohhot	23	2 (8.7)	0 (0)	1 (4.3)	3 (13.0)	0 (0)	1 (4.3)	0 (0)	1 (4.3)	2 (8.7)	0 (0)	2 (8.7)	0 (0)	0 (0)	6 (26.1)
Jinan	11	1 (9.1)	0 (0)	0 (0)	1 (9.1)	0 (0)	0 (0)	1 (9.1)	1 (9.1)	1 (9.1)	0 (0)	1 (9.1)	0 (0)	0 (0)	3 (27.3)
Harbin	16	1 (6.3)	0 (0)	0 (0)	1 (6.3)	0 (0)	1 (6.3)	0 (0)	1 (6.3)	0 (0)	0 (0)	0 (0)	0 (0)	1 (6.3)	3 (18.8)
Beijing	17	1 (5.9)	0 (0)	0 (0)	1 (5.9)	1 (5.9)	0 (0)	0 (0)	1 (5.9)	0 (0)	0 (0)	0 (0)	0 (0)	0 (0)	2 (11.7)
Total	67	5 (7.5)	0 (0)	1 (1.5)	6 (9.0)	1 (1.5)	2 (3.0)	1 (1.5)	4 (6.0)	3 (4.5)	0 (0)	3 (4.5)	0 (0)	1 (1.5)	14 (20.9)

E. coli strains. Among six STEC isolates, there were three isolates (13.0%) from Hohhot, one isolate (9.1%) from Jinan, one isolate (6.3%) from Harbin, and one isolate (5.9%) from Beijing, respectively. There were two *eae*-positive isolates from Hohhot (8.7%), one *eae*-positive isolates from Jinan (9.1%), and no *eae*-positive isolate from Harbin and Beijing. Moreover, the prevalence of ETEC strains were 9.1% from Jinan, 6.3% from Harbin, 5.9% from Beijing, and 4.3% from Hohhot, respectively. For ETEC-related virulence genes, the prevalence of *est*B, *est*A, and *elt* genes were 3.0% (2/67), 1.5% (1/67), and 1.5% (1/67), and there were one *elt*-positive isolate from Jinan (9.1%), two *est*B-positive isolates from Harbin (6.3%) and Hohhot (4.3%), and one *est*A-positive isolate from Beijing (5.9%). The *ipaH* was detected in only one *E. coli* strain from Harbin.

Antimicrobial Susceptibility Testing

The 67 isolates were exanimated by the disk diffusion method for susceptibility to 12 antibiotics. Antibiotic resistance on *E. coli* was observed to ampicillin (46.3%), amoxicillin-clavulanic acid (16.4%), tetracycline (13.4%), trimethoprim-sulfamethoxazole (13.4%), cefoxitin (11.9%), chloramphenicol (7.5%), kanamycin (7.5%), streptomycin (6.0%), tobramycin (4.5%), azithromycin (4.5%), ciprofloxacin (1.5%), and gentamicin (0; **Table 2**). Among isolates from Hohhot, the resistant to ampicillin (47.8%) was the most frequently observed, followed by amoxicillin-clavulanic acid (17.4%), tetracycline (13.0%), and sulfamethoxazole-trimethoprim (13.0%), and all investigated strains were sensitive to tobramycin, streptomycin, ciprofloxacin, and gentamicin. Among isolates from Jinan, the resistance to ampicillin and cefoxitin (45.5%) was the most frequently observed, and all investigated strains were sensitive to tobramycin, streptomycin, and gentamicin. Among isolates from Harbin, the resistance to ampicillin (43.8%) was the most frequently observed, followed by amoxicillin-clavulanic acid, tetracycline, sulfamethoxazole-trimethoprim, chloramphenicol, streptomycin, and tobramycin (12.5%), and all investigated strains were sensitive to ciprofloxacin and gentamicin. Among isolates from Beijing, the resistance to ampicillin (47.1%) was the most frequently observed, followed by streptomycin (12.5%), amoxicillin-clavulanic acid (11.8%), tetracycline (11.8%), and sulfamethoxazole-trimethoprim (11.8%), and all the investigated *E. coli* isolates were sensitive to ciprofloxacin, azithromycin, and gentamicin. Moreover, 38 strains (71.6%) were resistant to at least one antibiotic, and 13 isolates (19.4%) were resistant to more than three kinds of antibiotics.

Screening of Antibiotic Resistance Genes

The β-lactamase-encoding genes results were presented in **Table 3**. The prevalence of β-lactamase-encoding genes were 34.3% in 67 *E. coli* isolates and 45% in 40 β-lactam resistance *E. coli* isolates. The overall prevalences of bla_{SHV}, bla_{TEM}, bla_{CMY}, and $bla_{\text{CTX-M}}$ genes among *E. coli* isolates, which was narrow spectrum extended-spectrum β-lactamase-encoding genes, β-lactamase-encoding genes, AmpC, and β-lactamase-encoding genes, were 1.5, 1.5, 10.4, and 20.9%, respectively. In total,

TABLE 2 | Antibiotic resistance of strains.

Antibiotics	No. (%) of positive strains				
	Hohhot (*n* = 23)	Jinan (*n* = 11)	Harbin (*n* = 16)	Beijing (*n* = 17)	Total (*n* = 67)
Ampicillin	11 (47.8)	5 (45.5)	7 (43.8)	8 (47.1)	31 (46.3)
Amoxicillin-clavulanic acid	4 (17.4)	3 (27.3)	2 (12.5)	2 (11.8)	11 (16.4)
Tetracycline	3 (13.0)	2 (18.2)	2 (12.5)	2 (11.8)	9 (13.4)
Sulfamethoxazole-trimethoprim	3 (13.0)	2 (18.2)	2 (12.5)	2 (11.8)	9 (13.4)
Cefoxitin	1 (4.3)	5 (45.5)	1 (6.3)	1 (5.9)	8 (11.9)
Chloramphenicol	2 (8.7)	0 (0)	2 (12.5)	1 (5.9)	5 (7.5)
Kanamycin	2 (8.7)	1 (9.1)	1 (6.3)	1 (5.9)	5 (7.5)
Streptomycin	0 (0)	0 (0)	2 (12.5)	2 (11.8)	4 (6.0)
Tobramycin	0 (0)	0 (0)	2 (12.5)	1 (5.9)	3 (4.5)
Azithromycin	1 (4.3)	1 (9.1)	1 (6.3)	0 (0)	3 (4.5)
Ciprofloxacin	0 (0)	1 (9.1)	0 (0)	0 (0)	1 (1.5)
Gentamicin	0 (0)	0 (0)	0 (0)	0 (0)	0 (0)

TABLE 3 | β-lactamase genotypes identified in β-lactam-resistant *E. coli*.

Antibiotic	No. of positive strains	No. of positive strains				None
		bla_{SHV}	bla_{TEM}	bla_{CMY}	bla_{CTX-M}	
Ampicillin	26	0	8	1	0	17
Amoxicillin-clavulanic acid	4	0	0	2	0	2
Cefoxitin	3	0	0	0	1	2
Ampicillin, amoxicillin-clavulanic acid	2	0	1	0	0	1
Amoxicillin-clavulanic acid, cefoxitin	2	0	1	1	0	0
Ampicillin, amoxicillin-clavulanic acid, and cefoxitin	3	1	1	1	0	0
None	27	0	3	2	0	22
Total	67	1	14	7	1	44

71.4% of the isolates, which possessed the bla_{TEM} gene, were resistant to ampicillin. Around 57.1% of bla_{CMY} positive isolates were resistant to amoxicillin-clavulanic acid. Five (7.5%) isolates possessing bla_{TEM} or bla_{CMY} did not suggest β-lactamase antibiotic resistance.

Moreover, the presence of the *tet* genes, which were conferring resistance to tetracycline, were confirmed in seven tetracycline-resistance strains. None of the studied strains possessed *tet*A (**Table 4**).

DISCUSSION

In this research, 34.4% (67/195) of samples were positive for *E. coli* in raw milk. These results are significantly lower than that in previous studies. The incidence of *E. coli* in raw milk in India was 81.1% (Bhoomika et al., 2016), 75% in Bangladesh (Islam et al., 2016), 64.5% in Malaysia (Jayarao and Henning, 2001), and 45% in Northern China (Lan et al., 2017). In contrast, a much lower incidence (22.4%) of *E. coli* was discovered in raw milk in Sharkia Governorate (Awadallah et al., 2016). Moreover, our results are comparable with the findings of Ntuli et al. (2016), who reported 36% prevalence rate in bulk milk in South Africa, and Sharma et al. (2015), who reported 35.63% occurrence rate in raw milk in the Jaipur city of Rajasthan. Overall, the results indicated that *E. coli* is a common strain in raw milk collected from dairy herds of Northern China. The high prevalence of *E. coli* in raw milk and dairy products is a cause of concern because it is related to contamination from fecal sources and the consequent risk of enteric pathogenic microorganisms in food (Ombarak et al., 2016).

An important factor of *E. coli* infections is virulence factors. When *E. coli* carried some virulence genes, they could be potentially harmful to public consumers (Hinthong et al., 2017). In the study, 20.9% (14/67) of the tested raw milk possessing more than one virulence gene tested, may carried potentially pathogenic *E. coli*, as shown in **Table 3**. STEC, cause a life-threatening sequel, such as neurological disorder and hemolytic syndrome or HUS (Kaper et al., 2004), was found to be the most common pathogenic *E. coli* strain in raw milk. It has been reported that the virulence genes of STEC isolates were commonly implicated in many foodborne STEC outbreaks in the world (Beutin and Fach, 2015). In this study, the most common virulence genes in raw milk samples in Northern China were *stx* genes. The result was in agreement with Suojala et al. (2011), who reported the STEC (*stx*-positive isolates) was the most common *E. coli* type of raw milk with subclinical mastitis in Southern Finland, and by Lambertini et al. (2015), who found that the most frequently detected gene in raw milk of the United States northeastern was *stx*1. However, STEC or *stx* factors has been detected in the farms

TABLE 4 | Antimicrobial resistance genes among *E. coli*.

Phenotype		Genotype	
Antimicrobial agents	**No. of positive strains**	**Resistant genes or genetic elements studied**	**No. of positive strains**
Penicillin G	47	*blac*Z	30
Cefoxitin	23	*cfx*A	13
Tobramycin	3	*ant(4')*-Ia	2
Gentamicin	7	*aac*6'-*aph*2"	7
Chloramphenicol	4	*fex*A	0
		*cat*A	0
Tetracycline	7	*tet*K	1
		*tet*K + *tet*L	2
		*tet*M	3
		*tet*M + *tet*L	1
		*tet*A	0
Erythromycin	25	*erm*B	3
		*erm*B + *erm*C	3
		*erm*C	4
		*erm*C + *erm*A	1
		*erm*C + *msr*A	2
		*erm*C + *msr*B	1
		*msr*A	1
		*erm*A and/or *msr*B	0
Kanamycin	8	*ant(4')*-Ia	8
Lincomycin	28	*lin*A	5
Oxacillin	16	*mec*A	16
Streptomycin	5	*ant(6)*-Ia	0
Quinupristin-Dalfopristin	2	*vga*A and/or *vga*B	0

of United States and European at a low prevalence (Jayarao et al., 2006; Pradel et al., 2008; Van Kessel et al., 2011; Claeys et al., 2013; Ombarak et al., 2016).

Enteropathogenic *E. coli* is responsible for diarrhea in both developing and developed countries. As an important foodborne pathogen, EPEC has high isolation rate in retail foods in China (Zhang et al., 2016). EPEC were isolated from many animals, such as cattle, goat, sheep, chicken, gull, and pigeon (Gomez-Aldapa et al., 2016). In the study, three strains were *eae* genes-positive and *bfp* gene-negative, which could be classified as EPEC. Cortés et al. (2005) and Gomez-Aldapa et al. (2016) found that atypical EPEC strains were found in raw milk in Egypt, Saudi Arabia, and Slovakia. However, there is no report on the *eae*-positive *E. coli* strains found in mastitis cows in Iran and Thailand (Ghanbarpour and Oswald, 2010; Hinthong et al., 2017). Moreover, an increasing frequency of *eae*-negative isolates were postulated to have other putative adherence and virulence associated factors (Gomez-Aldapa et al., 2016). ETEC strains are usually transmitted by contaminated food. In the study, EPEC and ETEC strains were isolated from Hohhot and Jinan. EPEC/ETEC hybrid isolates were related to EPEC strain, and appeared to have acquired virulence genes by horizontal gene transfer (Hazen et al., 2017).

In the study, antimicrobial resistance was most frequently observed to ampicillin (46.3%). The susceptibility to amoxicillin can be predicted by antimicrobial resistance to ampicillin (CLSI, 2012). So the tested *E. coli* isolates may showed a high resistance to amoxicillin. Nam et al. (2009) reported that 32.2% *E. coli* strains from mastitis cow were resistant to ampicillin. However, the resistant rates in the study were much higher than those in South Korea from 2012 to 2015 (Tark et al., 2016) and in Northern Colorado (McConnel et al., 2016). Antibiotic susceptibility of *E. coli* was more important on choosing a suitable antibiotic for mastitis (Wang et al., 2016). The information of antibiotic use for dairy in Northern China has been investigated in our previous survey. Ampicillin was commonly used in dairy mastitis therapy (Liu et al., 2017). So, ampicillin is not a suitable treatment for mastitis caused by *E. coli* in Northern China.

In our previous survey, we found that five antibiotics (penicillin, ciprofloxacin, sulfamethoxazole-trimethoprim, streptomycin, and gentamicin) were commonly used in mastitis cow. In the study, most of tested strains showed an obvious antimicrobial resistance to ciprofloxacin, sulfamethoxazole-trimethoprim, and streptomycin. These results also indicated that there was a correlation between antibiotic use and antimicrobial resistance.

In the study, there were four β-lactamase resistance genes detected. The β-lactamase-encoding genes prevalence was 34.3% in 67 *E. coli* isolates. β-lactamase resistance genes, such as bla_{CMY}, bla_{SHV}, bla_{CTX-M}, and bla_{TEM} were detected in nine non-pathogenic *E. coli* isolates. So non-pathogenic *E. coli* can serve as an antibiotic resistance reservoir and could possibly transfer genes to other pathogenic *E. coli* strains, which can pose a threat to mastitis management programs of farm (Hu et al., 2016). The rate of $bla_{CTX-M,}$ bla_{CMY}, bla_{TEM}, and bla_{SHV} genes among *E. coli* was 1.5, 1.5, 10.4, and 20.9% in the study, respectively. The bla_{TEM} and bla_{CMY} genes were the most common, which is similar to several previous studies (Navajas-Benito et al., 2016; Gomi et al., 2017; Hinthong et al., 2017). The cephalosporins treatment in mastitis cattle also raised the proportion of bla_{TEM} in milk samples at the period of withdrawal ($p < 0.05$; Dong et al., 2021). The bla_{CTX-M}, which was the most important ESBL-related gene, it was associated with the geographic area (Su et al., 2016). However, bla_{CTX-M} was the most popular gene in Japan, United Kingdom, France, Netherlands, and Germany (Dahmen et al., 2013; Ohnishi et al., 2013; Timofte et al., 2014; Freitag et al., 2016; Santman-Berends et al., 2016).

Around 11.8% of *E. coli* stains showed resistance to tetracycline in the study. However, Su et al. (2016) reported that the tetracycline-resistance prevalence was 51%. Navajas-Benito et al. (2016) reported that antimicrobial resistance for tetracycline was detected in 19.2% of *E. coli* strains, which recovered from air and its surroundings in Spain. Antimicrobial resistance genes to tetracycline were tested in all the tetracycline-resistant isolates, and three tetracycline-resistant isolates harbored one tetracycline resistance gene *tet*B, which was the most frequent gene, and the studied *E. coli* did not possess *tet*A. However, Gomi et al. (2017) found that the prevalent of *tet*A was more than *tet*B in *E. coli* isolates. It was reported that one representative *E. coli* strain (No. JXLQYF114666) contained nine ARGs including *aph*(3")-Ib, bla_{TEM-1B}, bla_{CMY-2}, *aph*(6)-Id, *mdf*A, *sul*2, *tet*B, *cat*A2, and *dfrA14*, which result in resistance to seven important antibiotics classes (Liu et al., 2020). Moreover, the

phenotype-genotype discrepancies on the tetracycline-resistant *E. coli* were observed in the study. However, resistance genotypes on tetracycline, gentamicin, kanamycin, and oxacillin correlated well with resistance phenotypes in *E. coli* and *S. aureus* (Gomi et al., 2017). Therefore, it was still necessary to fully account of testing phenotypic susceptibility for resistance (Zhao et al., 2015). Further research should be carried out to analyze the genetic characteristics on antibiotic resistance by whole-genome approach, which may explain the phenotype-genotype discrepancies observed for many strains.

CONCLUSION

In conclusion, the antibiotic resistance on *E. coli* isolated from raw milk in Northern China was assessed for the first time. Our data indicated that *E. coli* isolates were widely present in raw milk samples in Northern China. A total 20.9% of the tested *E. coli* possessed one or more virulence genes, which showed a potential pathogenicity. *Escherichia coli* strains exhibited different levels of antimicrobial resistance, except gentamicin. Ampicillin should not be a suitable treatment of dairy herds for mastitis by *E. coli* in Northern China. Majority of *E. coli* were multiple-antibiotic resistant and co-carried many virulence genes, and it may pose great potential risk to public health. The possibility of transferring and transmitting resistance genes, between non-pathogenic and pathogenic *E. coli* isolates, should be evaluated in further studies.

DATA AVAILABILITY STATEMENT

The original contributions presented in the study are included in the article/**Supplementary Material**, further inquiries can be directed to the corresponding author.

AUTHOR CONTRIBUTIONS

HL, LM, and LD designed and performed the research. YZ helped with the data analysis. JW gave advices to the researchers. NZ gave the opinions on the research design. All authors contributed to the article and approved the submitted version.

FUNDING

This research was supported by China Agriculture Research System of MOF and MARA, The Agricultural Science and Technology Innovation Program (ASTIP-IAS12), The Scientific Research Project for Major Achievements of The Agricultural Science and Technology Innovation Program (CAAS-ZDXT2019004) and Project of Risk Assessment on Raw Milk (GJFP2019026).

SUPPLEMENTARY MATERIAL

The Supplementary Material for this article can be found online at: https://www.frontiersin.org/articles/10.3389/fmicb.2021.730656/full#supplementary-material

REFERENCES

Awadallah, M. A., Ahmed, H. A., Merwad, A. M., and Selim, M. A. (2016). Occurrence, genotyping, Shiga toxin genes and associated risk factors of *E. coli* isolated from dairy farms, handlers and milk consumers. *Vet. J.* 217, 83–88. doi: 10.1016/j.tvjl.2016.09.014

Beutin, L., and Fach, P. (2015). "Detection of Shiga toxin-producing *Escherichia coli* from nonhuman sources and strain typing," in *Enterohemorrhagic Escherichia coli and Other Shiga Toxin-Producing E. coli* (Washington, DC: American Society of Microbiology), 299–319.

Bhoomika, Sanjay, S., Anil, P., and Eknath, G. N. (2016). Occurrence and characteristics of extended-spectrum β-lactamases producing *Escherichia coli* in foods of animal origin and human clinical samples in Chhattisgarh, India. *Vet. World* 9, 996–1000. doi: 10.14202/vetworld.2016.996-1000

Claeys, W. L., Cardoen, S., Daube, G., Block, J. D., and Herman, L. (2013). Raw or heated cow milk consumption: review of risks and benefits. *Food Control* 31, 251–262. doi: 10.1016/j.foodcont.2012.09.035

CLSI (2012). *Performance Standards for Antimicrobial Susceptibility Testing. Document M100–S22*. Wayne, PA: Clinical and Laboratory Standards Institute (CLSI).

Cortés, C., Fuente, R., Blanco, J., Blanco, M., Blanco, J. E., Dhabi, G., et al. (2005). Serotypes, virulence genes and intimin types of verotoxin-producing *Escherichia coli* and enteropathogenic *E. coli* isolated from healthy dairy goats in Spain. *Vet. Microbiol.* 110, 67–76. doi: 10.1016/j.vetmic.2005.06.009

Dahmen, S., Métayer, V., Gay, E., Madec, J. Y., and Haenni, M. (2013). Characterization of extended-spectrum beta-lactamase (esbl)-carrying plasmids and clones of enterobacteriaceae causing cattle mastitis in France. *Vet. Microbiol.* 162, 793–799. doi: 10.1016/j.vetmic.2012.10.015

Da Silva, G., and Mendonça, N. (2012). Association between antimicrobial resistance and virulence in *Escherichia coli*. *Virulence* 3, 18–28. doi: 10.4161/viru.3.1.18382

Dong, L., Meng, L., Liu, H., Wu, H., Hu, H., Zheng, N., et al. (2021). Effect of therapeutic administration of β-lactam antibiotics on the bacterial community and antibiotic resistance patterns in milk. *J. Dairy Sci.* 104, 7018–7025. doi: 10.3168/jds.2020-20025

Douellou, T., Delannoy, S., Ganet, S., Mariani-Kurkdjian, P., Fach, P., Loukiadis, E., et al. (2016). Shiga toxin-producing *Escherichia coli* strains isolated from dairy products – genetic diversity and virulence gene profiles. *Int. J. Food Microbiol.* 232, 52–62. doi: 10.1016/j.ijfoodmicro.2016.04.032

EFSA (2015). Scientific opinion on the public health risks related to the consumption of raw drinking milk. *EFSA J.* 13:3940. doi: 10.2903/j.efsa.2015.4139

EFSA-ECDC (2012). Scientific report of EFSA and ECDC: the European Union summary report on trents and sources of zoonoses, agents and food-borne outbreaks in 2010. *EFSA J.* 10:2597. doi: 10.2903/j.efsa.2012.2669

Freitag, C., Michael, G. B., Kadlec, K., Hassel, M., and Schwarz, S. (2016). Detection of plasmid-borne extended-spectrum β-lactamase (ESBL) genes in *Escherichia coli* isolates from bovine mastitis. *Vet. Microbiol.* 200, 151–156. doi: 10.1016/j.vetmic.2016.08.010

Ghanbarpour, R., and Oswald, E. (2010). Phylogenetic distribution of virulence genes in *Escherichia coli* isolated from bovine mastitis in Iran. *Res. Vet. Sci.* 88, 6–10. doi: 10.1016/j.rvsc.2009.06.003

Gomez-Aldapa, C. A., Segovia-Cruz, J. A., Cerna-Cortes, J. F., Rangel-Vargas, E., Salas-Rangel, L. P., and Gutierrez-Alcantara, E. J. (2016). Prevalence and behavior of multidrug-resistant Shiga toxin-producing *Escherichia coli*, enteropathogenic *E. coli* and enterotoxigenic *E. coli* on coriander. *Food Microbiol.* 59, 97–103. doi: 10.1016/j.fm.2016.05.014

Gomi, R., Matsuda, T., Matsumura, Y., Yamamoto, M., Tanaka, M., Ichiyama, S., et al. (2017). Whole-genome analysis of antimicrobial-resistant and extraintestinal pathogenic *Escherichia coli* in river water. *Appl. Environ. Microbiol.* 78:e02703-16. doi: 10.1128/AEM.02703-16

Gonggrijp, M. A., Santman-Berends, I., Heuvelink, A. E., Buter, G. J., and Lam, T. (2016). Prevalence and risk factors for extended-spectrum β-lactamase-

and ampc-producing *Escherichia coli* in dairy farms. *J. Dairy Sci.* 99, 9001–9013. doi: 10.3168/jds.2016-11134

Hazen, T. H., Michalski, J., Luo, Q. W., Shetty, A. C., Daugherty, S. C., Fleckenstein, J. M., et al. (2017). Comparative genomics and transcriptomics of *Escherichia coli* isolates carrying virulence factors of both enteropathogenic and enterotoxigenic *E. coli*. *Sci. Rep.* 7:3513. doi: 10.1038/s41598-017-03489-z

Hernandes, R. T., Elias, W. P., Vieira, M. A., and Gomes, T. A. (2009). An overview of a typical enteropathogenic *Escherichia coli*. *FEMS Microbiol. Lett.* 297, 137–149. doi: 10.1111/j.1574-6968.2009.01664.x

Hinthong, W., Pumipuntu, N., Santajit, S., Kulpeanprasit, S., Buranasinsup, S., and Sookrung, N. (2017). Detection and drug resistance profile of *Escherichia coli* from subclinical mastitis cows and water supply in dairy farms in Saraburi Province, Thailand. *PeerJ* 5:e3431. doi: 10.7717/peerj.3431

Hu, Y., Yang, X., Li, J., Lv, N., Liu, F., Wu, J., et al. (2016). The transfer network of bacterial mobile resistome connecting animal and human microbiome. *Appl. Environ. Microbiol.* 82, 6672–6681. doi: 10.1128/AEM.01802-16

Islam, M. A., Kabir, S. M. L., and Seel, S. K. (2016). Molecular detection and characterization of *Escherichia coli* isolated from raw milk sold in different markets of Bangladesh. *Bangladesh J. Vet. Med.* 14, 271–275. doi: 10.3329/bjvm.v14i2.31408

Jayarao, B. M., Donaldson, S. C., Straley, B. A., Sawant, A. A., Hegde, N. V., and Brown, J. L. (2006). A survey of foodborne pathogens in bulk tank milk and raw milk consumption among farm families in Pennsylvania. *J. Dairy Sci.* 89, 2451–2458. doi: 10.3168/jds.S0022-0302(06)72318-9

Jayarao, B. M., and Henning, D. R. (2001). Prevalence of foodborne pathogens in bulk tank milk. *J. Dairy Sci.* 84, 2157–2162. doi: 10.3168/jds.S0022-0302(01)74661-9

Kaper, J. B., Nataro, J. P., and Mobley, H. L. (2004). Pathogenic *Escherichia coli*. *Nat. Rev. Microbiol.* 2, 123–140. doi: 10.1038/nrmicro818

Lambertini, E., Karns, J. S., Kessel, J., Cao, H., and Pradhan, A. K. (2015). Dynamics of *Escherichia coli* virulence factors in dairy herds and farm environments in a longitudinal study in the United States. *Appl. Environ. Microbiol.* 81, 4477–4488. doi: 10.1128/AEM.00465-15

Lan, X. Y., Zhao, S. G., Zheng, N., Li, S. L., Zhang, Y. D., Liu, H. M., et al. (2017). Short communication: microbiological quality of raw milk of raw cow milk and its association with herd management practices in Northern China. *J. Dairy Sci.* 100, 4294–4299. doi: 10.3168/jds.2016-11631

Lippolis, J. D., Holman, D. B., Brunelle, B. W., Thacker, T. C., Bearson, B. L., and Reinhardt, T. A. (2017). Genomic and transcriptomic analysis of *Escherichia coli* strains associated with persistent and transient bovine mastitis and the role of colanic acid. *Infect. Immun.* 86:e00566-17. doi: 10.1128/IAI.00566-17

Liu, H. M., Li, S. L., Meng, L., Dong, L., Zhao, S. G., Lan, X. Y., et al. (2017). Prevalence, antimicrobial susceptibility, and molecular characterization of *Staphylococcus aureus* isolated from dairy herds in northern China. *J. Dairy Sci.* 100, 8796–8803. doi: 10.3168/jds.2017-13370

Liu, J., Zhu, Y., Jay-Russell, M., Lemay, D. G., and Mills, D. A. (2020). Reservoirs of antimicrobial resistance genes in retail raw milk. *Microbiome* 8:99. doi: 10.1186/s40168-020-00861-6

McConnel, C. S., Stenkamp-Strahm, C. M., Rao, S., Linke, L. M., Magnuson, R. J., and Hyatt, D. R. (2016). Antimicrobial resistance profiles in *Escherichia coli* O157 isolated from Northern Colorado dairies. *J. Food Prot.* 79, 484–487. doi: 10.4315/0362-028X.JFP-15-321

Medeiros, P., Bolick, D., Roche, J. K., Noronha, F., Pinheiro, C., Kolling, G., et al. (2013). The micronutrient zinc inhibits EAEC strain 042 adherence, biofilm formation, virulence gene expression, and epithelial cytokine responses benefiting the infected host. *Virulence* 4, 624–633. doi: 10.4161/viru.26120

Nam, H. M., Lim, S. K., Kang, H. M., Kim, J. M., Moon, J. S., and Jang, K. C. (2009). Prevalence and antimicrobial susceptibility of gram-negative bacteria isolated from bovine mastitis between 2003 and 2008 in Korea. *J. Dairy Sci.* 92, 2020–2026. doi: 10.3168/jds.2008-1739

Navajas-Benito, E. V., Alonso, C. A., Sanz, S., Olarte, C., Martínez-Olarte, R., and Hidalgo-Sanz, S. (2016). Molecular characterization of antibiotic resistance in *Escherichia coli* strains from a dairy cattle farm and its surroundings. *J. Sci. Food Agric.* 97, 363–365. doi: 10.1002/jsfa.7709

Ntuli, V., Njage, P. M. K., and Buys, E. M. (2016). Characterization of *Escherichia coli* and other *Enterobacteriaceae* in producer-distributor bulk milk. *J. Dairy Sci.* 99, 9534–9549. doi: 10.3168/jds.2016-11403

Ohnishi, M., Okatani, A. T., Harada, K., Sawada, T., and Takahashi, T. (2013). Genetic characteristics of CTX-M-type extended-spectrum-β-lactamase (ESBL)-producing *Enterobacteriaceae* involved in mastitis cases on Japanese dairy farms, 2007 to 2011. *J. Clin. Microbiol.* 51, 3117–3122. doi: 10.1128/JCM.00920-13

Ombarak, R. A., Hinenoya, A., Awasthi, S. P., Iguchi, A., Shima, A., Elbagory, A. R. M., et al. (2016). Prevalence and pathogenic potential of *Escherichia coli* isolates from raw milk and raw milk cheese in Egypt. *Int. J. Food. Microbial.* 221, 69–76. doi: 10.1016/j.ijfoodmicro.2016.01.009

Pradel, N., Bertin, Y., Martin, C., and Livrelli, V. (2008). Molecular analysis of Shiga toxin-producing *Escherichia coli* strains isolated from hemolytic-uremic syndrome patients and dairy samples in France. *Appl. Environ. Microbiol.* 74, 2118–2128. doi: 10.1128/AEM.02688-07

Ribeiro, L. F., Barbosa, M. M. C., Pinto, F. R., Maluta, R. P., Oliveira, M. C., de Souza, V., et al. (2016). Antimicrobial resistance and virulence factors of *Escherichia coli* in cheese made from unpasteurized milk in three cities in Brazil. *Foodborne Pathog. Dis.* 13, 469–476. doi: 10.1089/fpd.2015.2106

Radostits, O. M., Gay, C. C., and Hinchcliff, K. W. (2007). Veterinary Medicine—A textbook of the diseases of cattle, horses, sheep, pigs, and goats. 10.ed. Philadelphia: Saunders. 673–762.

Ruegg, P. L., Oliveira, L., Jin, W., and Okwumabua, O. (2014). Phenotypic antimicrobial susceptibility and occurrence of selected resistance genes in gram-positive mastitis pathogens isolated from Wisconsin dairy cows. *J. Dairy Sci.* 98, 4521–4534. doi: 10.3168/jds.2014-9137

Rugeles, L. C., Bai, J., Martinez, A. J., Vanegas, M. C., and Gomez-Duarte, O. G. (2010). Molecular characterization of diarrheagenic *Escherichia coli* strains from stools samples and food products in Colombia. *Int. J. Food Microbiol.* 138, 282–286. doi: 10.1016/j.ijfoodmicro.2010.01.034

Santman-Berends, I., Gonggrijp, M. A., Hage, J. J., Heuvelink, A. E., Velthuis, A., and Lam, T. (2016). Prevalence and risk factors for extended-spectrum beta-lactamase or AMPC-producing *Escherichia coli* in organic dairy herds in the Netherlands. *J. Dairy Sci.* 562, 120–128. doi: 10.3168/jds.2016-11839

Sharma, S., Aarif, K., Dahiya, D. K., Jain, J., and Sharma, V. (2015). Prevalence, identification and drug resistance pattern of *Staphylococcus aureus* and *Escherichia coli* isolated from raw milk samples of Jaipur city of Rajasthan. *J. Pure Appl. Microbiol.* 9, 341–348.

Su, Y. C., Yu, C. Y., Tsai, Y. L., Wang, S. H., Lee, C. h., and Chu, C. (2016). Fluoroquinolone-resistant and extended-spectrum β-lactamase-producing *Escherichia coli* from the milk of cows with clinical mastitis in Southern Taiwan. *J. Microbiol. Immunol. Infect.* 49, 892–901. doi: 10.1016/j.jmii.2014.10.003

Suojala, L., Pohjanvirta, T., Simojoki, H., Myllyniemi, A. L., Pitkala, A., Pelkonen, S., et al. (2011). Phylogeny, virulence factors and antimicrobial susceptibility of *Escherichia coli* isolated in clinical bovine mastitis. *Vet. Microbiol.* 147, 383–388. doi: 10.1016/j.vetmic.2010.07.011

Tabaran, A., Mihaiu, M., Tabaran, F., Colobatiu, L., Reget, O., Borzan, M. M., et al. (2017). First study on characterization of virulence and antibiotic resistance genes in verotoxigenic and enterotoxigenic *E. coli* isolated from raw milk and unpasteurized traditional cheeses in Romania. *Folia Microbiol.* 62, 145–150. doi: 10.1007/s12223-016-0481-8

Tark, D. S., Moon, D. C., Kang, H. Y., Kim, S. R., Nam, H. M., Lee, H. S., et al. (2016). Antimicrobial susceptibility and characterization of extended-spectrum β-lactamases in *Escherichia coli* isolated from bovine mastitic milk in South Korea from 2012 to 2015. *J. Dairy Sci.* 100, 3463–3469. doi: 10.3168/jds.2016-12276

Timofte, D., Maciuca, I. E., Evans, N. J., Williams, H., Wattret, A., and Fick, J. C. (2014). Detection and molecular characterization of *Escherichia coli* CTX-M-15 and *Klebsiella pneumoniae* SHV-12 β-lactamases from bovine mastitis isolates in the United Kingdom. *Antimicrob. Agents Chemother.* 58, 789–794. doi: 10.1128/AAC.00752-13

Trevisani, M., Mancusi, R., Donne, G. D., Bacci, C., Bassi, L., and Bonardi, S. (2014). Detection of Shiga toxin (*Stx*)-producing *Escherichia coli* (STEC) in bovine dairy herds in northern Italy. *Int. J. Food Microbiol.* 184, 45–49. doi: 10.1016/j.ijfoodmicro.2013.12.033

Van Kessel, J. A. S., Karns, J. S., Lombard, J. E., and Kopral, A. C. A. (2011). Prevalence of *Salmonella enterica*, listeria monocytogenes, and *Escherichia coli* virulence factors in bulk tank milk and in-line filters from US dairies. *J. Food Prot.* 74, 759–768. doi: 10.4315/0362-028X.JFP-10-423

Wang, D., Zhang, L. M., Zhou, X. Z., He, Y. L., Yong, C. H., Shen, M. L., et al. (2016). Antimicrobial susceptibility, virulence genes, and randomly amplified polymorphic DNA analysis of *Staphylococcus aureus* recovered from bovine mastitis in Ningxia, China. *J. Dairy Sci.* 99, 9560–9569. doi: 10.3168/jds.2016-11625

Zhang, S. H., Wu, Q. P., Zhang, J. M., Lai, Z. P., and Zhu, X. M. (2016). Prevalence, genetic diversity, and antibiotic resistance of enterotoxigenic Escherichia coli in retail ready to eat foods in China. *China. Food Control.* 68, 236–243. doi: 10.1016/j.foodcont.2016.03.051

Zhao, S. G., Tyson, H., Chen, Y., Li, C., Mukherjee, S., Young, S., et al. (2015). Whole genome sequencing analysis accurately predicts antimicrobial resistance phenotypes in *Campylobacter* spp. *Appl. Environ. Microbiol.* 82, 459–466. doi: 10.1128/AEM.02873-15

Conflict of Interest: The authors declare that the research was conducted in the absence of any commercial or financial relationships that could be construed as a potential conflict of interest.

frontiers in Microbiology

ORIGINAL RESEARCH
published: 01 October 2021
doi: 10.3389/fmicb.2021.746632

The Possible Transmission and Potential Enterotoxicity of *Bacillus cereus* on Lettuce Farms in Five Chinese Provinces

Yang Qu[1,2], Chao Wei[3], Xiaohang Dai[3], Yalong Bai[1], Xin Zhao[4], Qingkuo Lan[4], Wenbo Wang[5], Yuanjuan Wu[5], Min Gao[6], Weihao Tang[6], Changyan Zhou[1,2] and Yujuan Suo[1,2]**

[1] Laboratory of Quality and Safety Risk Assessment for Agro-Products of Ministry of Agriculture and Rural Affairs, Institute for Agro-Food Standards and Testing Technology, Shanghai Academy of Agricultural Sciences, Shanghai, China, [2] Shanghai Co-Elite Agro-Food Testing Service Co., Ltd., Shanghai, China, [3] Laboratory of Quality and Safety Risk Assessment for Agro-Products of Ministry of Agriculture and Rural Affairs, Institute of Quality Standard and Testing Technology for Agro-Products of Sichuan Academy of Agricultural Sciences, Chengdu, China, [4] Institute of Germplasm Resources and Biotechnology, Tianjin Academy of Agricultural Sciences, Tianjin, China, [5] Laboratory of Quality and Safety Risk Assessment for Agro-Products of Ministry of Agriculture and Rural Affairs, Institute of Agricultural Standards and Testing Technology for Agri-Products, Shandong Academy of Agricultural Sciences, Jinan, China, [6] Laboratory of Quality and Safety Risk Assessment for Agro-Products Processing of Ministry of Agriculture and Rural Affairs, Institute of Food Science and Technology, Chinese Academy of Agricultural Sciences (CAAS), Beijing, China

OPEN ACCESS

Edited by:
Jun Wang,
Qingdao Agricultural University, China

Reviewed by:
Moutong Chen,
Guangdong Institute of Microbiology, Guangdong Academy of Sciences, China
Dapeng Wang,
Shanghai Jiao Tong University, China
Chao Qing Xie,
Shanghai Ocean University, China

***Correspondence:**
Changyan Zhou
zhouchangyan@saas.sh.cn
Yujuan Suo
suoyujuan@saas.sh.cn

Specialty section:
This article was submitted to Food Microbiology, a section of the journal Frontiers in Microbiology

Received: 24 July 2021
Accepted: 13 September 2021
Published: 01 October 2021

Citation:
Qu Y, Wei C, Dai X, Bai Y, Zhao X, Lan Q, Wang W, Wu Y, Gao M, Tang W, Zhou C and Suo Y (2021) The Possible Transmission and Potential Enterotoxicity of Bacillus cereus on Lettuce Farms in Five Chinese Provinces. Front. Microbiol. 12:746632. doi: 10.3389/fmicb.2021.746632

Bacillus cereus is a well-characterized human pathogen that produces toxins associated with diarrheal and emetic foodborne diseases. To investigate the possible transmission of *B. cereus* on lettuce farms in China and determine its enterotoxicity, (I) a total of 524 samples (lettuce: 332, soil: 69, water: 57, manure: 57, pesticide: 9) were collected from 46 lettuce farms in five Chinese provinces, (II) multilocus sequence typing (MLST) was used to classify *B. cereus* isolates and for trace analysis, and (III) the presence of toxin genes and enterotoxins (Hbl and Nhe) was detected in 68 strains. The results showed that one hundred and sixty-one lettuce samples (48.5%) tested positive for *B. cereus* at levels ranging from 10 to 5.3×10^4 CFU/g. Among the environmental sample categories surveyed, the highest positive rate was that of the pesticide samples at 55.6%, followed by soil samples at 52.2% and manure samples at 12.3%. Moreover, one hundred isolates of *B. cereus* yielded 68 different sequence types (STs) and were classified into five phylogenetic clades. Furthermore, Nhe toxin genes (*nheA*, *nheB*, *nheC*) were broadly distributed and identified in all 68 strains (100%), while Hbl toxin genes (*hblA*, *hblC*, *hblD*) were present in 61 strains (89.7%), *entFM* was detected in 62 strains (91.2%), and *cytK* was found in 29 strains (42.6%). All strains were negative for *ces*. As for the enterotoxin, Nhe was observed in all 68 isolates carrying *nheB,* while Hbl was present in 76.5% (52/68) of the strains harboring *hblC.* This study is the first report of possible *B. cereus* transmission and of its potential enterotoxicity on lettuce farms in

China. The results showed that soil and pesticides are the main sources of *B. cereus* on lettuce farms in China, and the possible transmission routes are as follows: soil-lettuce, manure-lettuce, pesticide-lettuce, manure-soil-lettuce, and water-manure-soil-lettuce. Furthermore, the *B. cereus* isolates, whether from lettuce or the environment, pose a potential risk to health.

Keywords: *Bacillus cereus*, lettuce farm, multilocus sequence typing (MLST), tracing analysis, enterotoxicity

INTRODUCTION

The World Health Organization recommends a daily intake of 400 g of fresh vegetables for improved health (Park et al., 2018). Lettuce is the most widely consumed fresh vegetable and is usually eaten raw with no or minimal processing, increasing the occurrence of lettuce-related foodborne outbreaks, which have gained attention among government agencies, industries, and the public (Bozkurt et al., 2021). Raw lettuce has been reported to harbor foodborne pathogens, such as *Bacillus cereus*, *Escherichia coli* O157:H7, *Salmonella*, and *Listeria monocytogenes* (Abadias et al., 2008; Park et al., 2018; Yu et al., 2019). A total of 597 outbreaks caused by *B. cereus* toxins involving 6,221 cases were reported in European Member States (MSs) from 2014 to 2016 due to the diarrhea and emesis (vomiting) caused by *B. cereus* (Osimani et al., 2018). Thus, the safety of *B. cereus* strains in lettuce should be considered.

Bacillus cereus is a spore-forming gram-positive species (Ceuppens et al., 2013) that is distributed among seven phylogenetic clades with nine species (Guinebretière et al., 2008), including (I) *B. cereus sensu stricto* and *B. cytotoxicus*, which cause foodborne illness (Dierick et al., 2005; Guinebretière et al., 2008); (II) *B. weihenstephanensis* and *B. mycoides*, which cause food spoilage (Meer et al., 1991); (III) *B. anthracis*, which causes anthrax in both humans and animals (Ivanova et al., 2003); (IV) *B. thuringiensis*, which is used as an insecticide in agriculture (Höfte and Whiteley, 1989); (V) *B. pseudomycoides,* which is considered a non-pathogenic environmental microorganism; (VI) *B. toyonensis*, which has recently been recognized as a putative probiotic species (Jiménez et al., 2013); and (VII) *B. wiedmannii*, which is a psychrotolerant cytotoxic species (Miller et al., 2016). Therefore, it is difficult to identify *B. cereus* isolates, and multilocus sequence typing (MLST) is recommended in combination with traditional methods to differentiate diverse species of *B. cereus* (Jung et al., 2011; Maiden et al., 2013; Otlewska et al., 2013; Castiaux et al., 2014; Zhuang et al., 2019).

Farm-to-fork supply chains are considered to be the source of *B. cereus* in lettuce, including field production, harvest, processing, packaging, transportation, retail, and home storage (Pang et al., 2017), and farm environments are the core source (Drewnowska et al., 2020). Moreover, MLST is a powerful method for tracing analysis based on genetic evolution, which can be determined by comparative analysis of alleles (Forsythe et al., 2014; Hammerum et al., 2015). Processing environments and packing areas have been found to be the sources most likely to be associated with *B. cereus* contamination in powdered infant formula production (Zhuang et al., 2019). The transmission of *B. cereus* in lettuce farms must be detected and monitored to promote food safety and human health.

In this study, the prevalence of *B. cereus* in lettuce and farm environments distributed in China was described. Genetic methods were applied to examine the phylogenetically diverse *B. cereus* isolates from lettuce and farm environments, and their associations were examined to identify the possible transmission of *B. cereus* in lettuce farms. In addition, the safety of *B. cereus* isolates was investigated by identifying virulence factors and enterotoxins from lettuce and in farm environments.

MATERIALS AND METHODS

Sample Collection and Isolation

A total of 524 samples were collected from 46 lettuce farms in five Chinese provinces from April 2019 to November 2020 (**Figure 1**). These samples were classified as lettuce (*Lactuca sativa L.*) ($n = 332$), soil ($n = 69$), water ($n = 57$), manure ($n = 57$), and pesticide ($n = 9$) samples; more details about the samples can be found in **Table 1**. The samples were transported to the laboratory in a cold box (4°C) within 2 h.

The *B. cereus* strains were isolated in accordance with GB4789.14-2014, the National Food Safety Standard for Food Microbiological Examination used in China. Genomic DNA was extracted from overnight cultures of *B. cereus* isolates in Luria-Bertani (LB) broth using a TIANamp Bacteria DNA Extraction Kit (Tiangen Biotech, Beijing, China) according to the manufacturer's protocol for gram-positive bacteria.

Phylogenetic Study

Isolates were characterized by using seven housekeeping genes (*glp*, *gmk*, *ilvD*, *pta*, *pur, pycA*, and *tpi*) with different primers and conditions (**Table 2**), which are provided in the *B. cereus* PubMLST database[1]. The PCR products were sequenced by Sangon Biotech (Shanghai, China) and submitted to the *B. cereus* PubMLST database to obtain the allele number. By combination of allele numbers for all seven housekeeping genes, a sequence type (ST) clonal complex could be obtained. New allele sequences and STs were submitted to the *B. cereus* PubMLST database and assigned by the MLST website administrator.

The phylogenetic study included all the isolates and nine references obtained from the NCBI database[2] (*B. anthracis* Ames Ancestor, *B. cereus* ATCC 1457, *B. cytotoxicus* NVH

[1]https://pubmlst.org/bcereus/

[2]https://www.ncbi.nlm.nih.gov/

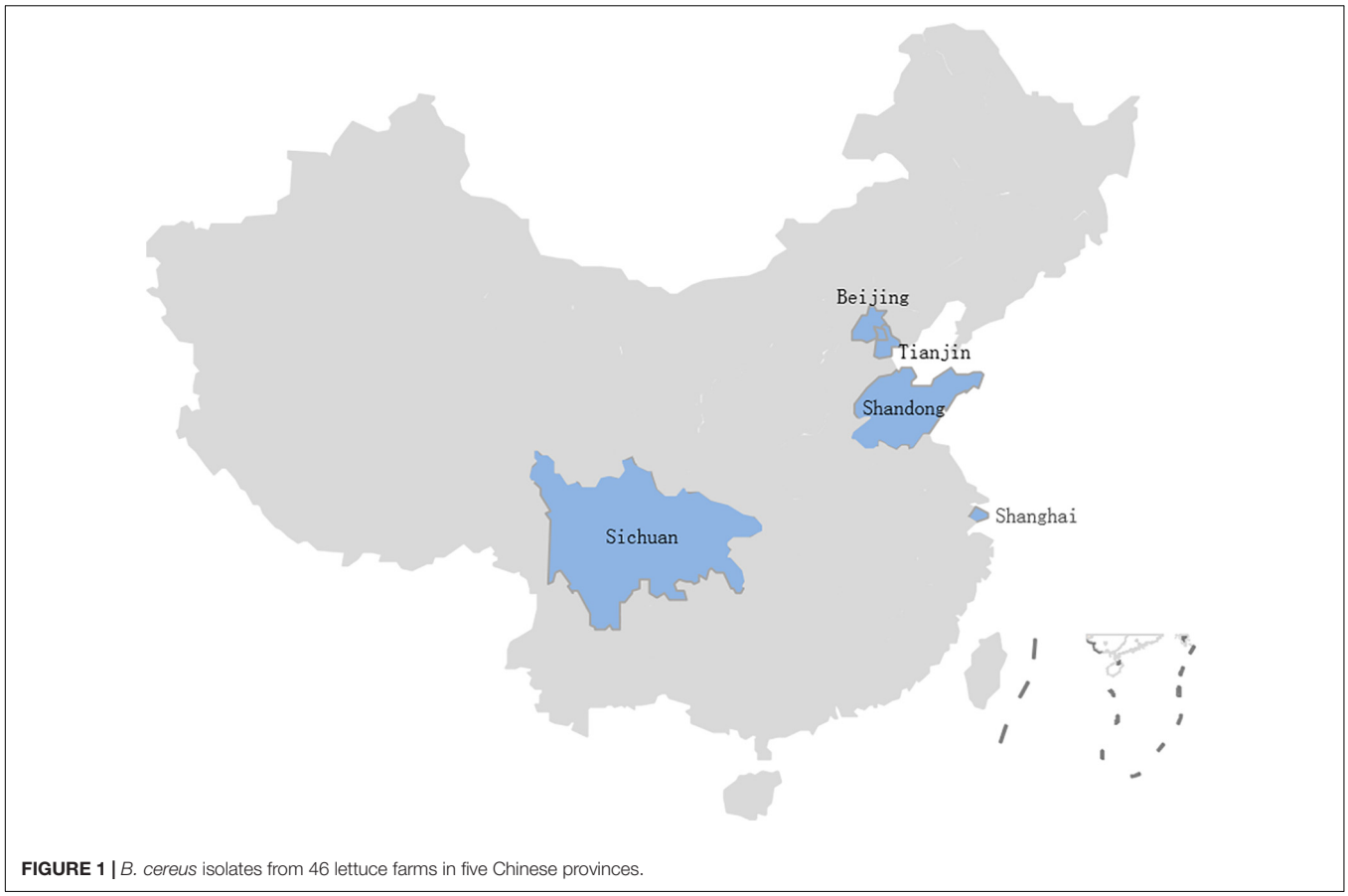

FIGURE 1 | *B. cereus* isolates from 46 lettuce farms in five Chinese provinces.

391-98, *B. mycoides* DSM 2048, *B. pseudomycoides* DSM 12442, *B. thuringiensis* ATCC 10792, *B. toyonensis* BCT-7112, *B. weihenstephanensis* WSBC 10204, *B. wiedmannii* FSL W8-1069) (Miller et al., 2018). The phylogenetic tree was constructed using the neighbor-joining (NJ) method in Molecular Evolutionary Genetic Analysis (MEGA-X) based on the concatenated sequences (2,829 bp) of the seven housekeeping genes (Kumar et al., 2018). In addition, 1,000 bootstrap replicates were used for branch quality.

Tracing Analysis

To analyze the relationship between different STs and sample sources, a minimum spanning tree was constructed with PHYLOViZ 2.0 software (Instituto de Microbiologia, Portugal) (Francisco et al., 2012) with the goeBURST algorithm and 1,000 bootstrap resamplings (Feil et al., 2004).

Detection of Virulence Genes

Nine virulence genes, namely, *hblA*, *hblC*, *hblD*, *nheA*, *nheB*, *nheC*, *entFM*, *cytK*, and *ces*, were identified according to a previous study (Stenfors and Granum, 2001; Guinebretière et al., 2002; Ehling-Schulz et al., 2005; Kim et al., 2011), and the primers and conditions are listed in **Table 2**. The 20 μL PCR mixture consisted of 10 μL of Taq^{TM} PCR Premix (Takara, China), 1 μL of diluted DNA, and 0.2 mM each primer.

Detection of the Enterotoxins

A Duopath® Cereus Enterotoxins kit (Merck, Kenilworth, NJ, United States) was used to detect Hbl (the lytic component L2, a subunit of toxin Hbl) and NheB (the binding component of the Nhe toxin), the detection limits for which were 20.0 and 6.0 ng/mL, respectively. Isolates were maintained on brain heart infusion (BHI; Co. CM1135, Oxoid, Hampshire, United Kingdom) agar plates at 4°C. Single colonies of bacteria were aseptically picked and cultured in 1 mL of CGY broth (with 1% glucose) and incubated for 4 h at 37°C. For testing, the cultures and Duopath® kit were both cooled to room temperature (20°C), and 150 μL of culture was pipetted into the circular sample port on the Duopath® kit. The results could be observed 30 min after applying the culture to the kit at room temperature (Krause et al., 2010).

RESULTS

Prevalence Analysis of *B. cereus* in Lettuce and Farm Environments

In this study, *B. cereus* was detected in 210 of the 524 (40.0%) samples from 46 lettuce farms (**Table 1**) distributed in five Chinese provinces (**Figure 1**). The positivity rates of

TABLE 1 | Prevalence and contamination level of *B. cereus* in different samples among 46 lettuce farms.

Sample types	Contamination rate[a]	Contamination level (CFU/g)			
		< 10	$10 \leq$ value $< 10^2$	$10^2 \leq$ value $< 10^4$	$10^4 \leq$ value $< 10^5$
Lettuce	48.5% (161/332)	51.5% (171/332)	22.0% (73/332)	25.9% (86/332)	0.6%(2/332)
Soil	52.2% (36/69)	47.8% (33/69)	10.1% (7/69)	34.8% (24/69)	7.3% (5/69)
Water	1.8% (1/57)	98.3% (56/57)	1.8% (1/57)	0.0% (0/57)	0.0% (0/57)
Manure	12.3% (7/57)	87.7% (50/57)	5.3% (3/57)	7.0% (4/57)	0.0% (0/57)
Pesticide	55.6% (5/9)	44.5% (4/9)	33.3% (3/9)	22.2% (2/9)	0.0% (0/57)
Total	40.0% (210/524)	60.0% (314/524)	16.6% (87/524)	22.1% (116/524)	1.3% (7/524)

[a]*Contamination rate = number of positive samples/total samples.*

TABLE 2 | Primers used in the study.

Primer	Sequence (50–30)	Target fragment length (bp)	Annealing temperature (°C)	References
glpF-F	GCG TTT GTG CTG GTG TAA GT	549	59	https://pubmlst.org/bcereus/
glpF-R	CTG CAA TCG GAA GGA AGA AG			
gmk-F	ATT TAA GTG AGG AAG GGT AGG	600	56	
gmk-R	GCA ATG TTC ACC AAC CAC AA			
ilvD-F	CGG GGC AAA CAT TAA GAG AA	556	58	
ilvD-R	GGT TCT GGT CGT TTC CAT TC			
pta-F	GCA GAG CGT TTA GCA AAA GAA	576	56	
pta-R	TGC AAT GCG AGT TGC TTC TA			
pur-F	CTG CTG CGA AAA ATC ACA AA	536	56	
pur-R	CTC ACG ATT CGC TGC AAT AA			
pycA-F	GCG TTA GGT GGA AAC GAA AG	550	57	
pycA-R	CGC GTC CAA GTT TAT GGA AT			
tpi-F	GCC CAG TAG CAC TTA GCG AC	553	58	
tpi-R	CCG AAA CCG TCA AGA ATG AT			
hblA-F	AAGCAATGGAATACAATGGG	1,154	56	Guinebretière et al., 2002
hblA-R	ACGAATGTAATTTGAGTCGC			
hblC-F	GATACTCAATGTGGCAACTGC	740	58	
hblC-R	TTGAGACTGCTCGTCTAGTTG			
hblD-F	AATCAAGAGCTGTCACGAAT	411	58	
hblD-R	CACCAATTGACCATGCTAAT			
nheA-F	GTTAGGATCACAATCACCGC	755	56	
nheA-R	ACGAATGTAATTTGAGTCGC			
nheB -F	CTATCAGCACTTATGGCAG	754	54	
nheB -R	ACTCCTAGCGGTGTTCC			
nheC -F	CGGTAGTGATTGCTGGG	564	58	
nheC-R	CAGCATTCGTACTTGCCAA			
entFM-F	AAAGAAATTAATGGACAAACTCAAACTCA	596	58	Guinebretière et al., 2002
entFM-R	GTATGTAGCTGGGCCTGTACGT			
cytK-F	GTAACTTTCATTGATGATCC	505	48	Stenfors and Granum, 2001
cytK-R	GAATACTAAATAATTGGTTTCC			
ces-F	GGTGACACATTATCATATAAGGTG	1,271	58	Ehling-Schulz et al., 2005
ces-R	GTAAGCGAACCTGTCTGTAACAACA			

B. cereus were 48.5% (161/332) for lettuce, ranging from 10 to 5.3×10^4 lg CFU/g, and the farm environment also contained *B. cereus*. Of these environmentally positive samples, the highest frequency of *B. cereus* was found in pesticides (55.6%), followed by soil (52.2%), manure (12.3%), and water (1.8%). Enumeration of *B. cereus* showed that 60.0% of the lettuce farm samples had counts below 10 CFU/g, 16.6% had counts in the range from 10–10^2 CFU/g, 22.1% had counts in the range from 10^2–10^4 CFU/g, and 1.3% had counts above 10^4 CFU/g. High counts ($>10^4$ CFU/g) were most frequently found in soil and lettuce.

Genetic Structure of *B. cereus* Populations

Considering the effect of source, location and sampling time, strains collected from the same lettuce or soil on the same farm during different sampling seasons were removed, and only 100 isolates that from lettuce, soil, pesticides, manure and water were selected for genetic structure analysis. A total of 65 different STs and seven clonal complexes (CCs) were identified among the isolates (**Figure 2**). Thirty-seven isolates were assigned to 31 new STs. Forty-seven of the 65 (72.3%) STs included only one isolate; however, the remaining 18 STs included more than one isolate. The most frequent ST was ST1000, comprising five isolates from lettuce and soil samples, which were found in Shanghai, Beijing, and Tianjin provinces.

The phylogenetic study was based on MLST, which clustered the STs into five phylogenetic clades (II to VI) (Guinebretière et al., 2008), and nine additional *B. cereus* clade species were included in phylogenetic analyses to serve as a reference (Miller et al., 2018). The most common clade was clade IV (50.8%), followed by clade III (20.0%), clade V (18.5%), clade II (6.2%), and clade VI (4.6%). Clade IV included both *B. cereus sensu stricto* ATCC 14579^T (ST4) and *B. thuringiensis* ATCC 10792^T as well as 33 STs obtained from five provinces that consisted of five CCs: CC8, CC18, CC56, CC229, and CC142. Frequent types of ST1000 and CC142 (11 STs) were observed in this clade. Clade III with 13 STs, in addition to the *B. anthracis* Ames ancestor, was represented by Shanghai (69.2%), Beijing (23.1%), and Tianjin (7.7%). Only CC205 (1 ST) was included in this clade. Clade V, with the *B. toyonensis* BCT-7112^T reference strain (ST111), contained 12 STs in five provinces and strains mainly from Shanghai (56.2%) and Beijing (25.0%), while other geographic locations were represented by less than 7.0% of isolates. ST1724, ST233, ST223, and ST281 were found in two different provinces, and isolates in clade V were clustered together in CC111 (7 STs). Clade II included the *B. wiedmannii* FSL W8-0169^T (ST1081) reference strain and four STs from Shanghai, Beijing, and Tianjin, while ST378 was found in both Shanghai and Tianjin. Clade VI contained both the *B. mycoides* DSM 2048^T and *B. weihenstephanensis* WSBC 10204^T reference strains as well as three STs in the Shanghai and Sichuan provinces. The isolates in clades II and VI were singletons. None of the *B. cereus* isolate strains were clustered with *B. pseudomycoides* DSM 12442^T within clade I or with *B. cytotoxicus* NVH 391-98^T within clade VII.

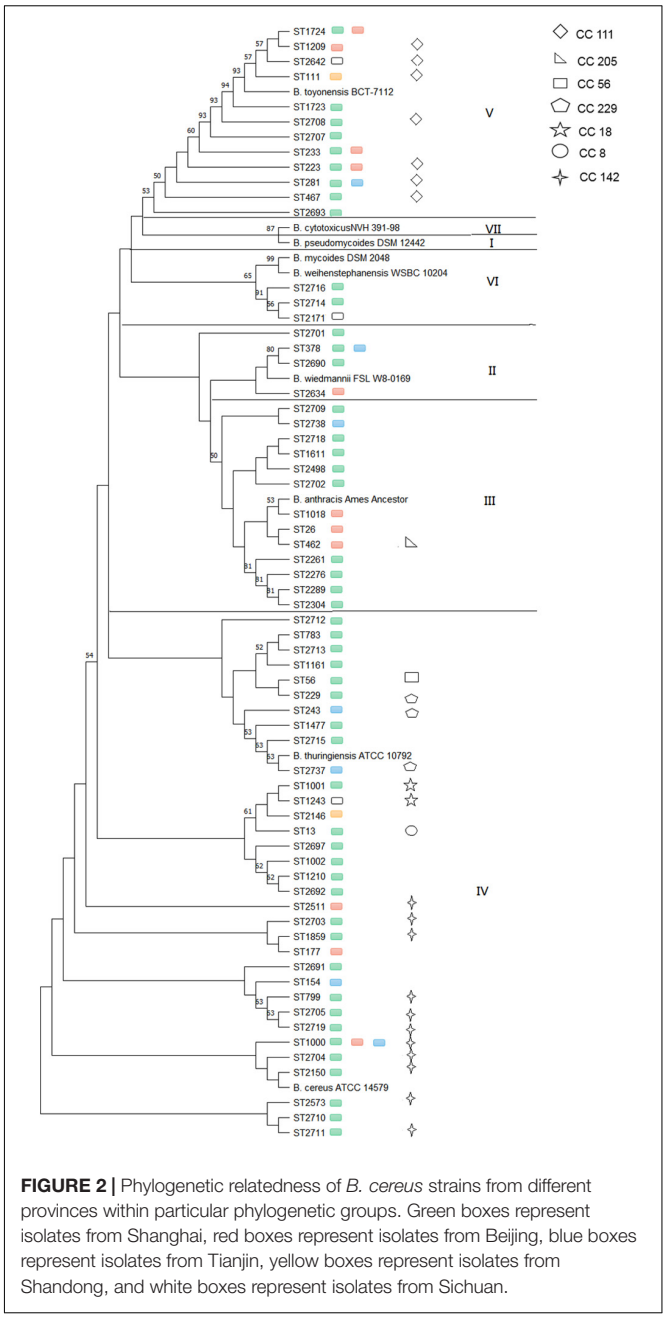

FIGURE 2 | Phylogenetic relatedness of *B. cereus* strains from different provinces within particular phylogenetic groups. Green boxes represent isolates from Shanghai, red boxes represent isolates from Beijing, blue boxes represent isolates from Tianjin, yellow boxes represent isolates from Shandong, and white boxes represent isolates from Sichuan.

Tracing Analysis

Among the 100 *B. cereus* isolates, 53 were collected from lettuce, 19 from soil, 14 from pesticide, 13 from manure, and 1 from water. A minimum spanning tree-like structure was drawn to show the link between the sample sources and different STs of *B. cereus* (**Figure 3**). The ST type in lettuce was associated with the environmental source, and there was no crossover between environmental samples. Isolates from lettuce and soil had seven identical STs, while manure had five STs, identical to lettuce. Pesticide and water also had one ST, consistent with lettuce. Five STs were associated with lettuce and soil, namely, ST223, ST229, ST378, ST799, and ST1000, while three STs (ST233, ST1724, and ST2692) were commonly recovered from lettuce and manure. Only ST2150 originated from lettuce and pesticide. Moreover, there were other STs from additional source categories: one major ST2498 was a prevalent ST type in lettuce, soil and manure. In addition, ST1210 was found in lettuce, soil, manure, and water.

Enterotoxic Potential of *B. cereus*

Sixty-eight strains were selected from lettuce farms, corresponding to sources and phylogenetic groups, for further enterotoxic potential (**Figure 4**). All isolates were tested *via* PCR for the presence of key toxin genes. (1) The most frequently

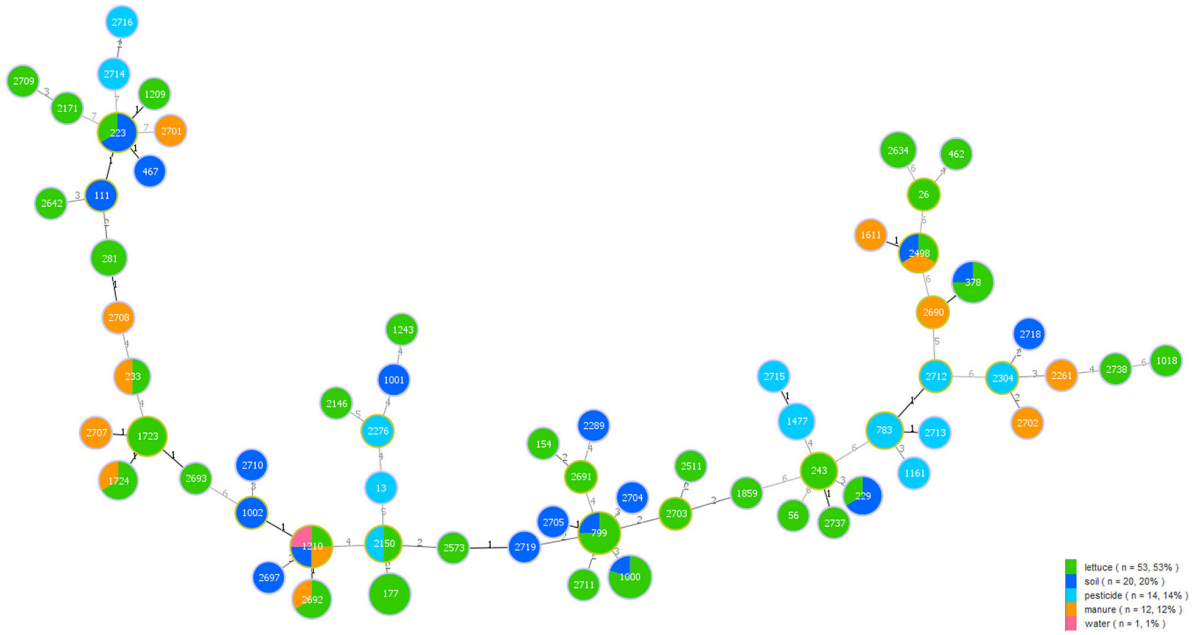

FIGURE 3 | Minimum spanning tree analysis of 100 *B. cereus* isolates collected from different sample categories on lettuce farms. The size of each circle indicates the number of STs. Different sample categories are represented by different colors, and the size of each color block represents the number of STs in that source.

distributed genes were those encoding the enterotoxin Nhe, namely, the *nheB*, *nheA* and *nheC* genes, which were detected in 100.0, 91.2, and 80.9% of the tested strains, respectively. While these *nheABC* genes (the strains were positive for *nheA*, *nheB*, and *nheC* at the same time) genes were all detected in 54 isolates in clades III and IV, *nheA* and *nheC* were detected less frequently in clades II, VI, and VI (23.1%∼80.0%). Isolates from lettuce, soil, water, manure, and pesticides all harbored the Nhe toxin genes (**Figures 3**, **4**). (2) Genes encoding Hbl (*hblA*, *hblC*, and *hblD*) were detected in 89.7% of the tested strains, and sixty-one Hbl PCR-positive isolates were distributed in clade II (100.0%), clade V (100.0%), clade IV (100.0%), clade IV (97.4%), and clade III (33.3%). *hblD* was the most commonly detected Hbl toxin genes (89.7%), while *hblA* and *hblC* were detected individually in 76.5 and 73.5% of the isolates, respectively. Fifty strains harbored *hblACD* (the strains were positive for *hblA*, *hblC*, and *hblD* at the same time). Among the sources, 100.0% of the water and pesticides isolates (1/1 water isolate), 92.0% of the lettuce isolates, 88.9% of the soil isolates, and 75.0% of the manure isolates harbored the Hbl toxin genes. (3) The *entFM* gene, encoding enterotoxin FM, was also broadly distributed (91.2%). All six PCR-negative isolates were present in clade IV and clade V. In addition, the *entFM* gene was detected in 100% of the isolates from all sources except lettuce and pesticides. Thus, the positive detection rate was still high in lettuce and pesticides, with values of 80.0 and 91.7%, respectively. (4) The *cytK* gene, encoding cytotoxin K, was detected in 42.6% of the strains. All PCR isolates positive for *cytK* represented clades III (88.9%), IV (51.3%), and II (20.0%). The strains harboring the *cytK* gene were isolated from all five sources. The highest percentage of *cytK* detected was 100.0%, which was observed in water (1/1 isolate), followed by 58.3% in pesticides, 50.0% in soil, 36.0% in lettuce, and 25.0% in manure. (5) The *ces* gene, encoding emetic toxin, known as cerulide synthetase, was not detected in the isolates.

All *B. cereus* isolates used in this study carried at least 3 of the 8 enterotoxin genes tested. The distribution of virulence genes was divided into 17 different profiles. Eighteen isolates possessed all eight virulence genes, which was one of the main gene profiles. The other main gene profile (18/68 of all isolates) was *hblA-hblC-hblD-nheA-nheB-nheC-entFM*. Only one isolate, SH-106 (ST2701), harbored the smallest virulence gene profile (*nheB-hblD-entFM*).

Nhe and Hbl, the most notable enterotoxins, were analyzed to obtain a broader view of the potential *B. cereus* enterotoxicity (**Figure 4**). Nhe was observed in the 68 isolates isolated from five sources and all phylogenetic groups, while Hbl was present in 76.5% (52/68) of the strains that were clustered into groups, with the exception of clade VI. The percentages of strains harboring Hbl were 100.0% in clade V, 84.6% in clade IV, 80.0% in clade II, and 22.2% in clade III. Among the sources, 100.0% of the water isolates (1/1), 92.0% of the lettuce isolates, 88.9% of the soil isolates, 66.7% of the manure isolates, and 33.3% of the pesticide isolates harbored Hbl. **Figure 4** also reveals the relationship between virulence genes and enterotoxins: (1) Nhe was expressed when the *nheB* gene was present, and (2) Hbl was detected when the strain harbored the *hblC* gene.

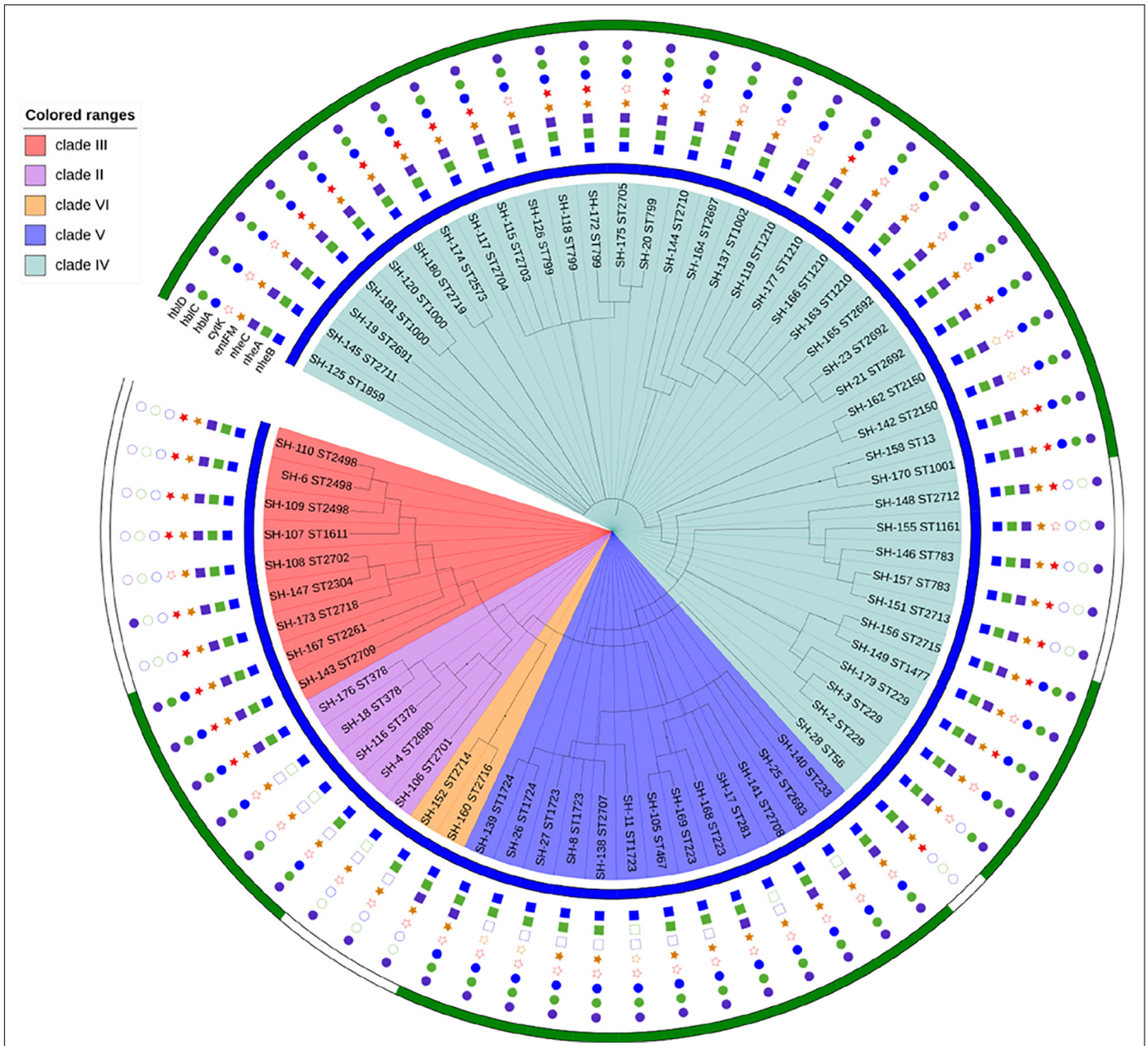

FIGURE 4 | Enterotoxic potential of 68 *B. cereus* strains. The blue color strip represents Nhe (enterotoxin), while green represents Hbl (enterotoxin). The blue square represents *NheB* (gene), the green square represents *nheA* (gene), the purple square represents *nheC* (gene), the orange star represents *entFM* (gene), the red star represents *cytK* (gene), the blue circle represents *hblA* (gene), the green circle represents *hblC* (gene), and the purple circle represents *hblD* (gene).

DISCUSSION

Bacillus cereus is widely distributed around the world, and some studies have evaluated *B. cereus* in vegetables (Gdoura-Ben Amor et al., 2018; Park et al., 2018; Yu et al., 2019), while few studies have examined it in planting environments (Drewnowska et al., 2020). In this study, we determined the occurrence of *B. cereus* on lettuce farms in five Chinese provinces and determined the possible contamination pathways. Moreover, the potential of the isolates to cause foodborne disease was evaluated based on their production of diarrheal and emetic toxins.

The overall prevalence (48.5%) of *B. cereus* observed in the current study was somewhat less than previous research (57.7%) about markets in China (Yu et al., 2019), but much less than that reported in some studies conducted in other countries, e.g., 84.0% in Mexico City (Flores-Urbán et al., 2014), 81.3% in Korea (Park et al., 2018), and 80.0% in Glasgow (Altayar and Sutherland, 2006). These results indicate that *B. cereus* is common in lettuce. Emetic syndrome and diarrheal diseases are often associated with *B. cereus* counts of at least 10^5 CFU/g (Osimani et al., 2018). In our study, concentrations below 10^5 CUF/g were found in all lettuce

samples. Thus, the loads at all levels were considered to be safe for consumption.

Multilocus sequence typing was used to evaluate the evolution and population diversity of *B. cereus*. The 100 *B. cereus* isolates from 46 lettuce farms represented 65 STs and seven CCs and were subtyped into five phylogenetic groups. ST233, ST378, ST1724, CC111, and CC142, which were crossed with different provinces, and each province had unique STs. Two strains isolated from lettuce and soil were assigned to ST26 and ST111, which were the same molecular types as those of the clinical isolates E6345 and F4794 (Hoffmaster et al., 2008). Eleven strains, except for those from pesticides, contained ST233, ST243, ST1001, ST1002, ST1210, and ST2171, which are listed as blood isolates in the *B. cereus* PubMLST database [3]. These results reveal a potential risk when consuming these lettuces directly or with minimal processing. ST1000 was the most frequent type in the 100 isolates and in lettuce, and ST177 was also a frequent type in lettuce, thus, these findings were different from the STs in vegetables on the Chinese market, in which ST26, ST770, and ST1605 were the most frequent types (Yu et al., 2019). Group IV was one of the three largest groups in this study, similar to its predominance in soil (Drewnowska et al., 2020). These results indicate the high genetic diversity of *B. cereus* isolates.

Soil and pesticides were the most frequently detected sources of *B. cereus* in our study, but the concentration in soil was higher than that in pesticides. In total, 7.3% of the soil samples had concentrations ranging from 2×10^4 to 5×10^5 CFU/g, which was consistent with previous studies (Drewnowska et al., 2020). Tracing analysis showed that soil, manure, pesticide and water had the same STs as lettuce, but soil and manure had more of these STs, indicating that *B. cereus* in lettuce was mainly from soil and manure. Additionally, the possible mechanism by which *B. cereus* spreads during lettuce planting were inferred as follows: soil-lettuce, manure-lettuce, pesticide-lettuce, manure-soil-lettuce, and water-manure-soil-lettuce. Quantitative microbial risk assessment of *E. coli* O157:H7 in lettuce revealed that bacterial concentration in soil, soil transfer by irrigation, and bacterial concentration in water were the most important input factors during lettuce preharvest (Pang et al., 2017; Bozkurt et al., 2021), which were partly consistent with our study and these indicated that the planting process needs to be controlled.

It has been demonstrated that *B. cereus* is the causative agent of two types of gastrointestinal diseases, namely, emetic syndrome and diarrheal syndrome (Osimani et al., 2018). The emetic form occurs due to a heat-stable toxin (cerulide) that is preformed in the food, while diarrhea is caused by the ingestion of viable cells, which produce enterotoxins in the small intestine (Osimani et al., 2018). In this study, in all the strains isolated from lettuce farms, only enterotoxins were detected, which was consistent with previous research (Park et al., 2018; Drewnowska et al., 2020).

Among the key toxin genes in *B. cereus* isolates, (1) the genes encoding the Nhe toxin were detected in 100.0% of the isolates in this study, especially *nheB,* which was distributed broadly. In addition, it has been shown that nearly 100.0% of *B. cereus* food poisoning outbreak strains harbor the Nhe toxin genes in Austria (Jessberger et al., 2019). (2) The genes encoding the Hbl toxin were present in 89.7% of the 68 isolates, which is somewhat higher than the value in Korea (Park et al., 2018), in which the *hblACD* genes were detected in 35.7% of lettuce isolates. In previous studies (Chon et al., 2015; Yu et al., 2019), the Hbl toxin genes were detected in 60.0% of *B. cereus* vegetable and soil isolates. (3) *EntFM* was detected in 91.2% of the strains, consistent with the results showing that 90.0 to 100.0% of *B. cereus* isolates harbored the *entFM* gene in *B. cereus* outbreak isolation (Jessberger et al., 2019). In total, 42.6% of the *B. cereus* isolates harbored the *cytK* gene. In Korea, 71.4% of the strains isolated from lettuce harbored *cytK* (Park et al., 2018), and *cytK* was present in 8.0 to 91.0% of the soil isolates (Drewnowska et al., 2020).

The enterotoxins Nhe and Hbl were detected by the Duopath® Cereus Enterotoxins test. Nhe was detected in 100.0% of the 68 isolates, and Hbl was observed in 76.5% of the isolates, thus the rates were higher than those of dairy-associated isolates among which tested positive for Nhe and 30.8% for Hbl (Miller et al., 2018). Moreover, 92.0% of the lettuce isolates harbored Hbl. Additionally, in this study, we found that (1) Nhe was expressed when the *nheB* gene was present. (2) Hbl was detected when the strain harbored the *hblC* gene. The Duopath® Cereus Enterotoxins test tracks Nhe by detecting the NheB component (encoded by *nheB*) in a sandwich complex with immobilized specific antibodies (Krause et al., 2010). NheA and NheC expression did not correlate with toxicity, while the expression of NheB showed a rough correlation with strain toxicity (Jessberger et al., 2019). In addition, the Duopath® Cereus Enterotoxins test detected Hbl based on gold-labeled monoclonal antibodies of Hbl lytic component L2 (Hbl-L2; encoded by *hblC*).

Taken together, the results of the present study showed that despite the high presence of *B. cereus* in lettuce and farm environment samples, the loads were at levels considered to be safe for consumption. However, pathogenic STs (ST26 and ST111) were detected in lettuce and soil, and all *B. cereus* strains tested in this study carried at least 3 of the 8 enterotoxin genes. Nhe and Hbl enterotoxins were the major toxins among the *B. cereus* strains tested. Additionally, *B. cereus* present in planting environments (soil, manure, pesticide, and water) could be easily transferred to lettuce. Our study provides useful information for improving the microbiological safety of fresh lettuce.

DATA AVAILABILITY STATEMENT

The original contributions presented in the study are included in the article/supplementary material, further inquiries can be directed to the corresponding author/s.

AUTHOR CONTRIBUTIONS

YQ, YS, and CZ conceived and designed the experiments. YQ, CW, XD, XZ, QL, WW, YW, MG, and WT performed the experiments. YQ analyzed the data and wrote the draft. YB

[3]https://pubmlst.org/bcereus/

contributed in the reagents/materials/analysis tools. YS and CZ supervised the research. YS revised the manuscript. All authors contributed to the article and approved the submitted version.

FUNDING

This study was supported by the Special Project of Agriculture Produce Quality Safety Risk Assessment (Grant No. GJFP2019005) from Ministry of Agriculture and Rural Affairs of the People's Republic of China and Youth Development Project (Grant No. 2020. No.1-7) from Institute for Agri-Food Standards and Testing Technology, Shanghai Academy of Agricultural Sciences.

ACKNOWLEDGMENTS

We would like to thank Shenghao Yu from the Information Application Research Center of Shanghai Municipal Administration of Market Supervision and Yiwei Dong from Changsha Tunkia Co., Ltd., for their assistance with the experiments.

REFERENCES

Abadias, M., Usall, J., Anguera, M., Solsona, C., and Viñas, I. (2008). Microbiological quality of fresh, minimally-processed fruit and vegetables, and sprouts from retail establishments. *Int. J. Food Microbiol.* 123, 121–129. doi: 10.1016/j.ijfoodmicro.2007.12.013

Altayar, M., and Sutherland, A. D. (2006). *Bacillus cereus* is common in the environment but emetic toxin producing isolates are rare. *J. Appl. Microbiol.* 100, 7–14. doi: 10.1111/j.1365-2672.2005.02764.x

Bozkurt, H., Bell, T., van Ogtrop, F., Phan-Thien, K. Y., and McConchie, R. (2021). Assessment of microbial risk during Australian industrial practices for *Escherichia coli* O157:H7 in fresh cut-cos lettuce: A stochastic quantitative approach. *Food Microbiol.* 95:103691. doi: 10.1016/j.fm.2020.103691

Castiaux, V., N'Guessan, E., Swiecicka, I., Delbrassinne, L., Dierick, K., and Mahillon, J. (2014). Diversity of pulsed-field gel electrophoresis patterns of cereulide-producing isolates of *Bacillus cereus* and *Bacillus weihenstephanensis*. *FEMS Microbiol. Lett.* 353, 124–131. doi: 10.1111/1574-6968.12423

Ceuppens, S., Boon, N., and Uyttendaele, M. (2013). Diversity of *Bacillus cereus* group strains is reflected in their broad range of pathogenicity and diverse ecological lifestyles. *FEMS Microbiol. Ecol.* 84, 433–450. doi: 10.1111/1574-6941.12110

Chon, J. W., Yim, J. H., Kim, H. S., Kim, D. H., Kim, H., Oh, D. H., et al. (2015). Quantitative prevalence and toxin gene profile of *Bacillus cereus* from ready-to-eat vegetables in South Korea. *Foodborne Pathog. Dis.* 12, 795–799. doi: 10.1089/fpd.2015.1977

Dierick, K., Van Coillie, E., Swiecicka, I., Meyfroidt, G., Devlieger, H., Meulemans, A., et al. (2005). Fatal family outbreak of *Bacillus cereus*-associated food poisoning. *J. Clin. Microbiol.* 43, 4277–4279. doi: 10.1128/jcm.43.8.4277-4279.2005

Drewnowska, J. M., Stefanska, N., Czerniecka, M., Zambrowski, G., and Swiecicka, I. (2020). Potential enterotoxicity of phylogenetically diverse *Bacillus cereus sensu lato* soil isolates from different geographical locations. *Appl. Environ. Microbiol.* 86:19. doi: 10.1128/aem.03032-19

Ehling-Schulz, M., Vukov, N., Schulz, A., Shaheen, R., Andersson, M., Märtlbauer, E., et al. (2005). Identification and partial characterization of the nonribosomal peptide synthetase gene responsible for cereulide production in emetic *Bacillus cereus*. *Appl. Environ. Microbiol.* 71, 105–113. doi: 10.1128/aem.71.1.105-113.2005

Feil, E. J., Li, B. C., Aanensen, D. M., Hanage, W. P., and Spratt, B. G. (2004). eBURST: inferring patterns of evolutionary descent among clusters of related bacterial genotypes from multilocus sequence typing data. *J. Bacteriol.* 186, 1518–1530. doi: 10.1128/jb.186.5.1518-1530.2004

Flores-Urbán, K. A., Natividad-Bonifacio, I., Vázquez-Quiñones, C. R., Vázquez-Salinas, C., and Quiñones-Ramírez, E. I. (2014). Detection of toxigenic *Bacillus cereus* strains isolated from vegetables in Mexico City. *J. Food Prot.* 77, 2144–2147. doi: 10.4315/0362-028x.Jfp-13-479

Forsythe, S. J., Dickins, B., and Jolley, K. A. (2014). Cronobacter, the emergent bacterial pathogen *Enterobacter sakazakii* comes of age; MLST and whole genome sequence analysis. *BMC Genomics* 15:1121. doi: 10.1186/1471-2164-15-1121

Francisco, A. P., Vaz, C., Monteiro, P. T., Melo-Cristino, J., Ramirez, M., and Carriço, J. A. (2012). PHYLOViZ: phylogenetic inference and data visualization for sequence based typing methods. *BMC Bioinform.* 13:87. doi: 10.1186/1471-2105-13-87

Gdoura-Ben Amor, M., Siala, M., Zayani, M., Grosset, N., Smaoui, S., Messadi-Akrout, F., et al. (2018). Isolation, identification, prevalence, and genetic diversity of *Bacillus cereus* group bacteria from different foodstuffs in Tunisia. *Front. Microbiol.* 9:447. doi: 10.3389/fmicb.2018.00447

Guinebretière, M.-H., Broussolle, V., and Nguyen-The, C. (2002). Enterotoxigenic profiles of food-poisoning and food-borne *Bacillus cereus* strains. *J. Clin. Microbiol.* 40, 3053–3056. doi: 10.1128/jcm.40.8.3053-3056.2002

Guinebretière, M. H., Thompson, F. L., Sorokin, A., Normand, P., Dawyndt, P., Ehling-Schulz, M., et al. (2008). Ecological diversification in the *Bacillus cereus* group. *Environ. Microbiol.* 10, 851–865. doi: 10.1111/j.1462-2920.2007.01495.x

Hammerum, A. M., Hansen, F., Skov, M. N., Stegger, M., Andersen, P. S., Holm, A., et al. (2015). Investigation of a possible outbreak of carbapenem-resistant *Acinetobacter baumannii* in Odense, Denmark using PFGE, MLST and whole-genome-based SNPs. *J. Antimicrob. Chemother.* 70, 1965–1968. doi: 10.1093/jac/dkv072

Hoffmaster, A. R., Novak, R. T., Marston, C. K., Gee, J. E., Helsel, L., Pruckler, J. M., et al. (2008). Genetic diversity of clinical isolates of *Bacillus cereus* using multilocus sequence typing. *BMC Microbiol.* 8:191. doi: 10.1186/1471-2180-8-191

Höfte, H., and Whiteley, H. R. (1989). Insecticidal crystal proteins of *Bacillus thuringiensis*. *Microbiol. Rev.* 53, 242–255.

Ivanova, N., Sorokin, A., Anderson, I., Galleron, N., Candelon, B., Kapatral, V., et al. (2003). Genome sequence of *Bacillus cereus* and comparative analysis with *Bacillus anthracis*. *Nature* 423, 87–91. doi: 10.1038/nature01582

Jessberger, N., Kranzler, M., Da Riol, C., Schwenk, V., Buchacher, T., Dietrich, R., et al. (2019). Assessing the toxic potential of enteropathogenic *Bacillus cereus*. *Food Microbiol.* 84:103276. doi: 10.1016/j.fm.2019.103276

Jiménez, G., Urdiain, M., Cifuentes, A., López-López, A., Blanch, A. R., Tamames, J., et al. (2013). Description of *Bacillus toyonensis sp. nov.*, a novel species of the *Bacillus cereus* group, and pairwise genome comparisons of the species of the group by means of ANI calculations. *Syst. Appl. Microbiol.* 36, 383–391. doi: 10.1016/j.syapm.2013.04.008

Jung, M. Y., Kim, J. S., Paek, W. K., Lim, J., Lee, H., Kim, P. I., et al. (2011). *Bacillus manliponensis sp. nov.*, a new member of the *Bacillus cereus* group isolated from foreshore tidal flat sediment. *J. Microbiol.* 49, 1027–1032. doi: 10.1007/s12275-011-1049-6

Kim, J. B., Kim, J. M., Cho, S. H., Oh, H. S., Choi, N. J., and Oh, D. H. (2011). Toxin genes profiles and toxin production ability of *Bacillus cereus* isolated from clinical and food samples. *J. Food Sci.* 76, T25–T29. doi: 10.1111/j.1750-3841.2010.01958.x

Krause, N., Moravek, M., Dietrich, R., Wehrle, E., Slaghuis, J., and Märtlbauer, E. (2010). Performance characteristics of the Duopath® cereus enterotoxins assay for rapid detection of enterotoxinogenic *Bacillus cereus* strains. *Int. J. Food Microbiol.* 144, 322–326. doi: 10.1016/j.ijfoodmicro.2010.10.008

Kumar, S., Stecher, G., Li, M., Knyaz, C., and Tamura, K. (2018). MEGA X: Molecular evolutionary genetics analysis across computing platforms. *Mol. Biol. Evol.* 35, 1547–1549. doi: 10.1093/molbev/msy096

Maiden, M. C., Jansen van Rensburg, M. J., Bray, J. E., Earle, S. G., Ford, S. A., Jolley, K. A., et al. (2013). MLST revisited: the gene-by-gene approach to bacterial genomics. *Nat. Rev. Microbiol.* 11, 728–736. doi: 10.1038/nrmicro3093

Meer, R. R., Baker, J., Bodyfelt, F. W., and Griffiths, M. W. (1991). Psychrotrophic *Bacillus spp*. in fluid milk products: a review. *J. Food Prot.* 54, 969–979. doi: 10.4315/0362-028x-54.12.969

Miller, R. A., Beno, S. M., Kent, D. J., Carroll, L. M., Martin, N. H., Boor, K. J., et al. (2016). B*acillus wiedmannii sp. nov*., a psychrotolerant and cytotoxic *Bacillus cereus* group species isolated from dairy foods and dairy environments. *Int. J. Syst. Evol. Microbiol.* 66, 4744–4753. doi: 10.1099/ijsem.0.001421

Miller, R. A., Jian, J., Beno, S. M., Wiedmann, M., and Kovac, J. (2018). Intraclade Variability in toxin production and cytotoxicity of *Bacillus cereus* group type strains and dairy-associated isolates. *Appl. Environ. Microbiol.* 84:17. doi: 10.1128/aem.02479-17

Osimani, A., Aquilanti, L., and Clementi, F. (2018). *Bacillus cereus* foodborne outbreaks in mass catering. *Int. J. Hosp. Manag.* 72, 145–153. doi: 10.1016/j.ijhm.2018.01.013

Otlewska, A., Oltuszak-Walczak, E., and Walczak, P. (2013). Differentiation of strains from the *Bacillus cereus* group by RFLP-PFGE genomic fingerprinting. *Electrophoresis* 34, 3023–3028. doi: 10.1002/elps.201300246

Pang, H., Lambertini, E., Buchanan, R. L., Schaffner, D. W., and Pradhan, A. K. (2017). Quantitative microbial risk assessment for *Escherichia coli* O157:H7 in fresh-cut lettuce. *J. Food Prot.* 80, 302–311. doi: 10.4315/0362-028x.Jfp-16-246

Park, K. M., Jeong, M., Park, K. J., and Koo, M. (2018). Prevalence, enterotoxin genes, and antibiotic resistance of *Bacillus cereus* isolated from raw vegetables in korea. *J. Food Prot.* 81, 1590–1597. doi: 10.4315/0362-028x.Jfp-18-205

Stenfors, L. P., and Granum, P. E. (2001). Psychrotolerant species from the *Bacillus cereus* group are not necessarily *Bacillus weihenstephanensis*. *FEMS Microbiol. Lett.* 197, 223–228. doi: 10.1111/j.1574-6968.2001.tb10607.x

Yu, P., Yu, S., Wang, J., Guo, H., Zhang, Y., Liao, X., et al. (2019). *Bacillus cereus* isolated from vegetables in china: incidence, genetic diversity, virulence genes, and antimicrobial resistance. *Front. Microbiol.* 10:948. doi: 10.3389/fmicb.2019.00948

Zhuang, K., Li, H., Zhang, Z., Wu, S., Zhang, Y., Fox, E. M., et al. (2019). Typing and evaluating heat resistance of *Bacillus cereus sensu stricto* isolated from the processing environment of powdered infant formula. *J. Dairy Sci.* 102, 7781–7793. doi: 10.3168/jds.2019-16392

Conflict of Interest: YQ, CZ, and YS are employed by Institute for Agro-Food Standards and Testing Technology, Shanghai Academy of Agricultural Sciences, Shanghai, China and Shanghai Co-Elite Agro-Food Testing Service Co., Ltd.

The remaining authors declare that the research was conducted in the absence of any commercial or financial relationships that could be construed as a potential conflict of interest.

Publisher's Note: All claims expressed in this article are solely those of the authors and do not necessarily represent those of their affiliated organizations, or those of the publisher, the editors and the reviewers. Any product that may be evaluated in this article, or claim that may be made by its manufacturer, is not guaranteed or endorsed by the publisher.

frontiers in Microbiology

ORIGINAL RESEARCH
published: 05 November 2021
doi: 10.3389/fmicb.2021.771770

Application of a 360-Degree Radiation Thermosonication Technology for the Inactivation of *Staphylococcus aureus* in Milk

*Jianwei Zhou[1], Lele Sheng[2], Ruiling Lv[3], Donghong Liu[2,3], Tian Ding[2,3] and Xinyu Liao[1,2]**

[1] School of Mechanical and Energy Engineering, Ningbotech University, Ningbo, China, [2] Department of Food Science and Nutrition, Zhejiang University, Hangzhou, China, [3] Ningbo Research Institute, Zhejiang University, Ningbo, China

Milk is easy to be contaminated by microorganisms due to its abundant nutrients. In this study, a 360-degree radiation thermosonication (TS) system was developed and utilized for the inactivation of *Staphylococcus aureus* in milk. The 360-degree radiation TS system-induced inactivation kinetics of *S. aureus* was fitted best by the Weibull model compared with biphasic and linear models. The treatment time, the exposure temperature, and the applied ultrasound power was found to affect the bactericidal efficacy of the 360-degree radiation TS system. Additionally, the TS condition of 200 W and 63°C for 7.5 min was successfully applied to achieve complete microbial inactivation (under the limit of detection value) in raw milk. The treatment of 360-degree radiation TS can enhance the zeta potential and decrease the average particle size of milk. It also exhibited better retainment of the proteins in milk compared with the ultrahigh temperature and conventional pasteurization processing. Therefore, the 360-degree radiation TS system developed in this study can be used as an alternative technology to assure the microbiological safety and retain the quality of milk, and the Weibull model could be applied for the prediction of the inactivation levels after exposure to this technology.

Keywords: 360-degree radiation thermosonication, inactivation kinetics, *Staphylococcus aureus*, quality characteristic, milk

OPEN ACCESS

Edited by:
Biao Suo,
Henan Agricultural University, China

Reviewed by:
Hongshun Yang,
National University of Singapore, Singapore
Libo Liu,
Northeast Agricultural University, China

***Correspondence:**
Xinyu Liao
xinyu_liao@zju.edu.cn

Specialty section:
This article was submitted to Food Microbiology, a section of the journal Frontiers in Microbiology

Received: *07 September 2021*
Accepted: *01 October 2021*
Published: *05 November 2021*

Citation:
Zhou J, Sheng L, Lv R, Liu D, Ding T and Liao X (2021) Application of a 360-Degree Radiation Thermosonication Technology for the Inactivation of Staphylococcus aureus in Milk. Front. Microbiol. 12:771770. doi: 10.3389/fmicb.2021.771770

INTRODUCTION

Milk contains a variety of nutritional compounds, especially high-quality proteins, making it one of the most popular food for human (Vartanian et al., 2007). In 2019, the global production of raw milk reached a value of 883.2 million tons (FAO, 2019). However, milk is also an ideal medium for the proliferation of pathogens, such as *Escherichia coli*, *Salmonella Thyphimurium*, and *Staphylococcus aureus*, making it a potential risk to food safety (Claeys et al., 2013; Zeinhom and Abdel-Latef, 2014; Rainard et al., 2018; Balasubramanian et al., 2019). Therefore, it is essential to control microbial contamination in the milk production process. Thermal treatments are the most widely used methods for the disinfection of milk, such as pasteurization and ultrahigh temperature processing (UHT) (Grant et al., 1996, 1998). However, heat may disrupt the thermosensitive nutrients in milk, which makes it difficult to meet the increasing nutrient requirements of consumers. Therefore, non-thermal processing technologies have emerged as alternatives to thermal methods for milk

processing (Aneja et al., 2014; Song et al., 2016; Liao et al., 2018; Makroo et al., 2020).

Ultrasound, as a promising non-thermal technology, has attracted much attention because of its low working temperature and maximum retainment of food quality (Tao and Sun, 2015). The phenomenon of acoustic cavitation is considered as the major contributor to the microbial inactivation induced by ultrasound exposure. When cavitation bubbles collapse in the liquid medium, both mechanical (e.g., shock waves, liquid microjets, and shear forces) and sonochemical (formation of H·, OH·, and H_2O_2) effects will be acted on the microbial cells (Ashokkumar, 2011; Chemat et al., 2011; Awad et al., 2012). However, the antimicrobial efficiency of individual ultrasound treatment was limited (Li et al., 2016). Ultrasound combined with mild heat as a novel hurdle technology, also called thermosonication (TS), is of great interest because of efficient microbial inactivation and less damages in food quality (Barba et al., 2017).

Horn probes (also called sonotrodes) are the most commonly used devices for the generation of ultrasound. To use, horn probes, with the diameter ranging 2–12.7 mm, are dipped into the liquid sample. For most of the horn probes, nearly all the ultrasonic energy is transmitted through the tip of the probe with a small area (Campoli et al., 2018; Carrillo-Lopez et al., 2020; Yuksel and Elgun, 2020). Generally, horn probe-based devices are suitable for the treatment of samples with a small volume in the laboratory scale. However, when scaling up to industrial application, the efficacy of the conventional horn probes might be compromised by the uneven radiation of the acoustic field and low ultrasound energy intensity applied in the treated samples with large volumes (Abesinghe et al., 2019).

The objectives of this study were to develop a large-volume 360-degree radiation TS system and to apply this technology for inactivating *S. aureus* in milk, one of the foodborne pathogens of concern in milk safety. The microbial inactivation efficacy of this novel TS treatment was estimated and compared with conventional UHT and pasteurization processing. The 360-degree radiation TS-induced killing curve of *S. aureus* was fitted with mathematical models to describe the inactivation kinetics. Additionally, the effect of this TS treatment on the physicochemical characteristics of milk was evaluated.

MATERIALS AND METHODS

Preparation of Bacterial Suspensions

Staphylococcus aureus strains of JPHG05A009-17, JP-GX07, and 5JP-HBA 2020 isolated from milk or milk product in China were used in this study. Bacterial culture was stored at −80°C in a mixture of glycerol and nutrient broth (NB) (Hope Bio-technology Co., Ltd., Qingdao, China) at a ratio of 1:1. Each strain was streaked and maintained on the Baird Parker (BP) (Hope Bio-technology Co., Ltd., Qingdao, China) medium supplemented with egg yolk tellurite emulsion (Hope Bio-technology Co., Ltd., Qingdao, China). A single colony of each strain was transferred into 100-ml NB, followed by incubation in a reciprocal shaker at 150 rpm and 37°C for 18 h. Subsequently, centrifugation (2,320 × *g*, 4°C, 10 min) was performed to collect *S. aureus* cells, which were washed twice by resuspension in sterile phosphate buffer solution (PBS) (pH 7.4). The suspensions of three *S. aureus* strains with the same volume were mixed thoroughly to prepare a cocktail inoculum, and the final concentration of the bacterial inoculum was approximately 10^9 CFU/ml, with determination through plating on the plate count agar.

Milk Preparation

Sterilized milk sample was purchased from a local market in Hangzhou, China. Raw milk without pasteurization was obtained from a farm in Hangzhou, China, and transported to the laboratory as soon as possible (less than 30 min). Milk samples with a volume of 270 ml were inoculated by *S. aureus* cocktail suspension (30 ml) to achieve the final bacterial concentration of approximately 10^8 CFU/ml in milk.

Thermosonication Treatment Conditions

In this study, a 360-degree radiation TS equipment (Ningbo Scientz Co., Ltd., Ningbo, China) was employed to treat the inoculated milk samples and consisted of an electrical power generator, an enclosed cylinder-shaped reactor, a circulating water bath, a transducer, and an ultrasonic probe (**Figure 1**). The sample reactor is an enclosed chamber covered with a heating jacket chamber, which is equipped with a heating water outlet and inlet and a temperature sensor. There are multiple transmitters distributed on the side surface of the ultrasonic probe, which can emit a more uniform sonication field throughout the liquid sample. All the ultrasonic transmitters are controlled by one ultrasonic transducer, which is fixed on the top of the enclosed chamber and connected with the ultrasonic probe. The transducer comprises a cylindrical barrel, of which a shell is made of stainless steel, and the multiple ultrasonic transduction components are installed in an inner cavity of the barrel along the axis. Each ultrasonic transduction component comprises a supporting block, wherein over two piezoelectric ceramic piece groups are arranged on the sides of each supporting block. Each piezoelectric ceramic piece group consists of over two piezoelectric ceramic wafers, and the electrodes are arranged on the end faces of the piezoelectric ceramic wafers. The piezoelectric ceramic piece groups are fixed with the supporting blocks through pressing the blocks correspondingly, and the ultrasonic transduction components are closely connected with the inner wall of the cylindrical barrel. It can prevent the dropping of the electrodes and the deformation fracture of the piezoelectric ceramics. Additionally, the transducer has the capability of emitting even ultrasonic within the radial direction range of 360-degrees, and a higher transduction efficiency can be achieved.

The milk sample was placed in the cylinder-shaped reactor with a volume of 300 ml and a diameter of 5 cm. The ultrasonic probe has a length of 8 cm and a diameter of 1.2 cm. Four transmitters are longitudinally distributed on the side surface of the ultrasonic probe at an interval of 3.5 cm. The ultrasonic frequency is 20 kHz, and the maximum input ultrasonic power is 900 W. The samples treated by TS conditions were divided into

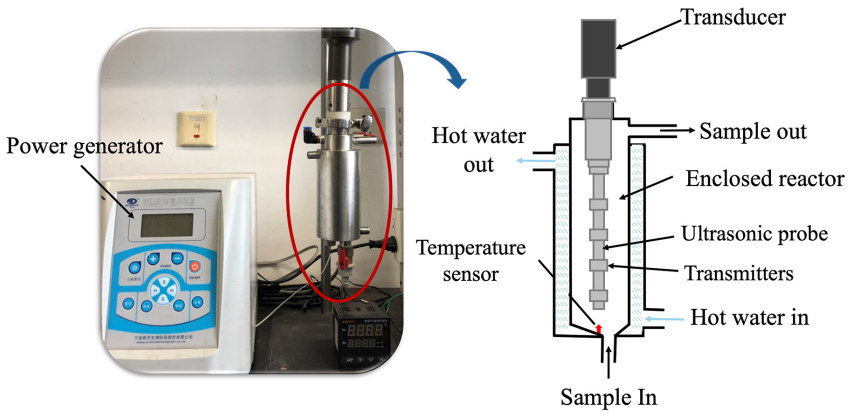

FIGURE 1 | Diagram of the 360-degree radiation thermosonication system.

four groups: 200 or 400 W at 55°C for 30 min and 200 or 400 W at 63°C for 15 min. The treatment temperature is achieved by the circulating water bath and controlled by a temperature sensor. The sample without TS treatment was set as the control.

Pasteurization and Ultrahigh Temperature Treatment

The pasteurization of the raw milk samples (300 ml) was performed by the 360-degree radiation TS equipment with an ultrasonic power of 0 W. The treatment temperature was set at 63°C and maintained for 30 min. Regarding UHT treatment, a commercial UHT system (TG-UHT-CH-DJ-nQJ, Shanghai Nanhua Transducer Manufacture Co., Ltd., Shanghai, China) was used for treating the raw milk samples at 121°C for 15 s.

Microbiological Analysis

Plate count method was used for the microbiological analysis. After various treatments, the milk samples were serially diluted with sterile 0.85% (m/v) saline solution. Then, a portion of diluent (0.1 ml) was spread on the BP medium supplemented with egg yolk tellurite emulsion. The plates were subsequently incubated in an incubator at 37°C for 48 h. The bacterial colonies grown on media was enumerated and expressed in $\log_{10}$ CFU/ml.

Establishment of the Inactivation Kinetic Model

The inactivation of *S. aureus* in milk samples by a 360-degree radiation TS was described using the Weibull model (Eq. 1), biphasic model (Eq. 2), and linear model (Eq. 3) (Chen et al., 2019; Shao et al., 2020; Zhao et al., 2020). The data were analyzed and fitted by non-linear least squares regression method.

$$log\left(\frac{N_t}{N_0}\right) = -\frac{1}{2.303}\left(\frac{t}{a}\right)^b \quad (1)$$

where N_0 is the initial counts of *S. aureus*, N_t is the survival of *S. aureus* at treatment time t, b represents the time scale parameter, and a is a dimensionless shape parameter.

$$log\left(\frac{N_t}{N_0}\right) = log\left[fe^{-Pt} + (1-f)\,e^{-Qt}\right] \quad (2)$$

where N_0 is the initial counts of *S. aureus*, N_t is the survival of *S. aureus* at treatment time t, P and Q represent the inactivated rates for two phases, and f and (1-f) are the ratios of TS-resistant and -susceptible *S. aureus* subpopulations, respectively.

$$log\left(\frac{N_t}{N_0}\right) = at + b \quad (3)$$

where N_0 is the initial count of *S. aureus*, N_t is the survival of *S. aureus* at treatment time t, and a represents the inactivated rate.

The fitness of models was estimated with the following goodness-of-fit indexes: the coefficient of determination (R^2, Eq. 4) and the root mean square error (RMSE, Eq. 5).

$$R^2 = 1 - \frac{SS_r}{SS_t} \quad (4)$$

where SS represents the residual sum of squares, and SS_t is the total sum of squares.

$$RMSE = \sqrt{\frac{\sum_{i=1}^{n}\left(y_{obs} - y_{pred}\right)^2}{n}} \quad (5)$$

where the variable y_{obs} was the logarithm value of *S. aureus* population estimated by the plate count method ($\log_{10}$ CFU/ml) in this study, y_{pred} corresponds to the logarithm value of the bacterial population ($\log_{10}$ CFU/ml) calculated by the fitted model, n is the total number of the observed data points, and p was the number of parameters for the estimated model.

Determination of the Physicochemical Characteristics of Milk

Color Properties

The color properties of milk samples after various treatments were measured using a Konica Minolta CM-600d spectrophotometer (Konica Minolta Holdings, Inc., Tokyo,

Japan) in the reflection mode at room temperature (25 ± 1°C). The parameters of L^* (lightness), a^* (redness and greenness), and b^* (yellowness and blueness) were obtained for calculation of the total color difference ΔE by Eq. 6 (Zhao et al., 2019; Feng et al., 2020):

$$\Delta E = \sqrt{\left(L^* - L_o^*\right)^2 + \left(a^* - a_o^*\right)^2 + \left(b^* - b_o^*\right)^2} \quad (6)$$

where L_0, a_0, and b_0 represented the color values of the milk sample before treatments.

pH

The pH of the milk samples was measured with a digital pH meter PHS-550 (Lohand Biological Co., Ltd., Hangzhou, China) at room temperature (25 ± 1°C).

Particle Size and Zeta Potential

After the different treatments, the particle size and zeta potential of the milk samples were determined using the Malvern Zetasizer Nano (ZS90; Malvern Panalytical Ltd., Malvern, United Kingdom) at room temperature (25 ± 1°C).

Total Protein Content

The total protein content (TPC) in the milk samples was measured according to the Kjeldahl method. Copper sulfate (0.4 g), potassium sulfate (6 g), and 20 ml sulfuric acid were added to a portion of milk sample (10 g) for the digestion to convert all the organically bonded nitrogen into ammonium ions. Subsequently, the ammonium ions are reacted with sodium hydroxide and transformed into ammonia, which dissolve in boric acid. Finally, the standard solution of hydrochloric acid (HCl) was used for titration to determine the nitrogen concentration. TPC (g/100 g) was calculated by the following equation:

$$x = \frac{(V_1 - V_0) \times c \times 0.0140}{m \times V_2/100} \times F \times 100 \quad (7)$$

where V_1 corresponds to the consumed volume (ml) of HCl standard titrant with concentration of c (M), V_0 is the consumed volume (ml) of HCl used for the blank sample (water), m was the quantity of the samples (g), V_2 represents the volume of the digested solution (ml), and F is the nitrogen-to-protein conversion coefficient, which is 6.38 for milk.

Statistical Analysis

All experiments in this study were performed in triplicate. Determining the statistical significance of the data was carried out using SPSS 22.0 (IBM Corp., Armonk, NY, United States) using one-way analysis of variance with Duncan's test for the *post-hoc* multiple comparison. A value of $p < 0.05$ was considered statistically different. The kinetic models were fitted to the data points with Origin 8.0 (OriginLab Corp., Northampton, MA, United States).

RESULTS AND DISCUSSION

360-Degree Radiation Thermosonication-Induced Heat Transfer Enhancement in Milk

During the 360-degree radiation TS treatment, the milk temperatures are controlled by circulating water in the jacket chamber covering the side surface of the sample reactor (**Figure 1**). As shown in **Figure 2**, the core temperature of the milk samples was increased to the target temperatures (55 or 63°C) in 5 min, and it was maintained at a relatively constant value with a deviation of less than 3.33°C from the target temperature. It demonstrated that the 360-degree radiation TS system could efficiently inhibit the perturbation of temperature. Without the ultrasonic effect, it required 18 min for the temperature in the core of milk sample to reach the target pasteurization temperature of 63°C. It might be attributed to the effect of acoustic cavitation during the ultrasound processing, which could accelerate the heat transfer efficiency between the milk samples in the reactor and the heating water in the jacket chamber (Kurbanov and Melkumov, 2003; Legay et al., 2011). When cavitation bubbles collapse, a large amount of energy can be generated, and violent impact and high-speed micro-jet are also formed, which greatly enhance the collision density. The thermal and velocity boundary layers are subsequently disrupted, which decreases the thermal resistance and creates microturbulence to achieve the heat transfer enhancement.

Inactivation of *S. aureus* Cocktail in Milk by 360-Degree Radiation Thermosonication

The survival levels of *S. aureus* cocktail in milk treated by the 360-degree radiation TS treatment are exhibited in **Table 1**. The 360-degree radiation TS-induced inactivation of *S. aureus* was affected

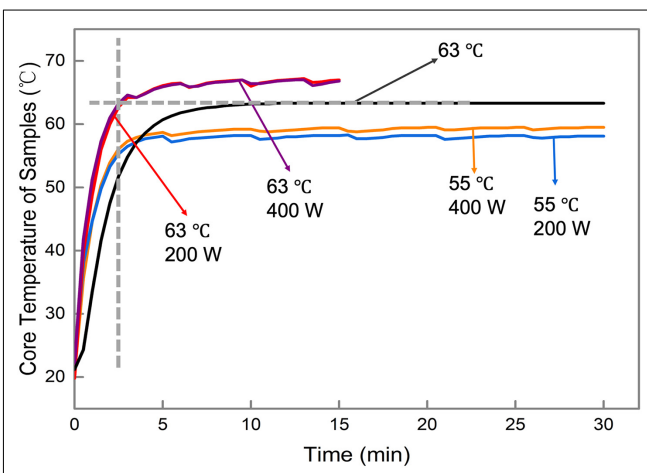

FIGURE 2 | Core temperature changes of samples under different treatment conditions. The black line shows the temperature change without ultrasonic treatment.

by the treatment time, the exposure temperature, and the applied ultrasound power.

As shown in **Table 1**, there is an inverse correlation between the *S. aureus* survival population and the treatment time or exposure temperature. With TS treatment at 63°C and 400 W, the survival levels of *S. aureus* were 8.12, 4.68, 3.79, 3.02, 1.99, and 1.59 log for 0-, 3-, 6-, 9-, 12-, and 15-min treatment time, respectively. When the exposure temperature decreased from 63 to 55°C, the remaining survival level increased from 1.59 to 3.93 logs for a treatment time of 15 min. The effect of ultrasound powers on TS-induced bactericidal efficacy is closely related to the exposure temperature. Under 55°C, the enhancement of ultrasound power contributed to the higher reduction of *S. aureus* in milk to some extent. When the exposure time was 15 min, the *S. aureus* cells were decreased by 3.86 log under an applied ultrasound power of 200 W, and it was 4.19 log reduction when the ultrasound power was increased to 400 W. However, when exposing the milk samples to 63°C, the survival levels of *S. aureus* were independent of ultrasound powers ($p > 0.05$).

Most of the commonly used ultrasonic horns have only one transmitter on the tip, which transfers nearly all the energy through one direction. In our previous study, it was found that the TS, combined with single-direction ultrasonic radiation (600 W) and 63°C, resulted in less than 99% reduction of *S. aureus* for 5 min (Li et al., 2019). Individual heat exposure has been reported to activate protective systems in bacteria cells, which could compromise the microbial inactivation level (Liu et al., 2020; Wu et al., 2021). In combination with ultrasonic field, the effect of ultrasound-induced cavitation contributes to the rupture of the microbial outer structure (e.g., cell wall/membranes), which weakened the heat tolerance of microorganisms and led to final cell death.

The 360-degree radiation TS treatment in this work under an applied ultrasound power of 200 W and a temperature of 63°C brought in over 99.9% inactivated level of *S. aureus* after 3 min of exposure. According to the performance criteria of milk processing published by FAO/WHO, the processing treatment should be designed to achieve at least a 5-log reduction of the target bacteria. In this study, a TS treatment of 63°C and 200/400 W for 9 min resulted in over 5-log reduction of *S. aureus*, while it required 40 min for an individual thermal treatment at 63°C to decrease *S. aureus* by over 5 logs. Considering the bactericidal efficacy and the energy consumption (the applied ultrasound power), the 360-degree radiation TS treatment of 63°C and 200 W was selected for further analysis in this study.

TABLE 3 | The total viable counts in milk before and after various treatments.

Treatments	Total viable counts (log_{10} CFU/ml)
Raw milk	3.25 ± 0.77
360-degree radiation thermosonication (200 W, 63°C, 7.5 min)	ND
UHT (121°C, 15 s)	ND
Pasteurization (63°C, 30 min)	ND

ND, non-detected (i.e., below the limit of detection).

TABLE 4 | pH, zeta potential, and particle size of milk after various treatments.

Treatments	pH	Zeta potential (mV)	Particle size (μm)
Raw milk	6.65 ± 0.04a	−23.0 ± 1.6a	7.59 ± 0.16c
360-degree radiation thermosonication (200 W, 63°C, 7.5 min)	6.66 ± 0.02a	−37.0 ± 0.4d	4.62 ± 0.14a
UHT (121°C, 15 s)	6.69 ± 0.01a	−30.4 ± 1.2c	6.08 ± 0.06b
Pasteurization (63°C, 30 min)	6.71 ± 0.04a	−26.4 ± 0.7b	6.00 ± 0.08b

Values with different lowercase letters in the same column showed a significant difference at $p < 0.05$.

TABLE 1 | Survival concentrations (log_{10} CFU/ml) of *S. aureus* after the 360-degree radiation thermosonication treatment under various conditions.

Treatment time (min)	Exposure temperature (°C)/Applied ultrasonic power (W)			
	55/200	55/400	63/200	63/400
3	7.46 ± 0.50C,b	6.90 ± 0.59D,b	4.79 ± 0.20E,a	4.68 ± 0.41D,a
6	5.89 ± 0.32B,b	5.47 ± 0.33C,b	3.62 ± 0.33D,a	3.79 ± 0.61C,a
9	5.38 ± 0.54B,c	4.60 ± 0.19B,b	2.65 ± 0.22C,a	3.02 ± 0.12B,a
12	5.00 ± 0.79B,C,c	4.10 ± 0.17AB,b	1.92 ± 0.17B,a	1.99 ± 0.24A,a
15	4.26 ± 0.28A,c	3.93 ± 0.16A,b	1.33 ± 0.17A,a	1.59 ± 0.22A,a

The initial concentration of bacterial cells was about 8.12 ± 0.05 log_{10} CFU/ml. The values are mean of triplicate measurements ± standard deviation. The values with different lowercase letters in the same row and uppercase letters in the same column showed a significant difference at $p < 0.05$.

TABLE 2 | The fitted parameters of linear model, biphasic model, and Weibull model.

Linear model				Biphasic model					Weibull model			
A	*B*	R^2	RMSE	*f*	*p*	*q*	R^2	RMSE	*a*	*b*	R^2	RMSE
−1.39 ± 0.76	−0.38 ± 0.07	0.866	76.08	0.996 ± 0.001	90091.86 ± 0.00	0.68 ± 0.17	0.985	6.33	0.02 1 ± 0.004	0.416 ± 0.001	0.999	0.36

TABLE 5 | The color changes of milk before and after various treatments.

Treatments	*L**	*a**	*b**	Δ*E*
Raw milk	87.38 ± 0.23a*	−2.00 ± 0.06b	4.67 ± 0.15a	0
360-degree radiation thermosonication (200 W, 63°C, 7.5 min)	90.75 ± 0.42c	−2.25 ± 0.04a	3.61 ± 0.04b	3.55 ± 0.40a
UHT (121°C, 15 s)	89.39 ± 0.08b	−1.79 ± 0.05c	2.60 ± 0.42c	2.91 ± 0.26b
Pasteurization (63°C, 30 min)	89.25 ± 0.42b	−1.98 ± 0.01b	4.01 ± 0.06b	1.99 ± 0.41c

Values with different lowercase letters in the same column showed a significant difference at $p < 0.05$.
The asterisk is used to differentiate the CIELAB system from ANLAB.

TABLE 6 | The total viable counts in milk before and after various treatments.

Treatments	Protein content (%)
Raw milk	3.28 ± 0.19b
360-degree radiation thermosonication (200 W, 63°C, 7.5 min)	3.22 ± 0.25b
UHT (121°C, 15 s)	3.02 ± 0.16b
Pasteurization (63°C, 30 min)	2.53 ± 0.38a

Values with different lowercase letters in the same column showed a significant difference at $p < 0.05$.

Establishment of Inactivation Kinetics

In order to predict the behavior of *S. aureus* cells in milk when exposed to the 360-degree TS treatment, the survival curve was fitted to linear and non-linear (Weibull and biphasic) models. R^2 and RMSE are the most commonly used indexes for the estimation of the goodness-of-fit of the models. A R^2 value close to 1 and a low RMSE value indicate that the fitted model exhibits a good fitting to data points.

As shown in **Table 2**, the values of R^2 and RMSE of the linear model are 0.866 and 76.08, respectively, which demonstrated that the inactivation kinetics of *S. aureus* by the 360-degree radiation TS treatment did not follow a linear pattern. Regarding non-linear models, the obtained values of R^2 for the fitted biphasic model and Weibull model are 0.985 and 0.999, respectively, which are close to 1. However, the value of RMSE of the fitted biphasic model is 6.33, which is much higher than that (0.36) of the fitted Weibull model in this study. Overall, the Weibull model is the most suitable model to describe the 360-degree radiation TS-induced inactivation kinetics of *S. aureus* in milk. Similarly, non-linear curves of TS-induced microbial inactivation have been observed in previous studies (Lee et al., 2009). In the study of Sasikumar et al. (2019), it was found that the inactivation level of *E. coli* by TS (1.95 W/50°C/21 min) in khoonphal juice was fitted well with the Weibull model, with an R^2 value of over 0.99 (Sasikumar et al., 2019).

The Weibull model is built by two parameters, including the scale parameter *a* (time) and the dimensionless shape parameter *b*. The shape parameter *b* not only accounts for the concavity of a survival curve but also is related to the physiological states of microorganisms (Surowsky et al., 2014). $b < 1$ indicates the upward concavity of a survival curve and that the remaining microbial subpopulation has the ability to adapt to the applied treatment, and $b > 1$ reflects the survival curve with a downward concavity and that the treatment results in accumulative damages on the remaining bacterial cells. As shown in **Table 2**, the *b* value of the fitted Weibull model in this work is 0.42, less than 1, indicating that the remaining *S. aureus* cells become increasingly damaged by the 360-degree radiation TS exposure. Based on the established Weibull model, the time to achieve a 5-log reduction is calculated to be 7.5 min. Therefore, the conditions of the 360-degree radiation TS treatment for the sterilization of milk are 200 W at 63°C for 7.5 min.

Application of 360-Degree Radiation Thermosonication for the Sterilization of Raw Milk

In order to validate the application of the 360-degree radiation TS treatment, it was further used for the sterilization of raw milk in comparison to commercial UHT processing (121°C, 15 s) and pasteurization (63°C, 30 min). As shown in **Table 3**, the initial bacterial contamination level in raw milk was 3.25 $\log_{10}$ CFU/ml. After all the treatments, the bacterial concentrations were decreased to be under the limit of detection (LOD), indicating that the 360-degree radiation TS treatment (200 W, 63°C, 7.5 min) in this work can be used as a promising technology for assurance of the microbiological safety of milk.

Physicochemical Property Changes of Raw Milk

Changes in pH, Particle Size, and Zeta Potential

The pH values of milk are stability indices of the casein micelles. The pH value of the untreated raw milk is 6.65, and no significant changes ($p > 0.05$) in pH values were found in the milk samples treated with the 360-degree radiation TS, UHT, and pasteurization (**Table 4**).

The zeta potential is an important index to reflect the stability of a colloidal system because it is generated from the interaction of all charged particles in the system (Shanmugam and Ashokkumar, 2014). As shown in **Table 4**, the zeta potential of raw milk was −23 mV, and it was significantly ($p < 0.05$) increased after various treatments. The milk treated with the 360-degree radiation TS exhibited the highest zeta potential, which might be attributed to the ultrasound-induced damage and interruption in the membrane of the fat globule, which could make the membrane more negatively charged and lead to an increase in zeta potential (Scudino et al., 2020). The enhancement of zeta potential caused by the 360-degree radiation treatment could improve the interaction of fat globules and protein micelles and thus strengthen the stability of milk (Shanmugam and Ashokkumar, 2014).

The average particle sizes of milk with various treatments are shown in **Table 4**. Untreated raw milk has an average particle size of 7.59 μm. It was found that all the treatments significantly reduced the particle size, and the A 360-degree radiation TS-treated milk exhibited the smallest particle size of milk with a value of 4.62 μm. The cavitation phenomenon was considered to be the major contributor to the reduction of the particle size of milk (Ertugay et al., 2004).

Changes in Color Characteristics

Color is one of the most important characteristics for milk sales, which is related to the dispersion of fat globules and casein micelles in the visible spectrum. The changes in the color characteristics of raw milk treated by 360-degree radiation TS, UHT, and pasteurization are shown in **Table 5**. Compared with the untreated raw milk, the L^* values (lightness) of milk were significantly increased, while the b^* values (yellow) of milk were significantly decreased after all the treatments. The more intense acoustic cavitation provides better homogenization of the milk due to the reduction of the fat globule size. Great changes in the size of the fat droplets are enough to change the light reflection (Owens et al., 2001). Regarding the a^* value (green), it was slightly increased after 360-degree radiation TS treatment, while UHT treatment resulted in a decrease in a^* value. Overall, the total color difference (ΔE) of 360-degree radiation TS-treated milk is 3.55, which exhibits an insignificant difference from that of UHT-treated milk and significantly higher than that of pasteurized milk.

Changes in the Total Protein Content

Protein is the most important component in milk, but it is sensitive to heat and easy to be denaturized. As shown in **Table 6**, the initial TPC was 3.53% in untreated raw milk. Both 360-degree radiation TS and UHT resulted in no significant changes of the TPC in milk. However, the TPC of pasteurized milk was significantly decreased to 2.53% ($p < 0.05$), which might have resulted from the heat-induced denaturation of proteins.

CONCLUSION

In the present study, a 360-degree radiation TS system was developed for the sterilization of milk. Compared with conventional pasteurization (63°C), the 360-degree radiation TS system enhanced the heat transfer rate in milk by over two times. Based on the established Weibull inactivation model, the treatment duration for the 360-degree radiation TS system to bring out a 5-log reduction was 7.5 min, which was much shorter than that of the common TS treatment combining the single-direction radiation ultrasonic horn and heat. Additionally, in this work, the 360-degree radiation TS system was successfully applied to achieve complete microbial inactivation (under LOD value) in raw milk. Regarding the effect on the physiochemical properties of milk, it was found that the treatment of 360-degree radiation TS can enhance the zeta potential and decrease the average particle size of milk. It also exhibited better retention of the proteins in milk compared with the UHT and conventional pasteurization processing. The 360-degree radiation TS technology can be utilized as a promising technology to assure the microbiological safety and retain the quality of milk.

DATA AVAILABILITY STATEMENT

The original contributions presented in the study are included in the article/supplementary material, further inquiries can be directed to the corresponding author/s.

AUTHOR CONTRIBUTIONS

XL and JZ conceived and designed the experiments. XL wrote the first draft of the manuscript. JZ performed the research and conducted the data analysis. LS, RL, DL, and TD contributed to the literature search and in reviewing and finalizing the manuscript. All authors have read and approved the final manuscript.

REFERENCES

Abesinghe, A. M. N. L., Islam, N., Vidanarachchi, J. K., Prakash, S., Silva, K. F. S. T., and Karim, M. A. (2019). Effects of ultrasound on the fermentation profile of fermented milk products incorporated with lactic acid bacteria. *Int. Dairy J.* 90, 1–14. doi: 10.1016/j.idairyj.2018.10.006

Aneja, K. R., Dhiman, R., Aggarwal, N. K., and Aneja, A. (2014). Emerging preservation techniques for controlling spoilage and pathogenic microorganisms in fruit juices. *Int. J. Microbiol.* 2014:758942. doi: 10.1155/2014/758942

Ashokkumar, M. (2011). The characterization of acoustic cavitation bubbles - an overview. *Ultrason. Sonochem.* 18, 864–872. doi: 10.1016/j.ultsonch.2010.11.016

Awad, T. S., Moharram, H. A., Shaltout, O. E., Asker, D., and Youssef, M. M. (2012). Applications of ultrasound in analysis, processing and quality control of food: a review. *Food Res. Int.* 48, 410–427. doi: 10.1016/j.foodres.2012.05.004

Balasubramanian, R., Im, J., Lee, J., Jeon, H., Mogeni, O. D., Kim, J. H., et al. (2019). The global burden and epidemiology of invasive non-typhoidal *Salmonella* infections. *Hum. Vaccin. Immunother.* 15, 1421–1426. doi: 10.1080/21645515.2018.1504717

Barba, F. J., Koubaa, M., do Prado-Silva, L., Orlien, V., and Sant'Ana, A. D. S. (2017). Mild processing applied to the inactivation of the main foodborne bacterial pathogens: a review. *Trends Food Sci. Technol.* 66, 20–35. doi: 10.1016/j.tifs.2017.05.011

Campoli, S. S., Rojas, M. L., do Amaral, J., Canniatti-Brazaca, S. G., and Augusto, P. E. D. (2018). Ultrasound processing of guava juice: effect on structure, physical properties and lycopene in vitro accessibility. *Food Chem.* 268, 594–601. doi: 10.1016/j.foodchem.2018.06.127

Carrillo-Lopez, L. M., Juarez-Morales, M. G., Garcia-Galicia, I. A., Alarcon-Rojo, A. D., and Huerta-Jimenez, M. (2020). The effect of high-intensity ultrasound on the physicochemical and microbiological properties of Mexican panela cheese. *Foods* 9:313. doi: 10.3390/foods9030313

Chemat, F., Zill, E. H., and Khan, M. K. (2011). Applications of ultrasound in food technology: processing, preservation and extraction. *Ultrason. Sonochem.* 18, 813–835. doi: 10.1016/j.ultsonch.2010.11.023

Chen, L., Zhang, H., Liu, Q., Pang, X., Zhao, X., and Yang, H. (2019). Sanitising efficacy of lactic acid combined with low-concentration sodium hypochlorite on

Listeria innocua in organic broccoli sprouts. *Int. J. Food Microbiol.* 295, 41–48. doi: 10.1016/j.ijfoodmicro.2019.02.014

Claeys, W. L., Cardoen, S., Daube, G., De Block, J., Dewettinck, K., Dierick, K., et al. (2013). Raw or heated cow milk consumption: review of risks and benefits. *Food Control* 31, 251–262. doi: 10.1016/j.foodcont.2012.09.035

Ertugay, M. F., Şengül, M., and Şengül, M. (2004). Effect of ultrasound treatment on milk homogenisation and particle size distribution of fat. *Turk. J. Vet. Anim. Sci.* 28, 303–308.

FAO (2019). *Food and Agriculture Data*. Available online at: http://www.fao.org/faostat/en/#data/QCL (assessed September 3, 2021).

Feng, X., Tjia, J. Y. Y., Zhou, Y., Liu, Q., Fu, C., and Yang, H. (2020). Effects of tocopherol nanoemulsion addition on fish sausage properties and fatty acid oxidation. *LWT Food Sci. Technol.* 118:108737. doi: 10.1016/j.lwt.2019.108737

Grant, I. R., Ball, H. J., and Rowe, M. T. (1998). Effect of high-temperature, short-time (HTST) pasteurization on milk containing low numbers of Mycobacterium paratuberculosis. *Lett. Appl. Microbiol.* 26, 166–170. doi: 10.1046/j.1472-765X.1998.00309.x

Grant, I. R., Ball, J. H., Neill, S. D., and Rowe, M. T. (1996). Inactivation of *Mycobacterium paratuberculosis* in cows' milk at pasteurization temperatures. *Appl. Environ. Microbiol.* 62, 631–636. doi: 10.1128/aem.62.2.631-636.1996

Halpin, R. M., Cregenzán-Alberti, O., Whyte, P., Lyng, J. G., and Noci, F. (2013). Combined treatment with mild heat, manothermosonication and pulsed electric fields reduces microbial growth in milk. *Food Control* 34, 364–371. doi: 10.1016/j.foodcont.2013.05.008

Kurbanov, U., and Melkumov, K. (2003). "Use of ultrasound for intensification of heat transfer process in heat exchangers," in *Proceedings of the International 2003 Congress of Refrigeration*, Washington DC, 1–5.

Lee, H., Zhou, B., Liang, W., Feng, H., and Martin, S. E. (2009). Inactivation of *Escherichia coli* cells with sonication, manosonication, thermosonication, and manothermosonication: microbial responses and kinetics modeling. *J. Food Eng.* 93, 354–364. doi: 10.1016/j.jfoodeng.2009.01.037

Legay, M., Gondrexon, N., Le Person, S., Boldo, P., and Bontemps, A. (2011). Enhancement of heat transfer by ultrasound: review and recent advances. *Int. J. Chem. Eng.* 2011:670108. doi: 10.1155/2011/670108

Li, J., Ahn, J., Liu, D., Chen, S., Ye, X., and Ding, T. (2016). Evaluation of ultrasound-induced damage to *Escherichia coli* and *Staphylococcus aureus* by flow cytometry and transmission electron microscopy. *Appl. Environ. Microbiol.* 82, 1828–1837. doi: 10.1128/AEM.03080-15

Li, J., Wang, J., Zhao, X., Wang, W., Liu, D., Chen, S., et al. (2019). Inactivation of *Staphylococcus aureus* and *Escherichia coli* in milk by different processing sequences of ultrasound and heat. *J. Food Saf.* 39:e12614. doi: 10.1111/jfs.12614

Liao, X., Li, J., Muhammad, A. I., Suo, Y., Chen, S., Ye, X., et al. (2018). Application of a dielectric barrier discharge atmospheric cold plasma (Dbd-Acp) for *Eshcerichia coli* inactivation in apple juice. *J. Food Sci.* 83, 401–408. doi: 10.1111/1750-3841.14045

Liu, Q., Chen, L., Laserna, A. K. C., He, Y., Feng, X., and Yang, H. (2020). Synergistic action of electrolyzed water and mild heat for enhanced microbial inactivation of *Escherichia coli* O157:H7 revealed by metabolomics analysis. *Food Control* 110:107026. doi: 10.1016/j.foodcont.2019.107026

Makroo, H. A., Rastogi, N. K., and Srivastava, B. (2020). Ohmic heating assisted inactivation of enzymes and microorganisms in foods: a review. *Trends Food Sci. Technol.* 97, 451–465. doi: 10.1016/j.tifs.2020.01.015

Owens, S. L., Brewer, J. L., and Rankin, S. A. (2001). Influence of bacterial cell population and pH on the color of nonfat milk. *LWT Food Sci. Technol.* 34, 329–333. doi: 10.1006/fstl.2001.0781

Rainard, P., Foucras, G., Fitzgerald, J. R., Watts, J. L., Koop, G., and Middleton, J. R. (2018). Knowledge gaps and research priorities in *Staphylococcus aureus* mastitis control. *Transbound. Emerg. Dis.* 65(Suppl. 1), 149–165. doi: 10.1111/tbed.12698

Sasikumar, R., Pradhan, D., and Deka, S. C. (2019). Effects of thermosonication process on inactivation of *Escherichia coli* and *Saccharomyces cerevisiae* and its survival kinetics modeling in khoonphal (*Haematocarpus validus*) juice to extend its shelf life. *J. Food Process. Preserv.* 43:e14220. doi: 10.1111/jfpp.14220

Scudino, H., Silva, E. K., Gomes, A., Guimaraes, J. T., Cunha, R. L., Sant'Ana, A., et al. (2020). Ultrasound stabilization of raw milk: microbial and enzymatic inactivation, physicochemical properties and kinetic stability. *Ultrason. Sonochem.* 67:105185. doi: 10.1016/j.ultsonch.2020.105185

Shanmugam, A., and Ashokkumar, M. (2014). Ultrasonic preparation of stable flax seed oil emulsions in dairy systems-physicochemical characterization. *Food Hydrocoll.* 39, 151–162. doi: 10.1016/j.foodhyd.2014.01.006

Shao, L., Dong, Y., Chen, X., Xu, X., and Wang, H. (2020). Modeling the elimination of mature biofilms formed by Staphylococcus aureus and *Salmonella* spp. Using combined ultrasound and disinfectants. *Ultrason. Sonochem.* 69:105269. doi: 10.1016/j.ultsonch.2020.105269

Song, K., Mohseni, M., and Taghipour, F. (2016). Application of ultraviolet light-emitting diodes (UV-LEDs) for water disinfection: a review. *Water Res.* 94, 341–349. doi: 10.1016/j.watres.2016.03.003

Surowsky, B., Frohling, A., Gottschalk, N., Schluter, O., and Knorr, D. (2014). Impact of cold plasma on *Citrobacter freundii* in apple juice: inactivation kinetics and mechanisms. *Int. J. Food Microbiol.* 174, 63–71. doi: 10.1016/j.ijfoodmicro.2013.12.031

Tao, Y., and Sun, D. W. (2015). Enhancement of food processes by ultrasound: a review. *Crit. Rev. Food Sci. Nutr.* 55, 570–594. doi: 10.1080/10408398.2012.667849

Vartanian, L. R., Schwartz, M. B., and Brownell, K. D. (2007). Effects of soft drink consumption on nutrition and health: a systematic review and meta-analysis. *Am. J. Public Health* 97, 667–675. doi: 10.2105/AJPH.2005.083782

Wu, J., Zhao, L., Lai, S., and Yang, H. (2021). NMR-based metabolomic investigation of antimicrobial mechanism of electrolysed water combined with moderate heat treatment against *Listeria monocytogenes* on salmon. *Food Control* 125: 107974. doi: 10.1016/j.foodcont.2021.107974

Yuksel, Y., and Elgun, A. (2020). Determination of the effect of high energy ultrasound application in tempering on flour quality of wheat. *Ultrason. Sonochem.* 67:105129. doi: 10.1016/j.ultsonch.2020.105129

Zeinhom, M. M. A., and Abdel-Latef, G. K. (2014). Public health risk of some milk borne pathogens. *Beni Suef Univ. J. Basic Appl. Sci.* 3, 209–215. doi: 10.1016/j.bjbas.2014.10.006

Zhao, L., Zhao, M. Y., Phey, C. P., and Yang, H. (2019). Efficacy of low concentration acidic electrolysed water and levulinic acid combination on fresh organic lettuce (*Lactuca sativa* Var. Crispa L.) and its antimicrobial mechanism. *Food Control* 101, 241–250. doi: 10.1016/j.foodcont.2019.02.039

Zhao, X., Chen, L., Zhao, L., He, Y., and Yang, H. (2020). Antimicrobial kinetics of nisin and grape seed extract against inoculated *Listeria monocytogenes* on cooked shrimps: survival and residual effects. *Food Control* 115:107278.

Conflict of Interest: The authors declare that the research was conducted in the absence of any commercial or financial relationships that could be construed as a potential conflict of interest.

Publisher's Note: All claims expressed in this article are solely those of the authors and do not necessarily represent those of their affiliated organizations, or those of the publisher, the editors and the reviewers. Any product that may be evaluated in this article, or claim that may be made by its manufacturer, is not guaranteed or endorsed by the publisher.

frontiers in Microbiology

ORIGINAL RESEARCH
published: 24 December 2021
doi: 10.3389/fmicb.2021.730733

Microbial-Maximum Likelihood Estimation Tool for Microbial Quantification in Food From Left-Censored Data Using Maximum Likelihood Estimation for Microbial Risk Assessment

Gyung Jin Bahk[1] and Hyo Jung Lee[2]*

[1] Department of Food and Nutrition, Kunsan National University, Gunsan, South Korea, [2] Department of Biology, Kunsan National University, Gunsan, South Korea

In food microbial measurements, when most or very often bacterial counts are below to the limit of quantification (LOQ) or the limit of detection (LOD) in collected food samples, they are either ignored or a specified value is substituted. The consequence of this approach is that it may lead to the over or underestimation of quantitative results. A maximum likelihood estimation (MLE) or Bayesian models can be applied to deal with this kind of censored data. Recently, in food microbiology, an MLE that deals with censored results by fitting a parametric distribution has been introduced. However, the MLE approach has limited practical application in food microbiology as practical tools for implementing MLE statistical methods are limited. We therefore developed a user-friendly MLE tool (called "Microbial-MLE Tool"), which can be easily used without requiring complex mathematical knowledge of MLE but the tool is designated to adjust log-normal distributions to observed counts, and illustrated how this method may be implemented for food microbial censored data using an Excel spreadsheet. In addition, we used two case studies based on food microbial laboratory measurements to illustrate the use of the tool. We believe that the Microbial-MLE tool provides an accessible and comprehensible means for performing MLE in food microbiology and it will also be of help to improve the outcome of quantitative microbial risk assessment (MRA).

Keywords: microbial measurement, microbial censored data, non-detection (ND), limit of quantification (LOQ), Excel spreadsheet, microbial risk assessment (MRA)

OPEN ACCESS

Edited by:
Jun Wang,
Qingdao Agricultural University, China

Reviewed by:
Qingli Dong,
University of Shanghai for Science and Technology, China
Zhaohuan Zhang,
Shanghai Ocean University, China

****Correspondence:***
Gyung Jin Bahk
bahk@kunsan.ac.kr

Specialty section:
This article was submitted to Food Microbiology, a section of the journal Frontiers in Microbiology

Received: *25 June 2021*
Accepted: *08 November 2021*
Published: *24 December 2021*

Citation:
Bahk GJ and Lee HJ (2021) Microbial-Maximum Likelihood Estimation Tool for Microbial Quantification in Food From Left-Censored Data Using Maximum Likelihood Estimation for Microbial Risk Assessment. Front. Microbiol. 12:730733. doi: 10.3389/fmicb.2021.730733

INTRODUCTION

A large number of experiments on the microbiological status of various foods and food products are carried out globally. These experiments involve the collection of large amounts of data. However, in attempts to estimate the concentration of various microorganisms in food samples, those present in quantities below the detection limit are either ignored or a specified value is substituted.

Abbreviations: CI, confidence intervals; LOD, limit of detection; LOQ, limit of quantification; MLE, maximum likelihood estimation; MRA, microbial risk assessment; ND, non-detection.

The statistical term for such results is "censored data," i.e., non-zero values which cannot be measured, but are known to be below some threshold level (Hornung and Reed, 1990). Moreover, in food microbiology, since these low bacterial counts are compared to the limit of quantification (LOQ) or the limit of detection (LOD) of the method of analysis, and not reported if found to be lower than these values, only a limited amount of data is available in most cases (Busschaert et al., 2010). In food microbial measurements, there were found to contain some values below the LOQ or LOD of the sampling and analytical methods, and some were very heavily censored; over 90% of the data were below the LOQ in some enumeration data sets (i.e., quantitative methods), with nearly 100% (i.e., totally left-censored results) being lower than the LOD in presence/absence tests (i.e., qualitative methods). When quantification of the microorganisms in these samples is not possible, and assumed positive samples fall below the LOQ or LOD, they are either ignored or a specified value is substituted at or below the LOQ or LOD (Hewett and Ganser, 2007; Lorimer and Kiermeier, 2007). The consequence of these approaches is that they may lead to the over or underestimation of quantitative results. As an example, Lorimer and Kiermeier (2007) and Busschaert et al. (2010) showed that the difference in quantitative results depending on whether or not censored data are considered. It is necessary, therefore, to use a method for calculating the parameters characterizing the statistical distribution, for example, the arithmetic mean exposures that considers the food microbial censored data.

A maximum likelihood estimation (MLE) approach can be applied to deal with these kinds of censored data sets. Hornung and Reed (1990) and Helsel (2005) previously published and implemented an analysis of methods, in which the techniques proposed included an MLE statistical method for estimating dataset descriptors in the presence of non-detectable values in environmental hygiene and chemistry analyses. Recently, in food microbiology, an MLE method that deals with food microbial censored results by fitting a parametric distribution has been introduced for analyzing data with microbial censored observations (Shorten et al., 2006; Lorimer and Kiermeier, 2007; Busschaert et al., 2010, 2011; Chik et al., 2018). These researchers suggested this MLE method to deal with non-detected microbes in food microbiological test results, and focused primarily on applying MLE to deal with quantitative data that are censored on one side due to an LOQ or LOD (Busschaert et al., 2010; Wang and Gui, 2020). This MLE approach can contribute significantly to the quantification of microbial censored data. Furthermore, using censored data is becoming increasingly important as quantitative microbial risk assessment (MRA) methodologies continue to make greater use of quantitative data (Lorimer and Kiermeier, 2007).

However, the current maximum likelihood approach has limited practical application in food microbiology, or in the food industry, and there exists little practical support in terms of implementing the suggested MLE statistical methods. In addition, it is difficult to confirm the results of MLE actually used in food microbial prevalence studies. In order to address these limitations, Lorimer and Kiermeier (2007) suggested using an Excel program (which, at the time, would have been difficult to implement) or a statistical package, such as free and open source statistical software. Boysen et al. (2013) also reported implementation of an MLE approach for estimating the normal distribution parameters using the Solver add-in for Excel 2010. However, this approach was only used for MRA self-performance, and was not released as a publicly available tool. Therefore, there seems to be no dedicated tool that can be used to easily implement MLE-based methods in food microbiology. Considering the growing number of people and food industries using MLE on censored data, the need for user-friendly MLE tools has become increasingly important.

The objective of this study was to develop a user-friendly MLE tool, which could be easily used in food microbiology without the need for understanding the underlying mathematical concepts. Here we report the development the Microbial-MLE tool, using the Solver add-in for Excel 2016. In addition, we illustrated approaches using this tool in case studies based on food microbial laboratory measurements. We believe the Microbial-MLE tool provides an accessible and easily comprehensible means of performing MLE analyses of food microbial censored data.

MATERIALS AND METHODS

Microbial-Maximum Likelihood Estimation Tool Configuration

The Microbial-MLE tool, included MLE techniques, was implemented in the Excel program with the Excel Solver add-in. As shown in **Figure 1**, the tool is composed of four sub-tools (QN_1, 2, 3, and 4), according to the type of microbiological enumeration test employed, i.e., whether data below the LOQ exists, and whether the data format is quantitative or semi-quantitative (interval data). QN_1 and 2 employ a general microbial concentration calculation method (i.e., no need to use MLE), and QN_3 and 4 are mainly used for MLE because of data occurring which is below the LOQ.

Maximum Likelihood Estimation for Microbial Censored Data

Maximum likelihood estimation is a method for estimating the parameters (e.g., mean and standard deviation) of a statistical distribution from observed data (Finkelstein and Verma, 2001) and is also used to fit a statistical distribution to a set of food microbial censored data (Busschaert et al., 2010). The method of MLE, assuming an underlying normal distribution for the logarithm 10 concentration (i.e., lognormal distribution), may be used to estimate the means and standard deviations for microbial censored data (Lorimer and Kiermeier, 2007).

The lognormal distribution has two parameters, the mean (μ) and the standard deviation (σ). Let $\ln(x_i)$ be the logarithm of the observed data value, x, of microbial sample i. Then, the probability distribution is defined by:

$$N(x_i, \mu, \sigma) = \frac{1}{\sqrt{2\Pi}\sigma} \exp\left[\frac{-\left(\ln(x_i) - \mu\right)^2}{2\sigma^2}\right] \quad (1)$$

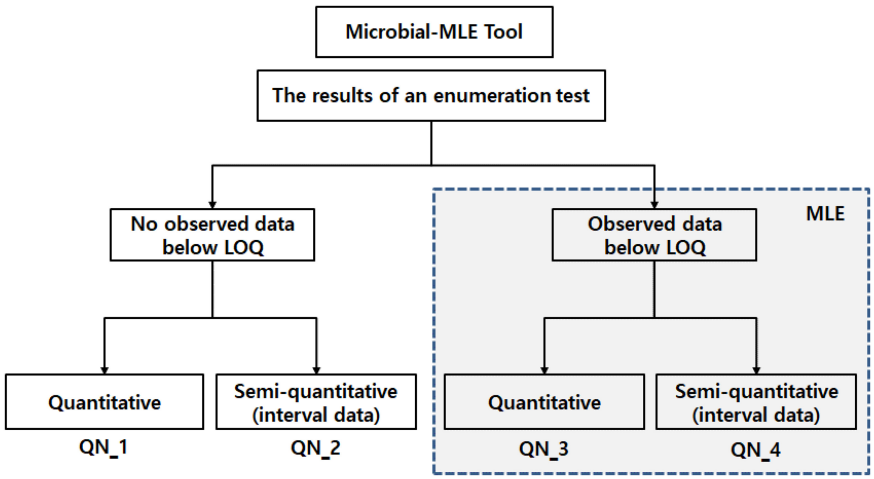

FIGURE 1 | Configuration of the Microbial-MLE tool composed of four sub-tools (QN_1, 2, 3, and 4), the blue dashed line indicates the steps in which MLE is used. LOQ, limit of quantification; MLE, maximum likelihood estimation. (Details for QN_1 and 2 can be seen in the Excel program in the supplement, QN_3 and 4 are shown in **Figures 3**, **4**).

If there are thus n observations, $y_1 = \ln(x_1)$, $y_2 = \ln(x_2)$ …and $y_n = \ln(x_n)$, from a lognormal distribution with the mean (μ) and the standard deviation (σ), the probability (P_N) of obtaining these values for the n observations is:

$$P_N(x_1, \ldots, x_n \mid \mu, \sigma) = \prod_{i=1}^{n} N(x_i, \mu, \sigma) \quad (2)$$

In the enumeration test result, if the LOQ or LOD is DL (CFU/g or ml) with non-detectable observations (m), the probability of observing a value less than DL is P_{DL}, in a normal distribution with mean (μ) and standard deviation (σ).

$$P_{DL} = \left(\int_{-\infty}^{DL} N(x; \mu, \sigma) \mathrm{ds} \right)^{m} \quad (3)$$

The probability of the microbial population distribution parameters mean (μ) and standard deviation (σ), given the observed data (n) and non-detectable observations (m), is defined by Finkelstein and Verma (2001); Shorten et al. (2006), and Hewett and Ganser (2007):

$$P\left(\mu, \sigma \mid \{x_i\}_{i=1}^{n}, m\right) = P_{DL} \times P_N \quad (4)$$

In statistical terminology this probability is called a likelihood, and the method of MLE finds those values of mean (μ) and the standard deviation (σ) that maximize this probability (Finkelstein and Verma, 2001).

Maximum Likelihood Estimation in Excel for Microbial Censored Data

We show how the previous MLE-related formulas (Eqs 1–4) are represented in Excel (Microsoft Excel 2016; Microsoft Corp., Redmond, WA, United States) spreadsheet (**Figure 2**). These probabilities (P_{DL}, P_N, and P) are programmed into spreadsheet. In the case of P_{DL}, in Excel, the function is NORMDIST. This function returns the normal cumulative distribution for the specified mean and standard deviation. **Figure 2** shows the maximization of the likelihood function using microbial censored data (Column A). The values in F3 and F4 as changing variable cells in Solver tool are the mean and standard deviation of the logarithms (Column C9:C18) of the observed microbial data values in Column A. The Solver tool in Excel will select the proper values in E5 and E6 to maximize the sum of the log-Likelihoods, which can be found in cell F7 as objective cell in Solver tool. In this Microbial MLE Tool, all of these calculations and processes were automated with the Excel macro functions.

Use of Microbial Maximum Likelihood Estimation Tool

In the Microbial MLE tool, each of these sub-tools is implemented in one spreadsheet and is divided into an input and an output part. As shown in the blue dashed lines on the left in **Figures 3**, **4**, the main input part consists of three input boxes: (1) sample size (g), (2) the volume of diluent used (ml), and (3) the observed measurement data, input as the results of quantitative (**Figure 3**) or semi-quantitative (**Figure 4**) enumeration tests (CFU/g or ml). Additionally, for QN_2 and 4 (interval data) there is an input for the dilution factor. Using (1) and (2) values, the LOQ is automatically calculated assuming a plating volume of 1 ml. After inputting these data, the "Calculate" button was clicked. The calculated results immediately appeared in the right-hand Output panel, as shown in **Figures 3**, **4**. In the output panel, the following information is displayed: estimated microbial concentration as mean and standard deviation (SD) with 95% confidence intervals (CI) (Log CFU/g or ml), and a plot showing the probability distribution for the concentration, displaying the mean, LOQ value, 5th and 95th percentile. All of the above can be found in the Excel sheet (**Supplementary Data**: Microbial-MLE Tool.xlsm) attached to this article.

	A	B	C	D	E	F	G
1	**Microbial**						
2	**data**	**(CFU/g or ml)**		**Log-Likelyhood of observation, given estimate of Mean and SD**	**Observed**		**Solver cells**
3					**Mean**	=AVERAGE(C9:C18)	Changing
4	9	<LOQ		=LN(NORMDIST(LN(A4),$F$3,$F$4,TRUE))	**SD**	=STDEV(C9:C18)	variable cells
5	9	<LOQ		=LN(NORMDIST(LN(A5),$F$3,$F$4,TRUE))			
6	9	<LOQ		=LN(NORMDIST(LN(A6),$F$3,$F$4,TRUE))	**Total**		
7	9	<LOQ		=LN(NORMDIST(LN(A7),$F$3,$F$4,TRUE))	**Log-Likelihood**	=SUM(D4:D18)	Objective cell
8	9	<LOQ		=LN(NORMDIST(LN(A8),$F$3,$F$4,TRUE))			
9	10	=LOQ	=LN(A9)	=LN((1/((2*PI())^0.5*$F$4))*EXP(-(1/2)*(C(A9)-$F$3)/$F$4)^2))	**Estimated (Log CFU/g or ml)**		
10	20	>LOQ	=LN(A10)	=LN((1/((2*PI())^0.5*$F$4))*EXP(-(1/2)*((C(A10)-$F$3)/$F$4)^2))	**Mean**	=LOG(EXP(F3))	
11	30	>LOQ	=LN(A11)	=LN((1/((2*PI())^0.5*$F$4))*EXP(-(1/2)*((C(A11)-$F$3)/$F$4)^2))	**SD**	=LOG(EXP(F4))	
12	50	>LOQ	=LN(A12)	=LN((1/((2*PI())^0.5*$F$4))*EXP(-(1/2)*((C(A12)-$F$3)/$F$4)^2))			
13	70	>LOQ	=LN(A13)	=LN((1/((2*PI())^0.5*$F$4))*EXP(-(1/2)*((C(A13)-$F$3)/$F$4)^2))			
14	100	>LOQ	=LN(A14)	=LN((1/((2*PI())^0.5*$F$4))*EXP(-(1/2)*((C(A14)-$F$3)/$F$4)^2))			
15	120	>LOQ	=LN(A15)	=LN((1/((2*PI())^0.5*$F$4))*EXP(-(1/2)*((C(A15)-$F$3)/$F$4)^2))			
16	150	>LOQ	=LN(A16)	=LN((1/((2*PI())^0.5*$F$4))*EXP(-(1/2)*((C(A16)-$F$3)/$F$4)^2))			
17	500	>LOQ	=LN(A16)	=LN((1/((2*PI())^0.5*$F$4))*EXP(-(1/2)*((C(A17)-$F$3)/$F$4)^2))			
18	1,200	>LOQ	=LN(A17)	=LN((1/((2*PI())^0.5*$F$4))*EXP(-(1/2)*((C(A18)-$F$3)/$F$4)^2))			
19							

FIGURE 2 | An Excel spreadsheet showing the structure of a template for Microbial MLE tool for an example of quantitative microbial censored data [$n = 15$, LOQ = 10 CFU/g or ml, Censored data% = 33.3%, (=5/15)].

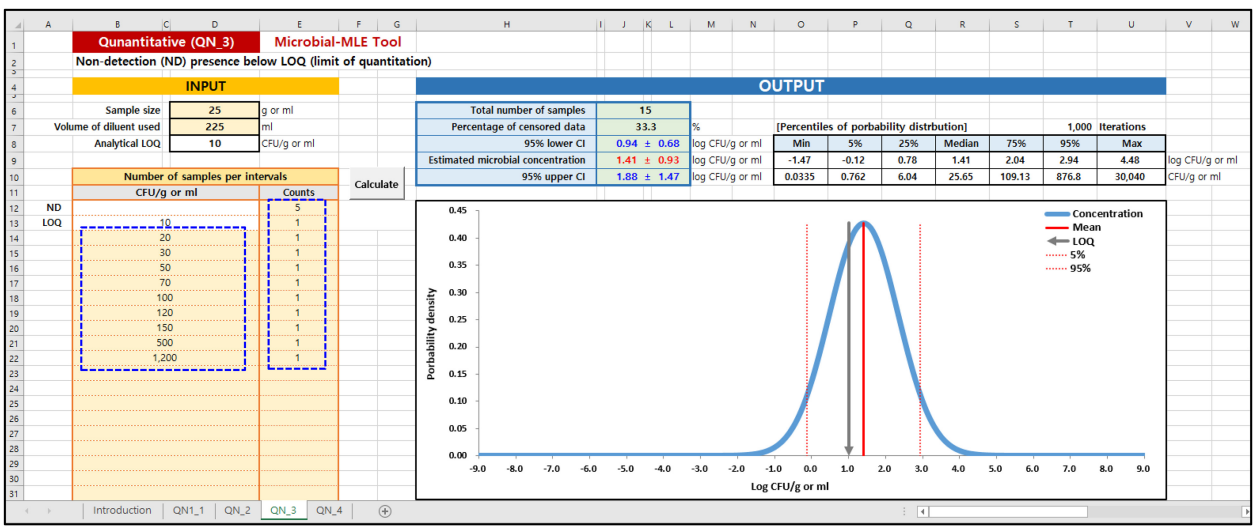

FIGURE 3 | Input and Output panels of the Microbial-MLE tool for quantitative data (QN_3). Data is entered into the pale-yellow cells (blue dashed lines). The entry values surrounded by blue dashed lines are the hypothetical data.

RESULTS

To show the result of Microbial-MLE tool, we used hypothetical data (presented in **Figure 3**) as an example for analyses involving quantitative left-censored data. This hypothetical data set comprises quantitative results with an LOQ of 10 CFU/g. In 5 of the 15 measurements (33%), the result is left-censored due to the LOQ. Using this tool, a normal distribution is estimated for these including censored data with 1.41 ± 0.93 log CFU/g as mean and standard deviation (**Figure 3**).

We illustrated, as case studies, microbial concentration estimation of left-censored food microbial data published in the literature (Jang et al., 2013; Chai et al., 2017), based on laboratory measurements using the developed Microbial-MLE tool. These data represented a variety of foods and microorganisms, and consisted mostly of semi-quantitative (interval) data. The LOQ of all these data sets was 10 CFU/g. The results of the estimated microbial concentrations using these data and the Microbial-MLE tool are shown in **Table 1**.

In cases 1 and 2, the results of the total coliforms and *Bacillus cereus* analyses in sandwiches (Jang et al., 2013), which were produced on-site and served in bakeries, cafe's, and sandwich bars in South Korea, were evaluated. The left-censored data due to the LOQ were in 214 (19%) and 1,008

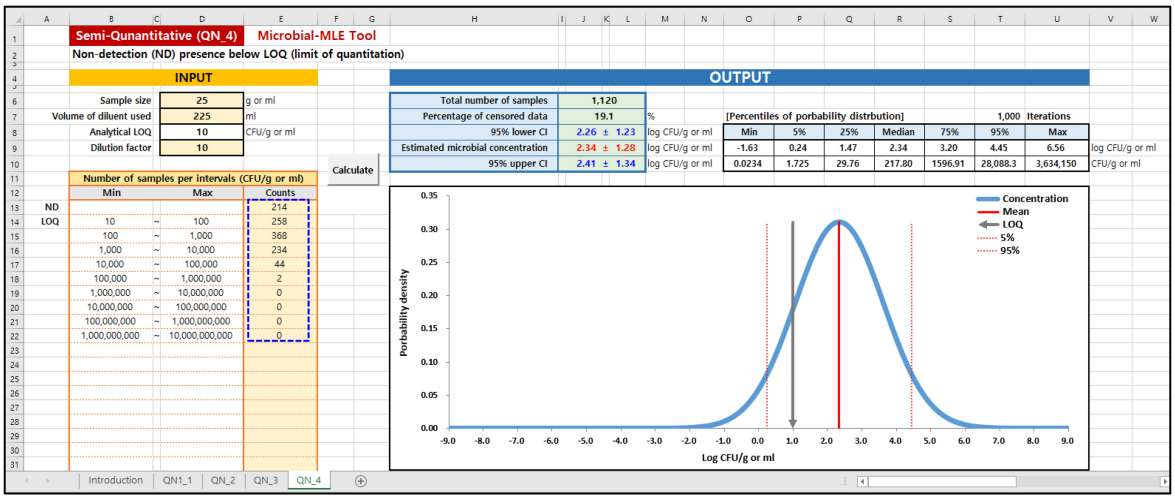

FIGURE 4 | Input and Output panels of the Microbial-MLE tool for semi-quantitative (interval) data (QN_4). Data is entered into the pale-yellow cells (blue dashed line). The values shown are those used in case 1 (**Table 1**).

TABLE 1 | The results of the estimated mean and standard deviation (SD) using the Microbial-MLE tool for four data sets (mainly semi-quantitative results) used as case studies.

Case number	Microorganisms	No. of samples (CFU/g)						Total	Reported Mean ± SD (log CFU/g)	Estimated Mean ± SD using this tool (log CFU/g)
		ND[1]	10∼10^2	10^2∼10^3	10^3∼10^4	10^4∼10^5	10^5∼10^6			
Case 1	Total coliforms	214	258	368	234	44	2	1,120	–	2.34 ± 1.28
Case 2	*B. cereus*	1,008	49	48	12	2	1	1,120	–	−2.76 ± 2.93
Case 3	Total coliforms	16	19	34	22	8	1	100	2.23 ± 1.32	2.57 ± 1.34
Case 4	*E. coli*	81	16	2	1			100	0.37 ± 0.35	−0.44 ± 1.63

[1]*ND, not detected; LOQ, 10 CFU/g.*

(90%) of 1,120 samples, in the total coliforms and *B. cereus* analyses, respectively. Using this tool, the logarithms of the including censored data of total coliforms and *B. cereus* have been estimated to have a normal distribution with 2.34 ± 1.28 and −2.76 ± 2.93 log CFU/g, respectively. In particular, the result of *B. cereus* showed a high censored percentage (90%), and a large SD with a wide distribution of up to 10^5∼10^6 CFU/g due to the presence of outliers.

Cases 3 and 4 consist of 100 measurements of the total coliforms and *Escherichia coli* in retail beef samples (Chai et al., 2017). The left-censored data due to the LOQ were in 16 (16%) and 81 (81%) of 100 samples, in the total coliforms and *E. coli* analyses, respectively. Using this tool, the logarithmic values of the analysis results are fitted to a normal distribution with 2.57 ± 1.34 and −0.44 ± 1.63 log CFU/g, respectively.

Cases 1 and 2 did not show self-estimated quantitative results in the reference article and were not compared with the estimated values with this tool. However, in cases 3 and 4 were presented self-estimated quantitative results (**Table 1**). The estimated mean and SD values (2.57 ± 1.34 log CFU/g) changed very little due to the small amount of censored data, in the order of 2.23 ± 1.32 log CFU/g, in the results of the total coliforms, while the estimated mean and SD values (−0.44 ± 1.63 log CFU/g) changed greatly from 0.37 ± 0.35 log CFU/g due the abundance of censored data in the results of the *E. coli* analysis (**Figure 5** and **Table 1**). This result shows the difference between the quantitative results when non-detected (left-censored) data is included and when it does not. Moreover, as shown in **Figure 5** (case 4), the result (0.37 ± 0.35 log CFU/g) does not converge to the maximum value given in **Table 1**.

DISCUSSION

To increase the use of MLE in food microbial measurements, a user-friendly Microbial-MLE tool based on an MLE statistical method was developed. This tool estimates the quantitative concentration levels of microorganisms using food microbial censored data from the results of laboratory measurements. The tool works in an easy-to-use Excel spreadsheet and does not require complex mathematical knowledge about MLE on the part of the user. Thus, using this tool, anyone can rapidly and easily estimate the concentration of microorganisms from a variety of measurement results, or from routine monitoring of foodborne pathogens in various foods and food products.

Microbiological tests are generally divided into qualitative (presence/absence test) and quantitative (enumeration test) methods (Jarvis, 2008). Qualitative methods are concerned

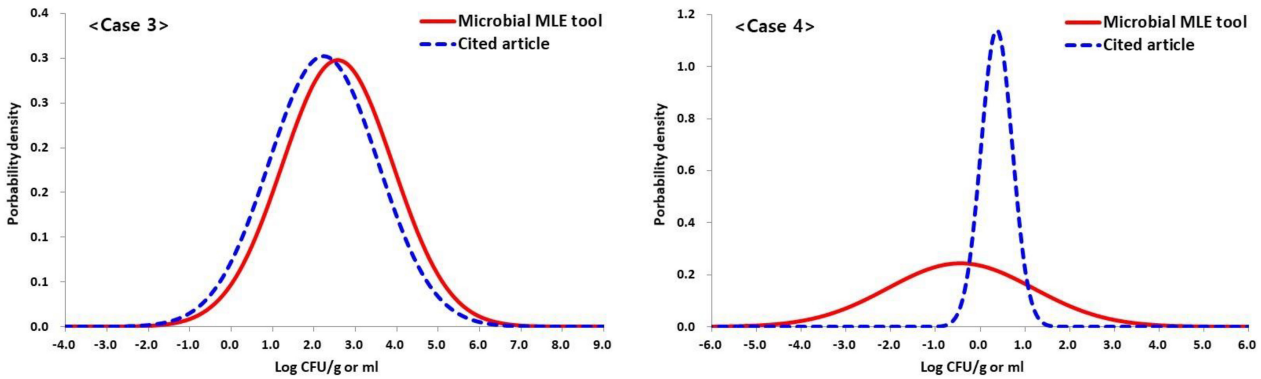

FIGURE 5 | Based on case 3 and three data set (n = 100, LOQ = 10 CFU/g) in **Table 1**, comparison of the results of estimated concentration of the total coliforms (case 3) and *E. coli* (case 4) in retail beef samples using the Microbial-MLE tool and the results presented in the cited literature (Chai et al., 2017) (Case 3: 2.57 ± 1.34 and 2.23 ± 1.32 log CFU/g, Case 4: –0.44 ± 1.63 and 0.37 ± 0.35 log CFU/g, estimated by the Microbial-MLE tool and in the cited article, respectively, and percentage of censored data in Case 3 and 4 are 16 and 81%, respectively). The larger the censored rate, the greater the difference, i.e., these results show the difference in quantitative results depending on whether or not censored data are included.

with investigating the presence or absence of a particular pathogen, such as specific foodborne pathogens (e.g., *Salmonella* spp. and *E. coli* O157:H7), even though quantitative method are available. On the other hand, quantitative methods are concerned with estimating microorganism concentrations, which may include total aerobic bacteria, coliforms and *E. coli*, as well as specific foodborne pathogens, such as *Staphylococcus aureus* and *B. cereus*. Currently, the tool we developed is only applicable to quantitative enumeration measurement results, and has not yet been applied to qualitative (presence/absence) test results possessing completely left-censored data (i.e., 100% censored data).

Microbial risk assessment is designed to quantitatively predict the probability of specific foodborne illness, such as pathogenic *E. coli* infections and salmonellosis, due to presence of causative pathogenic agents in the food products (Romero-Barrios et al., 2013). Thus, MRA have a requirement for quantitative data on the concentration of foodborne pathogens (Cassin et al., 1998; Boysen et al., 2013; Duarte et al., 2015), as microbiological contamination levels are often associated with predicted risk (Busschaert et al., 2010). The MLE method, which estimates values for the parameters that are most likely to have generated the observed measurements, can contribute to improving of the estimation for the concentration of microorganisms in foods, which is an important element of quantitative MRA.

The maximum likelihood method has been shown to produce unbiased estimates of both the mean and SD under a variety of conditions (Finkelstein and Verma, 2001). Moreover, the application of this MLE technique on microbial censored data has already been demonstrated to produce accurate and reliable results in food microbiology (Shorten et al., 2006; Lorimer and Kiermeier, 2007; Busschaert et al., 2010, 2011). However, despite many studies, the use of MLE method in food microbiology was, until recently, impractical, as MLE statistical methods are somewhat complex, and there was a lack of applicable tools with which to perform the necessary analyses. Previously, Lorimer and Kiermeier (2007) reported that MLE calculations could be performed by coding the methods manually and by using the Excel's Solver add-in. In addition, the "fitdistrplus" R-package is available and allows also fitting statistical distributions to datasets containing censored data (Pouillot and Delignette-Muller, 2010). The estimation results of our Microbial-MLE tool and this R-package were exactly the same. Cases involving more complex data sets (e.g., 100% censored data) require more complex models, e.g., combinations of MLE and bootstrapping methods (Busschaert et al., 2010), and zero-inflated Poisson models (Gonzales-Barron et al., 2010; Duarte et al., 2015). Currently, however, MLE is easily implemented in commonly available spreadsheet software such as Excel. We demonstrate how this MLE method may be implemented using Excel spreadsheet. Once the spreadsheet template is set up, it can be readily used to estimate the concentrations of microorganisms from microbial censored data sets.

CONCLUSION

In conclusion, our newly developed Microbial-MLE tool is simple to use and can rapidly estimate the best estimation concentrations of microorganisms from food microbial censored data, even if the user does not have deep knowledge of MLE. When reporting microbial measurement results, this tool can use censored data for analyzing the effectiveness of microbial interventions (Lorimer and Kiermeier, 2007). In addition, the tool will help improve the outcome of quantitative MRAs and can also be used as an educational tool for demonstrating MLE methods. However, this tool used only the parameters presented and did not take into account other parameters. Additionally, as mentioned above, the current tool is only available for quantitative enumeration test results and has not yet been applied to qualitative presence/absence test results, which are used for detecting the presence of most important foodborne pathogens. For use in various microbiological methods, future improvement and supplementation of to this tool should be undertaken.

DATA AVAILABILITY STATEMENT

The original contributions presented in the study are included in the article/**Supplementary Material**, further inquiries can be directed to the corresponding author.

AUTHOR CONTRIBUTIONS

GB and HL conceived of the study and participated in its design and coordination. Both authors reviewed and approved the final manuscript.

FUNDING

This work was supported by the National Research Foundation of Korea (NRF) grant funded by the Korea government (MSIT) (2019R1A4A102980111).

SUPPLEMENTARY MATERIAL

The Supplementary Material for this article can be found online at: https://www.frontiersin.org/articles/10.3389/fmicb.2021.730733/full#supplementary-material

REFERENCES

Boysen, L., Nauta, M., Duarte, A. S. R., and Rosenquist, H. (2013). Human risk from thermotolerant *Campylobacter* on broiler meat in Denmark. *Int. J. Food Microbiol.* 162, 129–134. doi: 10.1016/j.ijfoodmicro.2013.01.009

Busschaert, P., Geeraerd, A. H., Uyttendaele, M., and Van Impe, J. F. (2010). Estimating distributions out of qualitative and (semi) quantitative microbiological contamination data for use in risk assessment. *Int. J. Food Microbiol.* 138, 260–269. doi: 10.1016/j.ijfoodmicro.2010.01.025

Busschaert, P., Geeraerd, A. H., Uyttendaele, M., and Van Impe, J. F. (2011). Hierarchical bayesian analysis of censored microbiological contamination data for use in risk assessment and mitigation. *Food Microbiol.* 28, 712–719. doi: 10.1016/j.fm.2010.06.006

Cassin, M. H., Lammerding, A. M., Todd, E. C. D., Ross, W., and McColl, R. S. (1998). Quantitative risk assessment for *Escherichia coli* O157:H7 in ground beef hamburgers. *Int. J. Food Microbiol.* 41, 21–44. doi: 10.1016/s0168-1605(98)00028-2

Chai, C., Lee, S. Y., and Oh, S. W. (2017). Shelf-life charts of beef according to level of bacterial contamination and storage temperature. *LWT-Food Sci. Technol.* 81, 50–57.

Chik, A. H. S., Schmidt, P. J., and Emelko, M. B. (2018). Learning something from nothing: the critical importance of rethinking microbial non-detects. *Front. Microbiol.* 9:2304. doi: 10.3389/fmicb.2018.02304

Duarte, A. S. R., Stockmarr, A., and Nauta, M. J. (2015). Fitting a distribution to microbial counts: making sense of zeroes. *Int. J. Food Microbiol.* 196, 40–50. doi: 10.1016/j.ijfoodmicro.2014.11.023

Finkelstein, M. M., and Verma, D. K. (2001). Exposure estimation in the presence of nondetectable values: another look. *Am. Ind. Hyg. Assoc. J.* 62, 195–198. doi: 10.1080/15298660108984622

Gonzales-Barron, U., Kerr, M., Sheridan, J. J., and Butler, F. (2010). Count data distributions and their zero-modified equivalents as a framework for modelling microbial data with a relatively high occurrence of zero counts. *Int. J. Food Microbiol.* 136, 268–277. doi: 10.1016/j.ijfoodmicro.2009.10.016

Helsel, D. R. (2005). *Nondetects and Data Analysis: Statistics for Censored Environmental Data*. Hoboken, NJ: Wiley-Interscience, doi: 10.2136/vzj2005.0106br

Hewett, P., and Ganser, G. H. (2007). A comparison of several methods for analyzing censored data. *Ann. Occup. Hyg.* 51, 611–632. doi: 10.1093/annhyg/mem045

Hornung, R. W., and Reed, L. D. (1990). Estimation of average concentration in the presence of nondetectable values. *Appl. Occup. Environ. Hyg.* 5, 46–51. doi: 10.1080/1047322X.1990.10389587

Jang, H. G., Kim, N. H., Choi, Y. M., and Rhee, M. S. (2013). Microbiological quality and risk factors related to sandwiches served in bakeries, cafés, and sandwich bars in South Korea. *J. Food Prot.* 76, 231–238. doi: 10.4315/0362-028X.JFP-12-335

Jarvis, B. (2008). *Statistical Aspects of the Microbiological Examination of Foods*, 2nd Edn, Cambridge, MA: Academic Press.

Lorimer, M. F., and Kiermeier, A. (2007). Analysing microbiological data: Tobit or not Tobit? *Int. J. Food Microbiol.* 116, 313–318. doi: 10.1016/j.ijfoodmicro.2007.02.001

Pouillot, R., and Delignette-Muller, M. L. (2010). Evaluating variability and uncertainty separately in microbial quantitative risk assessment using two R packages. *Int. J. Food Microbiol.* 142, 330–340. doi: 10.1016/j.ijfoodmicro.2010.07.011

Romero-Barrios, P., Hempen, M., Messens, W., Stella, P., and Hugas, M. (2013). Quantitative microbiological risk assessment (QMRA) of food-borne zoonoses at the European level. *Food Control* 29, 343–349. doi: 10.1016/j.foodcont.2012.05.043

Shorten, P. R., Pleasants, A. B., and Soboleva, T. K. (2006). Estimation of microbial growth using population measurements subject to a detection limit. *Int. J. Food Microbiol.* 108, 369–375. doi: 10.1016/j.ijfoodmicro.2005.11.024

Wang, S., and Gui, W. (2020). Corrected maximum likelihood estimations of the lognormal distribution parameters. *Symmetry* 12:968. doi: 10.3390/sym12060968

Conflict of Interest: The authors declare that the research was conducted in the absence of any commercial or financial relationships that could be construed as a potential conflict of interest.

Publisher's Note: All claims expressed in this article are solely those of the authors and do not necessarily represent those of their affiliated organizations, or those of the publisher, the editors and the reviewers. Any product that may be evaluated in this article, or claim that may be made by its manufacturer, is not guaranteed or endorsed by the publisher.

Advantages of publishing in Frontiers

OPEN ACCESS
Articles are free to read for greatest visibility and readership

FAST PUBLICATION
Around 90 days from submission to decision

HIGH QUALITY PEER-REVIEW
Rigorous, collaborative, and constructive peer-review

TRANSPARENT PEER-REVIEW
Editors and reviewers acknowledged by name on published articles

Frontiers
Avenue du Tribunal-Fédéral 34
1005 Lausanne | Switzerland

Visit us: www.frontiersin.org
Contact us: frontiersin.org/about/contact

REPRODUCIBILITY OF RESEARCH
Support open data and methods to enhance research reproducibility

DIGITAL PUBLISHING
Articles designed for optimal readership across devices

FOLLOW US
@frontiersin

IMPACT METRICS
Advanced article metrics track visibility across digital media

EXTENSIVE PROMOTION
Marketing and promotion of impactful research

LOOP RESEARCH NETWORK
Our network increases your article's readership